

**Integrated bioprocess for conversion of xylose to xylonic acid
by recombinant *Corynebacterium glutamicum***

by

**LEKSHMI SUNDAR M S
10BB17J39013**

A thesis submitted to the
Academy of Scientific & Innovative Research
for the award of the degree of

DOCTOR OF PHILOSOPHY

in

SCIENCE

Under the Supervision of
Dr. K. Madhavan Nampoothiri



**CSIR-National Institute for Interdisciplinary Science and Technology
(NIIST), Industrial Estate, Thiruvananthapuram, Kerala - 695019**



Academy of Scientific and Innovative Research
AcSIR Headquarters, CSIR-HRDC campus
Sector 19, Kamla Nehru Nagar,
Ghaziabad, U.P. – 201 002, India

MAY – 2023



राष्ट्रीय अंतर्विषयी विज्ञान तथा प्रौद्योगिकी संस्थान
NATIONAL INSTITUTE FOR INTERDISCIPLINARY SCIENCE AND TECHNOLOGY

वैज्ञानिक तथा औद्योगिक अनुसंधान परिषद्
इन्टरडिप्लोम एस्टेट पी.ओ., पाप्पनकोड, तिरुवनन्तपुरम, भारत- 695 019

Council of Scientific & Industrial Research
Industrial Estate PO, Pappanamcode, Thiruvananthapuram, India - 695 019



CERTIFICATE

This is to certify that the work incorporated in this Ph.D. thesis entitled, "**Integrated bioprocess for conversion of xylose to xylonic acid by recombinant *Corynebacterium glutamicum***", submitted by **Ms. Lekshmi Sundar M S** to the Academy of Scientific and Innovative Research (AcSIR), in partial fulfillment of the requirements for the award of the Degree of **Doctor of Philosophy in Science**, embodies original research work carried out by the student. We, further certify that this work has not been submitted to any other University or Institution in part or full for the award of any degree or diploma. Research material(s) obtained from other source(s) and used in this research work has/have been duly acknowledged in the thesis. Image(s), illustration(s), figure(s), table(s) etc., used in the thesis from other source(s), have also been duly cited and acknowledged.

Lekshmi
18/5/23

Lekshmi Sundar M S

(Candidate)

Dr. K. Madhavan Nampoothiri
18/5/23

Dr. K. Madhavan Nampoothiri

(Supervisor)



डॉ. के. माधवन नम्पूतिरि, पीएच.डी., एफडीआरएस
Dr. K. MADHAVAN NAMPOOTHIRI, PH.D, FDRS
मुख्य वैज्ञानिक एवं प्रमुख / Chief Scientist & Head
माइक्रोबियल प्रक्रिया तथा प्रौद्योगिकी प्रभाग
Microbial Processes & Technology Division
सी एस आई आर-राष्ट्रीय अंतर्विषयी विज्ञान तथा प्रौद्योगिकी संस्थान
CSIR-National Institute for Interdisciplinary
Science and Technology (NIIST)
तिरुवनन्तपुरम / Thiruvananthapuram-695 019.

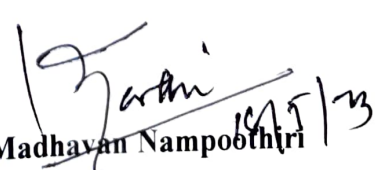
STATEMENTS OF ACADEMIC INTEGRITY

I **Lekshmi Sundar M S**, a Ph.D. student of the Academy of Scientific and Innovative Research (AcSIR) with Registration No. **10BB17J39013** hereby undertake that, the thesis entitled “**Integrated bioprocess for conversion of xylose to xylonic acid by recombinant *Corynebacterium glutamicum***” has been prepared by me and that the document reports original work carried out by me and is free of any plagiarism in compliance with the UGC Regulations on “*Promotion of Academic Integrity and Prevention of Plagiarism in Higher Educational Institutions (2018)*” and the CSIR Guidelines for “*Ethics in Research and in Governance (2020)*”.


Lekshmi Sundar M S

Trivandrum

It is hereby certified that the work done by the student, under my/our supervision, is plagiarism-free in accordance with the UGC Regulations on “*Promotion of Academic Integrity and Prevention of Plagiarism in Higher Educational Institutions (2018)*” and the CSIR Guidelines for “*Ethics in Research and in Governance (2020)*”.


Dr. K. Madhavan Nampoothiri



डॉ. के. माधवन नम्पूतिरि, Trivandrum
Dr. K. MADHAVAN NAMPOOTHIRI, PH.D, FRS
मुख्य वैज्ञानिक एवं प्रमुख / Chief Scientist & Head
माइक्रोबियल प्रक्रिया तथा प्रौद्योगिकी प्रभाग
Microbial Processes & Technology Division
सी एस आई आर-राष्ट्रीय अंतरविषयी विज्ञान तथा प्रौद्योगिकी संस्थान
CSIR-National Institute for Interdisciplinary
Science and Technology (NIIST)
तिरुवनन्तपुरम / Thiruvananthapuram-695 019.

DECLARATION

I, **Lekshmi Sundar M S**, bearing AcSIR Registration No. **10BB17J39013** declare:

- (a) that the plagiarism detection software is currently not available at my work-place institute.
- (b) that my thesis entitled, “**Integrated bioprocess for conversion of xylose to xylonic acid by recombinant *Corynebacterium glutamicum***” is plagiarism free in accordance with the UGC Regulations on “*Promotion of Academic Integrity and Prevention of Plagiarism in Higher Educational Institutions (2018)*” and the CSIR Guidelines for “*Ethics in Research and in Governance (2020)*”.
- (c) that I would be solely held responsible if any plagiarized content in my thesis is detected, which is violative of the UGC regulations 2018.


18/5/23
Lekshmi Sundar M S

Trivandrum

**Dedicated to my Family and
Friends**

ACKNOWLEDGEMENTS

I wish to offer my thanks first and foremost to my research supervisor Dr. K. Madhavan Nampoothiri for introducing me to this area of current interest and to many facets of bioprocess technology. I will be eternally grateful to him for his unwavering support and compassion over the years, as well as the time, supervision, knowledge, and resources he offered to help me to finish my studies.

It is my privilege to place on record my gratitude to Dr. C. Anandharamakrishnan, Director, CSIR-NIIST and Dr. A. Ajayaghosh, former Director, Dr. Rajeev K Sukumaran, former HOD, MPTD for providing all the necessary facilities in the Institute for my research work.

I would like to extend my warm regards and thanks to Dr. Binod Parameshwaran (DAC member), Dr. M. Arumugam (DAC member) and Dr. Dilip Kumar (DAC member) for the constant support and comments on my research.

I am thankful to Dr. Karunakaran Venugopal, Dr. Suresh C. H, and Dr. Laxmi Varma for their warm support as the AcSIR coordinators. I am grateful to the Academy of Scientific and Innovative Research (AcSIR), Ghaziabad, India for allowing my enrolment for the PhD program.

My sincere thanks to Prof. Dr. Volker F. Wendisch, Chair, Genetics of Prokaryotes, Center for Biotechnology, Bielefeld University, Bielefeld, Germany for his help during my course of research as my supervisor had a bilateral exchange project, Indo German program with him.

I acknowledge the technical help from other divisions (CSTD and MSTD) to carry out NMR, TGA and XRD analysis as part of my PhD work.

I am grateful to Dr. Krishna Kumar, ETD for his guidelines for the completion of CSIR 800 project, as part of the course work.

I would like to acknowledge the financial support from CSIR (JRF and SRF), Delhi in the form of fellowship, contingency and travel allowance for my PhD work.

I am thankful to Dr. Ramesh Kumar for his persistent help in sequencing facility. I would like to thank Er. Kiran kumar, Dr. Leena Devendra, Dr. Sindhu, for their immense support and ideas that helped me to carry out my work.

My special thanks to Dr. Susmitha A and Ms. Soumya M P for their ever willing help, encouragement, emotional support and inspiration.

I am thankful to Dr. Rajesh R.O, Dr. Hazeena S.H, Dr. Godan, Mr. Anoop, Mr Adarsh V P, Mr. Dileep, Ms. Athulya and Mr. Vijin for helping throughout my research. I sincerely thank my seniors of our group Dr. Kiran S Dhar, Dr. Nishanth Gopalan, Dr. Vivek, Dr. Dhanya for their advices during my tenure.

Words are inadequate in offering thanks to my lab mates Devi Rajan, Keerthi Sasikumar, Arun P M, Anandhu Suresh, Amrutha, Shehabaz Chekath, Reeba Parameshwaran, Anaswara P A, Vipin Krishnan, Sruthi C R, Taniya M S, Eveline Maria, Suryalekshmi V A, Sreelekshmi, Aswathy A, Gayathri G S. Kirti K, Sunitha Kumari, Lakshmi M, Alphy Maria Paul, Billu Abraham for their ever willing help and encouragement. I cherish the moments spent with all my friends in the division for the unforgettable lighter moments in the lab.

I extend my sincere thanks to Mr. Sivankutty, and Ms. Sasikala for the help rendered. I am very thankful to all the members of “Team Biotech”, old friends and resident friends for creating a unique, friendly and healthy working environment.

I take this opportunity to express my gratitude towards the scientists, technical and non-technical staff and friends for their immense help and support during my entire career in NIIST.

I owe a deep sense of gratitude to my mother, father, brother, husband, family members and teachers for their prayers, constant love, emotional support and inspiration.

Last but not least, I firmly hold that the Almighty have blessed me and enabled me to complete the book without any hindrance.

Thank you

Lekshmi Sundar M S

CONTENTS

LIST OF ABBREVIATIONS	ix
LIST OF FIGURES	xiv
LIST OF TABLES	xix

Chapter 1	Introduction and review of literature	1-28
1.1.	Introduction	2
1.2.	<i>Objectives of the study</i>	4
1.3.	Review of literature	6
1.3.1.	<i>Biomass as a raw material for value-added chemicals</i>	6
1.3.2.	<i>Composition analysis of biomass</i>	6
1.3.3.	<i>Pre-treatment of biomass</i>	7
1.3.3.1.	<i>Methods of pre-treatment</i>	7
1.3.3.1.a.	<i>Dilute acid</i>	9
1.3.3.1.b.	<i>Mild-alkali</i>	10
1.3.4.	Sugar acid	11
1.3.4.1.	<i>Xylonic acid</i>	11
1.3.4.2.	<i>Xylonic acid importance</i>	12
1.3.4.3.	<i>Native producers of xylonic acid</i>	13
1.3.4.4.	<i>Xylonic acid biosynthetic pathway</i>	15
1.3.4.5.	<i>Genetically modified strains for xylonic acid production</i>	17
1.3.4.6.	<i>Improvised bioprocesses for xylonic acid</i>	22
1.3.4.7.	<i>Bioconversion using immobilized biocatalyst</i>	22

1.3.4.8.	<i>Xylonic acid recovery and purification</i>	23
1.3.4.9.	<i>Non biological processes for xylonic acid synthesis</i>	23
1.3.4.10.	<i>Technology players for xylonic acid</i>	26
1.4.	Summary	27

Chapter 2	Materials and methods	29-48
------------------	------------------------------	--------------

2.1.	Introduction	30
2.2.	General materials	30
2.2.1.	<i>Microbial strains and plasmids</i>	30
2.2.2.	<i>Chemicals, reagents and kits</i>	31
2.3	General microbiology methods	32
2.3.1	<i>Microorganisms and their maintenance</i>	32
2.3.2	<i>Biomass determination</i>	32
2.3.3	<i>Cell density</i>	33
2.3.4	<i>Inoculum preparation</i>	33
2.3.5	<i>Fermentation</i>	33
2.3.6	<i>Preparation of Acid Pre-treated Liquor (APL)</i>	33
2.4	Analytical methods	34
2.4.1	<i>Estimation of Protein</i>	34
2.4.1.1	<i>Bradford Assay</i>	34
2.4.1.1.a	<i>Reagents</i>	34
2.4.1.1.b	<i>Procedure</i>	35
2.4.2	<i>Nucleic acids</i>	35
2.4.3	<i>HPLC Analysis of Sugars</i>	36

2.4.4	<i>HPLC analysis of Xylonic acid</i>	36
2.4.5	<i>HPLC analysis of Inhibitors</i>	37
2.5	Molecular biology methods	38
2.5.1	<i>Isolation of Genomic DNA</i>	38
2.5.2	<i>Isolation of Plasmid DNA</i>	39
2.5.3	<i>Polymerase Chain Reaction (PCR)</i>	41
2.5.4	<i>Sequencing of DNA</i>	42
2.5.5	<i>Restriction Digestion</i>	42
2.5.6	<i>Ligation</i>	43
2.5.7	<i>Preparation of competent cells and transformation</i>	43
2.5.7.1	<i>Competent cell preparation of E. coli (DH5α and BL21(DE3))</i>	43
2.5.7.2	<i>Transformation into competent cells of E. coli</i>	44
2.5.7.3	<i>Preparation of Electro competent cells of C. glutamicum</i>	44
2.5.7.4	<i>Electroporation and transformation into C. glutamicum</i>	45
2.5.8	<i>Agarose Gel Electrophoresis</i>	45
2.5.9	<i>Purification of xylose dehydrogenase enzyme</i>	46
2.5.10	<i>Poly Acrylamide Gel Electrophoresis (PAGE)</i>	46
2.6	Online tools and Softwares	47
2.7	Summary	48

Chapter 3	Metabolic engineering of <i>Corynebacterium glutamicum</i> for xylonic acid production from xylose	49-67
3.1	Introduction	50
3.2	Materials and Methods	51
3.2.1	<i>Microbial strains and culture conditions</i>	51
3.2.2	<i>Isolation and identification of pentose transporter (araE) gene from C. glutamicum ATCC 31831</i>	52
3.2.3	<i>Isolation of xylose dehydrogenase (xylB) and xylonolactonase (xylC) genes from xylose inducible xylXABCD operon</i>	53
3.2.4	<i>Cloning of xylB, xylC and xylBC genes into E. coli – C. glutamicum shuttle vector, pVWEx1, and transformation into C. glutamicum competent cells</i>	55
3.3.	Results	56
3.3.1	<i>E. coli – C. glutamicum shuttle vector</i>	56
3.3.2	<i>Amplification of araE gene from C. glutamicum ATCC 31831 and sequence confirmation</i>	57
3.3.3	<i>Isolation of genes from xylose operon of Caulobacter crescentus</i>	59
3.3.4	<i>Construction of pVWEx1-xylB, pVWEx1-xylC and pVWEx1-xylBC plasmid</i>	62
3.4	Discussion	65
3.5	Summary	66
Chapter 4	Production of xylonic acid by recombinant <i>Corynebacterium glutamicum</i> ATCC 31831 using synthetic medium	68-87
4.1	Introduction	69
4.2	Materials and methods	69
4.2.1	<i>Microbial strains and culture conditions</i>	69
4.2.2	<i>Comparative growth analysis of C. glutamicum ATCC 31831 and recombinant C. glutamicum ATCC 31831 (C. glu-xylB) in CGXII</i>	70

	<i>medium with xylose as carbon source</i>	
4.2.3	<i>Comparative growth analysis of C. glutamicum ATCC 31831 and recombinant C. glutamicum ATCC 31831 (C. glu-xyIB) strain in CGXII medium containing xylose and glucose mixture as carbon source</i>	70
4.2.4	<i>Screening of recombinant strains of C. glutamicum under different combinations of glucose and xylose for xylonic acid production</i>	70
4.2.5	<i>Medium engineering by response surface methodology (RSM) for xylonic acid production</i>	71
4.2.6	<i>Batch fermentation for xylonic acid production in 2.5 L fermentor</i>	72
4.3	Results	73
4.3.1	<i>Growth analysis of C. glutamicum ATCC 31831 and recombinant C. glu-xyIB (ATCC 31831) in CGXII medium with xylose as carbon source</i>	73
4.3.2	<i>Growth analysis of C. glutamicum ATCC 31831 and recombinant C. glu-xyIB (ATCC 31831) in CGXII medium containing xylose and glucose mixture as carbon source</i>	73
4.3.3	<i>Xylonic acid production by recombinant strains of C. glutamicum under different combinations of glucose and xylose</i>	74
4.3.4	<i>Expression analysis of xylose dehydrogenase (xyIB) gene</i>	77
4.3.5	<i>Role of araE pentose transporter for enhanced uptake of xylose and xylonic acid production</i>	78
4.3.6	<i>Statistical optimization of operational parameters for xylonic acid production</i>	79
4.3.7	<i>Xylonic acid production by batch fermentation in 2.5 L fermenter</i>	83
4.4	Discussion	84
4.5	Summary	87
Chapter 5	Scrutiny of different biomasses as raw material for the fermentative production of xylonic acid using recombinant <i>Corynebacterium glutamicum</i> ATCC 31831	88-109
5.1	Introduction	89

5.2	Materials and methods	90
5.2.1	<i>Raw material selection</i>	90
5.2.2	<i>Dilute acid pre-treatment of biomass</i>	91
5.2.3	<i>Compositional analysis of biomass</i>	91
5.2.4	<i>SEM analysis</i>	92
5.2.5	<i>Detoxification of pentose rich sawdust liquor</i>	92
5.2.6	<i>Fermentation</i>	93
5.2.7	<i>Influence of furan inhibitors on cell growth, xylose utilization and xylonic acid production</i>	93
5.3	Results	94
5.3.1	<i>Pre-treatment and composition analysis of biomass</i>	94
5.3.2	<i>Comparative study of xylonic acid production in acid pre-treated liquor (APL) of rice straw, wheat bran and sawdust</i>	96
5.3.3	<i>SEM analysis of sawdust</i>	98
5.3.4	<i>Detoxification of APL using INDION PA 500 adsorbent resin</i>	99
5.3.5	<i>Optimization of process parameters for xylonic acid production from APL of sawdust in 2.5L fermenter</i>	101
5.3.6	<i>The effect of HMF and furfural on xylonic acid fermentation</i>	103
5.4	Discussion	105
5.5	Summary	109

Chapter 6	Recovery, purification, and characterization of xylonic acid	110-126
------------------	---	----------------

6.1	Introduction	111
6.2	Materials and methods	112
	<i>Clarification of fermented broth</i>	112
6.2.1		

6.2.2	<i>Decolourization of clarified broth by activated charcoal</i>	113
6.2.3	<i>Crystallization of xylonic acid</i>	114
6.2.4	<i>Characterization of xylonic acid</i>	115
6.2.5	<i>Antibacterial property of xylonic acid</i>	116
6.3	Results	116
6.3.1	<i>Clarification</i>	116
6.3.2	<i>Decolourization</i>	117
6.3.3	<i>Xylonic acid recovery and purification</i>	118
6.3.4	<i>LC-MS, NMR, FTIR and HPLC characterization of xylonic acid crystal</i>	120
6.3.5	<i>Xylonic acid and antibacterial activity</i>	123
6.4	Discussion	123
6.5	Summary	126

Chapter 7	Bioconversion of xylose to xylonic acid by xylose dehydrogenase immobilized on ferromagnetic nanoparticles	127-147
------------------	---	----------------

7.1	Introduction	128
7.2	Materials and methods	129
7.2.1	<i>Heterologous expression and purification of xylose dehydrogenase of <i>Caulobacter crescentus</i></i>	129
7.2.2	<i>Determination of xylose dehydrogenase activity and bioconversion of xylose to xylonic acid</i>	131
7.2.3	<i>Immobilization of xylose dehydrogenase on magnetic nanoparticles</i>	131
7.2.4	<i>Optimization of immobilization conditions by statistical tool</i>	132
7.2.5	<i>Enzyme kinetics of xylose dehydrogenase</i>	133
7.2.6	<i>Validation of enzyme immobilization by FTIR and XRD</i>	133

7.2.7	<i>Reusability of immobilized xylose dehydrogenase</i>	134
7.3	Results	134
7.3.1	<i>Expression and purification of xylose dehydrogenase</i>	134
7.3.2	<i>Xylose dehydrogenase immobilization on magnetic nanoparticles</i>	135
7.3.3	<i>Optimization of the parameters for xylose conversion to xylonic acid</i>	136
7.3.4	<i>Enzyme kinetics of free and immobilized xylose dehydrogenase</i>	140
7.3.5	<i>Structural characterization of ferro-magnetic nano-particles and immobilized xylose dehydrogenase</i>	141
7.3.6	<i>Bioconversion of xylose into xylonic acid by immobilized xylose dehydrogenase under optimized parameters</i>	143
7.3.7	<i>Reusability of immobilized biocatalyst</i>	145
7.4	Discussion	145
7.5	Summary	147

Chapter 8	Summary and Conclusion	148-154
------------------	-------------------------------	----------------

Bibliography	155-178
---------------------	----------------

<i>ANNEXURE I- List of Instruments</i>	179
--	-----

<i>ANNEXURE II- Media Composition</i>	181
---------------------------------------	-----

<i>ANNEXURE III- Vector Details and Sequence</i>	184
--	-----

<i>ANNEXURE IV- AcSIR Course Work</i>	190
---------------------------------------	-----

Abstract of the Thesis	191
-------------------------------	------------

List of Publications	192
-----------------------------	------------

LIST OF ABBREVIATIONS

AD	Aldolase
ALD	Alcohol dehydrogenase
%	Percentage
°C	Degree celsius
μF	Micro farad
μg	Microgram
μgmL ⁻¹	Microgram per millilitre
μL	Microlitre
μm	Micromole
μmolmin ⁻¹	Micromole per minute
AGE	Agarose gel electrophoresis
ANOVA	Analysis of variance
APL	Acid pre-treated liquor
APS	Ammonium Persulfate
APTES	(3-Aminopropyl)triethoxysilane
ATCC	American type culture collection
ATP	Adenosine tri phosphate
AuNPs	Gold nanoparticles
BBD	Box Behnken design
BHI	Brain heart infusion
Bi ₂ S ₃	Bismuth sulfide
BLAST	Basic local alignment search tool
bp	Base pair
BSA	Bovine serum albumin
C ₅ H ₁₀ O ₆	Xylonic acid
CaCl ₂	Calcium Chloride
CaCO ₃	Calcium carbonate
CHF	Cascade hydrolysis and fermentation

COOH	Carboxyl group
CTAB	Cetyltrimethylammonium bromide
D ₂ O	Deuterium oxide
dATP	Deoxyadenosine triphosphate
dCTP	Deoxycytidine triphosphate
DCW	Dry cell weight
dGTP	Deoxyguanosine triphosphate
DMSO	Dimethyl sulfoxide
dNTP	Deoxynucleoside triphosphates
DO	Dissolved oxygen
dTTP	Deoxythymidine triphosphate
EDTA	Ethylenediaminetetraacetic acid
EtBr	Ethidium bromide
FDA	Food and drug administration
FP	Forward primer
FTIR	Fourier transmission infrared
g	Gravity
gg ⁻¹	Gram per gram
gL ⁻¹	Gram per litre
gL ⁻¹ h ⁻¹	Gram per litre per hour
GRAS	Generally regarded as safe
h	Hour
H ₂ O ₂	Hydrogen peroxide
H ₂ SO ₄	Sulphuric acid
HCl	Hydrochloric acid
HMF	Hydroxy methyl furfural
HPLC	High performance liquid chromatography
HT	Hydrotalcite
IPTG	Isopropyl β-D-1-thiogalactopyranoside
Kan	Kanamycin
Kan ^r	Kanamycin resistant

kb	Kilo base
kcat	Turnover number
KCl	Potassium chloride
kDa	Kilodalton
kV	Kilovolt
L	Litre
LB	Luria Bertani
LBHIS	Luria Bertani – Brain heart infusion – sorbitol medium
LCMS	Liquid chromatography – mass spectrometry
M	Molar
MCS	Multiple cloning site
mg	Milli gram
MgCl ₂	Magnesium chloride
mgmL ⁻¹	Milligram per millilitre
MgSO ₄ .7H ₂ O	Magnesium sulphate
MHA	Mueller Hinton agar
MIC	Minimum inhibitory concentration
mL	Millilitre
mM	Milli molar
mm	Millimeter
mM	Millimolar
MnSO ₄ .H ₂ O	Manganese sulphate
molL ⁻¹	Mole per litre
MOPS	3-(N-morpholino) propanesulfonic acid
MTCC	Microbial type culture collection
N	Normality
Na ₂ CO ₃	Sodium carbonate
Na ₃ PO ₄	Trisodium phosphate
NaCl	Sodium chloride
NAD	Nicotinamide adenine dinucleotide
NAD(P) ⁺	Nicotinamide adenine dinucleotide phosphate

NADP	Nicotinamide adenine dinucleotide phosphate
NaOH	Sodium hydroxide
NCBI	National Center for Biotechnology Information
NEB	New England Biolabs
NiCl ₂ .6H ₂ O	Nickel chloride
nm	Nanometer
NMR	Nuclear magnetic resonance
NREL	National renewable energy laboratory
OD	Optical density
Ori	Origin of replication
PAGE	Poly acrylamide gel electrophoresis
PCR	Polymerase chain reaction
Pd	Palladium
PDA	Photodiode array detector
PEG	Polyethylene glycol
pH	Potential of Hydrogen
pI	Isoelectric point
ppm	Parts per million
PPP	Pentose phosphate pathway
Pt	Platinum
p-value	Probability value
RI	Refractive index
RID	Refractive index detection
RP	Reverse primer
rpm	Revolutions per minute
RSM	Response surface methodology
RT	Room temperature
SDS	Sodium dodecyl sulphate
SEM	Scanning electron microscope
SHF	Separate hydrolysis and fermentation
SSF	Solid state fermentation

TCA	Tri carboxylic acid
TE	Tris-EDTA
TEMED	Tetramethylethylenediamine
Ti ₃ C ₂	Titanium carbide
TSS	Transformation and storage solution
UV	Ultra violet
v _v ⁻¹	Volume per volume
v _m	Vessel volume per minute
WT	Wild type
w _v ⁻¹	Weight per volume
w _w ⁻¹	Weight per weight
XA	Xyloic acid
XD	Xylonate dehydratase
XDH	Xylose dehydrogenase
XI	Xylose isomerase
XL	Xylonolactonase
XRD	X-ray diffraction
<i>xylB</i>	Xylose dehydrogenase
<i>xylC</i>	Xylonolactonase
ZnS	Zinc sulfide
ZnSO ₄ .7H ₂ O	Zinc sulphate
Ω	Ohms

LIST OF FIGURES

1.1	Schematic presentation of the overall work	5
1.2	Schematic structure of lignocellulose	7
1.3	Overview of different pre-treatment process	8
1.4	Chemical structure of xylonic acid	12
1.5	Xylose oxidative pathway for xylonic acid biosynthesis	16
2.1	Standard graph for Bradford assay	35
2.2	Standard graph of xylonic acid	37
3.1.a	pVWEx1 vector map	56
3.1.b	Restriction digestion confirmation of pVWEx1 digested with restriction enzymes EcoRI and Sall.	57
3.2	Gel picture showing the amplification of <i>araE</i> gene from genomic DNA of <i>C. glutamicum</i> ATCC 31831	58
3.3	The nucleotide sequence of <i>araE</i> gene isolated from <i>C. glutamicum</i> ATCC 31831	58
3.4	NCBI-BLAST analysis of <i>araE</i> gene sequence from <i>C. glutamicum</i> ATCC 31831	59
3.5	Graphical representation of <i>Caulobacter crescentus</i> xylose inducible <i>xylXABCD</i> operon	59
3.6	Gel picture showing the amplification of <i>xylB</i> , <i>xylC</i> and <i>xylBC</i> genes	60
3.7	The nucleotide sequence of <i>xylB</i> gene isolated from <i>xylXABCD</i> operon of <i>Caulobacter crescentus</i>	60
3.8	NCBI-BLAST analysis of <i>xylB</i> gene sequence from <i>Caulobacter crescentus</i>	61
3.9	The nucleotide sequence of <i>xylC</i> gene isolated from <i>xylXABCD</i> operon of <i>Caulobacter crescentus</i>	61
3.10	NCBI-BLAST analysis of <i>xylC</i> gene sequence from <i>Caulobacter crescentus</i>	61
3.11	Vector map of pVWEx1 derivatives (A) pVWEx1- <i>xylB</i> ; (B) pVWEx1- <i>xylC</i> and (C) pVWEx1- <i>xylBC</i>	62
3.12	Transformed colonies of <i>C. glutamicum</i> 31831 with (A) pVWEx1(control vector)	63

	(B) pVWEx1- <i>xylB</i> , (C) pVWEx1- <i>xylC</i> and (D) pVWEx1- <i>xylBC</i>	
3.13	Gel picture showing restriction digestion mapping of pVWEx1 recombinant plasmids containing <i>xylB</i> , <i>xylC</i> and <i>xylBC</i> genes in <i>C. glutamicum</i> ATCC 31831	64
3.14	Transformed colonies of <i>C. glutamicum</i> 13032 with (A) pVWEx1 (control vector), (B) pVWEx1- <i>xylB</i> , (C) pVWEx1- <i>xylC</i> and (D) pVWEx1- <i>xylBC</i>	64
3.15	Gel picture showing restriction digestion mapping of pVWEx1 recombinant plasmids containing <i>xylB</i> , <i>xylC</i> and <i>xylBC</i> genes in <i>C. glutamicum</i> ATCC 13032	65
4.1	Comparative growth analysis of <i>C. glutamicum</i> and recombinant <i>C. glutamicum</i> (<i>C. glu-xylB</i>) in CGXII medium containing 4% xylose as carbon source	73
4.2	Comparative growth analysis and sugar consumption by <i>C. glutamicum</i> ATCC 31831 and recombinant <i>C. glutamicum</i> ATCC 31831 (<i>C. glu-xylB</i>) in CGXII medium containing 1% glucose and 3% xylose as carbon source	74
4.3	Xylonic acid production by recombinant strains of <i>C. glutamicum</i> ATCC 31831 under different combinations of glucose (G) and xylose (X)	75
4.4	Xylonic acid production and sugar (xylose and glucose) utilization by recombinant strains of <i>C. glutamicum</i> ATCC 31831 under 0.5% glucose and 3.5% xylose	77
4.5	SDS-PAGE showing protein expression of xylose dehydrogenase enzyme of recombinant <i>C. glutamicum</i> (<i>C. glu-xylB</i>)	78
4.6	Xylonic acid production by <i>C. glu-xylB</i> ATCC 31831 (A) and <i>C. glu-xylB</i> ATCC 13032 (B)	79
4.7	Xylonic acid production by recombinant <i>C. glu-xylB</i> under optimized CGXII medium	80
4.8	Contour plots showing the effect of various parameters on xylonic acid production by <i>C. glu-xylB</i> (ATCC 31831)	81
4.9	Validation plot for xylonic acid production	83
4.10	Xylonic acid production and sugar consumption by recombinant <i>C. glu-xylB</i> in 2.5L fermenter	84
5.1	Different agro-industrial biomasses (A) Rice straw, (B) Wheat bran and (C) Sawdust	91

5.2	Composition analysis of rice straw, sawdust and wheat bran	94
5.3	Release of sugar (A), inhibitors (B) after the acid pre-treatment of biomass	95
5.4	Xylose utilization and xylonic acid production by <i>C. glu-xytB</i> in non-detoxified (A) rice straw, (B) wheat bran and (C) saw dust APL	97
5.5	SEM image of (A) raw sawdust (control) (B) acid pre-treated sawdust	98
5.6	Inhibitor (acetic acid, formic acid, furfural and HMF) removal by INDION PA 500 resin	100
5.7 A	HPLC chromatogram of non-detoxified sawdust APL	100
5.7 B	HPLC chromatogram of detoxified sawdust APL	101
5.7 C	Appearance of sawdust APL (a) before and (b) after treatment with INDION PA 500 resin	101
5.8	2.5L batch fermentation using recombinant <i>C. glu-xytB</i> in CGXII- sawdust APL production medium	103
5.9 A	Effect of furfural on xylose consumption and xylonic acid production	104
5.9 B	Effect of HMF on xylose consumption and xylonic acid production	105
6.1	Xylonic acid crystals obtained from CGXII synthetic medium (A) and sawdust APL-CGXII production medium (B)	119
6.2	Fluorescent image of (A) standard xylonic acid (B) xylonic acid crystal recovered from CGXII synthetic medium (C) xylonic acid crystal recovered from sawdust APL-CGXII medium	119
6.3	LCMS/MS spectrum of (A) standard xylonic acid (B) purified xylonic acid crystal	120
6.4	¹ H and ¹³ C NMR of (A) standard xylonic acid (B) purified xylonic acid crystal	121
6.5	FTIR spectrum of standard xylonic acid and purified xylonic acid crystal	122
6.6	HPLC chromatogram of (A) xylonic acid standard (B) purified xylonic acid crystal	122
6.7	Antimicrobial effect of xylonic acid against (a) <i>Staphylococcus aureus</i> MTCC 96, (b) <i>Escherichia coli</i> MTCC 443 and (c) <i>Salmonella enterica</i> MTCC 3224	123

7.1	Functionalization of ferromagnetic nanoparticles with APTES and glutaraldehyde for xylose dehydrogenase immobilization.	132
7.2	Expression of recombinant xylose dehydrogenase	135
7.3	Contour plot showing the effect of various parameters on bioconversion of xylose into xylonic acid by immobilized xylose dehydrogenase.	139
7.4	Lineweaver-Burk plots of free (A) and immobilized (B) xylose dehydrogenase.	140
7.5	FTIR data of individual peaks of Fe ₃ O ₄ iron particle, APTES – Glutaraldehyde modification and xylose dehydrogenase binding (A). Fe ₃ O ₄ magnetic nanoparticle with immobilized xylose dehydrogenase (B).	142
7.6	X-Ray Diffraction (XRD) pattern of magnetic nanoparticles (Fe ₃ O ₄)	143
7.7	Bioconversion of xylose into xylonic acid by immobilized xylose dehydrogenase	144
7.8	HPLC chromatogram of xylonic acid formation from xylose in the presence of immobilized xylose dehydrogenase	144
7.9	Operational stability of immobilized xylose dehydrogenase	145
8.1	Schematic representation of bioprocess for xylonic acid production from lignocellulosic biomass (sawdust APL)	152

LIST OF TABLES

1.1	Native strains reported for xylonic acid production	14
1.2	Genetically modified strains reported for xylonic acid production	21
2.1	Microbial strains and plasmids used in the study	30
2.2	Softwares used and its applications	47
3.1	Microbial strains and plasmid used in the study	51
3.2	Oligonucleotides for the amplification of <i>araE</i> , <i>xylB</i> , <i>xylC</i> and <i>xylBC</i> genes	53
3.3	PCR conditions for the amplification of <i>araE</i> , <i>xylB</i> , <i>xylC</i> and <i>xylBC</i> genes	54
4.1	Box-Behnken experimental design matrix with experimental values of xylonic acid production by <i>Corynebacterium glutamicum</i> ATCC 31831	72
4.2	Analysis of variance (ANOVA) for xylonic acid production using <i>C. glu-xylB</i>	82
5.1	Physio-chemical properties of sawdust liquor	98
5.2	Process parameters for xylonic acid production under submerged fermentation in 2.5L fermenter	102
6.1	Effects of various parameters on decolourization efficiency of fermented broth	117
6.2	Xylonic acid recovery yield from CGXII synthetic medium and sawdust APL-CGXII medium	118
7.1	Bacterial strains, vectors and primers used in the study	130
7.2	Optimization of xylose dehydrogenase binding on magnetic nanoparticles	136
7.3	Box–Behnken design matrix with response xylonic acid bioconversion by immobilized xylose dehydrogenase	136
7.4	ANOVA for xylonic acid production using immobilized xylose dehydrogenase	138
7.5	Kinetic constants of free and immobilized xylose dehydrogenase	141

Chapter 1

Introduction and review of literature

1.1. Introduction

The modern trend in bioprocessing focus on the use of advanced technologies such as synthetic biology, metabolic engineering, and systems biology to improve the efficiency and scalability of bioprocesses for the production of different products such as biofuels, biochemicals and pharmaceuticals. The single-use technologies improve the speed and flexibility of bioprocesses while also reducing costs and environmental impact. The concept of bio-refinery is getting more attractive because of the growing approach on using renewable energy sources and sustainable practices in bioprocessing operations. Lignocellulosic biomass is the most abundant renewable feedstock composed of cellulose (35% - 50%), hemicellulose (20% - 35%), and lignin (10% - 25%). Value addition of the biomass can be achieved through various processes such as converting it into biofuels, chemicals, or other materials. These processes can be done through chemical, physical or biological methodologies such as fermentation, pyrolysis, and gasification (Osman et al. 2021). But the biological conversion of lignocellulosic biomass into biofuels and platform chemicals can provide an alternative to fossil fuels, as well as to diversify the use of these resources increasing their economic value (Garba and Garba 2020).

Biomass holds an inexhaustible, far, wide and low-cost wellspring of sugars that can be used as renewable carbon source for the manufacture of synthetic compounds. Different horticultural build-ups contain around 20 - 30% hemicellulose (Iqbal et al., 2011). The second most prevalent sugar in these hydrolysates is D-xylose (30 - 40%), an important bio-resource for diverse chemicals and added value products (Dhiman et al., 2012; Lachke, 2002; Moyses et al., 2016). Thus, plant biomass has the potential to be utilised as renewable source for a variety of fuels and chemicals. The conversion of xylose to ethanol has been the focus of much of these investigations (Mohd Azhar et al., 2017). However, several recent studies have demonstrated that

bacteria can convert this pentose sugar to other valuable chemicals (Kwak et al., 2017). Both indigenous or engineered microorganisms were reported in literature capable of producing variety of chemicals (1,3-PDO, lactic acid, levulinic acid, 3-hydroxypropionic acid, 3-hydroxypropionaldehyde etc.) from biomass derived sugars (Isikgor and Remzi Becer 2015; Takkellapati et al. 2018).

Xylose derived sugar acid *i.e.*, xylonic acid ($C_5H_{10}O_6$) have gained much attention in the last decade and is still a thriving area of research (Kumar et al., 2018). Researchers contribute dedicated piece of works related to different pre-treatment strategies, strain improvement, advanced fermentation strategies to enhance the titer of xylonic acid (Ghaffar et al., 2017; Sapcı et al., 2016; Takata et al., 2014). The gradual switching from C6 sugars to under utilized C5 sugars of biomass is an important twist in the rapid growth of the alternate carbon source utilization in white biotechnology.

C5 sugar utilization presents several challenges due to the complex nature of the metabolic pathways involved. Very few microbes are reported for efficient C5 sugar metabolism. The breakdown of C5 sugar requires the action of several enzymes, and the low expression levels of these enzymes in microorganisms lead to inefficient metabolism of C5 carbon sources. Additionally, the presence of other sugars, such as glucose, can inhibit the uptake and utilization of C5 sugars. Therefore, optimizing microbial strains and metabolic pathways is important for efficient utilization of C5 sugars. Our group demonstrated the production of amino acids and xylitol from C5 sugars (Gopinath et al. 2011; Dhar et al. 2016). Based on this, we introduced metabolic pathway in *C. glutamicum* ATCC 31831 assimilating xylose for xylonic acid production.

1.2. Objectives of the study

- Amplification of xylose dehydrogenase (*xyl B*) and xylonolactonase (*xyl C*) genes from xylose inducible *xylXABCD* operon of *Caulobacter crescentus*
- Cloning and expression of *xyl B* and *xyl C* genes of *C. crescentus* in *C. glutamicum* ATCC 31831
- Fermentative production of xylonic acid by recombinant *C. glutamicum* using xylose from synthetic medium and from acid pre-treated liquor (APL) generated during biomass pre-treatment
- Downstream processing, purification and characterization of xylonic acid
- Bioconversion of xylose to xylonic acid by xylose dehydrogenase immobilized on ferromagnetic nanoparticles

1.2.a. Outline of the study

Given the current situation's increased importance of green energy technologies, it was worthwhile to research and expedite the prospect of far-ranging high-value chemicals generated from lignocellulosic pentose sugars. Therefore, we attempted to develop a microbial bioprocess for the production of xylonic acid which is a sugar acid and a versatile platform chemical with added value that could be integrated into a bio-refinery. It has diverse applications in the agricultural, medical, and pharmaceutical industries (Jin et al. 2022; Zomara et al. 2000). It is considered by the U.S. Department of Energy to be one of the top 30 chemicals of the highest value. Xylonic acid may also be used as a precursor for bio-plastic, polymer synthesis and other chemicals like 1,2,4-butanetriol (Niu Wei et al. 2003).

It is targeted to develop a bioprocess for the production of xylonic acid from agro-industrial residues and we selected the industrial microbe *Corynebacterium glutamicum* ATCC

31831 as the microbial workhorse and engineered towards the utilization of xylose released from lignocellulose. Heterologous expression of genes, xylose dehydrogenase (*xylB*) and xylonolactonase (*xylC*) of *Caulobacter crescentus* in *C. glutamicum* ATCC 31831 enabled the efficient conversion of xylose into xylonic acid. After the screening of different biomasses like rice straw, sawdust and wheat bran, sawdust was selected as the biomass for xylonic acid production. The method developed is suitable for knowledge-based bio-process evolution, which cuts down on experimental time and costs, and is easily adaptable to different strains and cultivation strategies. Fig.1.1. shows the schematic presentation of overall work.

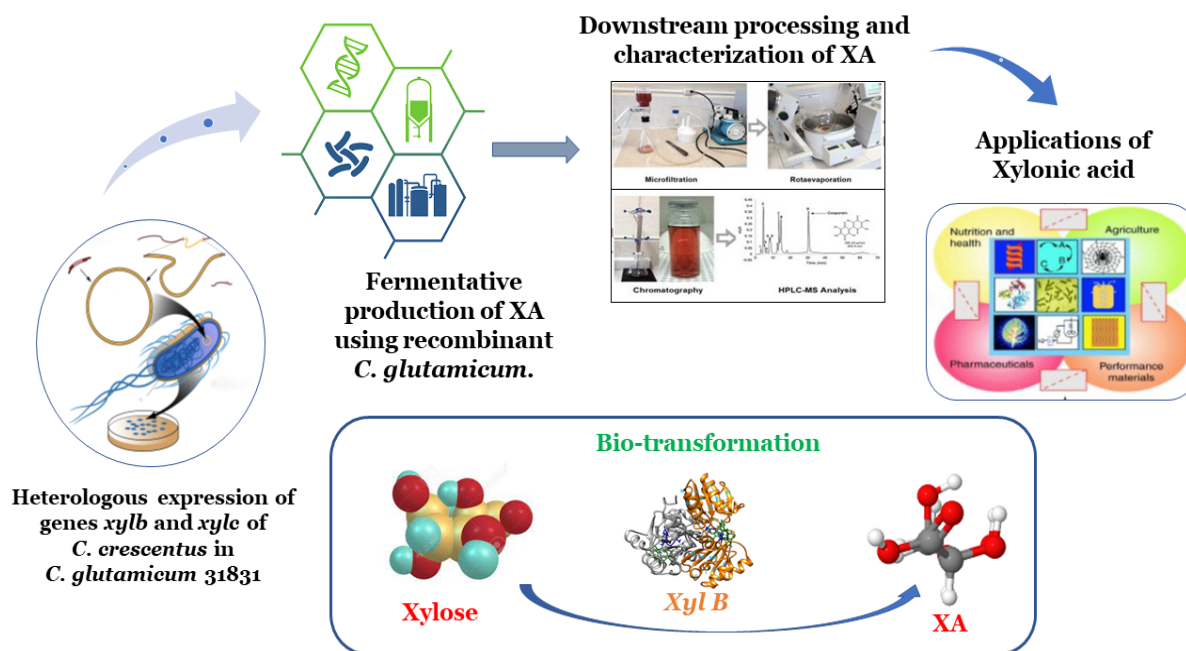


Fig.1.1. Schematic presentation of the overall work

1.2.b. Thesis layout

The thesis is framed into eight chapters, covering introduction about the work and objectives, a general methodology chapter, experimental chapters, summary and conclusion. The

working chapters deals with strain construction, xylonic acid production, process optimization, biomass utilization, downstream processing, and biotransformation using immobilized xylose dehydrogenase enzyme. Apart from that, a thorough review on the topic to find the gap areas, relevance and future prospects and bibliography is included. Separate annexures given for list of instruments, vector map and sequence and media composition.

1.3. Review of Literature

1.3.1. Biomass as a raw material for value-added chemicals

As an alternative carbon resource, biomass, a renewable, abundant, and locally accessible and carbon-neutral raw material become a natural choice. Lignocellulose is a complex carbohydrate polymer composed of cellulose, hemicellulose and an aromatic polymer lignin as well as the rich source of C6 and C5 sugars (Ruiz et al., 2013). Better exploitation of these sugars can support a diverse application in different industrial sectors like pharmaceuticals, food, cosmetics and agriculture. Sugars are primarily used as the source of energy and specifically xylose is used for the production of bio-ethanol, bio-butanol, bio-polymer, bio-hydrogen, 1,3-butanediol, 2,3-propanediol, organic acids, furfural, xylitol, single cell protein, amino acids and furans (furfural and 5-hydroxymethylfurfural: precursors for polyester, nylon, fuel, plastic, resin, fine chemicals) (de Sa' et al., 2020; Kim et al., 2017; Kudahettige-Nilsson et al., 2015; Wu et al., 2018).

1.3.2. Composition analysis of biomass

Lignocellulosic biomass is a complex abundant material that serves as an essential source of renewable energy and various bio-based products. It consists of three primary components: cellulose, hemicellulose, and lignin. Cellulose is a linear polymer of glucose and is the most

abundant component, accounting for up to 40 - 60% of the total weight of lignocellulosic biomass. Hemicellulose, on the other hand, is a branched polymer of different sugars, such as xylose, arabinose, and mannose, and accounts for about 20-35% of the total weight. Finally, lignin is a complex polymer composed of phenylpropanoid units and accounts for approximately 15-30% of the total weight (Zoghiami and Paës 2019). Fig.1.2. shows the schematic structure of lignocellulose (Baruah et al. 2018).

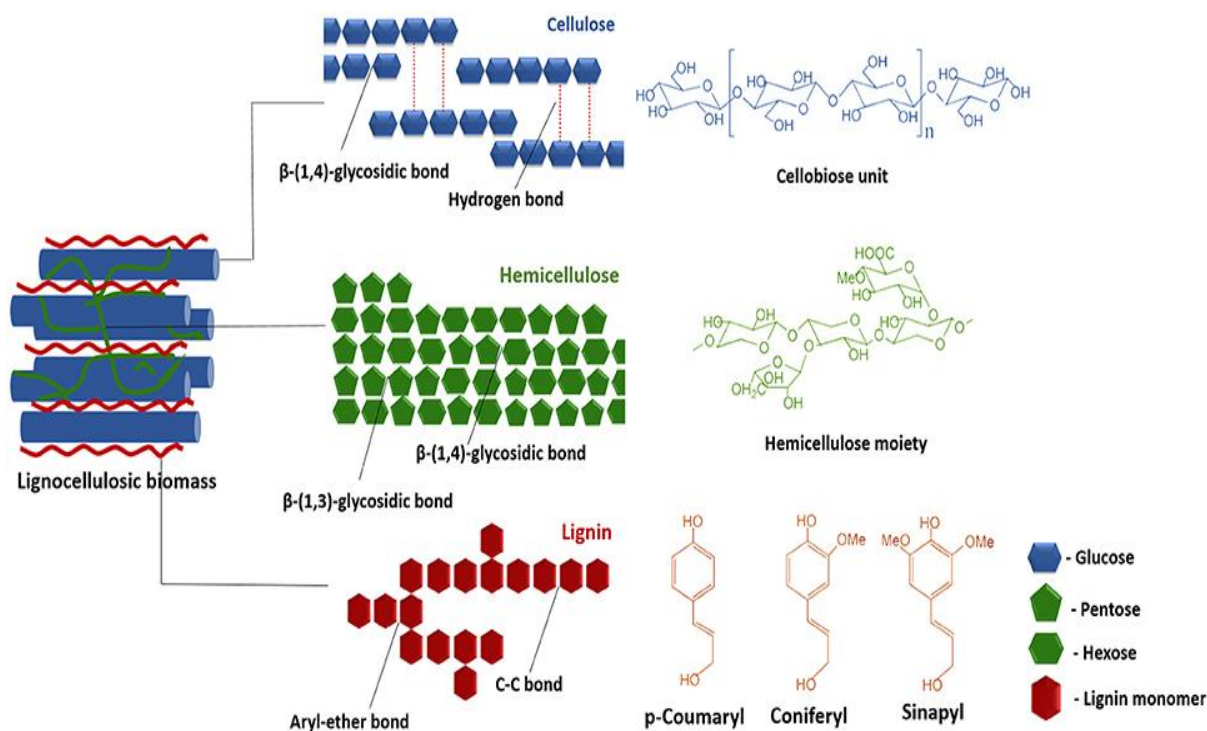


Fig.1.2. Schematic structure of lignocellulose

1.3.3. Pre-treatment of biomass

1.3.3.1. Methods of pre-treatment

The process of pre-treating lignocellulosic feedstocks is crucial in altering their structure and exposing the lignocellulosic fractions for efficient enzyme access during enzymatic hydrolysis, resulting in higher reducing sugar yields and rates (Alvira et al., 2010). The choice of

pre-treatment method and conditions depends on the type and composition of the biomass being used (Phwan et al. 2019). Fig.1.3. lists some of the most commonly used pre-treatment methods (Kumar and Sharma 2017).



Fig.1.3. Overview of different pre-treatment process

Saccharification is the prime and most important step in the processing of agricultural biomass. Chemical and enzymatic hydrolysis is the most prevalent saccharification techniques for the release and hydrolysis of polysaccharides in lignocellulosics. Chemical hydrolysis is of

two types, acid and alkali pre-treatment, where these methods used to break down the complex structure of biomass, making it more accessible for further processing, such as fermentation or enzymatic hydrolysis, to produce biofuels or other value-added products. Acid pre-treatment uses an acidic solution, such as hydrochloric acid, acetic acid and sulfuric acid to break down the lignocellulosic material, while alkali pre-treatment uses an alkaline solution, such as NaOH/KOH at high temperatures and pressures, to do the same. Both methods aim to remove lignin and open up hemicellulose and cellulose structure to make it more accessible to enzymes.

Lignocellulosic biomass pre-treatment methods can be broadly classified into two groups based on the type of treatment process employed: non-biological and biological. Non-biological methods do not involve any microbial treatments and can be divided into physical, chemical, and physico-chemical methods.

1.3.3.1.a. Dilute acid

Although acid treatment is the most frequently used traditional pre-treatment method for lignocellulosic feedstocks, it is not preferred due to the production of a significant amount of inhibitory substances such as furfurals, phenolic acids, aldehydes, and 5- hydroxymethylfurfural. Despite this, it is still the most widely used pre-treatment method on an industrial scale. Two types of acid pre-treatments are developed based on the end application. High-temperature (above 180°C) for a short duration (1–5 min) and low temperature (<120°C) for a long duration (30 - 90 min). In some cases, the acid itself hydrolyses the biomass into fermentable sugars, and the enzymatic hydrolysis step could be avoided. However, extensive washing is necessary to remove acid before fermentation of sugars (Sassner et al. 2008). Various acids have been used for the pre-treatment of different biomass, and the most commonly used acid is discussed here.

Dilute sulphuric acid H_2SO_4 is widely used in commercial acid pre-treatment, especially for switch grass, corn stover, spruce, and poplar (Kumar and Wyman 2009; Shuai et al. 2010; Digman et al. 2010; Xu et al. 2009). Pre-treating bermuda grass and rye straw with 1.5% sulphuric acid followed by diluted H_2SO_4 resulted in the generation of low levels of inhibitors and maximum sugar yield (Sun and Cheng 2005). The use of sulphuric acid for pre-treating lignocellulosic biomass is a conventional technique, primarily due to its affordability. However, acid treatment has some disadvantages, such as the production of inhibitory compounds and corrosion of the reaction vessel.

1.3.3.1.b. Mild-alkali

In contrast to acid treatment, alkali pre-treatment methods are generally performed at room temperature and pressure. Sodium hydroxide is the most commonly used alkali reagent and is the most effective (Kumar and Wyman 2009). Alkali reagents modify the structure of lignin, cause cellulose to swell and de-crystallize, and solvate hemicellulose (McIntosh and Vancov 2010; Cheng et al. 2010; Ibrahim et al. 2011). Optimization studies have been performed using sodium hydroxide, and mild alkali pre-treatment can be carried out at ambient conditions, but higher temperatures are required for longer durations (Sun et al. 1995). The only drawback of alkali treatment is its high downstream processing cost due to the large amount of water needed to remove salts from the biomass. A neutralizing step is also required to remove inhibitors and lignin.

The amount of glucose and xylose released during acid and alkali pre-treatment of lignocellulosic biomass can vary depending on various factors, such as the type of biomass, the pre-treatment conditions, and the analytical methods used to measure the released sugars.

1.3.4. Sugar acid

Sugar acids are a class of organic compounds that are derived from sugars. They are characterized by the presence of a carboxyl group (-COOH) attached to a sugar molecule. Sugar acids can be used as food additives, flavouring agents, and pH regulators. They can also be used in the production of various chemicals, such as biodegradable plastics and pharmaceuticals. Sugar acids are mainly synthesised via oxidation of corresponding mono or oligosaccharides. Both chemical and biological methods are used for sugar acid production. Aldonic, aldaric, and uronic acids are the three major class of sugar acids. The bio-refinery concept of producing biofuels and commodity chemicals from natural resource is gaining high interest due to its replacement with those produced from petroleum basis along with which sugar acids are also generating a lot of attention due to their potential as high value chemicals, and specifically as precursors of bio-plastics. Sugar acids are used as latent acid in food industry, and other application as pH regulator, sequestering agent and in pharmaceuticals (Mehtio et al., 2016). Xylose derived, sugar acid, xylonic acid generate interest as of the use of this molecule in the manufacture of synthetic polymers, including polyamides, polyesters and hydrogels. Further advancement of this xylonic acid would result in higher production volumes and thus help sustain the next generation bio refineries.

1.3.4.1. Xylonic acid

Xylonic acid, an oxidised five carbon derivative of xylose, is an excellent chemical platform with multifarious applications in the food, medicinal and agricultural fields. It is regarded as one of the top 30 highest-value chemicals by the U.S. National Renewable Energy Laboratory (NREL) and finds a number of applications in different fields as precursor for synthesis of polyamides, chelator, and as a dispersant, antibiotic, clarifying agent and health

enhancer (Byong-Wa et al. 2006; Toivari et al., 2012). The two potential routes for the synthesis of xylonic acid are chemical and biological oxidation. In chemical process xylonic acid oxidation is through a chemical catalyst (Pt/Au). In biological process biocatalysts dehydrogenase and lactonase oxidise xylose into xylonic acid. Biological oxidation is more sustainable, eco-friendly and cost-effective for industrial need compared to chemical process due to the lack of selectivity of the process (Mathews et al., 2015). Fig.1.4. shows the chemical structure of xylonic acid.

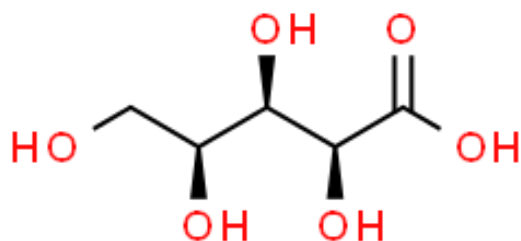


Fig.1.4. Chemical structure of xylonic acid

1.3.4.2. Xylonic acid importance

One of the three primary components of plant biomass is hemicellulose, which can be utilized to produce high value chemicals and fuels. The hemicellulose found in xylan is the source of xylose, which is the second most prevalent carbohydrate in nature as mentioned earlier. The prime requirement and crucial factor for accomplishing the high-value application of lignocellulose is the effective utilisation of xylose (Toivari et al. 2013). Through redox reaction, xylose can be transformed into a number of other compounds, such as xylonic acid (xylonate), lactic acid, formic acid, acetic acid, and xylitol (Kwak, S. and Jin, Y.S. 2017; Fehér et al. 2018). Among them, xylan hemicellulose is selectively oxidised to produce xylonic acid, which has superior biocompatibility, biodegradability, and thermal stability (Yim et al. 2017). By combining xylonic acid and viscose fibre, a fabric with a cooling effect can be produced based

on the properties of the heat absorption of xylonic acid and water. The outfits prepared are cooling and refreshing. In addition, xylonic acid functions well as both a green solvent and catalyst for the Biginelli reaction (Ma et al. 2016). Xylonic acid or its salts are being used in construction to great economic advantage, and are anticipated to take the place of the gluconic acid cement water reducer. The successful use of xylonic acid has enormous social and economic benefits and has contributed to protect the environment, which has increased desire in producing xylonic acid.

1.3.4.3. Native producers of xylonic acid

The biological conversion of pentoses to pentanoic acid is mainly attained by aerobic bacterial fermentation. At the end of the nineteenth century, microbial production of xylonic acid was recognised from pure xylose and several species like *Gluconobacter*, *Paraburkholderia*, *Pseudomonas*, *Pseudoduganella*, *Erwinia* and other microorganisms were reported to produce xylonic acid (Bondar et al., 2021; Sundar Lekshmi et al., 2019; Toivari et al., 2012). *Burkholderia sacchari* is a well-known industrial producer strain with a high capacity for incorporation into bio-refinery that uses biomass residues. The wild-type *B. sacchari* produced both xylitol and xylonic acid comparable with other high production hosts. The genetic level rewiring of its metabolic route, along with improvements in molecular modification methods and a better knowledge of metabolic fluxes through upcoming studies, will integrate its potential as a micro-production platform (Oliveira-Filho et al., 2021). Native xylonic acid producers, yield and titre reported are compiled in Table 1.1. For the production of xylonic acid with a titer near to the theoretical yield, metabolic engineering approaches based on genetic modulation were introduced recently.

Table. 1.1. Native strains reported for xylonic acid production

Species	Process	Yield (gg⁻¹)	Titer (gL⁻¹)	Volumetric productivity (gL⁻¹h⁻¹)	Reference
<i>Gluconobacter oxydans</i> ATCC 621	Batch	1.10	109	2.50	Toivari et al., 2012
<i>Gluconobacter oxydans</i> ATCC 621	Batch	1.10	107	2.20	VTT Technical research centre of Finland
<i>Gluconobacter oxydans</i> ATCC 621	Batch	1.00	41	1.00	VTT Technical research centre of Finland
<i>Gluconobacter oxydans</i> ATCC 621	Batch	-	66.42	-	Zhang et al., 2017
<i>Gluconobacter</i> <i>oxydans</i> DSM 2003	Batch	-	38.86	0.90	Zhang et al., 2016
<i>Gluconobacter</i> <i>oxydans</i> NL71	Batch	-	143.6	4.48	Dai et al., 2020
<i>Gluconobacter</i> <i>oxydans</i>	Batch	-	102.3	-	Zhou et al., 2016
<i>Gluconobacter</i> <i>oxydans</i> NL71	Batch	0.90	54.97	-	Zhu et al., 2015
<i>Gluconobacter oxydans</i> ATCC 621	Batch	1.10	51.00	1.80	VTT Technical research centre of Finland
<i>Gluconobacter oxydans</i> NL71	Batch	0.98	586.30	4.69	Zhou et al., 2015
<i>Gluconobacter oxydans</i>	Batch	-	329	6.70	Zhou et al., 2019
<i>Enterobacter cloacae</i>	Batch	~ 1.00	190	~ 1.00	Ishizaki et al., 1973
<i>Pseudomonas fragi</i> ATCC 4973	Batch	1.10	162	1.40	Buchert and Viikari 1988

<i>Pichia kudriavzevii</i>	Fed-Batch	1.00	171	1.40	Toivari et al., 2013
<i>Klebsiella pneumoniae</i>	Fed-Batch	1.11	103	1.30	Wang et al., 2016
<i>Paraburkholderia sacchari</i>	Fed-Batch	1.11	390	6.41	Bondar et al., 2021
<i>Pseudoduganella danionis</i>	Batch	0.65	6.5	0.54	Sundar Lekshmi et al., 2019

1.3.4.4. Xylonic acid biosynthetic pathway

The oxidative pathway for xylonic biosynthesis is divided into two routes: The Weimberg pathway and the Dahms pathway (Fig.1.5.). Native bacteria such as *Gluconobacter oxydans*, *Paraburkholderia sacchari*, *Caulobacter crescentus*, and *Pseudomonas taiwanensis* utilise this pathway to assimilate xylose into D-xylonolactone via enzyme xylose dehydrogenase (XDH) (Kohler et al., 2015; McClintock et al., 2017; Stephens et al., 2007). D-xylonolactone is then converted to D-xylonic acid by xylonolactonase (XL), which is further converted to the common intermediate, 2-keto-3-deoxy-xylonate, between the two pathways. 2-keto-3-deoxy-xylonate is converted to α -ketoglutarate via the Weimberg pathway, alternatively 2-keto-3-deoxy-xylonate is hydrolysed to pyruvate and glucoaldehyde via the Dahms pathway (Brüsseler et al., 2019).

The non-phosphorylative metabolic route has significant advantages over the oxidoreductase and isomerase pathways as it directly transforms xylose to pyruvate and α -ketoglutarate without entering PPP, reducing enzymatic conversions and ATP consumption. The incorporation of oxidative pathway enzymes aided the evolution of new recombinant strains producing a variety of useful chemicals (Banares et al., 2021; Domingues et al., 2021).

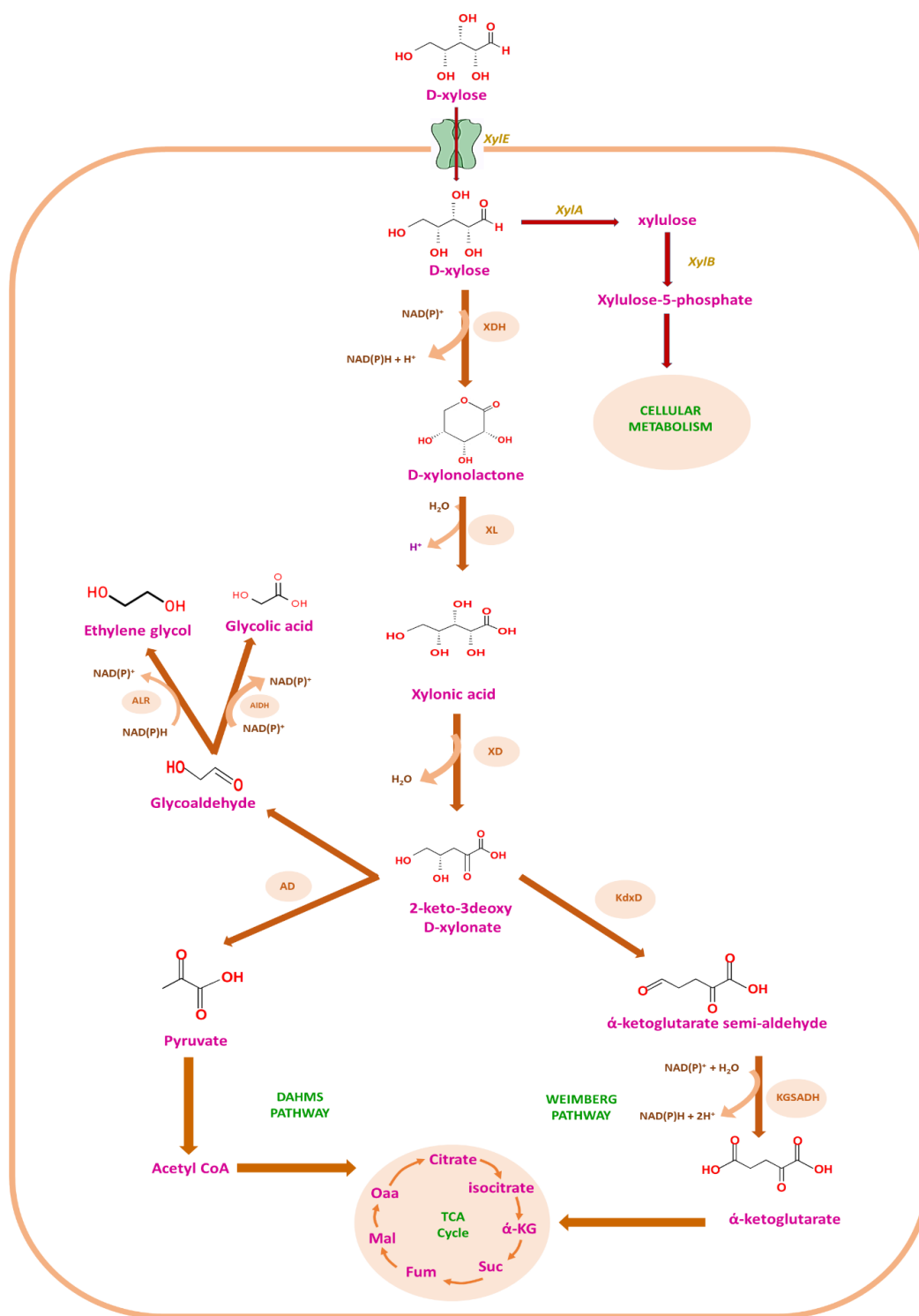


Fig.1.5. Xylose oxidative pathway for xylonic acid biosynthesis. Xylose is converted to D-xylonolactone by xylose dehydrogenase (XDH) and then to xylonic acid by xylonolactonase (XL) enzyme. Xylonic acid again converted to 2-keto 3-deoxy D-xylonate by

xylonate dehydratase (XD). 2-keto 3-deoxy D-xylonate is the common intermediate in both the Dahm's pathway and Weimberg pathway. In Dahm's pathway 2-keto 3-deoxy D-xylonate splits into pyruvate and glycoaldehyde via enzyme aldolase (AD). Pyruvate enters into TCA cycle as acetyl CoA, glycoaldehyde again converted to ethylene glycol via aldehyde dehydrogenase (ALR) and/or converted to glycolic acid via aldehyde dehydrogenase (AIDH), whereas in Weimberg pathway 2-keto 3-deoxy D-xylonate is oxidised to α -keto-glutarate semi-aldehyde by Ketodeoxy-Xylonate dehydratase (KdxD) and then enters TCA cycle as α -keto-glutarate by the enzymatic action of α -keto glutarate semi-aldehyde dehydrogenase (KGSADH).

1.3.4.5. Genetically modified strains for xylonic acid production

E. coli is an interesting model organism for producing biotechnologically valuable chemicals, because its metabolic routes and physiology are well understood, and there are several genetic and bioinformatic tools accessible. However, its prime genetic pathway for xylose metabolism is the XI pathway, *E. coli* does not natively produce xylonic acid from xylose. Nevertheless, metabolic engineering can be used to get around this limitation. In fact, the genetically modified strain accumulated xylonic acid after co-expression of two genes encoding xylose dehydrogenase (*xdh*) and xylonolactonase (*xylC*) from xylose operon of a heterologous Gram negative bacteria *Caulobacter crescentus*, as well as deletion of the genes encoding xylose isomerase and xylose kinase to block xylose utilisation via its native xylose isomerase pathway (Cao et al., 2013; Liu et al., 2012).

After *E. coli*, very recently *Corynebacterium glutamicum* has been reported for its potential in xylonic acid production from agro-residue. *C. glutamicum* is a Gram-positive, rod-shaped bacterium that has been considered as Generally Recognized as Safe (GRAS) by the United States Food and Drug Administration (FDA) for use as a food ingredient. *C. glutamicum* is most commonly used in industrial biotechnology for the production of amino acids, such as lysine, glutamate, and glutamine. It is also used in the production of enzymes, metabolites, and

other proteins. *C. glutamicum* is a well-known model organism for metabolic engineering. Its unique metabolic pathways make it an attractive organism for metabolic engineering projects. This is done by introducing genetic modifications to the organism to improve the efficiency of the metabolic pathways involved in the production of the desired product. It is widely used in industrial fermentation for the production of amino acids, peptides, polysaccharides, and enzymes. It is also employed in the manufacture of pharmaceuticals, vitamins, food additives, flavorings, and other products. It has been widely used in metabolic engineering studies, in order to improve L-glutamate production, to produce other amino acids, and other compounds, like vitamins and antibiotics, and also to study the basic biology of the organism. The genome of *C. glutamicum* has been sequenced, providing researchers with a wealth of information about the organism's genetic makeup and metabolic pathways. This information can be used to identify genes and pathways that can be manipulated to improve the organism's ability to produce a desired product.

Previous reports from our lab was also focused on the adaptability of *Corynebacterium glutamicum* in biomass hydrolysate and also its ability to grow in harsh conditions and to resist inhibitors were explored. *Corynebacterium glutamicum* was modified for C5 utilization and production of amino acids and xylitol from rice straw (Gopinath et al. 2011; Dhar et al. 2016).

In 2017 Yim et al (2017) explored *Corynebacterium glutamicum* for its potential in bioconversion of hemicellulosic biomass into speciality chemicals i.e xylan into xylonic acid. Heterologous expression of xylose specific transporter gene, *xylE*, of *Escherichia coli* along with xylose dehydrogenase and xylonolactonase genes, involved in xylonic acid metabolism, from *Caulobacter crescentus* were cloned for xylonic acid production. The metabolically engineered *C. glutamicum* successfully produced xylonic acid from biomass (Yim et al., 2017). D-xylose

dehydrogenase gene from *Caulobacter crescentus* was also expressed in yeast *Pichia kudriavzevii* VTT C-79090 T for xylonic acid production and the modified strain showed 100% conversion (Toivari et al., 2013). Herrera et al., (2021) engineered *Zymomonas mobilis* for conversion of sugarcane bagasse derived xylose to xylonic acid. The recombinant strain expressing xylose dehydrogenase gene (of *Paraburkholderia xenovorans*) allowed effective production of xylonic acid in shake flasks. The yeasts *Saccharomyces cerevisiae* and *Kluyveromyces lactis* were also modified in such a way showing the potential of prokaryotic systems for xylonic acid production (Nygard et al., 2011; Toivari et al., 2012). The studies on this sugar acid took a deviation to the practical application of xylonic acid as a concrete add-mixture in 2018.

Zhou et al., (2018) exploited *G. oxydans* for xylonic acid production from wheat straw hydrolysate as an economical source for industrial application. High titer of upto 210 g xylonic acid was produced by *G. oxydans* within one-day catalysis (Han et al., 2021). Calcium xylonate from lignocellulosic prehydrolysate (CXL) demonstrated to be a promising commercial precursor for concrete add-mixture with improved characteristics as a potential water reducer with high retardation capacity and compressive strength reinforcement and as a cost-competitive approach it has boosted the comprehensive utilization of lignocellulosic for xylonic acid production.

Klebsiella pneumonia a mutant strain (Δ gad) reported for producing both gluconic acid and xylonic acid from bamboo hydrolysate, where 14 gL⁻¹ xylonic acid and 33 gL⁻¹ gluconic acid were produced (Wang et al., 2016). *G. oxydans* the natural xylonic acid producer that has undergone extensive studies for this metabolite's synthesis reported with maximum yield of 586.30 gL⁻¹ (Zhou et al., 2015). Miao et al., (2015), sequenced the complete genome of *G.*

oxydans NL71 to understand the overall metabolism of xylose as well as the genome sequence elucidation paved the basis for both evolutionary studies and in the enhancement of the organism's biotechnological applications. This whole genome data is influential in understanding the metabolic mechanism occurring in the bacterial cells for the biotransformation of xylose into xylonic acid and the cellular resistance towards highly concentrated xylonic acid, xylose and inhibitors in the crude lignocellulosic hydrolysate. Table.1.2. compiles the metabolically engineered strains reported for xylonic acid production.

CRISPR-Cas9 technology is a dynamic genome editing tool, the vast scope of this technology will change the near future of biotechnology. A transitory CRISPR-Cas9 gene editing in *Candida glycerinogenes* enabled the co-production of xylonic acid and ethanol from lignocellulosic hydrolysate. For decades, *Candida glycerinogenes*, a potent industrial yeast with strong inhibitor resistance, has been used to produce glycerol. The absence of reduction division, whole genome, and the dearth of molecular tools, however, limited its genetic manipulation. The CRISPR-Cas9 system altered the genetic make-up of *C. glycerinogenes*. Single and multiple gene knock-outs were produced by targeting counter selectable marker genes (TRP1, URA3), and the auxotroph created employed as a background for targeting other genes (HOG1) with an 80% mutation efficiency. Furthermore, by knocking in the xylose dehydrogenase gene, a recombinant *C. glycerinogenes* strain was created, co-producing both ethanol (28 gL⁻¹) and xylonic acid (9 gL⁻¹) from xylose rich biomass hydrolysate. This strategy could countersign to unlock the application of CRISPR-cas9 genome editing in more organisms paving pathways producing diverse biochemicals (Zhu et al., 2019).

Table 1.2. Genetically modified strains reported for xylonic acid production

Species	Process	Yield (g g^{-1})	Titer (g L^{-1})	Volumetric productivity ($\text{g L}^{-1} \text{ h}^{-1}$)	Reference
<i>Saccharomyces cerevisiae</i> <i>Xyd1</i>	Batch	0.40	4	0.03	Toivari et al., 2010
<i>Saccharomyces cerevisiae</i> <i>SUS2DD</i>	Batch	0.40	3	0.02	Toivari et al., 2012
<i>Saccharomyces cerevisiae</i> <i>xylB</i>	Batch	0.80	17	0.23	Toivari et al., 2012
<i>Saccharomyces cerevisiae</i> <i>B67002 xylB</i>	Batch	0.80	43	0.44	Toivari et al., 2012
<i>Kluyveromyces lactis</i> <i>Xyd1</i>	Batch	0.60	19	0.16	Nygaard et al., 2011
<i>Kluyveromyces lactis</i> <i>Xyd1</i> ΔXYL1	Batch	0.40	8	0.13	Nygaard et al., 2011
<i>Aspergillus niger</i> ATCC 1015	Batch	0.80	10	0.12	VTT
<i>E. coli</i> W3110 EWX4	Batch	0.98	39.20	1.09	Liu et al., 2012
<i>E. coli</i> BL21 $\Delta\text{xylAB/pA-}$ <i>xdhxylC</i>	Batch	0.91	27.30	1.8	Cao et al., 2013
<i>E. coli</i> W3110 XGL4	Fed-Batch	1.09	108.2	1.8	Zhang et al., 2019
<i>Corynebacterium</i> <i>glutamicum</i> (ATCC 13032)	Batch	1.04	20.71	1.02	Yim et al., 2017
<i>Corynebacterium</i> <i>glutamicum</i> (ATCC 31831)	Batch	1.00	56.32	0.93	Sundar et al., 2020
<i>Zymomonas mobilis</i>	Batch	1.04	26.17	1.85	Herrera et al., 2021

1.3.4.6. Improvised bioprocesses for xylonic acid

Hou et al., (2018) illustrated the cascade hydrolysis and fermentation (CHF) strategy for the co-production of both gluconic acid and xylonic acid from highly viscous corn stover hydrolysate slurry. The high fermentation product yields of gluconic acid and xylonic acid (118.9 gL⁻¹ and 59.3 gL⁻¹ respectively) were reported exploiting *Gluconobacter oxydans* DSM 2003. This study signifies the economy and efficacy of CHF over traditional distinct hydrolysis and fermentation (SHF) as a practical fermentation strategy to be broadly extended to other value-added chemicals. Powdered activated carbon treatment improves xylonic acid synthesis from hemicellulose pre-hydrolysate. The use of powdered activated carbon lowered the viscosity of concentrated pre-hydrolysate and other non-sugar molecules, allowing lignocellulosic xylonic acid synthesis to be scaled up in an air-aerated and agitated bioreactor (Dai et al., 2020). Using straw pulping solid residue, a unique bio-refinery sequence was created, providing a variety of co-products such as xylonic acid, nitrogen fertiliser and ethanol. This method employs neutral sulphite pre-treatment, which resulted in 64.3 % delignification and also preserving cellulose and xylan (90 and 67.3%) under optimal conditions. Semi-simultaneous saccharification and fermentation (SSSF) and bio-catalysis methods were investigated after pre-treatment. With various solid loading, nearly 100 % xylonic acid got yielded from bio-catalysis of xylose remained in fermentation broth (Huang et al., 2018).

1.3.4.7. Bioconversion using immobilized biocatalyst

Immobilized biocatalyst technology has shown a great potential for xylonic acid production from xylose. Zdarta et al, (2019) reported the co-immobilization of glucose dehydrogenase and xylose dehydrogenase on mesoporous Santa Barbara Amorphous silica for simultaneous production of xylonic acid and gluconic acid. The reaction yield reached over 80%

even after 5 consecutive reaction steps (Zdarta et al. 2019). Similarly, the immobilization of xylose dehydrogenase (XDH) and alcohol dehydrogenase (ADH) on magnetite-silica core-shell particles was carried out to enable the simultaneous conversion of xylose into xylonic acid (XA) and the regeneration of cofactors in situ. The experiment showed that even after five cycles of reaction, the immobilized XDH and ADH retained more than 65% of their original properties, and the overall biocatalytic productivity was found to be 1.65 mM of xylonic acid per 1U of co-immobilized XDH (Bachosz et al. 2019). These findings indicate that the immobilized biocatalysts have several benefits over a free enzyme system, such as increased stability and activity.

1.3.4.8. Xylonic acid recovery and purification

For industrial applications, purity is a key criterion. Activated charcoal treatment and solvent extraction are the major downstream processes employed for xylonic acid recovery. Charcoal clarified broth is concentrated by rotary evaporator (usually at 70°C) and xylonic acid precipitate is recovered by ethanol precipitation (3:1 ratio). Another recovery process is the use of ion-exchange resin and crystallization, where anion exchange resin (D311) is employed for xylonic acid purification. The resin extracted eluate is concentrated into pure xylonic acid crystals (Liu et al., 2012; Wang et al., 2016; Zhang et al., 2020).

1.3.4.9. Non biological processes for xylonic acid synthesis

In the chemical process for the synthesis of chemicals from biomass, heterogeneous catalysis is important. In the realm of bio-refining, photocatalytic synthesis has steadily gained attention in addition to thermal catalytic synthesis.

Thermal catalysis is widely used to convert biomass into valuable compounds. Several works for the synthesis of xylonic acid were reported. The development of an efficient catalyst is

essential to achieve this process. Earlier reports of thermal catalytic synthesis used alkaline or organic systems, and noble metal catalysts were essential for the production of xylonic acid during the process. For example, Rafaideen et al. (2019) demonstrated that using a Pd/C catalyst, xylonic acid could be synthesized from an alkaline system with a pH of 10 (Rafaideen et al. 2019). The device could also successfully achieve the selective oxidation of glucose to gluconic acid (Chun et al. 2006). In addition, Tathod et al. (2014) claimed that Pt/hydrotalcite (HT) was essential for producing xylonic acid from xylose and that it could catalyze the conversion of xylose to xylonic acid at 50°C and atmospheric pressure with a 57% yield and 90% conversions (Tathod et al. 2014). It is because ultraviolet (UV) analysis was used to determine that in alkaline conditions, sugars remain in open-chain form in solution, exposing their CHO groups, which then get through oxidation and hydrogenation reactions to generate acids and alcohols. After that, it was discovered that adding Au-based catalyst significantly enhanced the catalytic efficiency. After few years, there has been a significant increase in the yield of the chemical synthesis of xylonic acid. Ma et al. (2018) developed a catalyst made of Au nanoparticles embedded in the inner wall of mesoporous alumina hollow nanospheres (Au@h-Al₂O₃). The results showed that the Au@h-Al₂O₃ catalyst performs effectively in non-alkaline environments. In the presence of Au@h-Al₂O₃ (20.00 mg) and oxygen pressure (3.00 MPa) at 130°C for 60 min, the yield of xylonic acid was 83.30% (Ma et al. 2018). Despite an increase in xylonic acid yield, the system exhibited high reaction temperature and the use of metal catalyst, which are not ideal for xylonic acid synthesis at an industrial level. A metal-free catalyst was designed for the production of xylonic acid from xylose to reduce the production costs. The doped graphitic N is the active site, according to the results. However, this work also had a number of flaws, including a low yield, a high reaction temperature, and an alkaline reaction media, which is

incompatible with needs for developing green chemistry. Therefore, it is essential to develop a safe, effective, and environmentally friendly xylonic acid production process.

Photocatalysis is a process in which a photocatalyst (such as titanium dioxide (TiO_2)) is used to facilitate a chemical reaction under the influence of light. In the case of xylonic acid production, photocatalysis is used to convert xylose into xylonic acid through a series of chemical reactions. The process typically involves the use of a photocatalyst, a source of light, and an oxidizing agent such as oxygen or hydrogen peroxide (H_2O_2). In a Na_2CO_3 solution, Zhou et al. (2017) used a catalyst composed of AuNPs/ TiO_2 (3.00 wt % Au) to oxidise xylose into xylonic acid. The production of xylonic acid was 96% when the light source was UV light (= 350-400 nm, 0.30 W cm^{-2}); however, the yield was 98% when the light source was visible light irradiation (= 420-780 nm, 0.30 W cm^{-2}). The results also showed that the band-gap photoexcitation of TiO_2 is favourable to the UV light, hence increasing the photocatalytic activity, whereas the surface plasmon resonance of AuNPs is favourable to the excitation of visible light (Zhou et al. 2017). Biomass was used as the raw material by Chen et al., (2021) who then used a hydrothermal process to synthesise $\text{TiO}_2/\text{Ti}_3\text{C}_2$ and in-situ developed TiO_2 nanoparticles on Ti_3C_2 nanosheets. $\text{TiO}_2/\text{Ti}_3\text{C}_2$ shown exceptional photocatalytic activity in the oxidation of xylose to xylonic acid when compared to raw TiO_2 . With a catalyst dosage of 30 mg and a KOH concentration of 0.08 molL^{-1} , the best yield of 64.20% was achieved (Chen et al. 2021). Li et al. (2021) have published a novel hydrothermal technique for the controllable one-step production of $\text{ZnS}@\text{Bi}_2\text{S}_3$ nanosheets. $\text{ZnS}@\text{Bi}_2\text{S}_3$ nanosheets showed a good band gap and outstanding stability when compared to pure Bi_2S_3 . In the presence of $\text{ZnS}@\text{Bi}_2\text{S}_3$ nanosheets (40 mg) with 0.08 molL^{-1} of KOH at 50°C during the reaction, the production of xylonic acid reached 74.20% (Li et al. 2021).

The chemical synthesis of xylonic acid has several drawbacks and disadvantages compared to biological production. Chemical process requires harsh reaction conditions, including high temperatures and strong acids, which can lead to the production of undesirable side products and can be energy-intensive. The chemical synthesis route is expensive, and the cost of the starting materials and reagents is high. Additionally, the chemical synthesis of xylonic acid often requires the use of hydrothermal process, toxic or hazardous chemicals, which can pose risks to workers and the environment. Furthermore, the process may produce large amounts of waste and requires specialized equipment for the purification of the product.

In contrast, biological production of xylonic acid using microbial fermentation can be performed under mild conditions, uses renewable resources, and has a lower environmental impact. Additionally, microbial production can produce high yields of pure product with fewer by-products and can be performed at lower costs than chemical synthesis. Therefore, while chemical synthesis of xylonic acid can be a useful tool in laboratory settings, it is not a feasible or sustainable method for large-scale production.

1.3.4.10. Technology players for xylonic acid

Recent scientific and applied research on xylonic acid has shown a significant amount of patent activity in the recent past, from 2008 to 2021, with a slight shift towards more scientific publications in recent years due to an increase in research on the acid's synthesis and application. Data from the last decade (2012-2021) shows that there were 214 scientific publications and 210 patent families related to xylonic acid, the data retrieved from Clarivate Analytics databases, Derwent Innovations Index, and the Web of Science. This indicates that scientific research has overtaken patent filing during this period. Of these publications, 68 were related to acid

production in scientific publications, while 36 were related to acid production in patent publications.

The leading players in the production of xylonic acid are biotech companies such as Novozymes (India) and Danisco (USA), as well as universities and research centers such as Julich (Germany), East China University of Science and Technology (China), and Shanghai Advanced Research Institute (China). These entities use various strategies, including genetically modified and non-modified microorganisms, bacteria, yeast, enzyme cocktails, and process improvements like enzyme immobilization, aeration, and downstream separation and purification. While hydrolysates from corncob have been evaluated, they are not commonly used as a substrate. The primary substrate for microbial production is pure pentoses, specifically xylose.

1.4. Summary

In recent years, bacteria and yeast strains have been developed to produce xylonic acid efficiently in defined media containing xylose. However, using agro-industrial by-products and residues, such as lignocellulosic hydrolysates, as raw materials for xylonic acid production is still a challenging process. The proportion of different sugars present in the hydrolysate and their impact on the microorganism's metabolism have not been fully considered. Moreover, lignocellulose-derived inhibitors pose a challenge to be overcome, and detoxification of hydrolysates has been pursued for bacterial cultivation. Therefore, the primary technical challenges for the industrial-scale production of xylonic acid include efficient conversion of biomass xylose in undetoxified lignocellulosic hydrolysates, also microorganisms which can uptake good level of xylose and which have efficient enzyme systems for its conversion to xylonic acid is preferred and it has to survive in harsh conditions where growth inhibitors are

present, also capable of performing for extended periods with high production efficiency, and scaling up the process beyond the few liters evaluated so far. In this thesis we tried to address all these lacunae related to the bioprocess.

Chapter 2

Materials and methods

2.1. Introduction

This chapter provides a detailed description of the materials and experimental procedures used to conduct the study. Standard protocols and details, information of instruments and equipments are provided. Individual chapters concerned with only very specific methodologies pertained to that chapter and all other standard microbiology, molecular biology and routine analytical experiments are described here.

2.2. General materials

2.2.1. Microbial strains and plasmids

Corynebacterium glutamicum ATCC 31831 procured from American Type Culture Collection (ATCC) was used mainly in this work for xylonic acid production. The details of all microbial cultures and vectors used in the study are presented in Table 2.1.

Table 2.1 Microbial strains and plasmids used in the study

Strains & Vector	Descriptions	Reference
Microbial strains		
<i>Corynebacterium glutamicum</i>	ATCC13032, Wild type (WT)	(Abe et al. 1967)
<i>Corynebacterium glutamicum</i>	ATCC 31831	(Kinoshita et al. 2004)
<i>E. coli</i> DH5 α	<i>Fthi-1 endA1 hsdR17(r-, m-) supE44 _lacU 169 f80lacZ_M15) recA1 gyrA96 relA1</i>	(Hanahan & Harbor 1983)
<i>E. coli</i> BL21(DE3)	F- ompT gal dcm lon hsdSB(rB- mB-) λ (DE3)	Novagen, USA
Plasmid vector		
pET 28a	Bacterial expression vector	Novagen, USA
pVWEx1	Kan ^r ; <i>E. coli</i> - <i>C. glutamicum</i> shuttle vector	(Peters-Wendisch et al. 2001) Gifted by Prof. Dr. Volker F Wendisch, Bielefeld University, Germany
Xylose operon	Xylose inducible <i>xylXABCD</i> operon	

2.2.2. Chemicals, reagents and kits

All chemicals used in this study were of analytical grade, procured from Merck (India), Sigma-Aldrich (USA) and Sisco Research Laboratories (SRL) (India). Culture medias (Luria Bertani (LB) and Brain Heart Infusion (BHI), media components comprise D-glucose, D-xylose, Tryptone, Yeast extract, $\text{FeSO}_4 \cdot 7\text{H}_2\text{O}$, $\text{MnSO}_4 \cdot \text{H}_2\text{O}$, $\text{ZnSO}_4 \cdot 7\text{H}_2\text{O}$, $\text{CuSO}_4 \cdot 5\text{H}_2\text{O}$, $\text{NiCl}_2 \cdot 6\text{H}_2\text{O}$, biotin, protocatechuate, $(\text{NH}_4)_2\text{SO}_4$, urea, KH_2PO_4 , K_2HPO_4 , $\text{MgSO}_4 \cdot 7\text{H}_2\text{O}$ and MOPS), staining reagents (crystal violet and safranin) were obtained from Himedia (India). Solvents (NaOH, HCl, H_2SO_4 , methanol, acetonitrile, formic acid, acetic acid, furfurals and syringaldehyde), Co-factors (NAD^+ & NADH) and antibiotic (kanamycin), solvents (ethanol, isopropanol and acetone for the recovery and purification of xylonic acid) were procured from Sisco Research Laboratories (SRL) (India). Xylonic acid standard (HPLC grade) procured from Sigma- Aldrich (USA). Details of the oligonucleotides (from New England Biolabs (NEB) Ipswich, (USA)) used for various experiments are mentioned in respective chapters.

Various molecular biology kits such as genomic DNA isolation kits, Plasmid isolation kits, PCR clean-up kits, and Gel extraction kits were obtained from Thermo scientific (Lithuania) and Qiagen, GmbH, Hilden (Germany). Restriction enzymes (BamHI, EcoRI, PstI), 2X Taq Master mix, Q5 High Fidelity Master mix, T4 DNA ligase, protein and DNA markers were purchased from New England Biolabs, NEB, Ipswich, (USA). Lysozyme and Bovine Serum Albumin (BSA) were procured from Himedia (India). Molecular biology grade chemicals like Agarose, Polyethylene glycol (PEG) MW 4000, Tris-base, Glycine, Ethylenediaminetetraacetic acid (EDTA), Glycerol were obtained from Sigma-Aldrich, (USA). Analytical grade solvents like Dimethyl sulfoxide (DMSO) and glacial acetic acid were purchased from Merck (India).

2.3. General microbiology methods

2.3.1. Microorganisms and maintenance

The wild type strain and all the recombinant strains of *Corynebacterium glutamicum* were maintained aerobically in Brain Heart Infusion (BHI) agar or broth (composition of media given in Annexure II) at 30°C. Antibiotic, kanamycin (25 µg mL⁻¹), supplementation was used for recombinant *C. glutamicum* strains carrying pVWEx1 plasmid. *E. coli* strains DH5α and BL21(DE3) were maintained aerobically in Luria Bertani (LB) agar or broth (composition of media given in Annexure II) at 37°C. All the cultures were grown in broth and stored at 4°C in respective agar plates and for long term preservation glycerol (20 %) stocks were made and stored at -80 °C.

2.3.2. Biomass determination

The microbial biomass was determined based on dry cell weight (dcw). The broth containing cells were separated by centrifugation at 6,000 g for 5 min. The supernatant was discarded and the pellet was dissolved in deionized water. The suspension was filtered through pre weighed 0.2 µm filters. The filter containing biomass was dried in hot air oven at 50°C for 12 h. The filter paper containing dried biomass was weighed and calculated the dry weight of biomass (dcw) in g L⁻¹.

$$\text{g cdwL}^{-1} = \frac{(w - w_0)}{v} \times 100$$

Whereas,

‘w’ is the weight of the filter paper with dried biomass in grams

‘w₀’ is the weight of the filter paper alone in grams.

‘v’ is the volume of broth taken (mL) for analysis

2.3.3. Cell density

The bacterial cell concentration was measured spectrophotometrically by suspending in sterile deionized water or fermentation media. 3 mL sample was taken in a quartz cuvette having a path length of 1 cm and optical density was measured at 600 nm using a spectrophotometer (UV-160A, Shimadzu, Japan).

2.3.4. Inoculum preparation

Single colony of *C. glutamicum* from BHI agar plate was inoculated into 15.0 mL test tube containing 5.0 mL sterile BHI medium. The medium was incubated aerobically at 30°C in a rotary shaker at 200 rpm for 16 h. 1 % (v/v⁻¹) of the grown culture with OD_{600 nm} of 0.8 was used as the pre-inoculum for batch fermentation studies. The recombinant *C. glutamicum* containing plasmid pVWEx1 and their derivatives were inoculated in BHI medium supplemented with kanamycin (25 µgmL⁻¹).

2.3.5. Fermentation

Batch fermentation was carried out in both 250 mL shake flasks with 100 mL production medium and 2.5L fermenter with 1L production medium at 30°C and 200 rpm for 120 h with an initial xylose concentration of 60 gL⁻¹. Downstream process for the purification and characterization of xylonic acid is described in detail in chapter 6. The production medium (CGXII medium) composition used in this study are listed in Annexure II.

2.3.6. Preparation of Acid Pre-treated Liquor (APL)

After the initial screening, the sawdust biomass was selected for the preparation of Acid Pre-treated Liquor. The biomass was dried, milled and sieved through 2.0 mm sieve to obtain fine

particles of similar size. The sawdust was hydrolysed by dilute acid hydrolysis. 1 % sulphuric acid (wv^{-1}) was used to soak the biomass with solid biomass loading of 15 % (wv^{-1}). The mixture was pre-treated at 121°C in an autoclave for 60 min. After the treatment, the biomass was washed with deionized water to wash out all the residual soluble sugar present in the biomass. The resultant wash out liquid *i.e.*, Acid Pre-treated Liquor (APL) was neutralized with calcium carbonate followed by fine adjustment with 10 N NaOH (pH 6.5). The APL was concentrated in a rotary vacuum evaporator (Buchi, India) to increase the sugar concentration according to the requirement. The APL concentrate was refined by centrifugation at 8000 rpm for 15 min followed by sterilization by filtration through $0.2\ \mu\text{m}$ filters.

2.4. Analytical methods

2.4.1. Estimation of Protein

2.4.1.1. Bradford Assay

The assay is based on the observation that the absorbance maximum for an acidic solution of Coomassie Brilliant Blue G-250 shifts from 465 nm to 595 nm when protein binds to it (Bradford 1976). The anionic form of the dye is stabilized by both hydrophobic and ionic interactions, which results in a discernible colour change. The experiment is effective because a dye-albumin complex solution's extinction coefficient is constant over a concentration range of 10 fold.

2.4.1.1.a. Reagents

- Bradford's Reagent (contains Coomassie Brilliant Blue G-250, phosphoric acid and methanol)
- Protein samples dissolved in appropriate buffer

2.4.1.1.b. Procedure

Protein samples were quantified spectrophotometrically using Infinite 200 PRO microplate reader at 595 nm along with Bradford reagent. Bovine serum albumin (BSA) was used as the standard. 10 μL of the sample was mixed with 300 μL of Bradford reagent and incubated for 5 min at RT. A standard curve was plotted against BSA concentration within a range of 0.5-3 mgmL^{-1} (Fig. 2.1). All the readings were taken in triplicates in a 96-well microtiter plate.

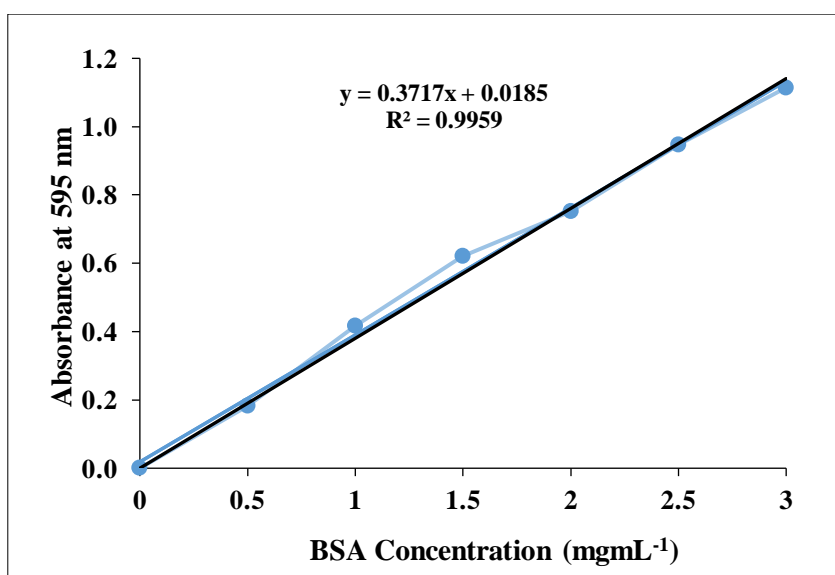


Fig. 2.1 Standard graph for Bradford assay

2.4.2. Nucleic acids

Qualitative and quantitative analysis of nucleic acids, DNA and RNA, were performed spectrophotometrically (ND-1000 UV-Vis Spectrophotometer (Nanodrop, USA)). 1-2 μL of the sample was analyzed by keeping it between two optical surfaces which define the path in vertical orientation. Each measurement has been carried out at both 1 mm and 0.2 mm path by the instrument automatically provided dynamic range of detection levels without sample dilutions (2 to 3700 $\text{ng}\mu\text{L}^{-1}$ dsDNA, 2 to 3000 $\text{ng}\mu\text{L}^{-1}$ RNA, 2 to 2400 $\text{ng}\mu\text{L}^{-1}$ ssDNA).

Nucleic acids and proteins share absorbance maxima at 260 and 280 nm respectively. The purity was determined based on the ratios of this absorbance. Pure DNA generally has a ratio ~ 1.8 , and ~ 2.0 for RNA. An absorbance at 230 nm considered as contamination, therefore ratio of A260/A230 also calculated. So the pure DNA and RNA will have higher A260/A230 ratio at a range of 2.0 and 2.2 respectively. The instrument was controlled with Nano Drop™ software which measures the A280/A260 and A260/A230 automatically to provide the purity and concentration of the samples.

2.4.3. HPLC analysis of sugars

The qualitative and quantitative analysis of sugars were performed with automated High Performance Liquid Chromatography (HPLC) system (Prominence UFLC, Shimadzu, Japan) equipped with auto sampler (SIL20AC-HT) and column oven (CTO-20AC). The sugars (D-glucose and D-xylose) were resolved with Phenomenex Razex RPM Pb²⁺ cation exchange monosaccharide column (300 x 7.5 mm) operated at 80°C using milliQ water (0.6 mLmin⁻¹) as mobile phase and detected using RI detector (RID, Refractive Index Detector-10A Shimadzu, Japan).

2.4.4. HPLC analysis of xylonic acid

The sugar acid (xylonic acid) was resolved with Phenomenex organic acid column (250 mm×4.6 mm×5 μm) operated at 55°C using 0.01N H₂SO₄ as mobile phase at a flow rate of 0.6 mLmin⁻¹ and detected using PDA detector (SPDM-20A, Shimadzu, Japan). The samples were centrifuged (13,000 rpm for 10 min at 4°C) and filtered using 0.2 μm filters (Pall Corporation, Port Washington, New York) for analysis.

For standard graph preparation, different concentration of xylic acid standard in the range 2, 4, 6, 8, 10 mgmL⁻¹ was prepared and were analysed in HPLC. Standard graph was plotted with different concentrations against the peak area generated in the chromatogram. Xylic acid production titer from batch fermentation was calculated from the standard curve. Fig.2.2. shows the standard graph of xylic acid.

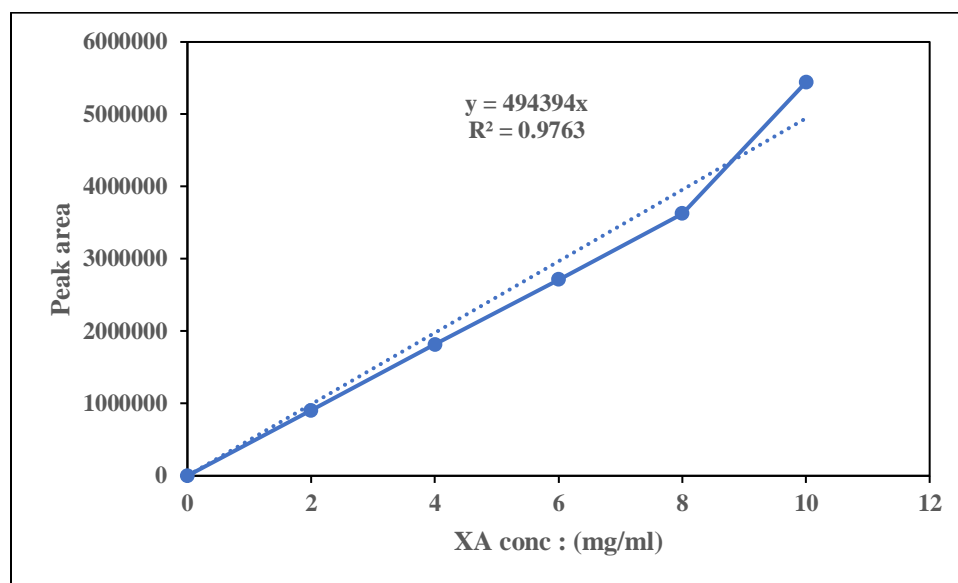


Fig.2.2. Standard graph of xylic acid

2.4.5. HPLC analysis of Inhibitors

The quantitative analysis of inhibitors such as formic acid, acetic acid, HMF and furfural in APL was carried out with Phenomenex organic acid column (250 mm×4.6 mm×5 μm) operated at 55°C using 0.01N H₂SO₄ as mobile phase at a flow rate of 0.6 mLmin⁻¹ and detected using PDA detector (SPDM-20A, Shimadzu, Japan). The samples were centrifuged (13,000 rpm for 10 min at 4°C) and filtered using 0.2 μm filters (Pall Corporation, Port Washington, New York) for analysis.

2.5. Molecular biology Methods

Unless specified, all the molecular biology techniques used for the experiments were adopted from the classical molecular biology methods provided in Sambrook and Russell (2001) unless otherwise specified. The buffers and reagents used in these methods were of sterile molecular biology grade.

2.5.1. Isolation of Genomic DNA

The genomic DNA isolation was performed by (cetyltrimethylammonium bromide) CTAB method (William et al., 2012). The bacterial cells from exponential stage were used for the genomic DNA isolation. 1.5 mL culture broth was centrifuged at 6,000 g for 5 min. After discarding the supernatant, the pellet was dissolved in TE buffer (10 mM Tris; 1 mM EDTA, pH 8.0) to get an OD of 1.0 at 600 nm. Around 740 μL cell suspension was transferred to a clean micro centrifuge tube. 20 μL lysozyme (10 mgmL^{-1}) was added to the cell suspension and mixed well. The mixture was incubated at 37°C for 10 to 60 min depending on the rigidity of the bacterial cell wall. Most of the gram positive bacterial cells need more time (30-60 min) for the lysis of cell wall. 40 μL SDS (10 %) was added to the lysate followed by 8 μL Proteinase K (20 mgmL^{-1}) and incubated at 55°C for 1 – 2 h. The complete lysis of cells can be confirmed on the basis of lucidity of the suspension. 100 μL NaCl (5 M) solution was added to the clear lysate and mixed well. This was followed by the addition of 100 μL , CTAB-NaCl (10: 4) solution. The thoroughly mixed solution was incubated at 65°C for 10 min. 500 μL Chloroform: Isoamyl alcohol (24:1) was added to the suspension and mixed well. The mixed solution was centrifuged at 14,000 g for 10 min at RT. The aqueous phase was transferred and added 500 μL of phenol: chloroform: isoamyl alcohol (25:24:1). The mixture was then centrifuged at 14,000 g for 15 min at RT. The aqueous phase was transferred to a new microfuge tube and 500 μL of Chloroform:

Isoamyl alcohol (24:1) was added once again. The contents were centrifuged again at 14,000 g for 10 min at RT. 400 μL of aqueous phase was transferred to a new microfuge tube and 240 μL of ice cold isopropanol (99 %) was added. After gentle mixing by inversion, the tubes were incubated at -20°C overnight. After the incubation the DNA precipitates formed was separated by centrifugation at 14,000 g for 15min at 4°C . The supernatant was discarded and the pellet was washed by suspending it in 500 μL ice cold ethanol (70 %, vv^{-1}). The pellet was recollected by centrifugation at 14,000 g for 5 min at 4°C . The washed pellet was air dried in a vacuum concentrator at room temperature (RT) for 10 min. The dried pellet was dissolved in 170 μL nuclease free water and mixed well by gentle pipetting with cut tip. 20 μL RNase I buffer (10 X) along with 10 μL RNase I (100 mgmL^{-1}) was added to the DNA solution and incubated at 37°C for 1 h to digest the residual RNA. The enzyme was inactivated by incubating the solution at 70°C for 15 min. After heat inactivation, the content was placed in ice to cool, and 20 μL of Sodium Acetate solution (3M) was added. 550 μL ice cold ethanol (99%) was added to the content and gently mixed by inverting the tubes. The mixed content was placed in -80°C for 2 h for the precipitation of DNA.

The precipitated DNA was separated by centrifugation at 14,000 g for 20 min in a cooling centrifuge. Supernatant was discarded and the pellet was washed with ice cold ethanol (70 %) as described earlier in the protocol. The washed pellet was air dried and dispensed in 100 μL TE buffer for storage at -80°C . The DNA was visualized in 1% pre-stained (EtBr) agarose gel (1 %) and quantified by UV-Vis spectrophotometer (Nanodrop, USA).

2.5.2. Isolation of Plasmid DNA

Plasmid DNA isolation was done using the QIAprep Spin Miniprep kit (Qiagen, Hilden, Germany) following the manufacturer's instructions. Briefly, prepared the culture by

inoculating it in 100 mL LB broth with $10 \mu\text{g mL}^{-1}$ of the desired antibiotics as per the plasmid used (kanamycin for pVWEx1) and incubated overnight at 37°C . Transferred 100 mL of the overnight grown culture into the centrifuge tubes and centrifuged at 6000 g for 15min at 4°C . Discarded the supernatant and re-suspended the pellet in 4 mL of P1 buffer (resuspension buffer). Added 4 mL of P2 buffer (lysis buffer) mix thoroughly by vigorously inverting 4-6 times and incubated at RT for 5 min. Added 4 mL of pre-chilled P3 buffer (wash buffer), mix thoroughly by vigorously inverting 4-6 times and incubated in ice for 15 min. After this step the mixture turns into a turbid form. After incubation, centrifuged at 14,000-18,000 g for 10 min at 4°C . Re-centrifuged if the supernatant is not clear. Again centrifuged at 20,000 g for 30 min at 4°C . Re-centrifuged at the same rpm for 15 min at 4°C . Equilibrated the Qiagen tip (column) with 4 mL of QBT buffer (equilibrium buffer) and empty it by gravity flow. Added the supernatant after centrifugation to the column and allowed it for gravity flow. Washed the column (twice) 2X 10mL with QC buffer (wash buffer). Allowed it to drain it by gravity flow. Eluted the DNA with 5 mL of QF buffer (elution buffer) into a clean 15 mL centrifuge tube. (For constructs larger than 45kb pre-warming the elution buffer to 65°C may help to increase the yield). Precipitated the DNA by adding 3.5 mL (0.7 volumes) isopropanol to elute the DNA mix. Washed the DNA pellet with 2 mL 70% ethanol and centrifuged at 15,000 g for 10 min. Carefully discarded the supernatant. Air dried the pellet for 5-10 min and re-dissolved the DNA in a suitable volume of nuclease free water. The presence and quality of the isolated plasmid was confirmed by performing an agarose gel electrophoresis (AGE). The purity of the DNA was visualized in 1% pre-stained (EtBr) agarose gel (1 %) and quantified by NanoDrop1000 spectrophotometer (NanoDrop Technologies, Inc. USA).

2.5.3. Polymerase Chain Reaction (PCR)

A typical polymerization reaction contains template DNA, thermotolerant DNA dependant DNA polymerase (Taq polymerase isolated from *Thermus aquaticus*) primers (single stranded fragments of DNA (20-50 nucleotides) initiates polymerization reaction), dNTPS (Deoxy Ribo Nucleotides (monomeric units of DNA), dATP, dGTP, dCTP and dTTP) and buffer containing salts for enzyme activity. For the amplification of DNA segment, the template double-stranded DNA (dsDNA) has to be denatured at high temperature (92 to 95°C) to get two pieces of single-stranded DNA (ssDNA). The two primers that are designed to match to the segment of template DNA gets attached to the targeted complementary ends of template DNA when the temperature was reduced to annealing Temperature (T_a). Generally, T_a was calculated from melting temperature (T_m) of the primers used, by subtracting 5 °C from the T_m of the primers. After the attachment of primers in the template the temperature was increased to 72°C for the polymerization reaction for the synthesis of two strands of DNA, which completes one cycle. As the process repeats over again 30 or 40 times the DNA segments increases to more than one billion copies. For polymerase chain reaction, oligonucleotides were designed using the software CloneManager 9. The PCR mixture was made with Nuclease free water, 10 X PCR Master mix (10 mM Tris-HCl, pH 8.3, 50 mM KCl, 200 μ M of each dNTPs), 1-5 mM $MgCl_2$, 0.5 μ M of forward and reverse primers, 1-10 ng template DNA and 1.25 U DNA polymerases. The PCR was carried out using automated PCR machines from BioRad, USA (MyCycler) and Eppendorff, Germany (Ep gradient). Depending up on the size of the template used the PCR starts with a single cycle of the initial denaturation reaction at 94°C for 2- 4 min. This was followed by a repeated (25 to 35) cycles of denaturation (94°C for 30sec), annealing ($T_m-5^\circ C$ for 30sec) and extension (72°C for 2 min k_b^{-1}). The final stage of the reaction was extension reaction at 72°C for

5 to 15min. The reaction was maintained at 4°C by the machine to stop the enzyme activity. Colony PCR was performed with heat denatured bacterial biomass pricked from single colony contains crude DNA as template.

In this work two genes namely, *xyI B* and *xyI C* were PCR amplified from xylose inducible *xyIXABCD* operon of *C. crescentus*. The specific PCR conditions and the PCR primers designed for them are all explained in detail in chapter 3, section 3.2.3.

2.5.4. Sequencing of DNA

Sequencing was performed with Sanger's (dideoxy termination) method using Gene analyzer 3500 (Thermo Fisher Scientific, USA). The instrument uses a fluorescence-based DNA analysis system that uses high resolution capillary electrophoresis technology. Gene specific primers are used for *xyIB* and *xyIC* gene amplification. PCR amplified gene was purified by gel extraction method and analyzed UV - Spectrophotometrically (Nanodrop, Technologies, Inc. USA). 20 ng of high purity DNA (A260/A280 ratio between 1.7 and 1.9) was used for sequencing.

2.5.5. Restriction Digestion

A typical 50 µL restriction digestion reaction contains DNA (10 µg), buffer (1X), restriction enzyme (10 U) and nuclease free water. The components were gently mixed by flicking the tube, and spin down for few seconds. The contents were incubated at 37°C for 1 to 6 h based on the efficiency of the enzymes. Similarly, for double digestion (restriction digestion with combination of enzymes), the compatible buffer used for the reaction was specified by manufacturers for better activity. One unit (1U) is the amount of enzyme required to digest 1 µg of DNA in 50 µL reaction volume with recommended buffer at 37°C for 1 h.

2.5.6. Ligation

Ligation reaction was performed in 20 μ L set-up. A typical reaction contains water, 1x T4 DNA ligase buffer ((40 mM Tris-HCl (pH 7.8), 10 mM MgCl₂, 10 mM DTT, 1 mM ATP), DNA fragments and finally T4 DNA ligase (1 Weiss U* = One Weiss unit is defined as the amount of enzyme required to convert 1 nmol of ³²P-labeled inorganic pyrophosphate into Norit adsorbable material in 20 min at 37°C, using specified reaction conditions). The contents were added and mixed by keeping the tube in ice, and incubated at 22°C for 10 to 30 min or 16°C for 12 h. The success rate of ligation was dependant on molar ratio of the fragments, enzyme units and incubation time. For a sticky end ligation of linear fragment 1:1 molar ratio of the fragment was maintained, whereas for linear vector – insert ligation, the molar ratio of the fragment was 1:3. For blunt end ligation of linear vector and insert was incubated for 1h at 22°C with 5 Weiss U of ligase and 1:5 molar ratio of fragments. *One Weiss unit is equivalent to approximately 200 cohesive end ligation units (CEU). One CEU is defined as the amount of enzyme required to give 50 % ligation of HindIII fragments of lambda DNA in 30 min at 16°C. The number of pmols of each fragment was calculated based on fragment length and weight.

$$\text{pmols} = (\text{weight in ng}) \times 1,000 / (\text{base pairs} \times 650 \text{ daltons})$$

2.5.7. Preparation of competent cells and transformation

2.5.7.1. Competent cell preparation of *E. coli* (DH5 α and BL21(DE3))

Competent cells of *E. coli* were prepared by TSS (Transformation and Storage Solution) method. Inoculated 2 mL of LB broth with single colony of *E. coli* in micro centrifuge tube and incubated at 37°C for overnight with shaking (200 rpm). Aseptically added 1 mL of overnight grown culture to sterile 100 mL LB broth and again incubated at 37°C with shaking for 2-4 h or until OD₆₀₀ = 0.4. Centrifuged the culture to obtain the pellet and to the pellet, added

pre-chilled TSS buffer, vortexed slightly to suspend the pellet and incubated in ice for 15 min. After the incubation, aliquoted 200 μL of cells to fresh sterile micro centrifuge tubes and stored at -80°C until use.

2.5.7.2. Transformation into competent cells of *E. coli*

After ligation, 20 μL of ligated product was mixed with 100 μL of freshly thawed *E. coli* competent cells and incubated on ice for 30 min. A heat shock at 42°C for 45 sec (water-bath) was given after the incubation. 900 μL of LB broth/SOC medium was added immediately after the heat shock and incubated at 37°C at 200 rpm for 1-1.5 h. After incubation, pelleted the cells by centrifugation at 6000 rpm for 10 min and resuspended the pellet in 100 μL of SOC medium. This 100 μL of the *E. coli* cells were spread plated on LB agar plate supplemented with kanamycin ($25 \mu\text{g mL}^{-1}$) and incubated at 37°C for 24 h.

2.5.7.3. Preparation of electrocompetent cells of *C. glutamicum* (van der Rest et al. 1999)

A single colony of *Corynebacterium glutamicum* was inoculated from a fresh plate (almost 2 days old) in 10 mL LB medium containing 2% (wv^{-1}) filter sterilized glucose and incubated at 30°C overnight (16 h) in a rotary shaker at 200 rpm. The overnight grown culture with an OD of 0.3 at 600 nm was inoculated into Epo medium (AnnexureII). Cells were allowed to grow in 500 mL conical flask at 18°C for 28 h with shaking at 120 rpm. When the OD at 600 nm reached 0.8 to 1.0. The culture was chilled on ice for 10 min and harvested by centrifugation for 10 min at 4000g. The cells were washed 4 times with 50 mL ice cold 10 % (vv^{-1}) glycerol and resuspended in 0.5 mL 10 % (vv^{-1}) glycerol. 100 μL aliquots were stored at -80°C .

2.5.7.4. Electroporation and transformation into *C. glutamicum*

The *C. glutamicum* cells were electroporated to achieve the transformation (Van *et al.*, 1999). Transformation of *C. glutamicum* is comparatively complex procedure. For electroporation, the competent *C. glutamicum* cells were thawed in ice. 1- 2 μ L plasmid DNA along with 100 μ L of *C. glutamicum* competent cells were added to pre-cooled electroporation cuvette (interelectrode distance 0.2 cm). Electroporation was performed with parameters set at 25 μ F, 600 Ω and 2.5 kv (2500 V) yielding a pulse duration of 10-12 min. Immediately after electroporation 1mL BHIS (Brain Heart Infusion and 0.5 M sorbitol) at room temperature was added to the cuvette and the suspension was transferred to eppendorf tube. For heat shock the cells in eppendorf tube was incubated for 6 min at 46°C in dry incubator. After heat shock cells were then incubated for 1 h at 30°C to allow for recovery and expression of antibiotic marker (kanamycin). 100 μ L of the cell suspension were then plated on selective LBHIS medium containing 25 μ g kanamycin per mL and incubated at 30°C for 16 to 24 h. The transformants appeared on the plate after 24 h incubation. The positive transformant colonies were confirmed by colony PCR and were sub cultured and used for further study. The transformation efficiency was calculated using the following equation:

2.5.8. Agarose Gel Electrophoresis

DNA (genomic, plasmid, PCR products) and RNA were resolved by Agarose Gel Electrophoresis (0.8 – 1.2 %). The gels were prepared in 1X TAE buffer (40 mM Tris acetate and 1 mM EDTA) and DNA and RNA were visualized in pre-stained (Ethidium bromide) gel under far UV (320 nm) illumination using Chemi, Biorad, USA.

2.5.9. Purification of xylose dehydrogenase enzyme

Single colony of recombinant *E. coli* BL21 (DE3) carrying the recombinant vector pET28a-*xyIB* from LB agar plate was inoculated in LB broth and incubated overnight at 37°C. 1 mL of pre-inoculum (OD_{600 nm} 0.8) was added to 100 mL of LB broth. The culture was incubated at 37°C until an OD of 0.4 – 0.6, IPTG (1mM) induction was done and again incubated at 37°C for 3 h. The cells were harvested by centrifugation, frozen, thawed, and resuspended in 0.5 M phosphate buffer. The cell resuspension was sonicated (Time: 6 min, Pulse: 10 s on and 10 s off, Amplitude: 40 %) and centrifuged on an orbital shaker for 30 min at 13,000 g. The cell free supernatant was filtered (0.2 mm filter) and allowed to pass through His-Trap HP column, and an imidazole gradient (50 – 500 mM) in buffer (50 mM Na₃PO₄ buffer pH 7.2, and 300 mM NaCl) was used to elute the recombinant protein bound to the column. The purified protein was collected and stored at -80°C.

2.5.10. Poly Acrylamide Gel Electrophoresis (PAGE)

The molecular weight of proteins was determined by 12 % Sodium Dodecyl Sulphate (SDS) - Poly Acrylamide Gel Electrophoresis (PAGE) (Laemmli *et al.*, 1970). The separating gel was prepared in separating buffer (325 mM Tris-HCl, pH- 8.8) comprised of 12 % Acrylamide-Bis acrylamide (29:1), 0.1 % SDS, and 0.1 % APS and 0.01 % TEMED. The stacking gel prepared in Stacking buffer (75 mM, Tris-HCl, pH- 6.8) with 5 % Acrylamide-Bis acrylamide (29:1), 0.1 % SDS, 0.1 % APS and 0.01 % TEMED. The protein samples were loaded with loading dye (0.25M Tris-HCl pH 6.8), 4% SDS, 20% glycerol, 0.002 % bromophenol blue) and Tris-Glycine buffer was used as running buffer. The separated proteins were stained with Coomassie Brilliant Blue-R 250.

2.6. Online tools and Softwares

Different online tools and softwares were used for data analysis and validation. Table 2.2 comprises a list of the genome analytic tools and softwares used in the study.

Table.2.2. Softwares used and its applications

Software	Applications	Source
BioRender	Create and draw scientific diagrams, and illustrations	https://www.biorender.com
BLAST	Sequence homology search and potential functional relationships	https://blast.ncbi.nlm.nih.gov/Blast.cgi
ChemDraw	Draw and edit chemical structures and reactions as well as biological objects and pathways	https://chemdrawdirect.perkinelmer.cloud/js/sample/index.html
Clone Manager 9	Primer designing, simulate restriction digests and PCR reactions, and performs sequence analysis and annotations	https://scied.com/dl_cm9.htm
ClustalW	Multiple sequence alignment to compare DNA or protein sequences to identify similarities and differences and infer evolutionary relationships	https://www.genome.jp/tool-s-bin/clustalw
Expasy ProtParm tool	Provides information about protein sequence, including its molecular weight, theoretical pI, amino acid composition, and other physicochemical properties which helps to understand the behavior and function of protein	https://web.expasy.org/protparam/
Image Lab	Gel documentation (Nucleic acid and protein)	www.biorad.com
LC solution	HPLC chromatograms – allows data analysis and management	www.shimadzu.com
OriginPro 8.5	Scientific graphing, statistical analysis and modeling	https://www.originlab.com/origin
SnapGene	Enables DNA sequence visualization, sequence annotation, sequence editing, cloning, protein visualization, and simulating common cloning methods	https://www.snapgene.com/

Minitab 17 Process optimization, data analysis and quality control. Also enables to make informed decisions based on findings <https://www.minitab.com/>

2.7. Summary

The chapter describes the procurement details of the major materials and general standard methods adopted throughout this work and this includes basic microbiology methods, analytical methods, molecular biology methods and online tools and softwares. The analytical methods for detecting proteins, sugars, nucleic acids etc. briefed here. The detection and quantitative analysis of xylonic acid, which is the focus of this thesis is elaborated in this chapter. Unless specified, the general fermentation conditions are also described. However, very specific experiments and working details are represented in respective chapters.

Chapter 3

Metabolic engineering of *Corynebacterium glutamicum* for xylonic acid production from xylose

3.1. Introduction

Xylose is one of the lignocellulosic pentoses found in nature (Zhao et al. 2020). The use of xylose as a feedstock in industrial fermentation processes has become increasingly important due to its abundance in lignocellulosic biomass, which is a sustainable and renewable source of energy (Brat D et.al 2009). Most microorganisms typically used in fermentation, such as yeasts and bacteria, can readily ferment glucose, but they cannot efficiently metabolize xylose. The fermentation of xylose requires specific enzymes and metabolic pathways that are not present in all microorganisms. For example, the yeast *Saccharomyces cerevisiae*, which is commonly used in industrial fermentation processes, cannot efficiently ferment xylose (Moysés et al. 2016). However, some other microorganisms, such as certain strains of bacteria and fungi, such as *Candida* and *Pichia* have the ability to convert xylose to useful products through a metabolic pathway known as the xylose fermentation pathway or pentose phosphate pathway (PPP). Xylose fermentation can be used to produce a variety of products, including biofuels like ethanol and butanol, as well as other valuable chemicals like amino acid, diamines, sugar alcohol *etc* (Gopinath et al. 2011; Meiswinkel et al. 2012; Wendisch et al. 2022). Also researchers precisely introduce specific genes to metabolise xylose into desired product. For example, the bacterium *Escherichia coli* has been engineered to express xylose isomerase (*xyIA*), an enzyme that converts xylose into xylulose, which can then be used by the cells for energy and biosynthesis (Zhao et al. 2020).

This chapter describes about the construction and evaluation of recombinant *Corynebacterium glutamicum* for xylonic acid synthesis from xylose. Distinctly, *Corynebacterium glutamicum* ATCC 31831 is selected as the host, as it harbours an inbuilt AraE pentose transporter which facilitates the easy uptake of pentose sugars (xylose and arabinose)

(Kawaguchi et al. 2009). Bio-production of xylonic acid from xylose is an enzymatic reaction catalyzed by NAD(P)⁺ dependant xylose dehydrogenase (xylB) and xylonolactonase (XylC) enzymes. Both the genes xylose dehydrogenase (*xylB*) and xylonolactonase (*xylC*) were amplified from *Caulobacter crescentus* xylose-inducible *xylXABCD* operon (CC0823–CC0819) (Stephens et al. 2007) and cloned into pVWEx1 *E. coli* – *C. glutamicum* shuttle vector. Subsequently the recombinant plasmid was transferred to *Corynebacterium glutamicum* ATCC 31831 competent cells and the kanamycin resistant positive colonies were selected and confirmed for further studies.

3.2. Materials and Methods

3.2.1. Microbial strains and culture conditions

Microbial strains and plasmids used in this study are listed in Table 3.1. For genetic manipulations, *E. coli* strains were grown at 37°C in Luria–Bertani (LB) medium. *C. glutamicum* strains were grown at 30°C in Brain Heart Infusion (BHI) medium and in case of recombinants appropriate antibiotics (kanamycin 25 µg mL⁻¹) were supplemented. Culture growth was measured spectrophotometrically at OD₆₀₀ nm using a UV–VIS spectrophotometer (UVA-6150, Shimadzu, Japan).

Table 3.1. Microbial strains and plasmid used in the study

Strains & Vector	Descriptions	Reference
<i>Microbial strains</i>		
<i>Corynebacterium glutamicum</i>	ATCC13032, Wild type (WT)	Abe et al. 1967
<i>Corynebacterium glutamicum</i>	ATCC 31831	Kinoshita et al. 2004
<i>Escherichia coli</i> DH5α	<i>Fthi-1 endA1 hsdR17(r-, m-)</i> <i>supE44_lacU169 f80lacZ_M15)</i> <i>recA1gyrA96 relA1</i>	Hanahan and Harbor 1983
<i>Escherichia coli</i> BL21 (DE3)	F- ompT gal dcm lon hsdSB(rB- mB-) λ(DE3)	Novagen, USA

Plasmid vector

pVWE _{x1}	Kan ^r ; <i>E. coli</i> - <i>C. glutamicum</i> shuttle vector	Peters-Wendisch et al. 2001
Xylose operon	Xylose inducible <i>xylXABCD</i> operon	Gifted by Prof. Dr. Volker F Wendisch, Bielefeld University, Germany

*Kan^r – Kanamycin resistance

3.2.2. Isolation and identification of pentose transporter (*araE*) gene from *C. glutamicum* ATCC 31831

In this study the main focus is the value addition of pentose sugar derived from lignocellulosic biomass into platform chemical xylonic acid. Pentose sugar uptake by the host organism is inevitable. *C. glutamicum* ATCC 31831 harbouring AraE pentose transporter protein which facilitates the easy uptake of pentose sugar was selected as the host organism for the study. For the confirmation of the presence of transporter the *araE* gene encoding the pentose transporter was amplified and isolated from *C. glutamicum* ATCC 31831 genomic DNA. For that, single colony of *C. glutamicum* ATCC 31831 was inoculated into 15.0 mL test tube containing 5.0 mL sterile BHI medium. The medium was incubated aerobically at 200 rpm in a rotary shaker for 16 h at 30°C. The cells from 2 mL broth were harvested by centrifugation at 6,000 g in a cooling centrifuge. Genomic DNA was isolated from the cells using the protocol (William et al., 2012) mentioned in Chapter 2 (2.5.2). The DNA was resolved in separated (EtBr) agarose gel (0.8 %) electrophoresis and visualized under gel documentation unit (Chemi Doc, BioRad, USA). The isolation of *araE* gene from the genomic DNA was performed by PCR amplification (My Cycler, Eppendorff, Germany). The oligonucleotides forward and reverse primers (Table 3.2) used for the reaction were custom made using the software clone manager

based on the sequence (NC_011916.1) available in NCBI- database using Primer BLAST (NCBI) and were procured from NEB Inc. The PCR condition for the reaction is mentioned in Table.3.3

3.2.3. Isolation of xylose dehydrogenase (*xylB*) and xylonolactonase (*xylC*) genes from xylose inducible *xylXABCD* operon

Xylose dehydrogenase (*xylB*), xylonolactonase (*xylC*) and *xylBC* genes together of *Caulobacter crescentus* were amplified from the xylose-inducible *xylXABCD* operon (CC0823–CC0819) by polymerase chain reaction (PCR) (My Cycler, Eppendorff, Germany) (Stephens et al. 2007) with appropriate primers as shown in Table 3.2. The oligonucleotides forward and reverse primers used for the reaction were custom made using the software clone manager based on the sequence available in NCBI- database using Primer BLAST (NCBI) and were procured from NEB Inc. The PCR condition for the reaction is mentioned in Table 3.3.

Table 3.2. Oligonucleotides for the amplification of *araE*, *xylB*, *xylC* and *xylBC* genes

Gene	Primer	Restriction enzyme
<i>araE</i>	FP: TAGGGATCCATGGCAGGGCACATCATCCGCTCAGAC	BamHI
	RP: GATGAATTCTCAGACCCTGGCCTTGGTGCCGTGAGCCTC AATC	EcoRI
<i>xyl B</i>	FP: CGCCAAGCTTGCATGCCTGCAGTAAAGGAGATATACATA TGTCTCAGCCATCTATCC	Pst I
	RP: CGAGCTCGGTACCCGGGGATCCCTTCACGCTGGGCCGGG ATG	BamHI
<i>xyl C</i>	FP: CGCCAAGCTTGCATGCCTGCAGTAAAGGAGATATACATA TGACCGCTCAAGTCACTTG	Pst I
	RP: CGAGCTCGGTACCCGGGGATCCGGGCGTGCGGTTAGAC AAGG	Bam HI

<i>xyl BC</i>	FP1: CGCCAAGCTTGCATGCCTGCAGTAAAGGAGATATACAT ATGTCCTCAGCCATCTATCC	Pst I
	RP 2 with linker: <u>CCCATCCACTAAACTTAAACATCAACGCCAGCCGGCGTTCGAT</u> CC	-
	FP 3 with linker: <u>TGTTTAAGTTTAGTGGATGGGATGACCGCTCAAGTCACTTGC</u> GTATGGG	Bam HI
	RP4: CGAGCTCGGTACCCGGGGATCCGGGCGTGCGGTTAGAC AAGG	

Table 3.3. PCR conditions for the amplification of *araE*, *xylB*, *xylC* and *xylBC* genes

<i>araE</i>					
Denaturation	35 Cycles			Final Extension	Hold
	Denaturation	Annealing	Extension		
95°C- 5 min	95°C- 30 sec	57°C- 1 min	72°C- 30 sec	72°C- 5 min	4°C- ∞
<i>xylB</i>					
Denaturation	35 Cycles			Final Extension	Hold
	Denaturation	Annealing	Extension		
95°C- 5 min	95°C- 30 sec	60°C- 1 min	72°C- 30 sec	72°C- 5 min	4°C- ∞
<i>xylC</i>					
Denaturation	35 Cycles			Final Extension	Hold
	Denaturation	Annealing	Extension		
95°C- 5 min	95°C- 30 sec	55°C- 1 min	72°C- 30 sec	72°C- 5 min	4°C- ∞
<i>xylBC</i>					
Denaturation	35 Cycles			Final Extension	Hold
	Denaturation	Annealing	Extension		
95°C- 5 min	95°C- 30 sec	65°C- 1 min	72°C- 30 sec	72°C- 5 min	4°C- ∞

3.2.4. Cloning of *xylB*, *xylC* and *xylBC* genes into *E. coli* – *C. glutamicum* shuttle vector, pVWEx1, and transformation into *C. glutamicum* competent cells

The isolated *xylB* and *xylC* genes of size (747 bp - *xylB*, 870 bp - *xylC*) were purified by gel elution, verified by sequencing and cloned separately into the restriction digestion site (*Bam*HI/*Pst*I) of pVWEx1 shuttle vector. The recombinant plasmids so-called pVWEx1-*xylB* and pVWEx1-*xylC*.

Also genes *xylB* and *xylC* were tailored together for the construction of recombinant pVWEx1-*xylBC* plasmid. The gene amplification for the tailoring reaction was performed with specially designed primer with linker sequence *xylBC* FP and *xylBC* RP (Table 3.2) under PCR conditions mentioned in Table 3.3. The gene size of *xylBC* is 1811 bp.

The recombinant plasmids pVWEx1-*xylB*, pVWEx1-*xylC* and pVWEx1-*xylBC* were transformed independently into *E. coli* DH5 α cells and the transformants bearing pVWEx1 derivatives were screened in LB medium supplemented with kanamycin (25 $\mu\text{g mL}^{-1}$). Competent cells of *C. glutamicum* ATCC 13032 and ATCC 31831 were prepared (Chapter 2 section 2.5.9) and the recombinant plasmids were electroporated (Biorad, USA) (Chapter 2 section 2.5.10) into both the *C. glutamicum* strains with parameters set at 25 μF , 600 Ω and 2.5 kV, yielding a pulse duration of 10 ms and the positive clones were selected in LBHIS kanamycin (25 $\mu\text{g mL}^{-1}$) plates (van der Rest et al. 1999). The transformants containing gene insert were analysed by colony PCR (Chapter 2 section 2.5.4) using gene specific primers i.e *xylB* FP and *xylB* RP for *xylB* gene, *xylC* FP and *xylC* RP for *xylC* gene and *xylBC* FP and *xylBC* RP for *xylBC* genes (Table 3.2). The PCR samples were analyzed by pre-stained (EtBr) agarose gel (1.0 %) electrophoresis and visualized under gel documentation unit (Chemi Doc, BioRad,

USA). The amplicons were gel purified, sequenced (Sanger's method) and the sequences obtained were analysed and confirmed by NCBI- BLAST.

3.3. Results

3.3.1. *E. coli* – *C. glutamicum* shuttle vector

The pVWEx1 shuttle vector is a plasmid vector used for recombinant protein expression in both bacterial and eukaryotic host cells. pVWEx1 vector can replicate in both Gram-positive and Gram-negative bacteria. It contains an origin of replication (*ori*) from *Escherichia coli* and a replication origin (*oriV*) from the *Streptomyces* species. This vector has a multiple cloning site (MCS) for the insertion of foreign DNA, and a *lacZ* alpha-complementation system for screening recombinant clones. It also has a kanamycin resistance gene as a selectable marker for bacteria that carry the plasmid and also promoter and termination sequences. Fig.3.1.a. shows the pVWEx1 vector map and Fig.3.1.b. shows the single and double digestion profile of the vector.

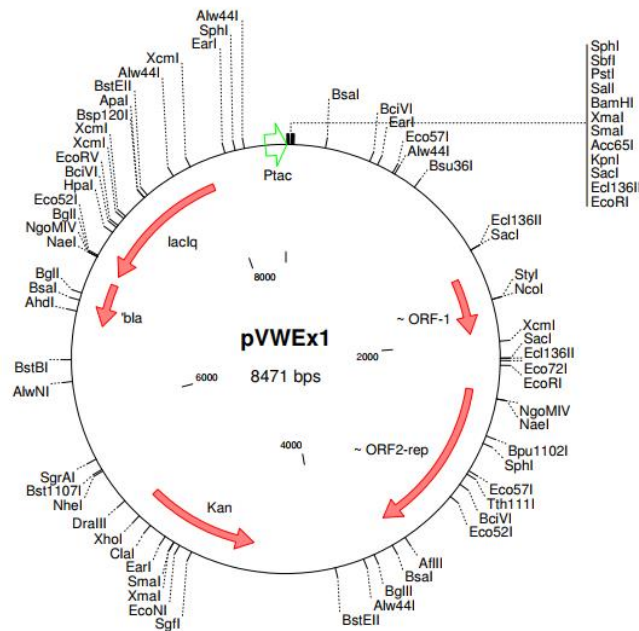


Fig.3.1.a. pVWEx1 vector map (giving sequence in Annexure III)

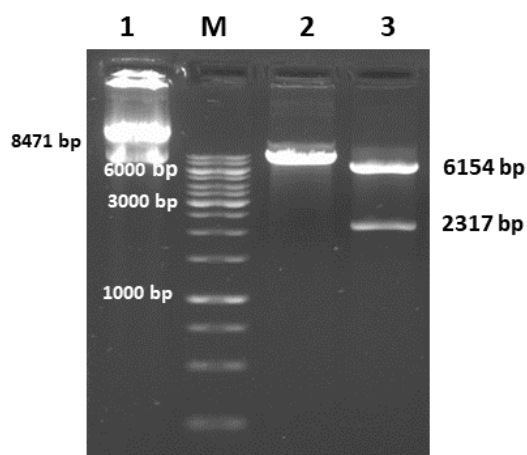


Fig.3.1.b. Restriction digestion confirmation of pVWEx1 digested with restriction enzymes EcoRI and Sall. Lane M: 1 kb DNA molecular weight marker; Lane 1: pVWEx1 native plasmid; Lane 2: linearized plasmid on digestion with Sall; Lane 3: double digested fragments with EcoRI and Sall.

3.3.2. Amplification of *araE* gene from *C. glutamicum* ATCC 31831 and sequence confirmation

The AraE pentose transporter protein that plays an important role in transporting pentose sugars across the cell membrane in bacteria. Specifically, it is responsible for the uptake of xylose and arabinose, five carbon sugars that is commonly found in plant cell wall, into the bacterial cells (Zhao et al. 2020). The function of AraE pentose transporter is regulated by a number of factors, including the presence of other sugars in the extracellular environment. Fig.3.2. shows the amplification of *araE* gene from genomic DNA of *C. glutamicum* ATCC 31831. Sequencing analysis also confirms the presence of AraE pentose transporter in *C. glutamicum* ATCC 31831. The 1140 bp sequence of *araE* gene (Fig.3.3.) was analysed and verified by NCBI-BLAST, showed 100% (Fig.3.4.) similarity to the reported sequences available in the nucleotide database.

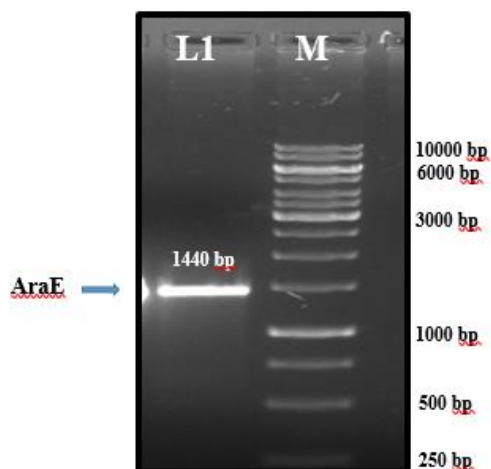


Fig.3.2. Gel picture showing the amplification of *araE* gene from genomic DNA of *C. glutamicum* ATCC 31831. Lane M: 1 kb DNA molecular weight marker; Lane 1: Pentose transporter gene (*araE*) (1440 bp)

```

ATGGCAGGGCACATCATCCGCTCAGACAGCCGGCCAATCGAAGGAGTAATGATGACAGAGA
CTGTTCAACAAACCAAGAAGATCCCCGACCGTACATCTACTTCTTCGGTTCATTTCGGCGGGA
TTCTCTTCGGCTACGACATCGGCGTGATGACCGGCGCCCTCCCTTTCCTACAGAGTGACTGGA
ACATCCAGCACGAAGCCGCCATCATCGGCTGGATCACCTCTTCGCTCATGCTTGGCGCCGCTCT
TCGGCGGTGTA CTGCGGCCAGCTCTCCGACAAGCTCGGCCGCCGCAAATGATCCTCTTCT
CTGCGCTGGTATTCATGATCTTCTCACTCGGCTGCGCGGTGCTCCGGACGGCGGCTGGGTCT
TCCTGGCCATCGTCCGCGTGTTCTCGGACTCGGCGTCGGCGCAGCCTCCGCCCTCGTCCCCG
CCTACATGTCCGAAATGGCGCCCCGGAAGATCCGCGGCCGGCTCTCCGGCCTCAACCAGACG
ATGATCGTCTCCGGTATGCTCGCCTCTACATTGTGCTTATTTCTGCGAAACCTCCACGAGA
CCACCGCATGGCGGCTCATGCTCGGGCTCGCCGCAATCCCTGCCCTCGTCTCTTCTCGGTG
TGCTGCGCCTGCCGGAATCCCCGCGTTTCTCATCAAGAACGGCCGCATCGAAGAGGCCCGC
ACCGTGCTCAGTTACATCCGCGATAACGACGCCATCGATTCCGAGCTCAAGAACATCCAGGA
GACCGCCGAACTGGAGAACGCCATCCAGGCCAAGACCAGACTCGCGACCCTATTCAGCGGAC
GCTACCGCTACCTCGTCGACGCCGGTGTGCGGTGTCGCTGCCTTCCAGCAGTTCAGGGCGCGA
ACGCCATCTTCTACTACATCCCGCTCATCGTCGAGAAGGCCTCCGGCACCAGGGCGTCCAATG
CGCTCATGTGGCCGATCATCCAGGGCGTCATCCTAGTTCTCGGTTCCCTGCTGTTTCATGGTCAT
CGCCGACAAGTTCAACCGACGCACCCTGCTCACAGTCGGAGGCACGGTCATGGGCCTGTCTTT
CCTCTTCCCACCTTCATTCACATGACGATCCCGGATGCCAACCCTCATGATGATCGTGGTCTT
CCTGTCCATCTACGTGGCCTTCTACTCCTTTACCTGGGCCCGCTGACCTGGGTTCATCGTTGGC
GAGATCTTCCCGTTAGCCATCCGCGGCCGCGCCTCCGGATTGGCGTCTCTTCAACTGGATC
GGTTCCTTCTCCGTCGGCTTACTTTTCCCAATTATGACCGCCAGATGACCCAGGACGCGGTC
TTCGCGATCTTCGGCATCATCTGTATCCTCGGTGTCCTGTTTCGTCGATTCTCGTCCCAGAGA
CCCGCGGACGCACACTCGAGGAGATTGAGGCTCACGGCACCAAGGCCAGGGTCTGA

```

Fig 3.3. The nucleotide sequence of *araE* gene isolated from *C. glutamicum* ATCC 31831

Download ▾ GenBank Graphics

Corynebacterium glutamicum DNA, L-arabinose utilization gene cluster, strain: ATCC 31831

Sequence ID: [AB447371.1](#) Length: 12108 Number of Matches: 1

Range 1: 382 to 1821 GenBank Graphics ▾ Next Match ▲ Previous Match

Score	Expect	Identities	Gaps	Strand
2660 bits(1440)	0.0	1440/1440(100%)	0/1440(0%)	Plus/Minus

```

Query 1   ATGGCAGGGCACATCATCCGCTCAGACAGCCGGCCAATCGAAGGAGTAATGATGACAGAG 60
          |||
Sbjct 1821 ATGGCAGGGCACATCATCCGCTCAGACAGCCGGCCAATCGAAGGAGTAATGATGACAGAG 1762

Query 61   ACTGTTCAACAAACCAAGAAGATCCCCGACCGTACATCTACTTCTTCGGTTCATTTCGGC 120
          |||
Sbjct 1761 ACTGTTCAACAAACCAAGAAGATCCCCGACCGTACATCTACTTCTTCGGTTCATTTCGGC 1702

Query 121  GGGATTCTCTTCGGCTACGACATCGGCGTGATGACCGGCGCCCTCCCTTTCTACAGAGT 180
          |||
Sbjct 1701 GGGATTCTCTTCGGCTACGACATCGGCGTGATGACCGGCGCCCTCCCTTTCTACAGAGT 1642

```

Fig.3.4. NCBI-BLAST analysis of *araE* gene sequence from *C. glutamicum* ATCC 31831

3.3.3. Isolation of genes from xylose operon of *Caulobacter crescentus*

The genes for the metabolic pathway were isolated from *Caulobacter crescentus* xylose operon (*xyIXABCD*) (Fig.3.5) by PCR. The amplification of *xyIB*, *xyIC* and *xyIBC* genes are shown in Fig.3.6.

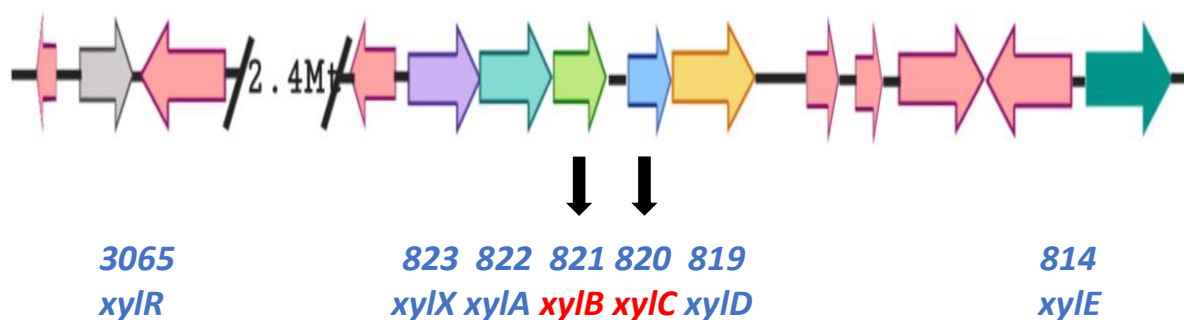


Fig.3.5. Graphical representation of *Caulobacter crescentus* xylose inducible *xyIXABCD* operon

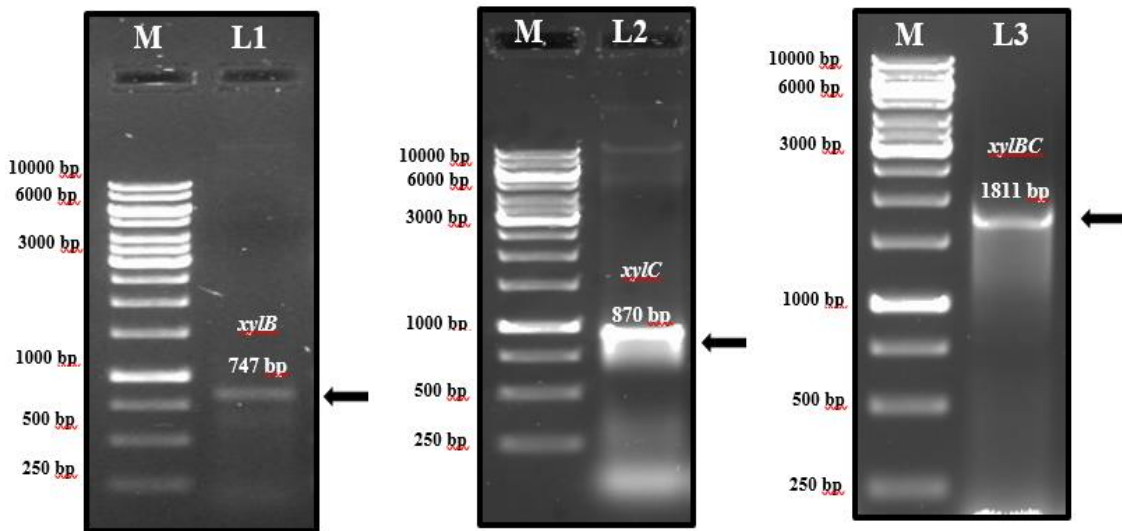


Fig.3.6. Gel picture showing the amplification of *xylB*, *xylC* and *xylBC* genes. Lane M :1 kb DNA molecular weight marker; Lane 1 (L1) : xylose dehydrogenase (*xylB*) gene (747 bp); Lane 2 (L2) : xylonolactonase (*xylC*) gene (870 bp) and Lane 3 (L3) : *xylBC* gene (1811 bp).

The 747 bp gene sequences of *xylB* (Fig.3.7.) and 870 bp gene sequence of *xylC* (Fig.3.8.) obtained were analysed and verified by NCBI-BLAST, showed 99% (Fig.3.9.) and 100% (Fig.3.10.) similarity to the reported sequences available in the nucleotide database.

```

ATGTCCTCAGCCATCTATCCCAGCCTGAAGGGCAAGCGCGTCGTCATCACCGGCGGGCGGC
TCGGGCATCGGGGCCGGCCTCACCGCCGGCTTCGCCGTCAGGGCGCGGGTGATCTTCCT
CGACATCGCCGACGAGGACTCCAGGGCTCTTGAGGCCGAGCTGGCCGGCTCGCCGATCCC
GCCGGTCTACAAGCGCTGCGACCTGATGAACCTCGAGGCGATCAAGGCGGTCTTCGCCGA
GATCGGCGACGTCGACGTGCTGGTCAACAACGCCGGAATGACGACCGCCACAAGCTGG
CCGACGTGACCGGCGCCTATTGGGACGAGCGGATCAACGTCAACCTGCGCCACATGCTGT
TCTGCACCCAGGCCGTCGCGCCGGGCATGAAGAAGCGTGCCGGCGGGGCGGTGATCAAC
TTCGGTTCGATCAGCTGGCACCTGGGGCTTGAGGACCTCGTCCTCTACGAAACCGCCAAG
GCCGGCATCGAAGGCATGACCCGCGCGCTGGCCCGGGAGCTGGGTCCCGACGACATCCG
CGTCACCTGCGTGGTGCCGGGCAACGTCAAGACCAAGCGCCAGGAGAAGTGGTACACGC
CCGAAGGCGAGGCCAGATCGTGGCGGCCAATGCCTGAAGGGCCGCATCGTCCCGGAG
AACGTGCGCCGCGTGGTGCTGTTCTGTCCTGGCCTCGGATGACGCGTCGCTCTGCACCGGCCAC
GAATACTGGATCGACGCCGGCTGGCGTTGA

```

Fig 3.7. The nucleotide sequence of *xylB* gene isolated from *xylXABCD* operon of *Caulobacter crescentus*

Download ▾ GenBank Graphics

Caulobacter crescentus NA1000, complete genome
Sequence ID: [CP001340.1](#) Length: 4042929 Number of Matches: 1

Range 1: 942458 to 943204 [GenBank](#) [Graphics](#) ▾ Next Match ▲ Previous Match

Score	Expect	Identities	Gaps	Strand
1367 bits(740)	0.0	745/747(99%)	2/747(0%)	Plus/Minus
Query 1		ATGTCCTCAGCCATCTATCCAGCCTGAAGGGCAAGCGCGTCGTATCACCGCGCGCGC		60
Sbjct 943204		ATGTCCTCAGCCATCTATCCAGCCTGAAGGGCAAGCGCGTCGTATCACCGCGCGCGC		943145
Query 61		TCGGGCATCGGGCCGGCTCACCGCCGGCTTCGCCCGTCAGGGCGCGG--GTGATCTTC		118
Sbjct 943144		TCGGGCATCGGGCCGGCTCACCGCCGGCTTCGCCCGTCAGGGCGCGGAGGTGATCTTC		943085
Query 119		CTCGACATCGCCGACGAGGACTCCAGGGCTCTTGAGGCCGAGCTGGCCGGCTCGCCGATC		178
Sbjct 943084		CTCGACATCGCCGACGAGGACTCCAGGGCTCTTGAGGCCGAGCTGGCCGGCTCGCCGATC		943025

Fig 3.9. NCBI-BLAST analysis of *xylB* gene sequence from *Caulobacter crescentus*

```

ATGACCGCTCAAGTCACTTGCATATGGGATCTGAAGGCCACGTTGGGCGAAGGCCCGATCTG
GCATGGCGACACCCTGTGGTTCGTCGACATCAAGCAGCGTAAAATCCACAACACCACCCCG
CCACCGGCGAGCGCTTCAGCTTCGACGCGCCGGATCAGGTGACCTTCCTCGCGCCGATCGTCG
GCGCGACCGGCTTTGTCGTCGGTCTGAAGACCGGGATTCACCGCTTCCACCCGGCCACGGGCT
TCAGCCTGCTGCTCGAGGTCGAGGACGCGGCGCTGAACAACCGCCCCAACGACGCCACGGTC
GACGCGCAAGGCCGTCTGTGGTTCGGCACCATGCACGACGGGGAAGAGAACAATAGCGGCT
CGTCTATCGGATGGACCTCACCGGCGTCGCCCGGATGGACCGCGACATCTGCATCACCAC
GGCCCGTGCCTCGCCGACGGCAAGACCTTCTACCACACCGACACCCTGGAAAAGACGAT
CTACGCCTTCGACCTGGCCGAGGACGGCCTGCTGTGAACAAGCGCGTCTTCGTGCAGTTTCG
CCTGGGCGACGATGTCTATCCGGACGGTTCGGTTCGTCGATTCCGAAGGCTATCTGTGGACCGC
CCTGTGGGGCGGTTTCGGCGCGGTCCGCTTCTCGCCGCAAGGCGACGCCGTGACGCGCATCG
AACTGCCCGCCCCAACGTCACCAAGCCCTGCTTCGGCGGGCCTGACCTGAAGACCCTCTATT
TCACCACCGCCCGCAAGGGCCTGAGCGACGAGACCTGGCCAGTACCCGCTGGCCGGCGGT
GTGTTCCCGTTCGGTTCGATGTGGCCGGCCAACCCAGCATGAGGTCCGCTTGTCTAA

```

Fig 3.8. The nucleotide sequence of *xylC* gene isolated from *xylXABCD* operon of *Caulobacter crescentus*

Download ▾ GenBank Graphics

Caulobacter crescentus NA1000, complete genome
Sequence ID: [CP001340.1](#) Length: 4042929 Number of Matches: 1

Range 1: 941464 to 942333 [GenBank](#) [Graphics](#) ▾ Next Match ▲ Previous Match

Score	Expect	Identities	Gaps	Strand
1607 bits(870)	0.0	870/870(100%)	0/870(0%)	Plus/Minus
Query 1		ATGACCGCTCAAGTCACTTGCATATGGGATCTGAAGGCCACGTTGGGCGAAGGCCCGATC		60
Sbjct 942333		ATGACCGCTCAAGTCACTTGCATATGGGATCTGAAGGCCACGTTGGGCGAAGGCCCGATC		942274
Query 61		TGGCATGGCGACACCCTGTGGTTCGTCGACATCAAGCAGCGTAAAATCCACAACACCAC		120
Sbjct 942273		TGGCATGGCGACACCCTGTGGTTCGTCGACATCAAGCAGCGTAAAATCCACAACACCAC		942214
Query 121		CCCGCCACCGGCGAGCGCTTCAGCTTCGACGCGCCGGATCAGGTGACCTTCCTCGCGCCG		180
Sbjct 942213		CCCGCCACCGGCGAGCGCTTCAGCTTCGACGCGCCGGATCAGGTGACCTTCCTCGCGCCG		942154

Fig 3.10. NCBI-BLAST analysis of *xylC* gene sequence from *Caulobacter crescentus*

3.3.4. Construction of pVWEx1-*xylB*, pVWEx1-*xylC* and pVWEx1-*xylBC* plasmid

The xylose metabolizing genes *xylB* and *xylC* were cloned individually as well as together under IPTG inducible Ptac promoter of pVWEx1 shuttle vector to obtain recombinant pVWEx1-*xylB*, pVWEx1-*xylC* and pVWEx1-*xylBC* plasmids shown in Fig.3.11.

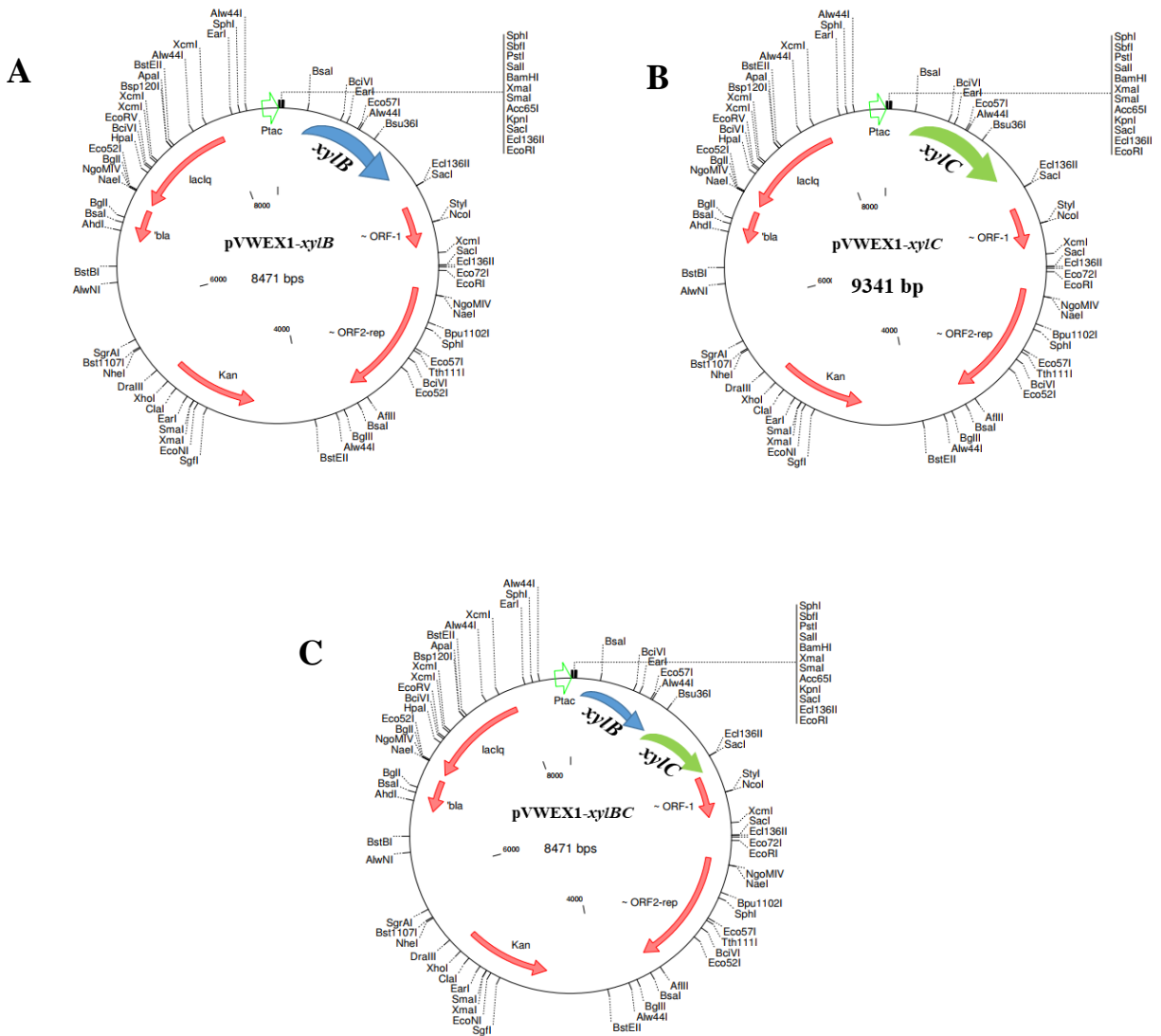


Fig.3.11. Vector map of pVWEx1 derivatives (A) pVWEx1-*xylB*; (B) pVWEx1-*xylC* and (C) pVWEx1-*xylBC*

The recombinant plasmids pVWEX1-*xylB*, pVWEX1-*xylC* and pVWEX1-*xylBC* were transformed into competent cells of both *C. glutamicum* ATCC 31831 (Fig.3.12) and *C. glutamicum* ATCC 13032 (Fig.3.14) under electroporation conditions, resistance: 600 Ω ; capacitance: 25 μ F and conductivity: 2.5 kv. The positive colonies were selected in kanamycin (25 μ g mL^{-1}) supplemented LBHIS plates.

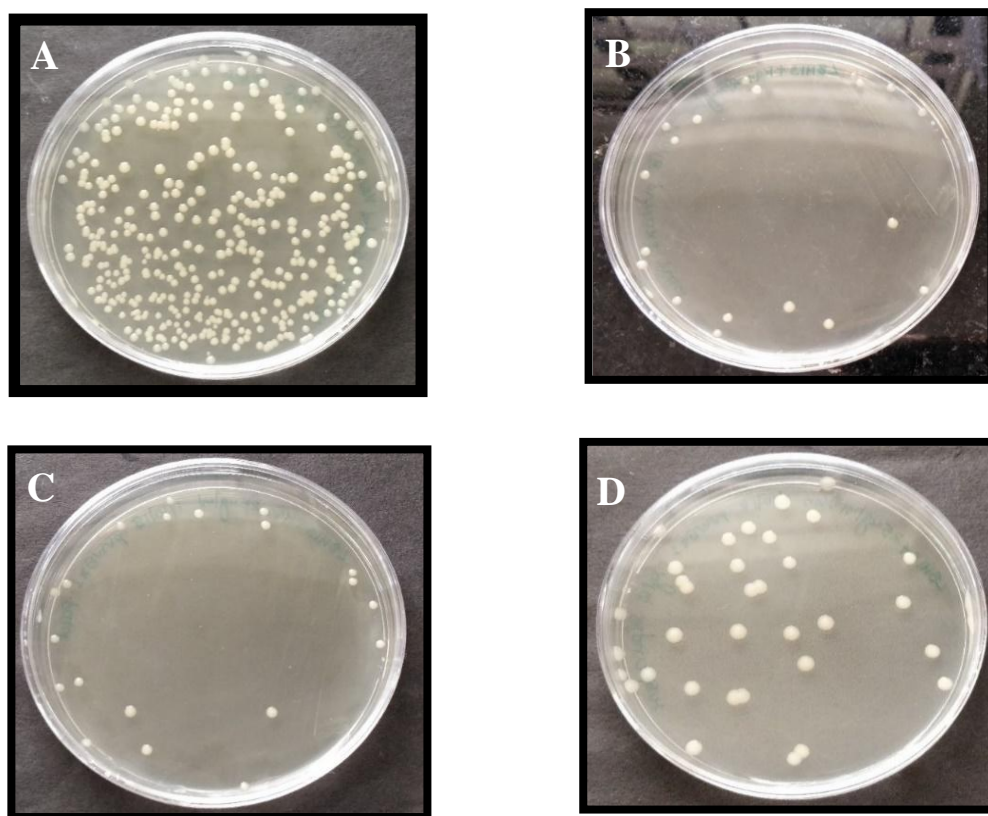


Fig.3.12. Transformed colonies of *C. glutamicum* 31831 with (A) pVWEX1(control vector) (B) pVWEX1-*xylB*, (C) pVWEX1-*xylC* and (D) pVWEX1-*xylBC*

Genes in the recombinant plasmid (pVWEX1-*xylB*, pVWEX1-*xylC* and pVWEX1-*xylBC*) were confirmed by restriction digestion mapping with restriction enzymes BamHI and PstI in both *C. glutamicum* 31831 (Fig.3.13) and *C. glutamicum* 13032 (Fig.3.15).

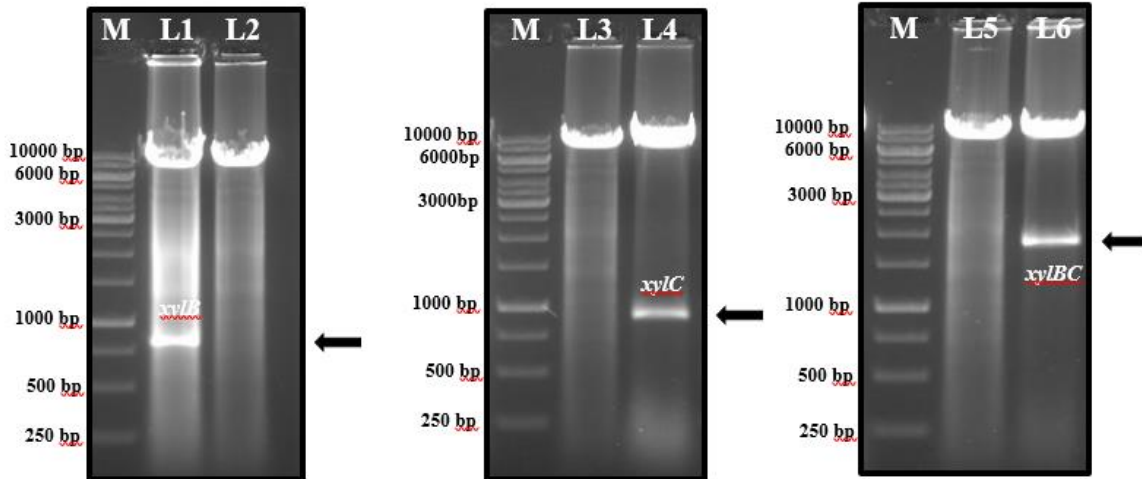


Fig.3.13. Gel picture showing restriction digestion mapping of pVWEx1 recombinant plasmids containing *xylB*, *xylC* and *xylBC* genes in *C. glutamicum* ATCC 31831. Lane L2, L3 and L5 shows the empty vector pVWEx1. Lane M: 1kb DNA ladder. Lane L1: pVWEx1 with *xylB*; Lane L4: pVWEx1 with *xylC* and Lane L6: pVWEx1 with *xylBC*. Lanes L1, L4 and L6 shows the recombinant vector digested with combinations of restriction enzymes BamHI and PstI, where the gene insert got released *xylB* (747 bp), *xylC* (870 bp) and *xylBC* (1811 bp) respectively.

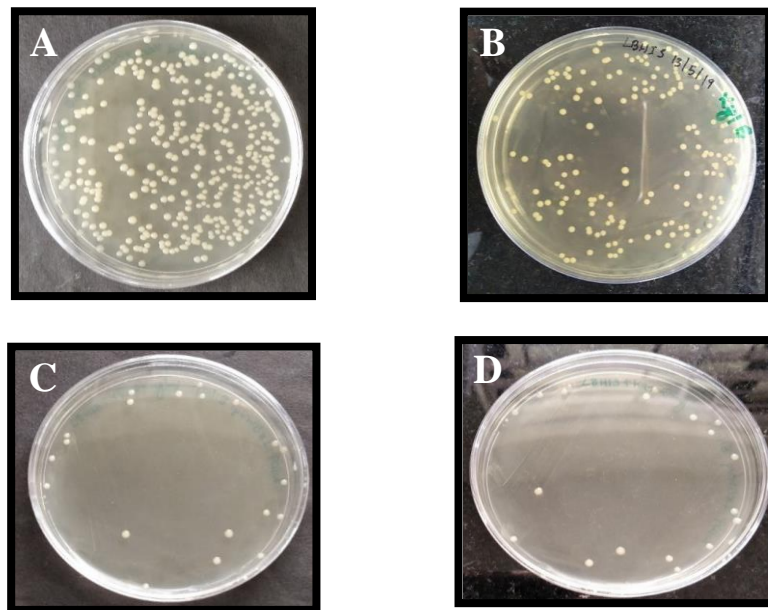


Fig.3.14. Transformed colonies of *C. glutamicum* 13032 with (A) pVWEx1 (control vector), (B) pVWEx1-*xylB*, (C) pVWEx1-*xylC* and (D) pVWEx1-*xylBC*

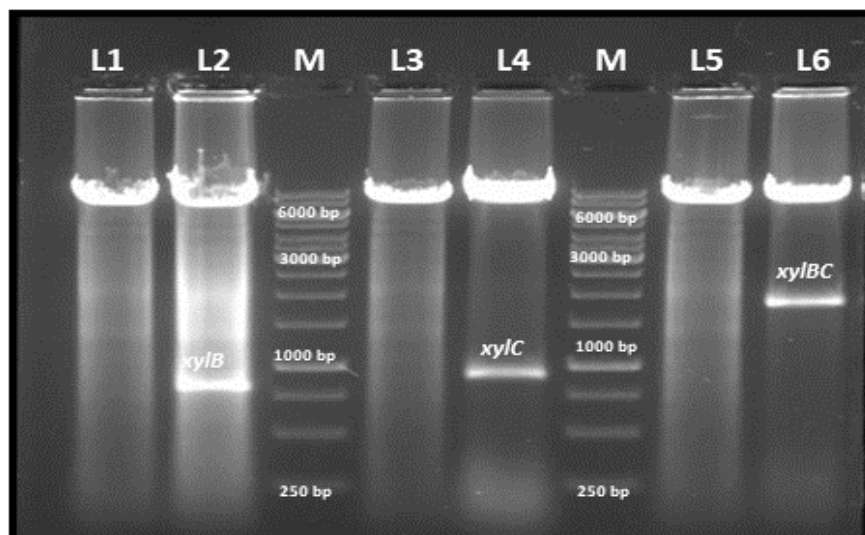


Fig.3.15. Gel picture showing restriction digestion mapping of pVWEx1 recombinant plasmids containing *xylB*, *xylC* and *xylBC* genes in *C. glutamicum* ATCC 13032. Lane L1, L3 and L5 shows the empty vector pVWEx1. Lane M: 1kb DNA ladder. Lane L2: pVWEx1 with *xylB* (747 bp); Lane L4: pVWEx1 with *xylC* (870 bp) and Lane L6: pVWEx1 with *xylBC* (1811 bp). Lanes L2, L4 and L6 shows the recombinant vector digested with combinations of restriction enzymes BamHI and PstI, where the gene insert got released *xylB* (747 bp), *xylC* (870 bp) and *xylBC* (1811 bp) respectively.

3.4. Discussion

The production of xylonic acid by microorganisms has been known since the late 19th century, (Herrera et al. 2021). Many types of bacteria, including *Pseudomonas*, *Acetobacter*, *Aerobacter*, *Gluconobacter*, *Erwinia* and similar genera, have been found to be capable of producing xylonic acid (Buchert J 1988). Later on xylonic acid production has been achieved by modifying different types of yeast strains and the bacterium *Escherichia coli*. This was accomplished through the incorporation of genes that encode for xylose dehydrogenase, as demonstrated in studies conducted by (Toivari et al. in (2010), Nygård et al. in (2011), and Liu et al. in (2012).

The synthetic pathway is more suitable for *C. glutamicum* compared to *E. coli* while wild type *C. glutamicum* ATCC 13032 lacks natural xylose catabolism and allosteric sugar competition (Kawaguchi et al., 2009). In *C. glutamicum* ATCC 31831 xylonic acid synthesis from xylose is achieved with the catalysis of two enzymes (xylose dehydrogenase and xylonolactonase) which was adopted from a Gram negative bacterium *Caulobacter crescentus*. Where xylose dehydrogenase catalyse the conversion of xylose into xylonolactone and xylonolactonase converts xylonolactone into xylonic acid. Similarly, Yim et al in (2017) metabolically engineered *C. glutamicum* for xylonic acid production from xylose. Along with xylose metabolizing genes they also introduced *xylE* transporter gene for easy uptake of C5 sugar and its conversion into xylonic acid.

Despite a few bacterial species having demonstrated xylose dehydrogenase activity such as *Trichoderma reesei*, *Pseudomonas fragi*, *Arthrobacter sp.*, only one xylose dehydrogenase with high specificity, catalytic activity and stability for xylose has been discovered in *C. crescentus*. *Caulobacter crescentus* xylose dehydrogenase has a high affinity for xylose because it has a specific structural arrangement that allows for optimal binding of the xylose substrate (Stephens et al. 2007). The evolution of genetically modified production strains unveils revolutionary opportunities for the advancement of strong industrial formulas in the manufacture of xylonic acid

3.5. Summary

Xylose dehydrogenase (*xyl B*) and xylonolactonase (*xyl C*) genes involved in xylonic acid metabolism were amplified from *Caulobacter crescentus* xylose inducible *xylXABCD* operon. The purified *xyl B* (747 bp), *xyl C* (870 bp) and *xyl BC* (1811 bp) genes were restriction digested with BamHI and PstI enzymes and cloned into pVWEx1 (*E. coli/Corynebacterium*) shuttle

vector. The pVWEx1 derivatives were transformed into two different strains of *C. glutamicum*. One wild type *C. glutamicum* ATCC 13032 and the other harbouring AraE pentose transporter protein i.e, *C. glutamicum* ATCC 31831. The positive recombinant strains *C. glu-xylB*, *C. glu-xylC* and *C. glu-xylBC* were selected in kanamycin ($25 \mu\text{g mL}^{-1}$) plates and were confirmed by plasmid double digestion and insert release. The presence of pentose transporter gene in *C. glutamicum* ATCC 31831 was confirmed by *araE* gene amplification and sequencing from the genomic DNA of *C. glutamicum* ATCC 31831.

Chapter 4

Production of xylonic acid by recombinant *Corynebacterium glutamicum* ATCC 31831 using synthetic medium

4.1. Introduction

Functional recombinant *C. glutamicum* which can metabolize lignocellulosic xylose to xylonic acid was constructed in view of value addition of Acid Pre-treated Liquor (APL) generated by the bio-ethanol industries. After constructing xylose utilizing strains they have to be validated and for that initially studies were conducted in defined CGXII synthetic medium to see whether they can use xylose as sole carbon source, and also to analyse the potential for multiple sugar utilization.

This chapter deals with the functional validation of xylose metabolizing recombinant strains of *C. glutamicum* for xylonic acid production in defined synthetic medium. Initially, the *Caulobacter crescentus* NAD⁺ dependent xylose dehydrogenase (*xylB*) and xylonolactonase (*xylC*) genes separately as well as together (*xylBC*) were expressed in *C. glutamicum*. Fermentation studies for xylose uptake and conversion rate, xylonic acid production were carried out by recombinant strains in flask level in synthetic medium. Among which the best strain showed relatively higher xylonic acid production titer was screened out for further studies. After screening the best recombinant strain, the process parameters were optimized using statistical tool Response Surface Methodology (RSM) for maximal xylonic acid production. With the optimized parameters the process was evaluated at bioreactor (2.5 L) level as well.

4.2. Materials and Methods

4.2.1. Microbial strains and culture conditions

C. glutamicum strain ATCC 31831 and ATCC 13032 were grown at 30°C in Brain Heart Infusion (BHI) medium. *C. glutamicum* ATCC 31831 which harbours AraE pentose transporter facilitates the uptake of pentose sugars and its metabolism. For comparative analysis, *C. glutamicum* strain ATCC 13032 which lacks AraE pentose transporter was used as control strain.

Fermentation studies were carried out using all the recombinant strains of *C. glutamicum* constructed for xylonic acid synthesis such as *C. glu-xylB* (over expressing xylose dehydrogenase), *C. glu-xylC* (over expressing xylonolactonase) and *C. glu-xylBC* (over expressing both xylose dehydrogenase and xylonolactonase). CGXII basal medium (Keilhauer et al., 1993) modified with altering sugar composition was used as fermentation medium. Details of the media components are described in Annexure II.

4.2.2. Comparative growth analysis of C. glutamicum ATCC 31831 and recombinant C. glutamicum ATCC 31831 (C. glu-xylB) in CGXII medium with xylose as carbon source

Initially, the efficacy of *C. glutamicum* ATCC 31831 and recombinant *C. glutamicum* ATCC 31831 (*C. glu-xylB*) to utilize xylose for the growth was analysed. Pure culture of both the strains were inoculated into CGXII medium with 4% xylose as carbon source and incubated at 30°C. Samples were collected at regular intervals of 12 h to measure the OD of the culture at 600 nm.

4.2.3. Comparative growth analysis of C. glutamicum ATCC 31831 and recombinant C. glutamicum ATCC 31831 (C. glu-xylB) strain in CGXII medium containing xylose and glucose mixture as carbon source

Initially *C. glutamicum* was supplemented with xylose alone as the carbon source as mentioned in section 4.2.2. With a very poor growth rate in the presence of xylose alone, a minimum level of glucose (1%) was added to the CGXII medium along with xylose (3%).

4.2.4. Screening of recombinant strains of C. glutamicum under different combinations of glucose and xylose for xylonic acid production

All the recombinant strains of *C. glutamicum* constructed for xylonic acid synthesis were subjected to submerged fermentation in CGXII medium. Different combinations of glucose

(G) and xylose (X) (0.1% G and 3.9% X, 0.25% G and 3.75% X and 0.5% G and 3.5% X) were supplemented in separate batches. Fermentation was carried out in 100 mL of the medium dispensed in 250 mL Erlenmeyer flask supplemented with antibiotic (kanamycin ($25 \mu\text{g mL}^{-1}$)) and inoculated with 16 h old recombinant strains (1% (v v^{-1}) inoculum). The flasks were incubated at 200 rpm for 120 h at 30°C . The expression of recombinant genes were induced with IPTG (1 mM) after inoculation. Samples were collected at regular interval of 12 h and centrifuged at 6000 g for 5 min. The culture supernatant was analyzed for sugar utilization and xylonic acid production by HPLC (Chapter 2, section 2.4.2).

4.2.5. Medium engineering by response surface methodology (RSM) for xylonic acid production

From the growth analysis and xylose uptake studies, *C. glu-xyIB* (ATCC 31831) with xylose dehydrogenase gene was selected for xylonic acid production. Response surface methodology was applied to identify the operating variables that have a significant effect on xylonic acid production. A Box Behnken experimental design (BBD) (Box and Behnken 1960) with four independent variables that may affect xylonic acid production, including $(\text{NH}_4)_2\text{SO}_4$ ($2.5\text{-}12.5 \text{ g L}^{-1}$), urea ($4.5\text{-}18.5 \text{ g L}^{-1}$), xylose ($30\text{-}90 \text{ g L}^{-1}$) and inoculum ($7.5\text{-}15\% \text{ (v v}^{-1})$) were studied at three levels -1, 0 and +1 which correspond to low, medium and high values respectively (Table 4.1). Responses were measured as titer (g L^{-1}) of xylonic acid. The statistical as well as numerical analysis of the model was evaluated by analysis of variance (ANOVA) (Table 4.2) which included p-value, regression coefficient, effect values and F-value using Minitab 17 software.

Table 4.1. Box-Behnken experimental design matrix with experimental values of xylonic acid production by *Corynebacterium glutamicum* ATCC 31831

Run Order	Urea (gL ⁻¹)	Xylose (gL ⁻¹)	(NH ₄) ₂ SO ₄ (gL ⁻¹)	Inoculum (% vv ⁻¹)	Xylonic acid (gL ⁻¹)
1	11.5	60	7.5	11.25	56.12 ± 0.3
2	11.5	90	2.5	11.25	59.79 ± 0.2
3	11.5	30	12.5	7.5	25.06 ± 0.1
4	4.5	30	7.5	15	21.36 ± 0.4
5	18.5	60	2.5	15	52.48 ± 0.3
6	11.5	30	2.5	7.5	25.06 ± 0.2
7	11.5	90	12.5	15	58.42 ± 0.1
8	4.5	60	12.5	11.25	30.34 ± 0.4
9	18.5	90	7.5	15	58.80 ± 0.3
10	4.5	90	7.5	11.25	45.75 ± 0.3
11	18.5	60	12.5	15	48.98 ± 0.1
12	11.5	60	7.5	15	56.02 ± 0.2
13	11.5	60	7.5	11.25	56.32 ± 0.3
14	18.5	30	7.5	11.25	28.35 ± 0.4
15	4.5	60	2.5	7.5	28.82 ± 0.2

4.2.6. Batch fermentation for xylonic acid production in 2.5 L fermenter

The fermentation was carried out in 2.5 L Infors HT multifors fermenter with automated system for pH, temperature and DO. The working volume was set to 1.0 L with sterile medium and inoculated with freshly prepared 16 h old *C. glu-xyIB* cells (11.25 % (vv⁻¹) inoculum). The genes were induced with 1mM IPTG immediately after inoculation of the production medium. The DO was set at 10% with a variable stirrer speed 50 to 200 rpm under a static aeration rate 2.0 vvm. Samples were taken at 12 h intervals and analyzed for sugar utilization and xylonic acid production. The effect of dissolved oxygen (DO; 0, 10, 20, 30 and 40%) was also analyzed. The

DO was maintained with help of cascade action of aeration (0.2 vvm) and agitation (200 rpm) during fermentation. The control of fermentation study was carried out at 200 rpm agitation without aeration.

4.3. Results

4.3.1. Growth analysis of *C. glutamicum* ATCC 31831 and recombinant *C. glu-xytB* (ATCC 31831) in CGXII medium with xylose as carbon source

It was observed that both the strains could grow in xylose medium but the growth rate was very low. After 120 h growth analysis *C. glutamicum* ATCC 31831 reached an OD₆₀₀ value of 0.4 on the other hand recombinant *C. glu-xytB* reached an OD₆₀₀ value of 0.7. On correlation it was noticed that recombinant strain is picking up better growth than wild type strain (Fig.4.1).

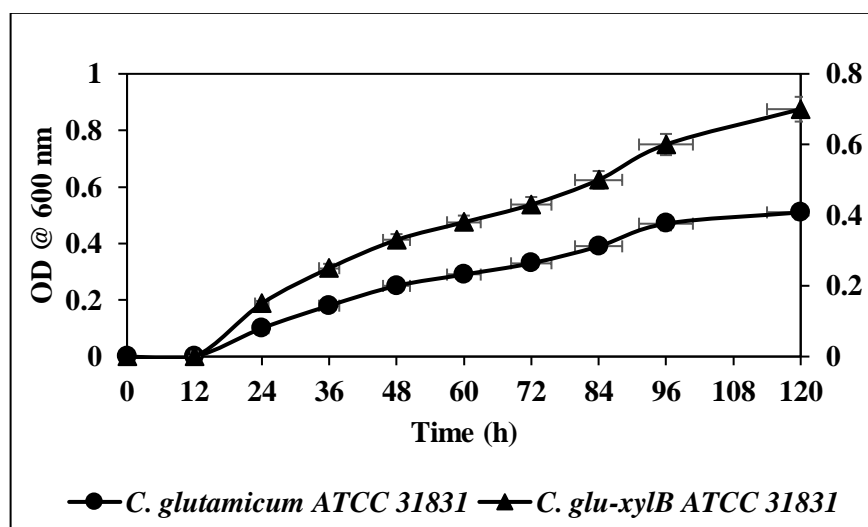


Fig.4.1. Comparative growth analysis of *C. glutamicum* and recombinant *C. glutamicum* (*C. glu-xytB*) in CGXII medium containing 4% xylose as carbon source

4.3.2. Growth analysis of *C. glutamicum* ATCC 31831 and recombinant *C. glu-xytB* (ATCC 31831) in CGXII medium containing xylose and glucose mixture as carbon source

In bacterial growth, the carbon source is used as the primary energy source for metabolism and biosynthesis. On comparative growth analysis of wild type and recombinant *C.*

glu-xykB in CGXII medium containing 1% glucose and 3% xylose as carbon source, it was observed that in the presence of glucose both the strains showed more than two-fold increase in growth rate i.e., in the case of *C. glutamicum* 31831 strain growth rate increased to 1.4 from 0.4 OD value and that of *C. glu-xykB* 31831 recombinant strain growth rate increased to 1.8 from 0.7 OD value (Fig.4.2). Also from the graph it was observed that after 48 h both the strains completely utilized glucose. Coming to xylose consumption, recombinant strain consumed 25 % more xylose compared to wild type strain after 120 h fermentation.

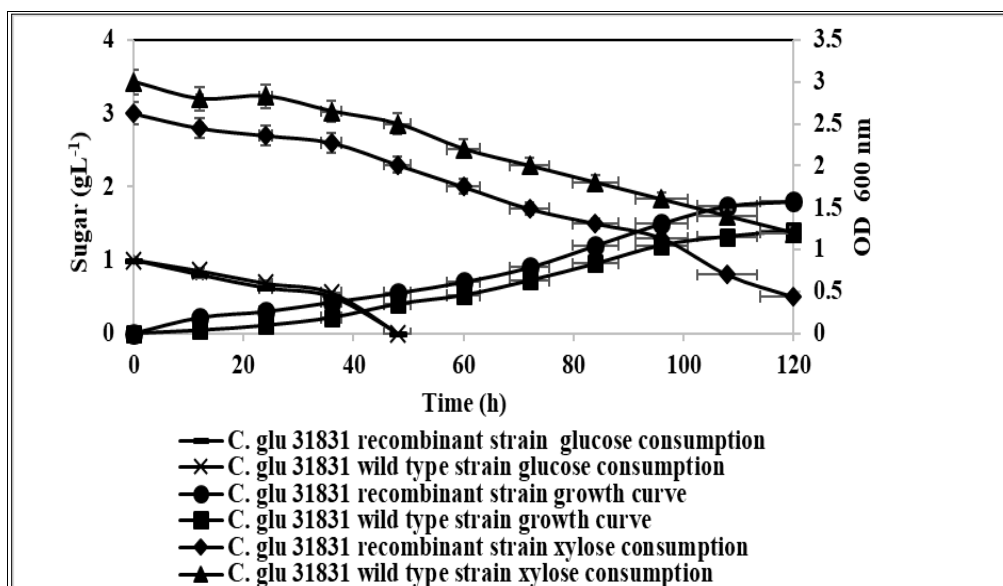


Fig.4.2. Comparative growth analysis and sugar consumption by *C. glutamicum* ATCC 31831 and recombinant *C. glutamicum* ATCC 31831 (*C. glu-xykB*) in CGXII medium containing 1% glucose and 3% xylose as carbon source

4.3.3. Xylonic acid production by recombinant strains of *C. glutamicum* under different combinations of glucose and xylose

The production of xylonic acid from glucose and xylose in *Corynebacterium* involves the oxidation of xylose to xylonic acid through the action of two enzymes: xylose dehydrogenase and xylonolactonase. These enzymes are highly specific for xylose and allows for the efficient

conversion of xylose to xylonic acid. Different combinations of sugars were supplemented to screen down the combination were minimum glucose concentration required for good growth and production. From the series of sugar combinations (0.1% G and 3.9% X, 0.25% G and 3.75% X and 0.5% G and 3.5% X), ranging from low to high it was observed that 0.5% glucose and 3.5% xylose showed maximum xylonic acid production from all the recombinant strains (Fig.4.3 A, B, C, D).

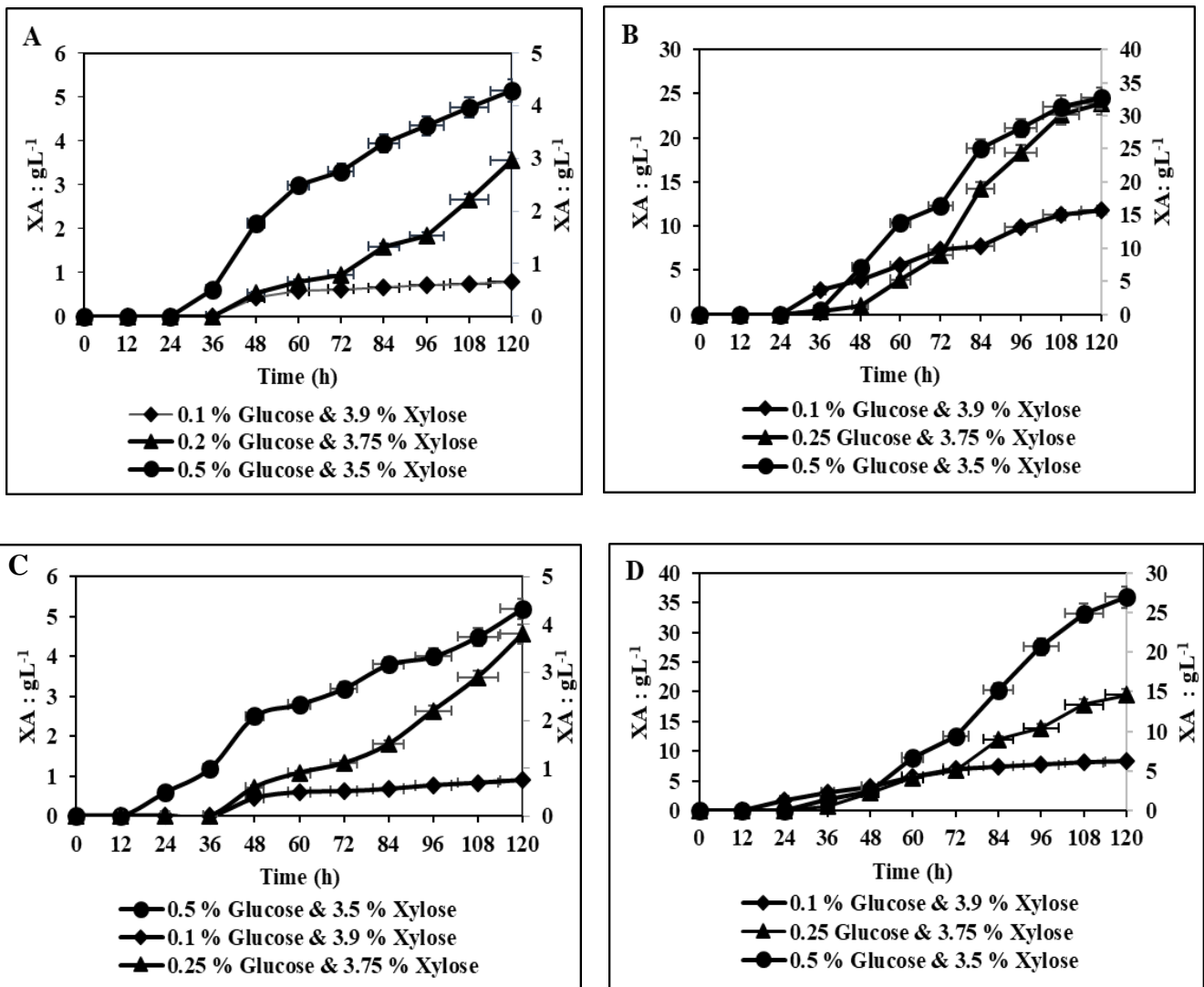
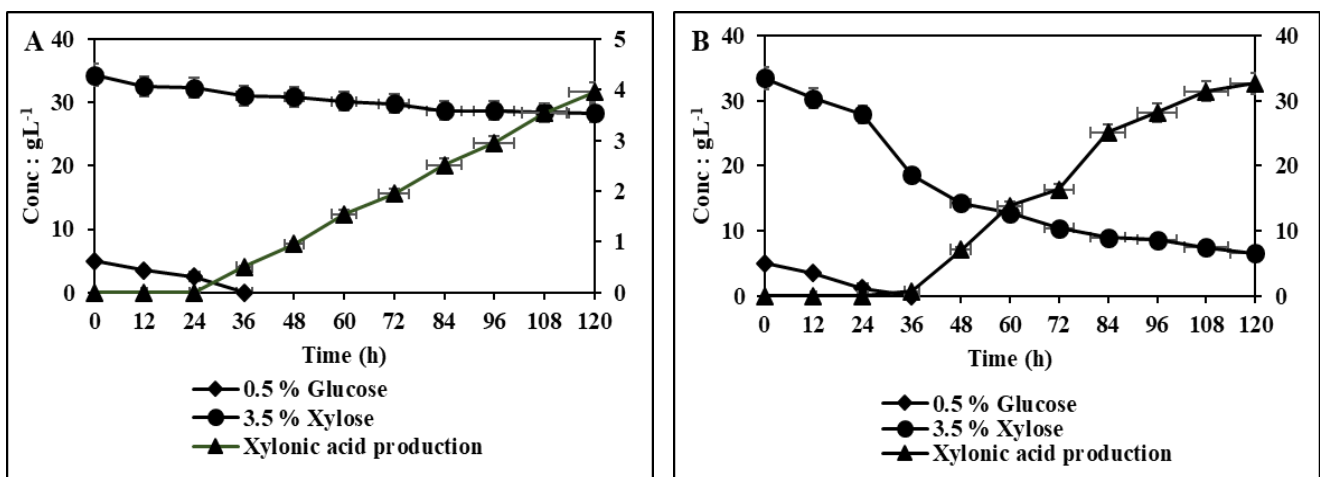


Fig.4.3. Xylonic acid production by recombinant strains of *C. glutamicum* ATCC 31831 under different combinations of glucose (G) and xylose (X) (0.1% G and 3.9% X, 0.25% G and 3.75%

X and 0.5% G and 3.5% X). *C. glu-pVWEx1* (control strain) (A), *C. glu-xylB* (B), *C. glu-xylC* (C) and *C. glu-xylBC* (D).

Discussing the production of each strain from 3 different combinations of xylose and glucose, *C. glu-pVWEx1* (control with empty vector) produced 0.77 gL⁻¹, 3.54 gL⁻¹ and 4.28 gL⁻¹ XA, *C. glu-xylB* produced 15.3 gL⁻¹, 32.12 gL⁻¹ and 33.5 gL⁻¹ XA, *C. glu-xylC* produced 0.9 gL⁻¹, 3.8 gL⁻¹ and 5.2 gL⁻¹ XA, *C. glu-xylBC* produced 8.2 gL⁻¹, 12.5 gL⁻¹ and 26.5 gL⁻¹ XA respectively. From this data 0.5% glucose and 3.5% xylose was selected as the optimum sugar (glucose) concentration for maximal xylonic acid production from synthetic CGXII medium with 4% sugar formulation.

Coming into the detailed analysis of XA production and sugar utilization from 0.5% glucose and 3.5% xylose it was observed that *C. glu-xylB* showed higher titer of 33.5 gL⁻¹ XA compared to *C. glu-xylBC* where the production is only 26.5 gL⁻¹. The control strain *C. glu-pVWEx1* and *C. glu-xylC* showed comparable titers of approximately 4 gL⁻¹ after 120 h fermentation (Fig.4.4 A, B, C, D). Therefore, *C. glu-xylB* showing higher titer was selected as the best strain for further investigation.



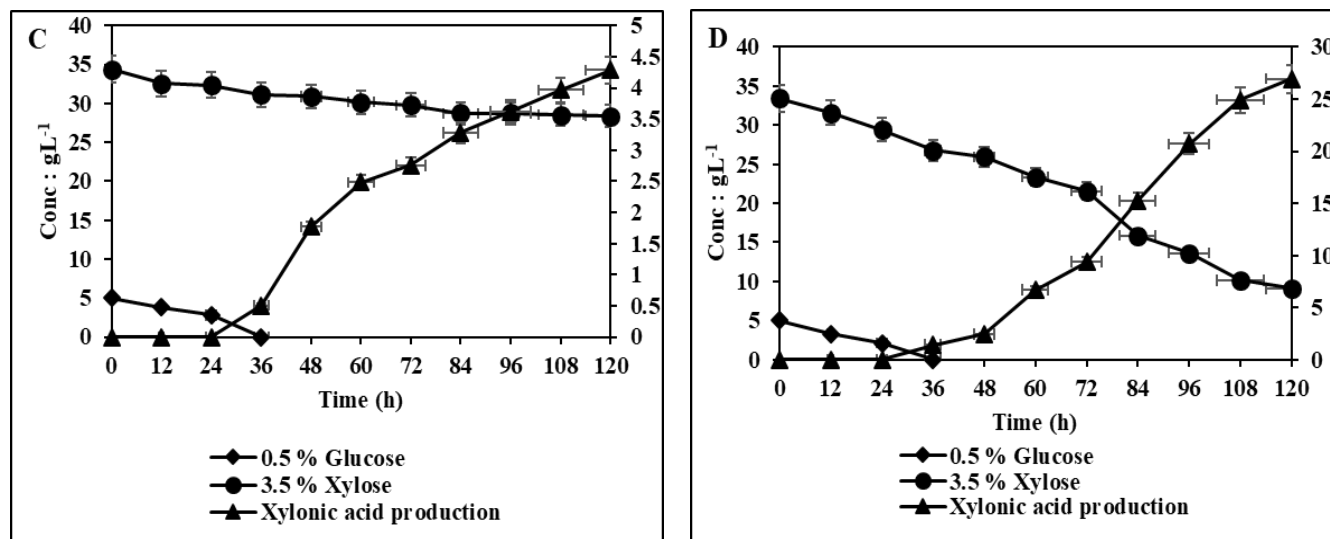


Fig.4.4. Xylonic acid production and sugar (xylose and glucose) utilization by recombinant strains of *C. glutamicum* ATCC 31831 under 0.5% glucose and 3.5% xylose. *C. glu-pVWEx1* (A), *C. glu-xylB* (B), *C. glu-xylC* (C) and *C. glu-xylBC* (D).

4.3.4. Expression analysis of xylose dehydrogenase (*xylB*) gene

On examining all the recombinant strains, it was observed that *C. glu-xylB* is showing better production. That is, *xylB* gene encoding xylose dehydrogenase enzyme alone is capable of converting xylose into xylonic acid. Similar observation was reported by Yim et.al (2017) where *C. glutamicum* metabolically engineered with xylose dehydrogenase gene alone could mediate the consolidated conversion of hemicellulosic biomass into xylonic acid.

For the expression analysis of xylose dehydrogenase gene, the recombinant strain *C. glu-xylB* was cultured in LB broth and IPTG (1Mm) induction was done to promote the expression of recombinant protein. After incubation for 48 h at 30°C the cells were harvested and sonicated to release the recombinant protein. The crude protein obtained was quantified to be 15.8 mgL⁻¹ and characterized using SDS-PAGE (Fig.4.5).

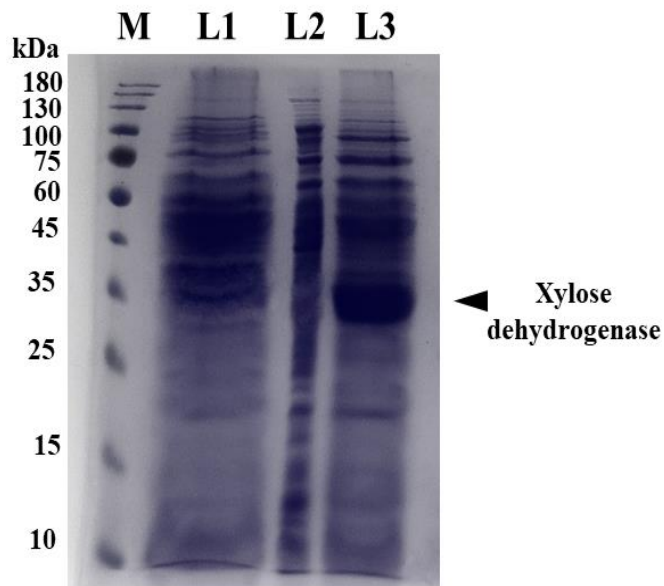


Fig.4.5. SDS-PAGE showing protein expression of xylose dehydrogenase enzyme of recombinant *C. glutamicum* (*C. glu-xydB*). Lane M: Protein molecular weight marker; Lane 1: *C. glu-pVWEx1*-induced (control); Lane 2: *C. glu-xydB* un-induced and; Lane 3: *C. glu-xydB* induced.

4.3.5. Role of araE pentose transporter for enhanced uptake of xylose and xylonic acid production

Functional analysis of *araE* pentose transporter gene in *C. glutamicum* ATCC 31831 was evaluated by carrying out a comparative production study with recombinant *C. glutamicum* ATCC 13032. Both the strains grew well in the CGXII production medium and metabolized xylose to xylonic acid. After 120 h fermentation, the recombinant strain, ATCC 13032 produced 27.66 gL⁻¹ of xylonic acid whereas ATCC 31831 produced 33.5 gL⁻¹ xylonic acid (Fig.4.6). It was observed that better uptake of the pentose sugar was also exhibited by *C. glutamicum* ATCC 31831, i.e., 88% consumption compared to 83% by ATCC 13032 after 120 h fermentation. Thus, the presence of *araE* transporter and its influence in xylose uptake and metabolism in recombinant *C. glu-xydB* ATCC 31831 was confirmed.

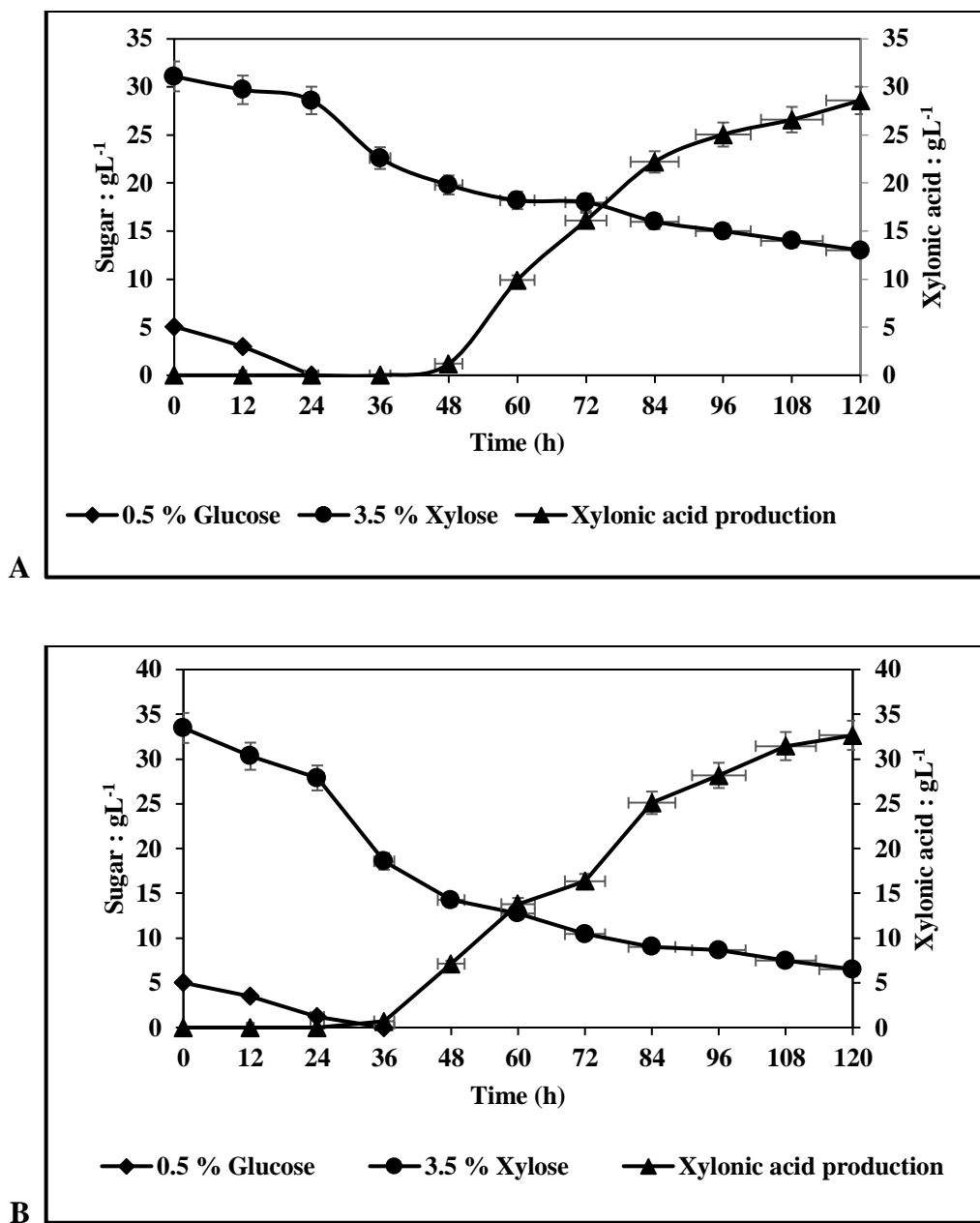


Fig.4.6. Xylonic acid production by *C. glu-xylB* ATCC 31831 (A) and *C. glu-xylB* ATCC 13032 (B)

4.3.6. Statistical optimization of operational parameters for xylonic acid production

The objective of the experimental design was medium engineering for maximum xylonic acid production. There were a total of 15 runs for optimizing the four individual parameters in

the current BBD. Experimental design and xylonic acid yield are presented in Table 4.1. The polynomial equation obtained for the model was as given below:

$$\text{Xylonic acid (gL}^{-1}\text{)} = -48.7 - 0.45 X_1 + 3.5 X_2 + 0.220 X_3 + 2.058 X_4 - 0.019 X_1^2 - 0.2139 X_2^2 - 0.0423 X_3^2 - 0.01943 X_4^2 - 0.075 X_1 X_2 + 0.0416 X_1 X_3 - 0.0119 X_1 X_4 + 0.526 X_2 X_3 + 0.0482 X_2 X_4 - 0.00128 X_3 X_4$$

where X_1 , X_2 , X_3 and X_4 are xylose, $(\text{NH}_4)_2\text{SO}_4$, urea and inoculum concentration respectively. Maximum production efficiency ($0.47\text{g}^{-1}\text{L}^{-1}\text{h}^{-1}$) was observed with Run No.13 where the concentration of parameters were urea 11.5 gL^{-1} , xylose 60 gL^{-1} , $(\text{NH}_4)_2\text{SO}_4$ 7.5 gL^{-1} and inoculum 11.25% (vV^{-1}) and xylonic acid titer was $56.32 \pm 0.3\text{ gL}^{-1}$ (Fig.4.7). It indicates that $(\text{NH}_4)_2\text{SO}_4$, inoculum concentration and xylose have a significant positive effect than urea on xylonic acid yield.

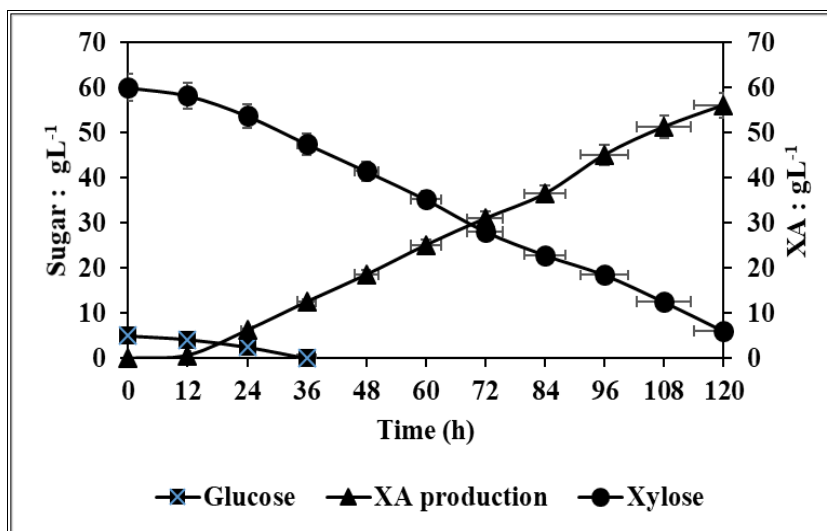


Fig.4.7. Xylonic acid production by recombinant *C. glu-xylB* under optimized CGXII medium composition, where $56.32 \pm 0.3\text{ gL}^{-1}$ xylonic acid was produced from 60 gL^{-1} xylose after 120 h fermentation.

Response surface curves were plotted to find out the interaction of variables and to determine the optimum level of each variable for maximum response. The contour plot

showing the interaction between a pair of factors on xylonic acid yield is given in Fig.4.8 (A to F). Major interactions studied are of inoculum and xylose concentration (A), xylose and urea concentration (B), $(\text{NH}_4)_2\text{SO}_4$ and urea concentration (C), effect of inoculum and $(\text{NH}_4)_2\text{SO}_4$ concentration (D), effect of $(\text{NH}_4)_2\text{SO}_4$ and xylose concentration (E) and the interaction of inoculum and urea concentration (F).

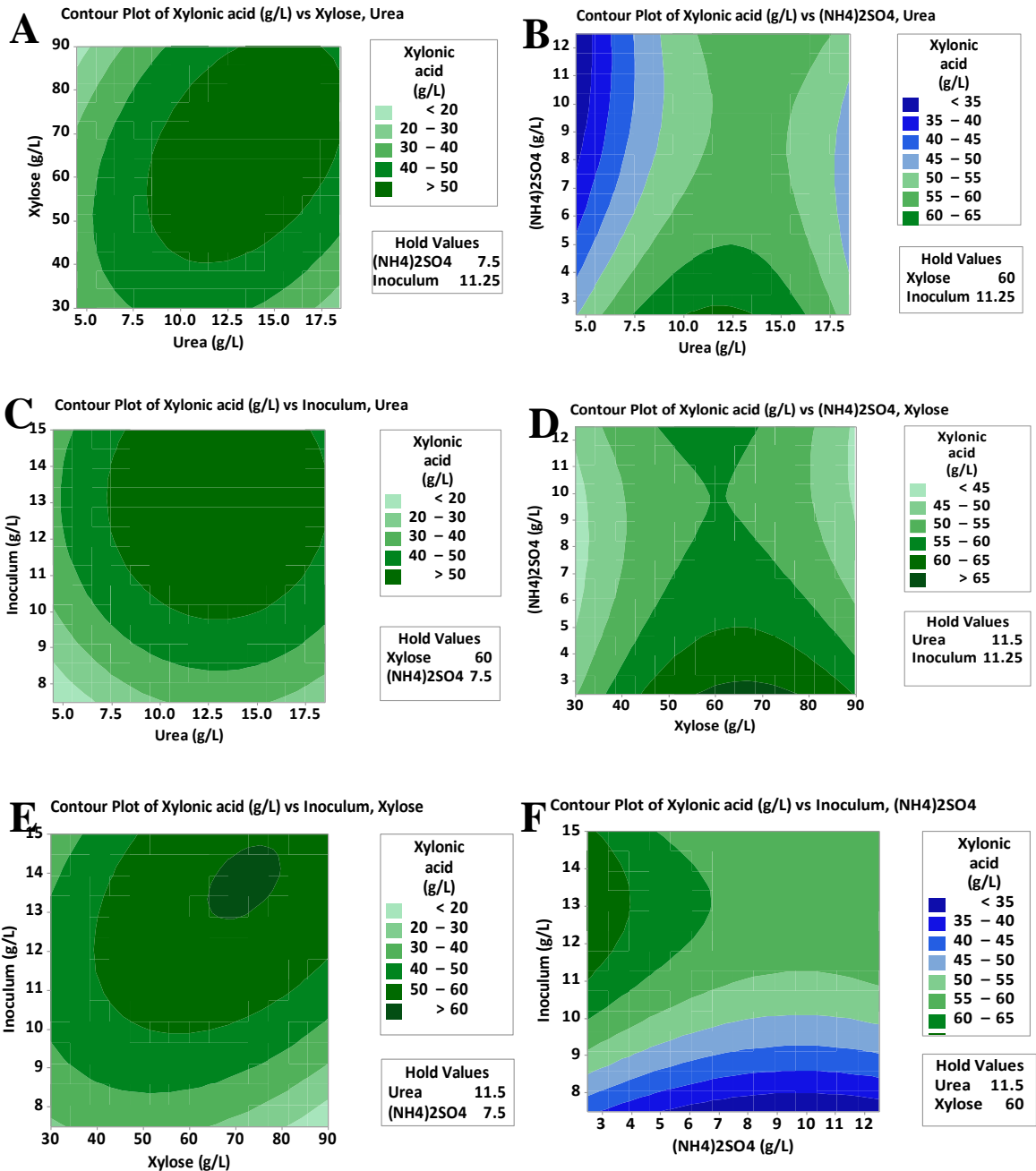


Fig.4.8. Contour plots showing the effect of various parameters on xylonic acid production by *C. glu-xylB* (ATCC 31831). A: Effect of inoculum and xylose. B: Effect of xylose and urea. C: Effect of $(\text{NH}_4)_2\text{SO}_4$ and urea. D: Effect of inoculum and $(\text{NH}_4)_2\text{SO}_4$. E: Effect of $(\text{NH}_4)_2\text{SO}_4$ and xylose F: Effect of inoculum and urea.

The ANOVA of response for xylonic acid is shown in Table 4.2. The R^2 value explains the variability in the xylonic acid yield associated with the experimental factors to the extent of 97.48%.

Table 4.2. Analysis of variance (ANOVA) for xylonic acid production using *C. glu-xylB*

Source	DF	Adj SS	Adj MS	F	P
Regression	12	3583.09	298.591	6.45	0.142
Linear	4	1688.94	422.234	9.11	0.101
Square	4	1249.59	312.398	6.74	0.133
Interaction	4	284.83	71.208	1.54	0.431
Residual error	2	92.66	46.328		
Lack-of-fit	1	92.66	92.657		
Pure error	1	0.00	0.000		
Total	14	3675.75			

$S = 6.80649$, $R\text{-Sq} = 97.48\%$, $R\text{-Sq (pred)} = 0.00\%$ and $R\text{-Sq (adj)} = 82.35\%$

ANOVA shows the statistical difference between the parameters being compared. It shows that $(\text{NH}_4)_2\text{SO}_4$, inoculum concentration and xylose have a statistically significant positive influence on xylonic acid production compared to urea having less effect. ANOVA table draw inference that the xylonic acid production increases with increase in concentration of the parameters $(\text{NH}_4)_2\text{SO}_4$, inoculum and xylose concentration.

Fig.4.9 shows the validation plot evaluating the performance of the statistical tool RSM for xylonic acid production. It is the plot of the predicted value from the model versus the actual value from the experimental data. The validation plot for maximal xylonic acid production, where maximum production can be obtained is 67.33 gL^{-1} from 90 gL^{-1} xylose. Whereas from the experiment the production was $56.32 \pm 0.3 \text{ gL}^{-1}$ XA from 60 gL^{-1} xylose.

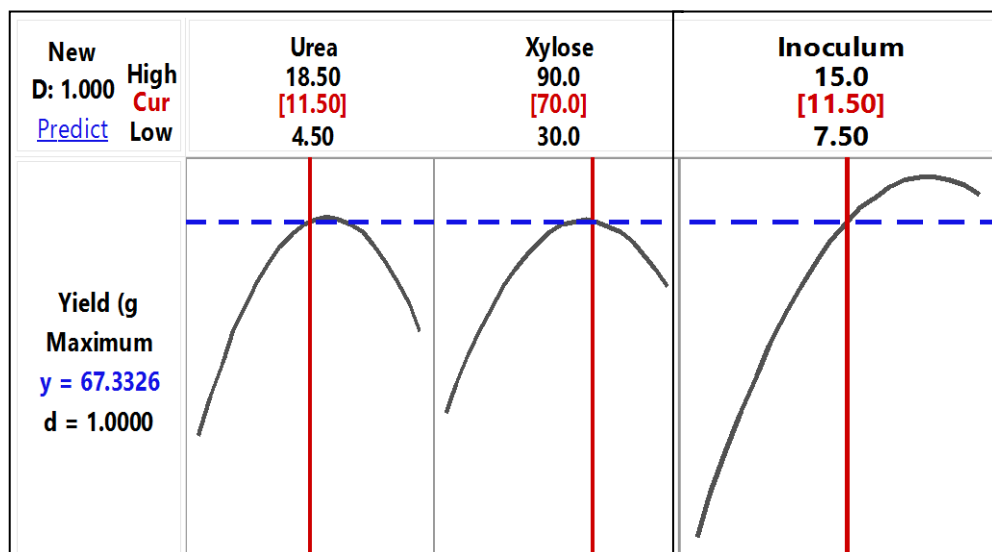


Fig.4.9. Validation plot for xylonic acid production

4.3.7. Xylonic acid production by batch fermentation in 2.5 L fermenter

The batch fermentation with optimized conditions was performed in Infors HT multiform fermenter with automated controls for pH, temperature and DO. The optimized CGXII medium containing sugar mixtures (glucose (5 gL^{-1}), xylose (60 gL^{-1})) found to have better production of $50.5 \pm 0.2 \text{ gL}^{-1}$ xylonic acid after 120 h fermentation (Fig.4.10) with a yield of 0.93 gg^{-1} xylose and a volumetric productivity of $0.42 \text{ gL}^{-1}\text{h}^{-1}$. 83% of xylose was successfully converted to xylonic acid indicating a good conversion efficiency of the process.

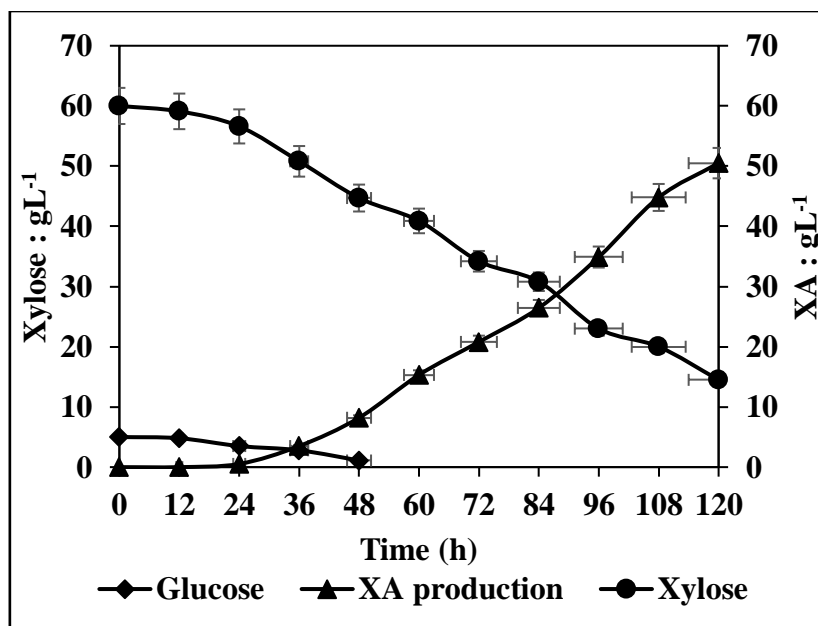


Fig.4.10. Xylonic acid production and sugar consumption by recombinant *C. glu-xyIB* in 2.5L fermenter

4.4. Discussion

Heterologous expression of genes for the production of varied value-added chemicals were successfully carried out in *C. glutamicum*, for example, the production of amino acids, sugar alcohol, organic acid, diamines, glycolate and 1,5-diaminopentane (Buschke et al. 2013; Meiswinkel et al. 2013; Zahoor et al. 2014; Pérez-García et al. 2016; Dhar et al. 2016). *C. glutamicum* being a versatile industrial microbe and the availability of genetic engineering tools makes it a rapid and rational manipulation host for diverse platform chemicals.

Corynebacterium glutamicum ATCC 31831 grew on pentose as the sole carbon source. The gene cluster responsible for pentose utilization comprised a six cistron transcriptional unit with a total length of 7.8 kb. The sequence of the *C. glutamicum* ATCC 31831 *ara* gene cluster containing gene *araE*, encodes pentose transporter, facilitates the efficient uptake of pentose sugar (Kawaguchi et al. 2009). Previous studies have also reported the role of *araE* pentose

transporter in *Corynebacterium glutamicum* ATCC 31831 and its exploitation for the production of commodity chemicals like 3HP and ethanol (Becker et al. 2018). In the present study, *Corynebacterium glutamicum* ATCC 31831 with an inbuilt AraE pentose transporter exhibited an effectual consumption of xylose as well as its conversion to xylonic acid. Therefore, *Corynebacterium glutamicum* ATCC 31831 selected as the host organism for xylonic acid production.

To construct a xylonic acid pathway in *C. glutamicum*, the *xylB* and *xylC* gene from *Caulobacter crescentus* was introduced. *C. crescentus xylB* was preferred due to its higher enzymatic activity compared to xylose dehydrogenases from other sources like *T. reesei* or *B. subtilis* (Toivari et al. 2012).

Xylose can be metabolized in four different routes (I) The oxido-reductase pathway, (II) The isomerase pathway, (III) The Weimberg pathway, an oxidative pathway and (IV) The Dahms pathway (Cabulong et al. 2018). Xylose once inside the cell gets converted to xylonolactone and then into xylonic acid on the expression of *xylB* (xylose dehydrogenase) and *xylC* (xylonolactonase) genes. These two enzymes are involved in both the Weimberg and Dahms pathway where xylose is metabolized to xylonic acid (Brüsseler et al. 2019). In the present study, it was observed that only the xylose dehydrogenase enzyme activity is good enough for xylonic acid production. Without the dehydrogenase activity, the lactonase activity alone cannot do the conversion of xylose to xylonic acid. Further, the xylonolactonase expression along with xylose dehydrogenase resulted in xylonic acid production but not that efficient as dehydrogenase alone with the case of *C. glutamicum*. It was reported that, xylonolactone once formed can be converted to xylonic acid either by the spontaneous oxidation of lactone or through the enzymatic hydrolysis of xylonolactonase enzyme (Buchert and Viikari

1988). *Corynebacterium glutamicum* being an aerobic organism, direct oxidation of xylonolactone to xylonic acid is more favorable inside the cell.

Previous studies have also shown that xylose dehydrogenase (*xydB*) activity alone in *C. glutamicum* can result in the production of xylonic acid (Yim et al. 2017).

Several bacteria, especially *Gluconobacter oxydans* and *Pseudomonas fragi*, have been found to exhibit elevated levels of xylonic acid in the extracellular medium. Production titer of 109 gL⁻¹ xylonic acid from 100 gL⁻¹ xylose by *Gluconobacter oxydans* and 162 gL⁻¹ xylonic acid from 150 gL⁻¹ xylose by *Pseudomonas fragi* were reported (Buchert and Viikari 1988). A modified strain of *E. coli* was engineered to synthesize xylonic acid. *E. coli*'s native metabolic pathway for xylose catabolism was blocked through the disruption of the xylose isomerase (XI) and xylulose kinase (XK) genes. Xylonic acid producing *E. coli* was created by introducing xylose dehydrogenase gene from *Caulobacter crescentus*. The resulting recombinant *E. coli* produced upto 39.2 gL⁻¹ xylonic acid from 40 gL⁻¹ xylose in minimal medium (Liu et al. 2012). The expression of *xydB*, an NAD⁺-dependent xylose dehydrogenase, from *Caulobacter crescentus* in *Saccharomyces cerevisiae* B67002 *xydB* resulted in the production of 43 g xylonic acid from 49 g of xylose (Toivari et al. 2012). In 2017 Yim et al explored *Corynebacterium glutamicum* for its potential in bioconversion of hemicellulosic biomass i.e xylan into xylonic acid. Heterologous expression of xylose specific transporter gene, *xylE*, of *Escherichia coli* along with xylose dehydrogenase and xylonolactonase genes, involved in xylonic acid metabolism, from *Caulobacter crescentus*, also an engineered xylan degrading module with two xylan degrading enzymes endoxylanase and xylosidase were cloned for xylonic acid production. The metabolically engineered *C. glutamicum* produced 6.23 gL⁻¹ xylonic acid from 20 gL⁻¹ xylan (Yim et al., 2017). Here in this study the recombinant strain *C. glu-xydB* also produced a

comparable titer of $56.32 \pm 0.3 \text{ gL}^{-1}$ xylonic acid from 60 gL^{-1} xylose in synthetic CGXII medium. The detailed analysis of the recombinant strains developed for its productivity and competence in biomass is described in the following Chapter 5.

4.5. Summary

An efficient one step bioconversion system for xylose to xylonic acid is developed. Xylonic acid production was found higher for the recombinant *C. glutamicum* 31831 having the AraE transporter protein than the recombinant *C. glutamicum* 13032 which is devoid of it, emphasizing the higher uptake of xylose in the presence of the transporter protein. Among the recombinant *C. glutamicum* 31831 strains constructed, the maximum xylonic acid production was obtained using *C. glu-xylB* followed by *C. glu-xylBC*. Media engineering was carried out with the statistical tool response surface methodology (RSM) to improve the production of xylonic acid. RSM aided to narrow down the most influencing parameters and its optimization on xylonic acid production. $56.32 \pm 0.3 \text{ gL}^{-1}$ xylonic acid was produced from 60 gL^{-1} xylose (conversion 76.4%) under optimum concentrations of CGXII medium components such as (xylose (60 gL^{-1}), glucose (5 gL^{-1}), urea (11.5 gL^{-1}), $(\text{NH}_4)_2\text{SO}_4$ (7.5 gL^{-1}) and inoculum ($11.25\% \text{ vV}^{-1}$) in the flask level with a yield of 1.04 gg^{-1} xylose and productivity $0.5 \text{ gL}^{-1}\text{h}^{-1}$. In 2.5L (fermenter) level, from 60 gL^{-1} of xylose, the production titer was $50.5 \pm 0.2 \text{ gL}^{-1}$ XA (conversion 66%) with a yield of 0.93 gg^{-1} xylose and a productivity of $0.42 \text{ gL}^{-1}\text{h}^{-1}$.

Chapter 5

**Scrutiny of different biomasses as raw material for the
fermentative production of xylonic acid using
recombinant *Corynebacterium glutamicum* ATCC
31831**

5.1. Introduction

The majority of modern chemical products are made from non-renewable sources such as coal, natural gas, and petroleum, which account for 85% of energy use (Hoffert et al. 2002; Goldemberg 2007). These resources are not sustainable and release carbon dioxide when burned, which contributes to global warming and accounts for over half of all warming factors (Wilbanks et al. 2014). To create a more sustainable economy that relies on renewable resources, there is growing interest in alternative energy sources that do not require the extraction of fossil fuels. Biomass resources offer a way to produce a range of products including chemicals, materials, energy, and food (Torres-Mayanga et al. 2019). The concept of bio-refining is similar to traditional petroleum refining, but instead uses biomass as the raw material to create a variety of products, including commodities and specialty chemicals (Castilla-Archilla et al. 2019). This approach has gained attention as a promising alternative to the traditional use of fossil fuels.

Biomass can be used as a feedstock for the production of biofuels such as bioethanol and biodiesel, which can replace fossil fuels and help reduce greenhouse gas emissions from the transportation sector. Additionally, biomass can be used to produce biogas through anaerobic digestion, which can be used for electricity generation or as a fuel for transportation. Apart from this, nowadays, bio-refineries produce a range of valuable compounds and commodities using industrial microorganisms such as *Escherichia coli*, *Saccharomyces cerevisiae*, and *Corynebacterium glutamicum* (Arnone et al. 2020). Among the industrial microbes, *C. glutamicum* has several advantages and is considered one of the most promising for producing value-added platform chemicals and polymers. Firstly, *C. glutamicum* has low extracellular protease activity and can secrete functional precursor proteins that are properly folded (Liu et al. 2015). Secondly, it has a weak carbon catabolite inhibitory effect, which allows it to use mixed

sugars as a carbon source without significant growth retardation (Baritugo et al. 2018). Thirdly, it is robust and tolerant to various toxic compounds, including organic acids, furfural, and toxic aromatic compounds (Gopinath et al. 2011; Kogure and Inui 2018; Conrady et al. 2019). Moreover, it maintains a strong catalytic function and high cell growth under growth-inhibiting conditions, making it particularly useful for lignocellulose treatment and environmental pollutant degradation. Fourthly, *C. glutamicum* has a wide spectrum of natural carbon source substrates, including five-carbon sugars, six-carbon sugars, monosaccharides, and toxic aromatic compounds (Choi et al. 2019). It can be used to produce a variety of compounds and can convert cheap biomass into high-value products. Additionally, *C. glutamicum* is safe, has a clear genetic manipulation background, and is an excellent candidate for bio-refining raw materials (Kitade et al. 2020).

This chapter deals with the fermentative production of xylonic acid from biomass and from the preliminary screening of different biomass, sawdust was selected as the optimized raw material for subsequent studies.

5.2. Materials and Methods

5.2.1. Raw material selection

Different agro-industrial residues like rice straw, wheat bran and sawdust (Fig.5.1.) were screened for fermentable sugar release and subsequently to convert to xylonic acid. Rice straw and wheat bran were purchase from local markets in Pappanamcode, Trivandrum, Kerala, India. Sawdust collected from M. S. Sawmills, Kollam, Kerala, India. Samples were milled and crushed into fine particles, and 10 mm-sized particles were sieved for processing. Samples were then dried and moisture content measured before pre-treatment.



Fig.5.1. Different agro-industrial biomasses (A) Rice straw, (B) Wheat bran and (C) Sawdust

Rice straw, wheat bran and sawdust were selected considering the relative low cost in the market and easy availability in the local market which can reduce transportation costs. The high energy content of the biomass ensures an efficient energy source for the process.

5.2.3. Dilute acid pre-treatment of biomass

For dilute acid pre-treatment, biomasses were pre-soaked in sulphuric acid (H_2SO_4) for 45 min and then treated at 121°C for 1h with 15% (ww^{-1}) biomass loading and 1% (ww^{-1}) acid concentration in separate batches. After pre-treatment, the liquid fraction with sugar monomers xylose and glucose were separated from the slurry using muslin cloth. The aqueous fraction was neutralized to pH 7 with NaOH (10 N) solution and sugar released were quantified using HPLC (Chapter 2, section 2.4.2). Residues left after pre-treatment was dried and powdered for compositional analysis.

5.2.3. Compositional analysis of biomass

Compositional analysis of biomasses were carried out according to NREL protocol (Sluiter et al, 2012). Moisture content of the biomass was determined; 300 mg of dry biomass was transferred into a conical flask. 3 mL of 72% H_2SO_4 (concentrated sulphuric acid) was

added to the flask and mixed well. The flasks were heated at 30 - 40°C in a water bath at 100 rpm for 2h. After boiling the flasks were allowed to cool and filtered the contents of the flask through a Whatman No.1 filter paper (Merck, India). The residue was dried at 105°C for 24h and the clear supernatant was neutralized adding CaCO₃ and subjected for HPLC to determine the monosaccharide content. Lignin in the non-neutralized filtrate was determined by diluting it 20 times using double distilled water and measured the absorbance at 205 nm in spectrophotometer. Weight of the Whatman No.1 filter paper cake was determined and transferred into a crucible and heated in a muffle furnace at 575°C for 6 h. After heating, cooled the crucible in a desiccator and weighed to determine the ash content.

5.2.4. SEM analysis

The surface property of the biomass was determined by Scanning Electron Microscopy. The differences in the sawdust structure before and after acid pre-treatment were visualized through SEM (JEOL JSM-5600, Japan). Finely powdered sawdust biomass was mounted on brass stub coated with conductive material gold. The sample was placed in the SEM chamber and electron beam was directed at the sample, and the secondary electrons were collected by the detector to generate images at a magnification of 1500 x.

5.2.5. Detoxification of pentose rich sawdust liquor

Acid pre-treated sawdust liquor (APL) was concentrated using rotavapor (Buchi, India) at 60°C to achieve a xylose concentration of 20 - 50% (vv⁻¹). INDION PA 500 non-ionic, adsorbent resin (Indion resins, Gujarat) used for inhibitor removal, was washed with water for 30 min. The resin was then activated with methanol. Detoxification experiments were conducted in batch mode at room temperature. The resins were mixed into the APL in a 1:15 (wv⁻¹) ratio. At various

time intervals, samples were collected and analysed for inhibitor and monomeric sugar content. The resin was regenerated after each detoxification cycle by washing them with methanol and water.

5.2.6. Fermentation

For shake flask fermentation, the recombinant strain *C. glu-xytB* was grown in 25 mL of Brain Heart Infusion (BHI) medium (with kanamycin 25 $\mu\text{g mL}^{-1}$) at 30°C overnight with shaking at 200 rpm. An aliquot of overnight grown culture was inoculated into 100 mL CGXII sawdust APL production medium (pH 6.5) (Annexure II) containing 1 mL 1% trace metals, 60 g L^{-1} xylose, and 8 g L^{-1} glucose supplemented with kanamycin (25 $\mu\text{g mL}^{-1}$). *xytB* gene was induced by adding 1mM IPTG to the inoculated culture for xylose metabolism. All the 250 mL Erlenmeyer flasks with 100 mL of production medium were then incubated at 30°C with shaking at 200 rpm.

Batch fermentations were carried out in a 2.5 L scale laboratory fermenter (Infors HT fermenter, Switzerland) containing 1.0 L of CGXII sawdust APL production medium with an initial xylose concentration of 60 g L^{-1} . The process parameters were set at temperature (30°C), inoculum (10% v v^{-1}), agitation speed (200 rpm), aeration (1.5 vvm) and pH 6.5. Samples were collected at regular intervals of 12 h and the cell free culture supernatant was subjected for the detection of xylonic acid as well as xylose level.

5.2.7. Influence of furan inhibitors on cell growth, xylose utilization and xylonic acid production

A screening study was conducted to analyze the effect of furan inhibitors which are normally present in APL of any biomass. Fermentation was carried out in CGXII synthetic

medium in 250 mL shake flasks with working volume of 100 mL at 30°C for 120 h with an initial xylose concentration of 60 gL⁻¹. Hydroxy methyl furfural (HMF) and furfural (Cas no. 67470 and 98011, Sigma Aldrich - Merck, India) of varying concentrations 0.5 gL⁻¹, 1.0 gL⁻¹, 1.5 gL⁻¹ and 2.0 gL⁻¹ were added to the CGXII synthetic production medium respectively to study its impact on xylose utilization and xylonic acid production.

5.3. Results

5.3.1. Pre-treatment and composition analysis of biomass

Fig.5.2. shows the compositional analysis results of rice-straw, sawdust and wheat bran. From composition analysis it was observed that all the biomass is rich in cellulose content in the range 45 - 50%, hemicellulose (20 - 25%) and lignin content (20 - 30%). Relatively higher hemicellulosic content obtained from sawdust APL i.e, 45.55 ± 6.5% cellulose, 24.41± 3.5% hemicellulose and 29.05 ± 0.5% lignin.

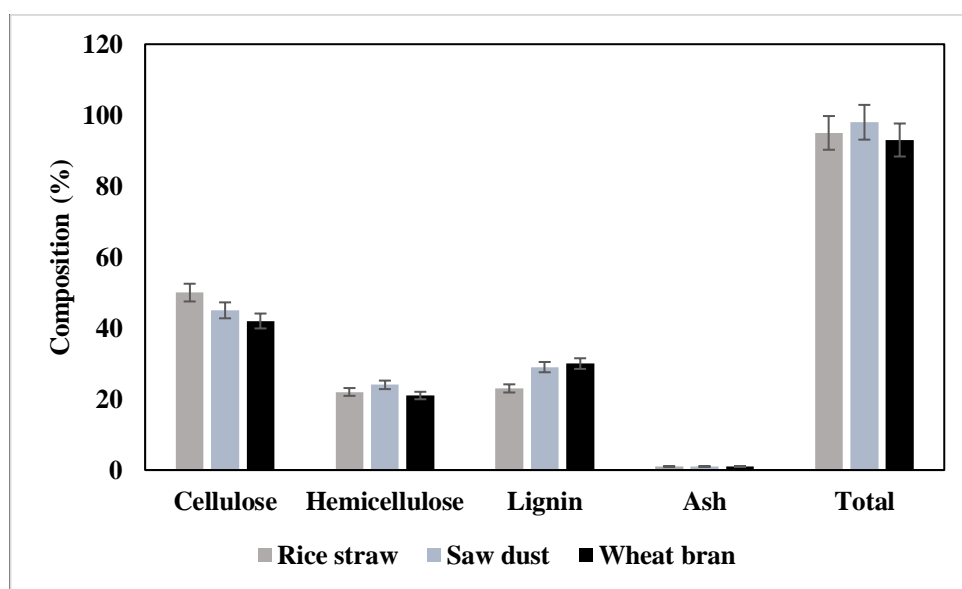


Fig.5.2. Composition analysis of rice straw, sawdust and wheat bran

Depending on the composition of biomass the fermentable sugars and inhibitors released from different biomass varies. As it is evident from Fig.5.3A. shows the concentration of sugars released and Fig.5.3B. shows the concentration of inhibitors released from the biomass after acid pre-treatment. Higher C5 sugar release *i.e.*, xylose – 23 gL⁻¹ obtained from sawdust and also comparatively lower inhibitor release (HMF – 1.1 gL⁻¹ and Furfural – 1.5 gL⁻¹) obtained from sawdust biomass. Acid pre-treatment is favourable for C5 sugar release. As our target is xylose sugar, biomass that yields more of xylose *i.e.*, sawdust was selected as the raw material for the study.

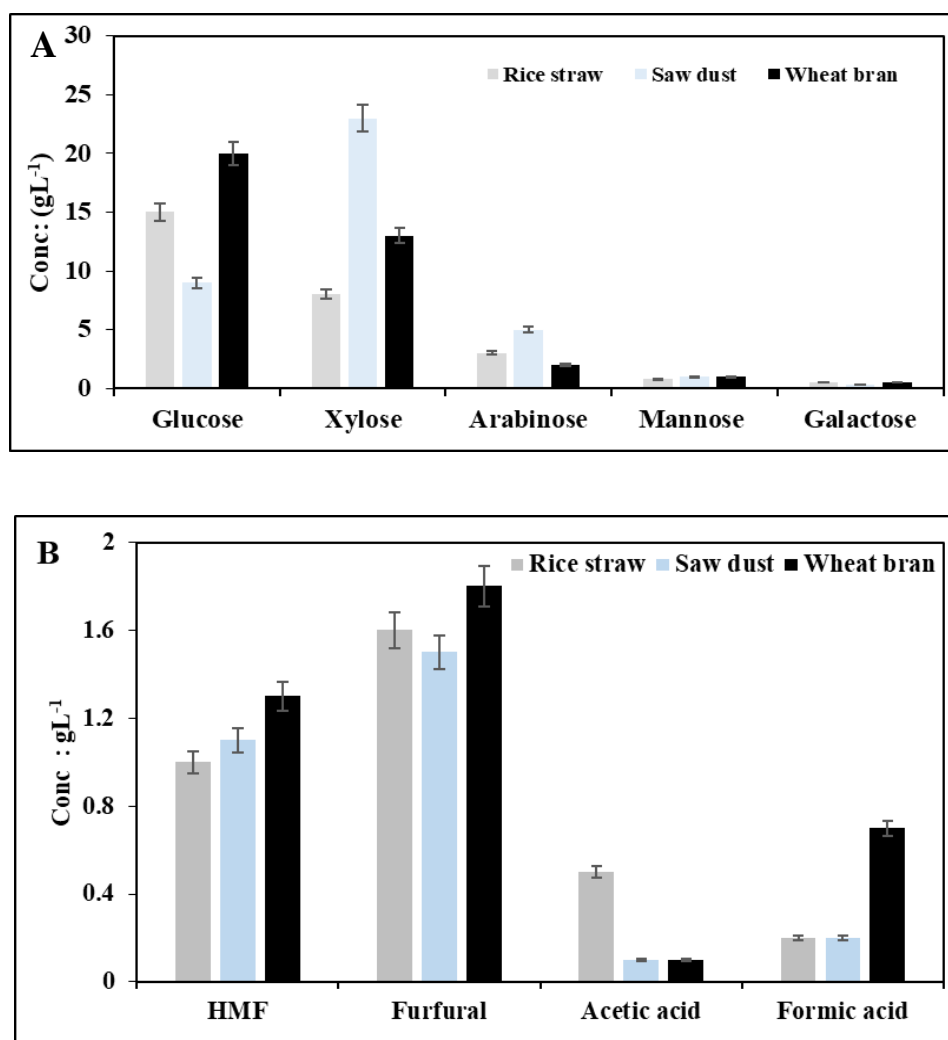
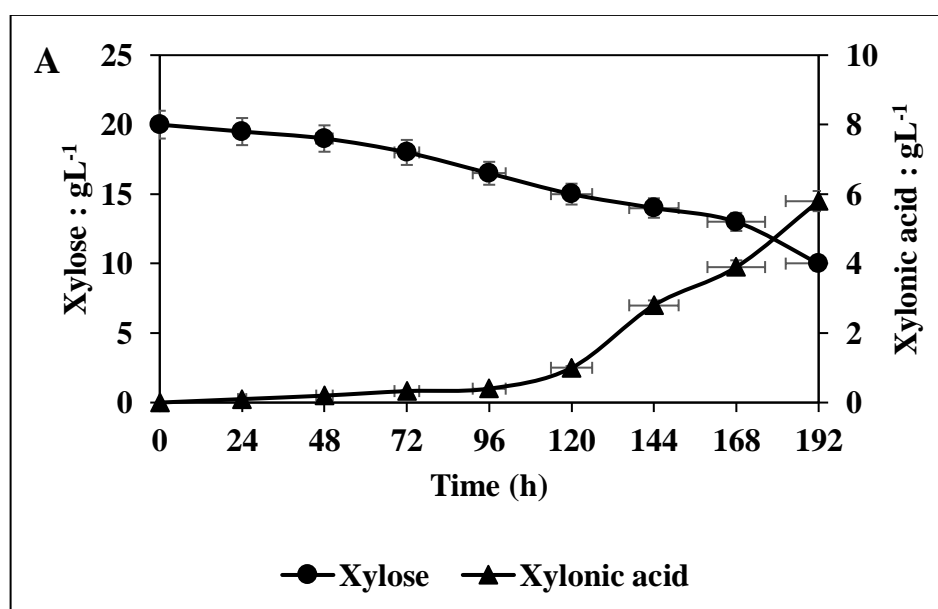


Fig.5.3. Release of sugar (A), inhibitors (B) after the acid pre-treatment of biomass

5.3.2. Comparative study of xylonic acid production in acid pre-treated liquor (APL) of rice straw, wheat bran and sawdust

Fermentation studies were carried out in 250 mL Erlenmeyer flask containing 100 mL CGXII medium where APL from biomass containing xylose was used as the carbon source for xylonic acid production. Independent experiments were done with APL from rice straw, wheat bran and sawdust biomass, the flasks were incubated at 30°C for 192 h. Comparative analysis was done to evaluate the potential of *C. glutamicum* to grow in non-detoxified APL from different biomass and to metabolise xylose into xylonic acid. Fig.5.4 A, B and C depicts the xylose utilization and xylonic acid production by *C. glu-xylB* (in rice straw, wheat bran and sawdust APL respectively). The initial concentration of xylose in APL was 20 gL⁻¹ (*i.e.*, without concentrating the APL). After fermentation it was observed that *C. glu-xylB* could grow and metabolise xylose from sawdust APL, better than other two biomass APL, with a titer of 7.5 gL⁻¹ xylonic acid which was higher than those from wheat bran and rice straw that is 5.1 gL⁻¹ and 5.8 gL⁻¹ respectively. Due to the presence of higher concentration of inhibitors in rice straw and wheat bran APL the production titer was also low.



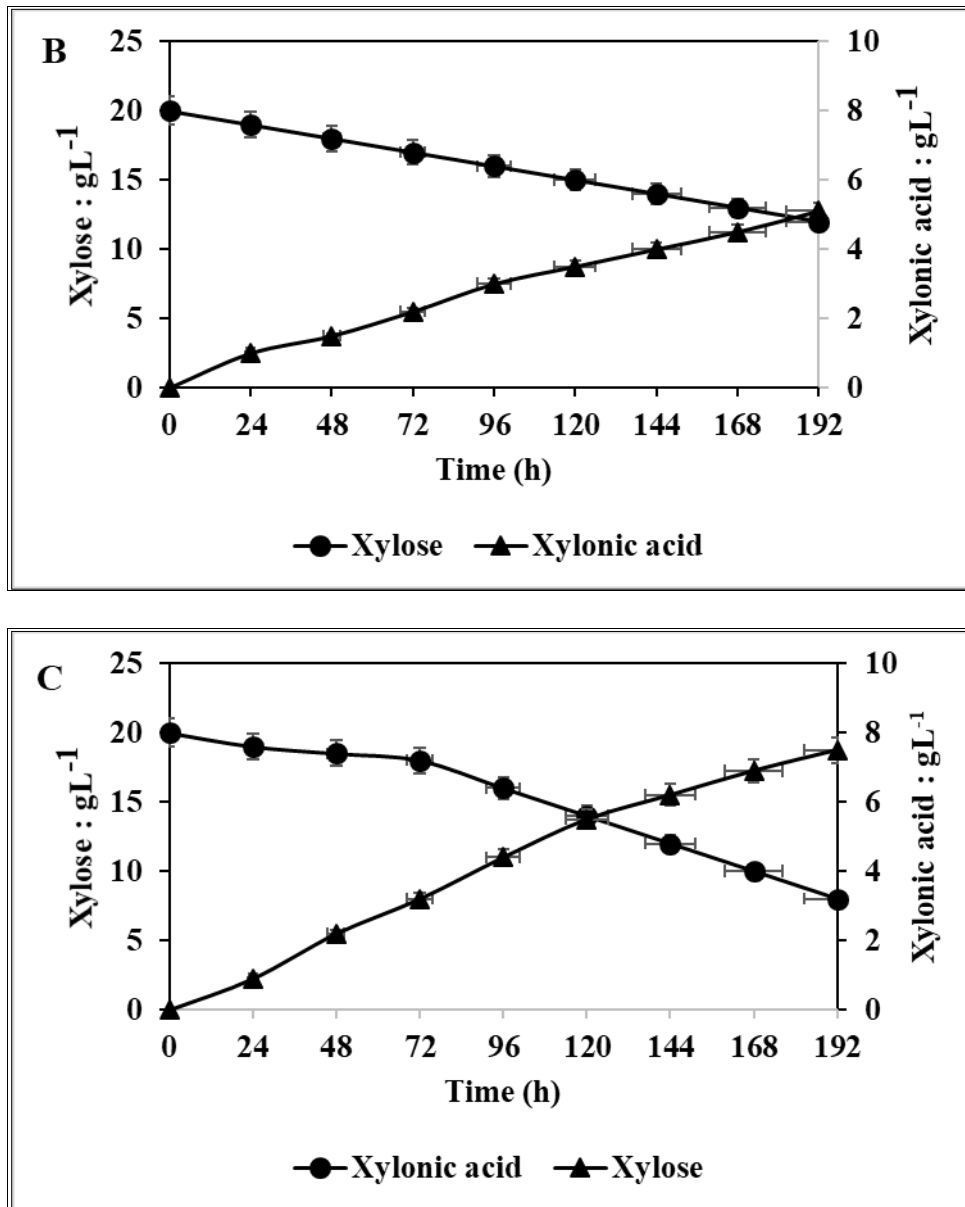


Fig.5.4. Xylose utilization and xylonic acid production by *C. glu-xyIB* in non-detoxified (A) rice straw, (B) wheat bran and (C) saw dust APL

Based on more xylose utilization, lower inhibitor concentration and better production titer, sawdust was selected as the biomass for further study. The physio-chemical characteristics of sawdust APL are given in Table.5.1.

Table.5.1. Physio-chemical properties of sawdust liquor

Sl.no.	Parameters	Value
1.	Cellulose (%)	45.55 ± 6.5
2.	Hemicellulose (%)	24.41 ± 3.5
3.	Lignin (%)	29.05 ± 0.5
4.	Total nitrogen (%)	1.8
5.	Total phosphate (mgL ⁻¹)	0.5 ± 0.31
6.	pH	6.7
7.	Total Dissolved solids (TDS) (mgL ⁻¹)	408 ± 0.1
8.	Dissolved Oxygen (DO) (mgL ⁻¹)	2.2 ± 2.1
9.	Oxidation Reduction Potential (ORP) (mgL ⁻¹)	95 ± 0.20
10.	Total Chemical Oxygen Demand (TCOD) (mgL ⁻¹)	237.6 ± 0.64
11.	Soluble Chemical Oxygen Demand (SCOD) (mgL ⁻¹)	216 ± 0.35

5.3.3. SEM analysis of sawdust

Fig. 5.5A and B shows the SEM image of raw (control) and acid pre-treated saw dust biomass. It is visible that after pre-treatment, the possible degradation of lignin and hemicellulose is happened and it caused the distortion or the opening up of the biomass wall.

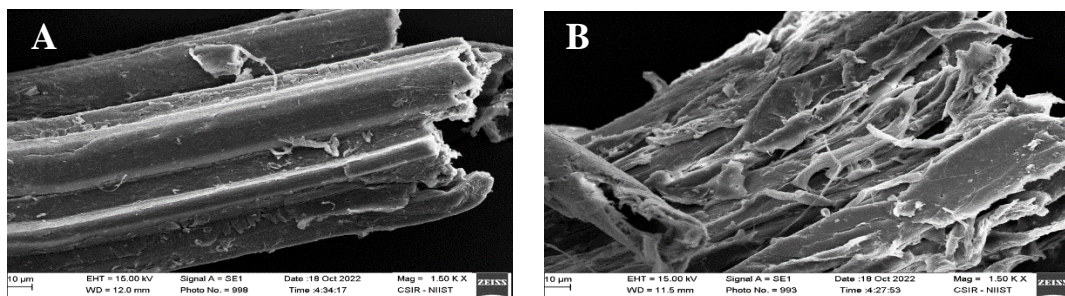


Fig.5.5. SEM image of (A) raw sawdust (control) (B) acid pre-treated sawdust (magnification – 1500 x)

5.3.4. Detoxification of APL using INDION PA 500 adsorbent resin

INDION PA 500 resin is a non-ionic, hydrophobic cross-linked polymer beads. The adsorbent resin was observed to be effective in removing 88% inhibitors (furfural, hydroxyl methyl furfural (HMF), acetic acid, and formic acid) present in APL. The resins were regenerated using 70% ethanol and water to desorb the adsorbed inhibitors and, to calculate the number of cycles for which the adsorbent resins could be reused. The APL was further detoxified using the regenerated resins. The resin could retain its adsorption capacity for up to 4 cycles with approximately 60% removal of inhibitors (Fig.5.6.). Effective removal of furans from APL can be correlated to higher surface area and aromatic nature of the resin. Its pore size distribution also makes it an excellent choice for the removal of a wide variety of large organic molecules from polar solvents. The resins could also adsorb the sugars present in APL during the detoxification process.

Fig.5.7A and 5.7B demonstrates the HPLC chromatogram of non-detoxified and detoxified sawdust APL and Fig.5.7C. shows the appearance of sawdust APL before and after treatment with resin. From the chromatogram it is observed that the APL contains higher concentration of furan inhibitors such as HMF and furfural, after treatment with the resin the concentration of the inhibitors got reduced, 90% removal of inhibitors in the first cycle. Because sugars are the primary pre-requisite for fermentation to value-added products, a suitable resin for large-scale processes should have less sugar adsorption.

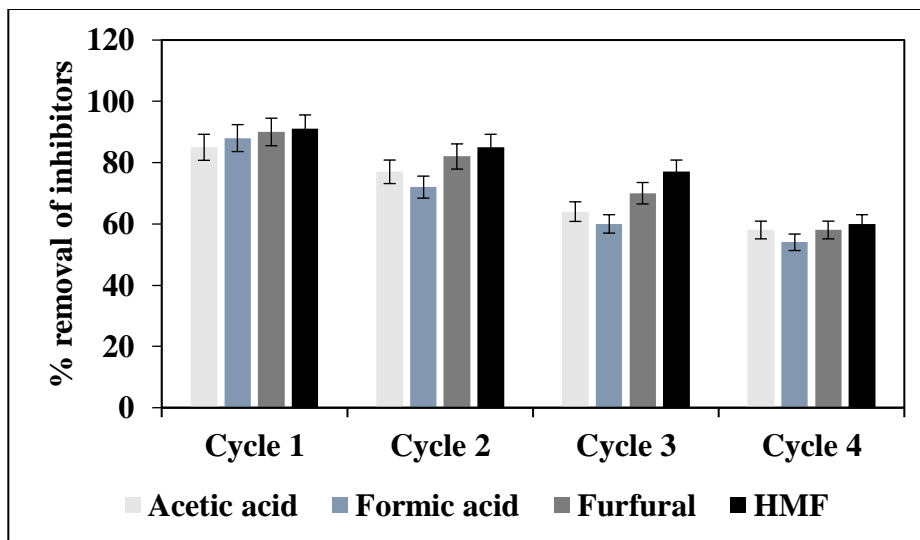


Fig.5.6. Inhibitor (acetic acid, formic acid, furfural and HMF) removal by INDION PA 500 resin

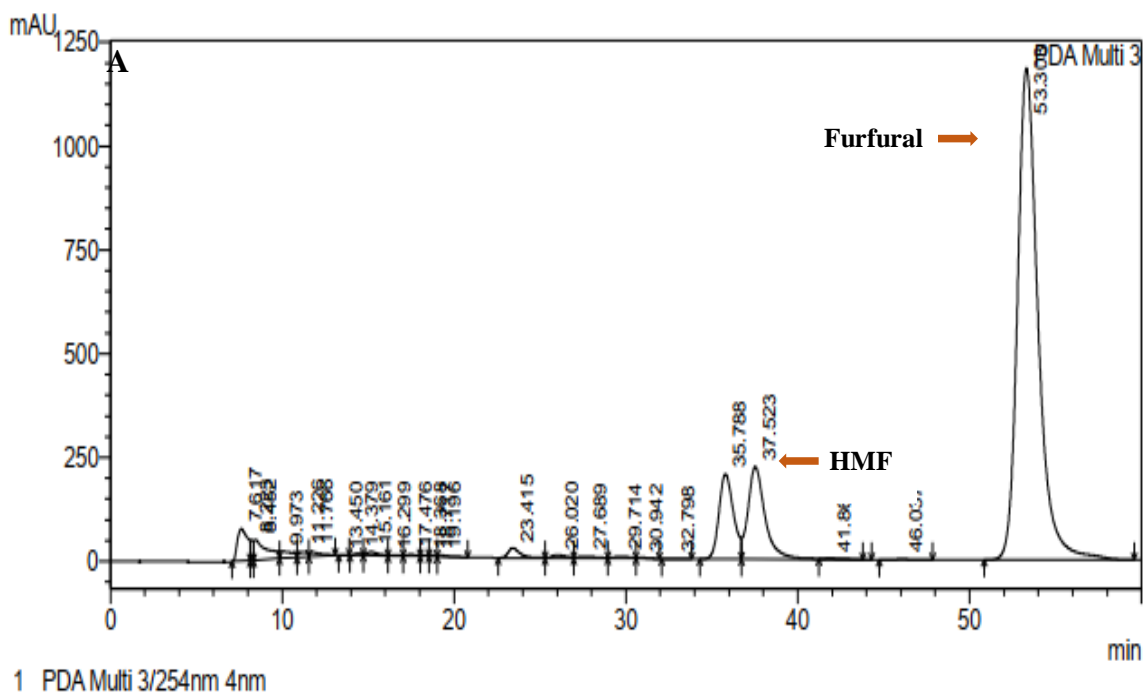


Fig.5.7A. HPLC chromatogram of non-detoxified sawdust APL

*(Peak area: HMF – 15245, Furfural – 1854834)

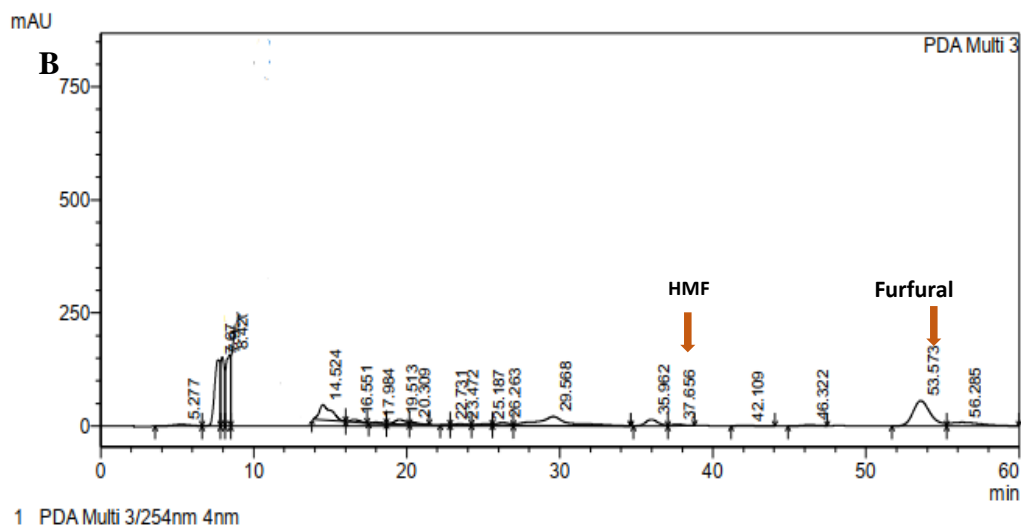


Fig. 5.7B. HPLC chromatogram of detoxified sawdust APL

*(Peak area: HMF – 1841, Furfural – 7321)



Fig. 5.7C. Appearance of sawdust APL (a) before and (b) after treatment with INDION PA 500 resin.

5.3.5. Optimization of process parameters for xylonic acid production from APL of sawdust in 2.5L fermenter

The optimization of process parameters typically involves adjusting factors such as temperature, pH, agitation speed, dissolved oxygen and substrate concentration to maximize the yield of the product. pH experiments showed that the maximum xylonic acid production ($48.5 \pm 0.20 \text{ gL}^{-1}$) from 60 gL^{-1} xylose occurred at an initial pH of 6.5. With xylose alone in the medium the organism struggled to pick up the sufficient growth rate, glucose supplementation was

essential to initiate cell division and hence optimized the initial glucose level to be 8 gL⁻¹ to reach sufficient cell growth and xylose utilization. The effects of changing dissolved oxygen concentrations during fermentation revealed that the highest xyloonic acid production occurred in the range of 1.5 and 2.0 vvm and thus 1.5 vvm set as optimum level of DO. Similarly, 10 – 12 (% vv⁻¹) inoculum resulted in the maximum titers of 48 ± 0.20 gL⁻¹ and 50 ± 0.20 gL⁻¹ and as the difference is marginal, 10 (% vv⁻¹) inoculum fixed as the optimum inoculum percentage (Table.5.2.). So, the parameter levels: xylose 60 gL⁻¹, glucose 8 gL⁻¹, DO 1.5 vvm and inoculum 10 % were optimized for maximal xyloonic acid yield in 2.5 L fermenter.

Table.5.2. Process parameters for xyloonic acid production under submerged fermentation in 2.5L fermenter

Parameters	Glucose (gL ⁻¹)	Xylose (gL ⁻¹)	DO (vvm)	Inoculum (% vv ⁻¹)	Xyloonic acid (gL ⁻¹)
Glucose concentration	2				-
	4				-
	6	60	1.5	10	22.3 ± 0.2
	8				45.5 ± 0.1
	10				36.2 ± 0.2
Xylose concentration		40			15.4 ± 0.3
		50			20.9 ± 0.2
	8	60	1.5	10	48.5 ± 0.2
		70			34 ± 0.2
		80			32.5 ± 0.1
Oxygen			0.5		24.8 ± 0.2
			0.8		28.9 ± 0.3
	8	60	1.0	10	31.6 ± 0.1
			1.5		47 ± 0.3
			2.0		50 ± 0.2
Inoculum size				3	8.5 ± 0.2
				5	18.6 ± 0.1
	8	60	1.5	8	32.8 ± 0.3
				10	48.5 ± 0.2
				12	50 ± 0.2

With the optimized process parameters, the recombinant strain *C.glu-xylB* produced $48.5 \pm 0.20 \text{ gL}^{-1}$ xylonic acid from 60 gL^{-1} xylose with a yield of 0.89 gg^{-1} xylose and productivity $0.30 \text{ gL}^{-1}\text{h}^{-1}$ (Fig.5.8.). Corresponding to the theoretical yield of xylonic acid from xylose *i.e* 73.67 %, the % yield obtained was 63% and that of xylose conversion efficiency of the strain *C.glu-xylB* was observed to be 86.6%.

$$\% \text{ Yield} = \frac{\text{Experimental yield}}{\text{Theoretical yield}} \times 100$$

Theoretical yield (73.67)

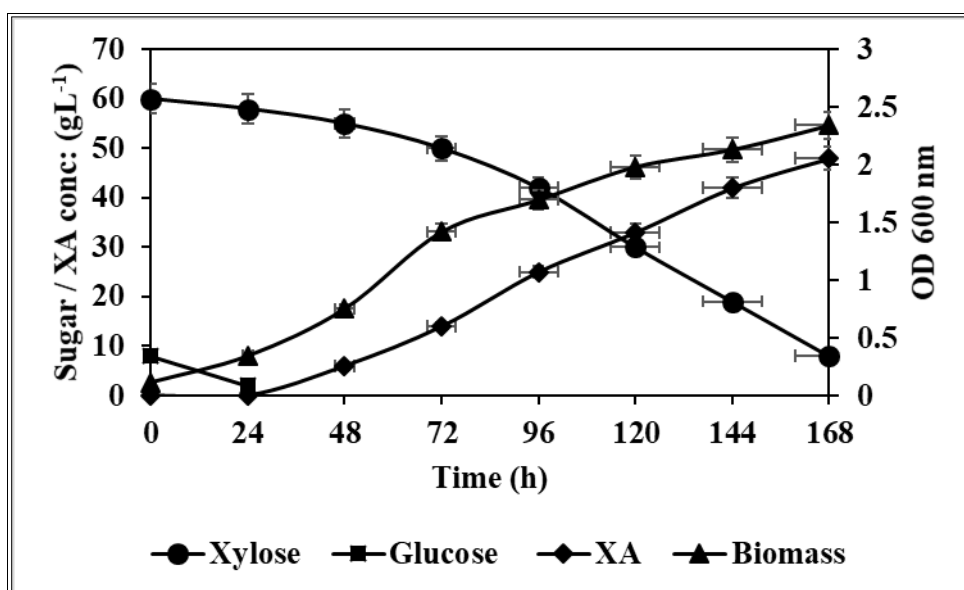


Fig.5.8. 2.5L Batch fermentation using recombinant *C. glu-xylB* in CGXII- sawdust APL production medium. The data shows cell growth, sugar utilization (glucose and xylose) and xylonic acid production by recombinant *C. glu-xylB*

5.3.6. The effect of HMF and furfural on xylonic acid fermentation

Fig.5.9A and B shows the inhibitory effects of furfural and HMF at its different concentrations (0.5, 1.0, 1.5 and 2.0 gL^{-1}) in synthetic CGXII production medium and it is

observed that the addition of inhibitors increased the lag phase of bacterial growth. As the concentration of inhibitors increases the uptake of xylose and its conversion into xylonic acid decreased. From Fig.5.9A. it is observed that with the addition of 0.5 gL^{-1} furfural, almost 20 gL^{-1} xylose remained unutilized after 120 h fermentation and the yield was 33 gL^{-1} against the control (i.e., in the absence of inhibitors) where residual xylose was 7 gL^{-1} and that of xylonic acid production was 53 gL^{-1} . As the concentration further increased, the growth, xylose utilization and xylonic acid production gradually decreased and at 2.0 gL^{-1} furfural, the organism was found to be unable to grow and no sugar uptake and production were noticed. Similarly, in Fig.5.9B. in the presence of 0.5 gL^{-1} HMF the inhibitory effect was higher compared to furfural where 25 gL^{-1} xylose remained unutilized yielding only 30 gL^{-1} xylonic acid against control i.e., 53 gL^{-1} xylonic acid after 120 h fermentation. The inhibitory effect of HMF was greater than that of furfural, and at 2.0 gL^{-1} HMF concentration, there was no xylonic acid production.

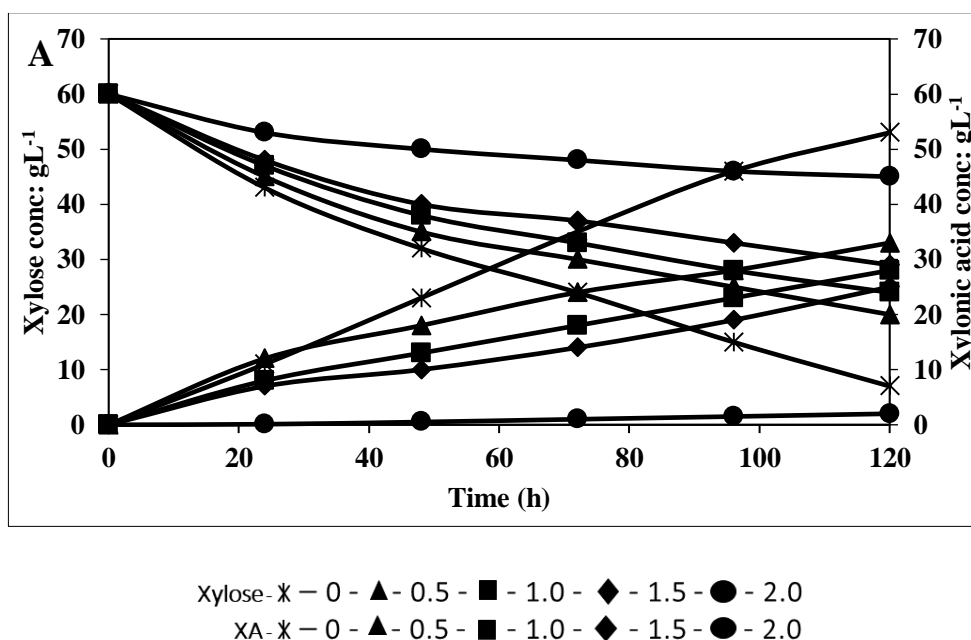


Fig.5.9A. Effect of furfural on xylose consumption and xylonic acid production

* Xylose consumption and xylonic acid production in the presence of different concentration

of furfural (cross – 0 gL⁻¹ furfural, filled triangle – 0.5 gL⁻¹ furfural, filled square – 1.0 gL⁻¹ furfural, filled diamond – 1.5 gL⁻¹ furfural, filled circle – 2.0 gL⁻¹ furfural.)

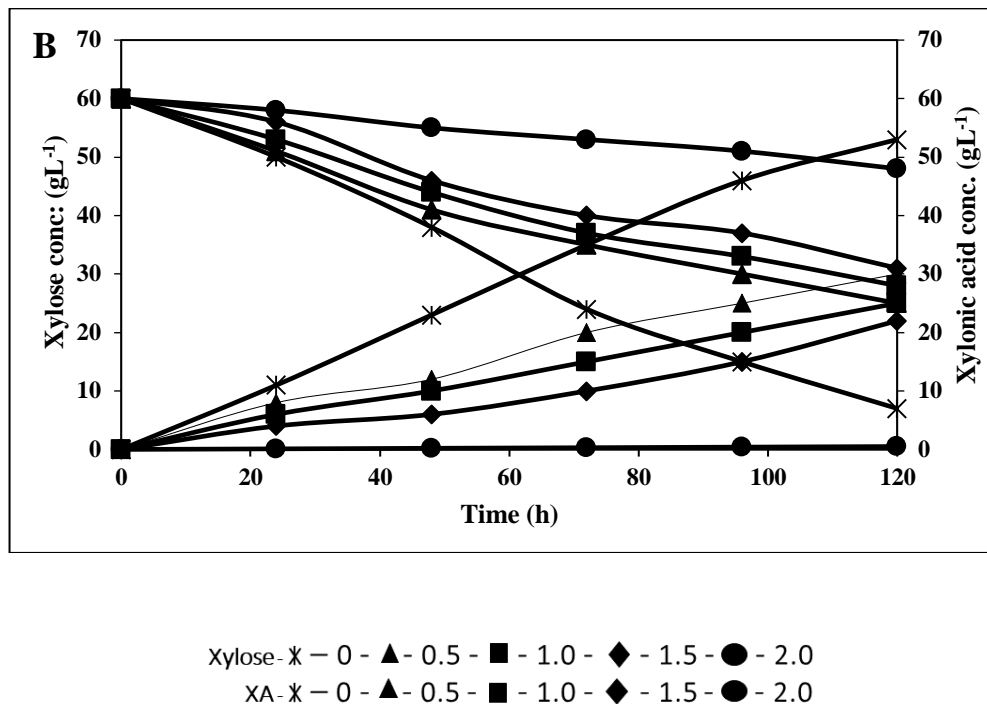


Fig.5.9B. Effect of HMF on xylose consumption and xylic acid production

* Xylose consumption and xylic acid production in the presence of different concentration of HMF (cross – 0 gL⁻¹ HMF, filled triangle – 0.5 gL⁻¹ HMF, filled square – 1.0 gL⁻¹ HMF, filled diamond – 1.5 gL⁻¹ HMF, filled circle – 2.0 gL⁻¹ HMF)

On exploring the effect of inhibitors, furfural and HMF, in APL on xylic acid production, it was observed that both the inhibitors had an inhibitory effect on fermentation reaction. The effect of HMF was found to be higher than furfural on xylic acid fermentation.

5.4. Discussion

Dilute acid pre-treatment is an effective and affordable technique for release of fermentable sugars from biomass. The acid pre-treated liquor (APL) is the valuable source of

hexoses and pentoses from the hemicellulose fraction in the biomass. As already mentioned rice straw, wheat bran and sawdust were selected as the raw material for the study.

Rice straw is the by-product of rice cultivation and is composed of the leaves, stems, and husks of the rice plant. It is one of the most abundant agricultural residues worldwide, with an estimated annual production of over 700 million tons. Rice straw has many potential applications, including as animal feed, soil amendment, and as a feedstock for biofuel production. However, rice straw is often considered a waste product and can pose environmental challenges if not properly managed. It can be a significant source of air pollution when burned in the fields, which is a common practice in many rice-producing regions. Therefore, alternative uses for rice straw, such as its use as a feedstock for biofuel production, can help reduce environmental impacts while providing a valuable resource.

Wheat is one of the most widely cultivated cereal crops in the world, and as a result, wheat bran is also a widely available by-product of wheat milling. Wheat bran can be used as a raw material for value addition in the production of various products. For example, it can be used to produce biofuels, such as biogas and bioethanol. The high cellulose and hemicellulose content of wheat bran make it a suitable feedstock for biofuel production. In addition, wheat bran can be used in the production of value-added products such as dietary supplements, functional foods, and biodegradable packaging materials.

The timber market in India is experiencing a significant growth, resulting in the generation of large amounts of sawdust as a major by-product of wood processing. It is crucial to adopt a sustainable approach to manage this waste and make use of it effectively. Currently, sawdust is commonly utilized in direct combustion methods to generate heat as a loose biomass,

which poses significant environmental hazards. In contrast sawdust containing fermentable sugar can be valorised into biofuels and high value products.

Fermentative production of xylonic acid from sugar mixtures i.e, from acid pre-treated lignocellulosic liquor using recombinant *C. glutamicum* has been carried out. The utilization of recombinant *C. glutamicum* for the efficient bioconversion of xylose present in biomass acid pre-treated liquor (APL) to xylonic acid was validated. The fermentative production of xylonic acid from xylose using various genetically modified organisms has been studied (Yim et al. 2017; Herrera et al. 2021). However, this is the first attempt that describes about the functional validation of a recombinant *C. glutamicum* ATCC 31831 for xylonic acid production from lignocellulosic biomass derived xylose.

The recombinant strain, *C.glu-xylB* produced $48.5 \pm 0.20 \text{ gL}^{-1}$ xylonic acid from 60 gL^{-1} xylose, with a yield of 0.89 gg^{-1} xylose and a productivity of $0.30 \text{ gL}^{-1}\text{h}^{-1}$. Although the theoretical yield of xylonic acid from xylose is 76.4 %, the yield obtained was 63 %. However, the xylose conversion efficiency of the strain *C.glu-xylB* was 86.6%. These results of xylonic acid productivity and yields are quite competitive compared to previous results obtained using other hosts *Zymomonas mobilis* ($0.32 \text{ gL}^{-1}\text{h}^{-1}$, 1.07 gg^{-1}), *Candida glycerinogenes* ($0.77 \text{ gL}^{-1}\text{h}^{-1}$, 0.83 gg^{-1}), *Komagataella phafi* ($0.14 \text{ gL}^{-1}\text{h}^{-1}$, 0.37 gg^{-1}) and *Komagataella phafi* ($0.16 \text{ gL}^{-1}\text{h}^{-1}$, 0.43 gg^{-1}) (Herrera et al. 2021; Qiao et al. 2021; Ramos et al. 2021).

While examined the production of xylonic acid in a defined medium *Gluconobacter* seems to be the most promising microorganism. However, the slow growth rate of *Gluconobacter*, the need for a more complex growth medium, low tolerance to hydrolysates, and promiscuous oxidizing enzymes may hinder the scale-up of the process (Zhou et al. 2019). Another potential xylonic acid producer, *P. sacchari*, has not yet been evaluated on

hemicellulosic hydrolysates, so it is unclear how its xylonic acid production will be affected in an industrial setting (Bondar et al. 2021). Despite the various applications of xylonic acid and the involvement of numerous players in the development of biotechnological processes, there is currently no industrial-scale production of xylonic acid, and the use of lignocellulosic hydrolysates as a feedstock poses the first hurdle towards industrialization. The presence of microbial growth inhibitory compounds, such as acetic acid and furaldehydes in the raw material is one of the primary challenges associated with this. These furan derivatives (Furfural and HMF) are the family of by-products from heat-processed pentose and hexose, and are the significant group of inhibitors in the pre-hydrolysate and were thought to be the most significant fermentation inhibitors for diverse bacteria (Jilani et al. 2020). The development and viability of several bacteria, yeasts, and fungi are negatively impacted by furan derivatives once the concentration exceeds 1.0 gL^{-1} (Chandel et al. 2013). These derivatives have been shown to inhibit fermentation processes by affecting the viability of microorganisms and activity of enzymes involved in the process, for example inhibiting the enzymes involved in glucose metabolism leading to decrease in energy production (Li et al. 2022).

Here comes the role of *C. glutamicum* the most potent industrial microbe that has undergone significant modifications to use pentose sugars from hemicellulosic biomass more effectively, achieved by introducing new and alternative pathways for their assimilation (Gopinath et al. 2012; Dhar et al. 2016). Due to its natural characteristics, such as weak carbon catabolite repression and resistance to toxic inhibitors, as well as its engineered abilities, (Choi et al. 2019) *C. glutamicum* can be considered as one of the best candidates for biomass valorisation for value addition.

5.5. Summary

Bioconversion of xylose derived from lignocellulosic biomass to xylonic acid was analyzed with recombinant strains of *C. glutamicum*. In this chapter it is demonstrated the value addition of biomass derived xylose to xylonic acid. Composition analysis (for fermentable sugars and inhibitor content) of different biomass and quantification was done using HPLC. The acid pre-treated sawdust liquor (APL) contained 45.55 ± 6.5 % cellulose, 24.41 ± 3.5 % hemicellulose and 29.05 ± 0.5 % lignin. Based on higher xylose content and relatively lower inhibitor release, saw dust was used as the raw material for xylonic acid production. Improved product quality, yield and processing efficiency was achieved by detoxifying the sawdust APL with INDION PA 500 resin. The resin could remove 90% inhibitors present in the APL. Under optimized process conditions recombinant *C. glu-xyIB* produced 48.5 ± 0.2 gL⁻¹ xylonic acid from 60 gL⁻¹ saw dust derived xylose with a yield of 0.89 gg⁻¹ xylose and productivity of 0.3 gL⁻¹h⁻¹.

Chapter 6

Recovery, purification, and characterization of xylonic acid

6.1. Introduction

Xyloic acid (XA) is a naturally occurring organic acid, primarily found in the form of esters in various plant species. It is a colourless, crystalline solid that is soluble in organic solvents and has a mild, sweet odour. In terms of its structure, xyloic acid consists of a carboxylic acid functional group (-COOH) and a hydroxyl group (-OH) attached to a linear carbon chain. It is considered as a monocarboxylic acid, meaning it has only one carboxyl group in its structure. An understanding of the properties of purified xyloic acid is essential for the proper utilisation of the xyloic acid in various sectors. The purification of xyloic acid from heterogeneous fermented broth is a difficult task. Though there are different methods of purification strategies (Cao and Xu 2019; Dai et al. 2020) the key issue is the composition of fermented liquor.

Purification of xyloic acid typically involves a series of steps that separate and remove impurities from the starting material. The specific methods used can vary depending on the source of the xyloic acid and the desired level of purity. One common approach involves the use of column chromatography. This involves passing the starting material through a column packed with a stationary phase that selectively retains xyloic acid while allowing impurities to pass through. The pure xyloic acid can then be recovered and purified (Wang et al. 2016). Another commonly used method for xyloic acid purification is distillation. This involves heating the starting material to boiling point and condensing the vapour produced to collect the pure xyloic acid. This method can be effective for removing impurities such as water, alcohols, and other volatile compounds. Other techniques that may be used in xyloic acid purification include recrystallization, which involves dissolving the starting material in a suitable solvent and then allowing it to crystallize out as pure xyloic acid, and crystallization from a super cooled

solution, which involves cooling the starting material below its normal melting point to encourage the formation of pure xylonic acid crystals (Zhang et al. 2017). Regardless of the specific methods used, the purification of xylonic acid is often a multi-step process that requires careful monitoring and control to ensure the desired level of purity is achieved.

This chapter portrays the purification of xylonic acid from CGXII synthetic medium where xylose used as main carbon source and also from sawdust APL-CGXII medium where the xylose present in the acid pre-treated liquor of saw dust used as the carbon source. Here, solvent precipitation is employed for downstream processing, where three different solvents (ethanol, acetone and isopropanol) were attempted. The xylonic acid was crystallized and analysed by HPLC, LC-MS, and ^1H and ^{13}C NMR.

6.2. Materials and Methods

Heterogeneous fermented broth (sawdust APL-CGXII medium) and CGXII synthetic medium containing residual sugars and xylonic acid was used for purification studies. Composition of CGXII medium is given in Annexure II. Solvents such as ethanol, isopropanol and acetone were purchased from SRL Pvt. Ltd (India) for the recovery and purification of xylonic acid.

Details of soluble protein estimation (Bradford, 1976) and HPLC analysis are described in Chapter 2, section 2.4.1. and section 2.4.3. respectively.

6.2.1. Clarification of fermented broth

Xylonic acid fermentation was carried out in 2.5L fermenter with a working volume of 1L, where the initial xylose concentration was fixed at 60 gL^{-1} . 1L of fermented culture broth (CGXII synthetic medium and sawdust APL-CGXII medium) was centrifuged at 6,000 g for 10

min to remove the cell biomass present in the broth. The supernatant was concentrated 10 times by evaporation in a rotary vacuum concentrator (Buchi, India) at 65°C. The concentrated crude broth was adjusted to pH 7.0 with 10 N NaOH. The mixture was incubated at 20°C for 12 h for the precipitation of soluble proteins. The protein precipitate that formed was separated by centrifugation at 8,000 g for 8 min. The resultant cleared broth was analysed for protein estimation (Bradford, 1976) and the percentage of protein removal from fermented broth was calculated using the formula given below.

Percentage of protein removal (%) =

$$\frac{\text{Protein content of crude broth (mg)} - \text{Protein content of clarified broth (mg)}}{\text{Protein content of crude broth (mg)}} \times 100$$

Protein content of crude broth (mg)

6.2.2. Decolourization of clarified broth by activated charcoal

Activated charcoal was used to decolourize clarified broth. Activated charcoal has a large surface area and a high adsorption capacity, which makes it an effective adsorbent for removing impurities, including pigments, from fermented broth (Wang et al. 2022). To use activated charcoal for decolourization, it is typically added to the clarified broth in small amounts, and the mixture is stirred/shaken to allow the activated charcoal to adsorb the pigments. The mixture is then filtered to remove the activated charcoal, resulting in a decolourized broth. It is important to note that activated charcoal can also adsorb other compounds in the broth, including sugars and the compound of interest, so it is essential to use the appropriate amount and type of activated charcoal to minimize these effects.

Here we standardized the conditions for decolourization of fermented sawdust APL-CGXII medium and CGXII medium based on the maximum decolourization efficiency (D). The

decolourization efficiency (%) was calculated on the basis of the absorbance (OD at 420 nm) of the sample before and after the decolourization process. The effect of different parameters such as carbon concentration, pH, temperature and contact time on decolourization efficiency were analysed. For this, 10 mL of clarified fermented broth was adjusted to pH (5.0 to 9.0) was treated with activated carbon (1 to 20 % (wv⁻¹)). The mixture was incubated at various temperatures (30 to 60°C) for 2 h at 200 rpm. The samples were taken at every 30 min and filtered through Whatman No.1 filter paper (Merck, India) for the analysis of decolourization. The parameters that led to the increased decolourization efficiency were taken into consideration for the development of standard decolourization procedure for fermented sawdust APL-CGXII medium and CGXII synthetic medium.

$$\text{Decolourization (D)} = \frac{A_0 - A}{A_0} \times 100$$

A_0

Where,

A_0 - absorbance before decolourization

A - absorbance after decolourization

6.2.3. Crystallization of xylonic acid

Xylonic acid can be crystallized from a solution by cooling the solution to its saturation point, and then slowly removing the solvent to cause the xylonic acid to come out of solution and form crystals (Zhang et al. 2017). Other factors that can influence the crystallization process include the concentration of the solution, the presence of other impurities or substances, and the temperature and cooling rate of the solution. To obtain high-quality crystals, it may be necessary

to perform multiple crystallization steps, or to carefully control the conditions of the crystallization process.

For a comparative analysis we have used three solvents for downstream processing i.e., ethanol, acetone and isopropanol. After fermented broth (1L) clarification and activated charcoal treatment the supernatant was filtered and concentrated using a rotary evaporator (65°C). The solvents (ethanol, acetone and isopropanol) were added to the broth (in separate batches) in the ratio (3:1) vv⁻¹ to concentrate and precipitate xylonic acid. The xylonic acid crystals were formed after 72h at 4°C. The bigger crystals (5-10 mm) were separated by filtration and analysed its purity. The purity was determined by HPLC chromatograms in comparison with chromatogram of standard xylonic acid.

6.2.4. Characterization of xylonic acid

FTIR spectra of xylonic acid was performed on an FTIR spectrometer (IR-Tracer, Shimadzu, Japan), with a wave number of 4000 to 400 cm⁻¹. ¹H and ¹³C nuclear magnetic resonance (NMR) (Bruker, Germany) performed for the identification and quantification of the functional groups and structural features of the molecule. High Performance Liquid Chromatography (HPLC, Shimadzu Corporation, Kyoto, Japan) was done (in organic acid column with 0.01N H₂SO₄ as mobile phase) to determine the purity and composition of the crystal. The purity was determined from the peak area of HPLC chromatogram. Liquid chromatography-mass spectroscopy (LC-MS/MS system Nexera with LCMS-8045 Shimadzu Corporation, Kyoto, Japan) was employed to identify the molecular mass of xylonic acid.

$$\text{Purity \%} = \frac{\text{Area of xylonic acid peak}}{\text{Total area of all peaks}} \times 100$$

6.2.5. Antibacterial property of xylonic acid

The antibacterial activity of xylonic acid crystals against *Escherichia coli* MTCC 443, *Staphylococcus aureus* MTCC 96, and *Salmonella enterica* MTCC 3224 were assessed. The bacterial strains were grown in LB broth. To test the efficacy of xylonic acid, used Kirby Bauer assay, which is a modified disc diffusion assay (Hudzicki 2009). Bacterial cultures were grown in LB broth until an $OD_{600\text{ nm}}$ of 0.6 and 100 μl of the cultures were spread onto MHA plates, then filter paper discs loaded with xylonic acid (concentration range 1-10 mgmL^{-1}) were placed on the bacterial spread. The xylonic acid diffuses out of the disc and into the media where it is taken up by the growing cells. The area with no bacterial growth surrounding the disc forms the zone of inhibition.

6.3. Results

Xylonic acid was purified from heterogeneous fermented broth containing various residual sugars and other components by a sequential method such as clarification, decolourization, filtration and crystallization. The purity and identity of xylonic acid was verified by HPLC, FTIR and NMR spectroscopy.

6.3.1. Clarification

The 1L concentrated heterogeneous fermentation broth obtained after the separation of biomass was subjected to precipitation of soluble protein at 20°C under pH 8.0 with 5 % lead acetate (wv^{-1}) and calculated the percentage of protein removal from the clarified fermented broth using Bradford's method. From the results it could be seen that 85.6 ± 2.0 % of protein removal was achieved.

6.3.2. Decolourization

Effect of different charcoal concentration studies showed the maximum efficiency of decolourization (75.6 ± 0.6 %) with 20 % charcoal. pH studies revealed the optimum was the control pH (pH 6) for maximum percentage of decolourization efficiency. Study of the influence of contact time on decolourization efficiency of clarified sawdust APL showed that 120 min was the best contact time. The results of incubation temperature studies showed that maximum decolourization efficiency (94 %) was attained when incubated at 60°C for 120 min (Table 6.1).

Table 6.1. Effects of various parameters on decolourization efficiency of fermented broth

Parameters	Activated charcoal (wv ⁻¹) %	Temperature °C	pH	Contact time (min)				Decolorization %
				30	60	90	120	
Activated charcoal (wv ⁻¹) %	5	40	6	25	27	30	35	
	10			27	30	35	37	
	15			36	40	45	50	
	20			41	49	51	55	
	25			50	58	65	71	
Temperature °C	20	20	6	24	37	42	52	
		30		51	60	65	73	
		40		65	71	82	85	
		50		67	90	91	93	
		60		75	92	93	94	
pH	20	40	5	51	60	65	68	
			6	50	59	67	70	
			7	42	52	65	68	
			8	34	41	45	50	
			9	33	36	43	47	

The results also showed that there were marginal differences in decolourization efficiency with incubation time (30, 60, 90 & 120 min). By considering the process economy, the decolourization parameters selected were 20 % (wv⁻¹) charcoal, pH 6.0, temperature 60°C and incubation time of 120 min.

6.3.3. Xylonic acid recovery and purification

Ethanol precipitation was found to be efficient to separate xylonic acid from the fermentation broth. After downstream processing, 40.81 gL⁻¹ (95.5% purity) and 30.8 ± 0.4 gL⁻¹ (89 % purity) xylonic acid crystals were recovered from 1L CGXII synthetic medium and sawdust APL-CGXII production medium. Fig.6.1A and B shows the xylonic acid crystals obtained from the CGXII-synthetic production medium and sawdust APL-CGXII production medium. To visualize the intensity of purity, epifluorescence image of xylonic acid crystal was also recorded (Fig.6.2) using a fluorescent microscope (Leica DM 2500 epifluorescent) equipped with UV filter. The intensity of fluorescence shows the purity and quality of the xylonic crystal. Xylonic acid recovery, yield and purity from CGXII synthetic medium and sawdust APL-CGXII medium is given in Table 6.2.



Fig.6.1. Xylonic acid crystals obtained from CGXII synthetic medium (A) and sawdust APL-CGXII production medium (B)

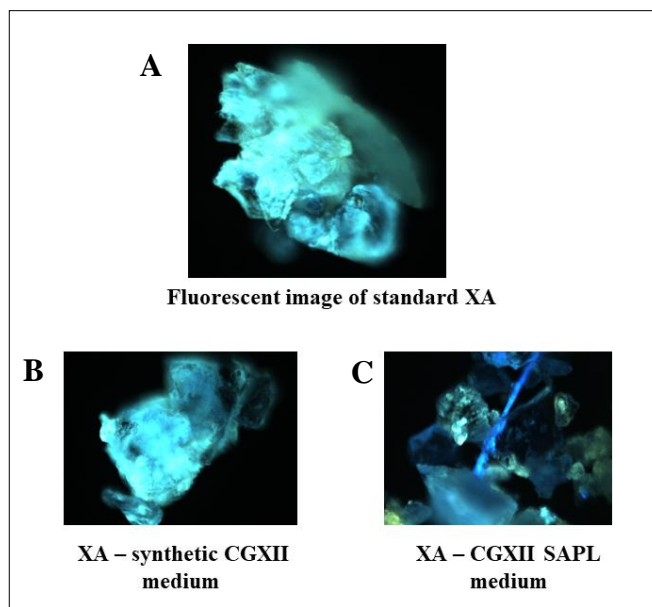


Fig.6.2. Fluorescent image of (A) standard xylonic acid (B) xylonic acid crystal recovered from CGXII synthetic medium (C) xylonic acid crystal recovered from sawdust APL-CGXII medium

Table 6.2. Xylonic acid recovery yield from CGXII synthetic medium and sawdust APL-CGXII medium

Medium	Solvent used for downstream processing	Total (gL ⁻¹)	Loss (gL ⁻¹)	% recovery	Yield (gL ⁻¹) crystal form	% purity of xylonic acid (from peak area)
CGXII synthetic medium	Acetone	56.31	18.9	66.4 %	37.41	89 %
	Ethanol	56.31	15.5	72.4 %	40.81	95.5 %
	Isopropanol	56.31	17.2	69.4 %	39.11	90 %
Sawdust APL-CGXII medium	Ethanol	48.5	17.7	63.5 %	30.80	89 %

6.3.4. LC-MS, NMR, FTIR and HPLC characterization of xylonic acid crystal

Confirmation of the purified crystals to be xylonic acid is done with the help of varying analytical techniques such as LC-MS, NMR, FTIR and HPLC.

The molecular mass of xylonic acid was determined *via* LCMS. 0.01-1 $\mu\text{g mL}^{-1}$ concentration of the sample in milliQ was analysed for mass detection. The molecular mass of the purified xylonic acid crystal was confirmed against the mass of standard xylonic acid which is 165 (Fig.6.3 A and B).

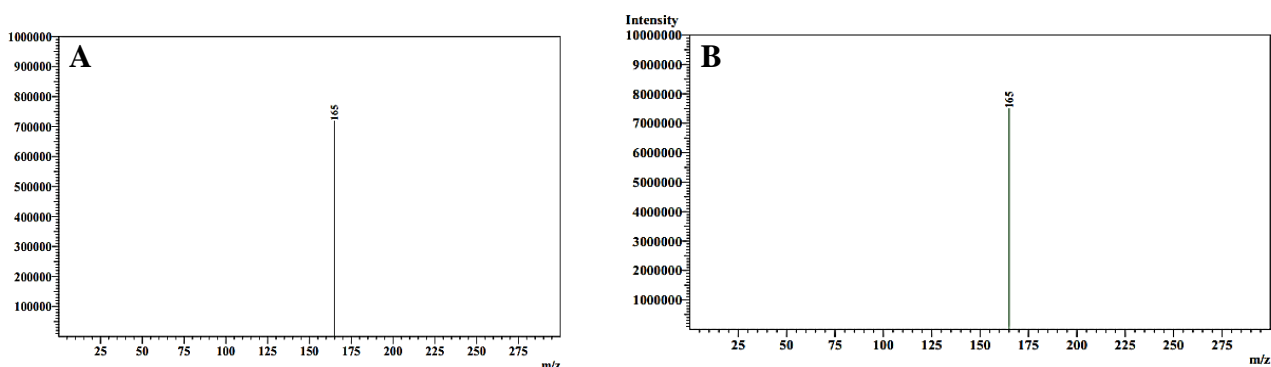


Fig.6.3. LCMS/MS spectrum of (A) standard xylonic acid (B) purified xylonic acid crystal

NMR spectrum for xylonic acid was obtained in Proton and Carbon Nuclear Magnetic Resonance Spectroscopy (^1H and ^{13}C NMR). 5 mg of purified xylonic acid crystals were dissolved in 600 μl NMR grade deuterium water (D_2O) (Merck, India) for analysis. The NMR spectrum of the crystal obtained was comparable to the spectral graph produced with standard xylonic acid, where the spectral peak in the range of 3.966 and 3.971 ppm in standard xylonic acid ^{13}C NMR and xylonic acid crystal (sample) ^{13}C NMR indicated the presence of carbonyl carbon in xylonic acid (Fig.6.4 A and B). On comparing the chemical shift of the peak in sample against that in standard xylonic acid it was found that the chemical environment around the nucleus is similar in both the spectrum. Also, the number and relative intensities of the peaks in the sample when compared to the standard identified the presence of a specific carboxylic acid group in both the crystal sample and standard xylonic acid.

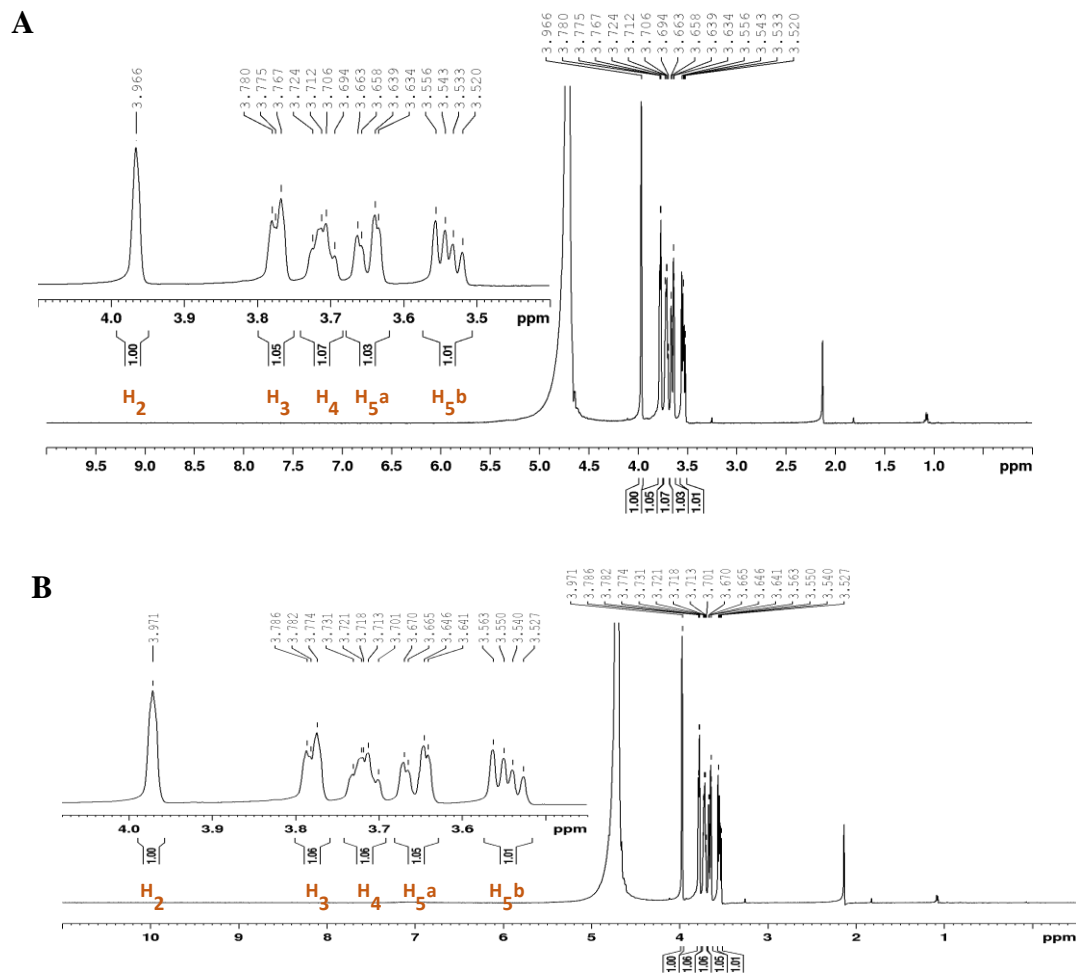


Fig.6.4. ^1H and ^{13}C NMR of (A) standard xylonic acid (B) purified xylonic acid crystal

FTIR measurements were carried out for both the xylonic acid standard and purified crystals from fermentation broth. The peak of OH (O-H stretch) was found at 3197.98 cm^{-1} and the carbonyl (C=O) stretch was observed at 1579.70 cm^{-1} . The presence of specific OH and carbonyl stretch confirms the crystals as xylonic acid and the data obtained was comparable with the standard xylonic acid spectrum (Fig.6.5).

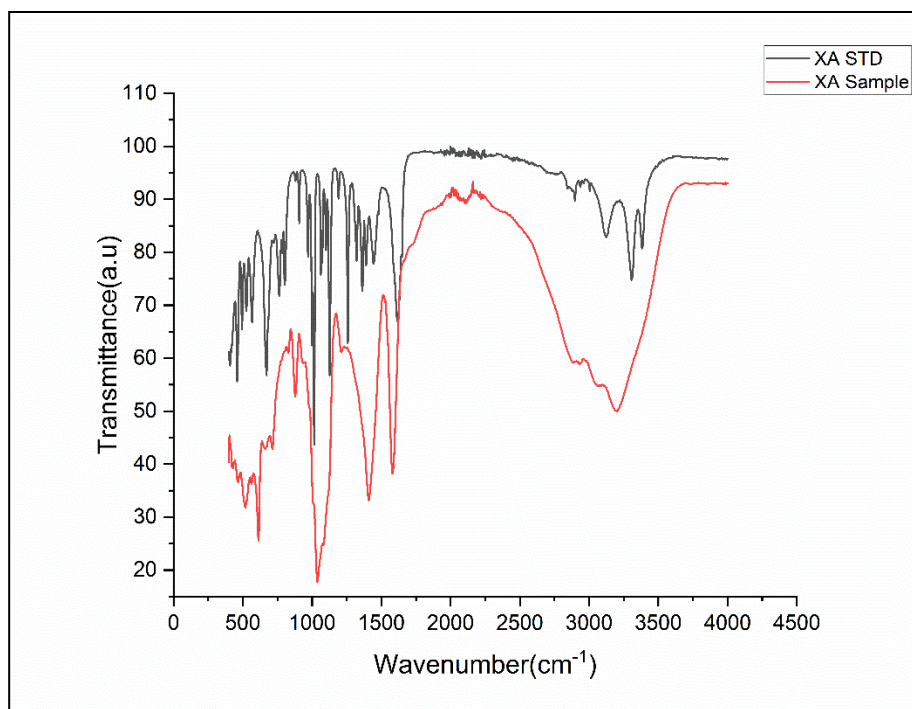


Fig.6.5. FTIR spectrum of standard xylic acid and purified xylic acid crystal

HPLC chromatogram was used to determine the purity of crystals in comparison to the chromatogram of standard xylic acid. HPLC analysis (peak area) demonstrated that the purity of the crystals was as high as 95 % (Fig.6.6 A and B).

Purity of XA (%) =

$$\frac{\text{HPLC peak area of purified XA from the fermentation broth (10 mgmL}^{-1}\text{)} * 100}{\text{HPLC peak area of standard XA (10 mgmL}^{-1}\text{)}}$$

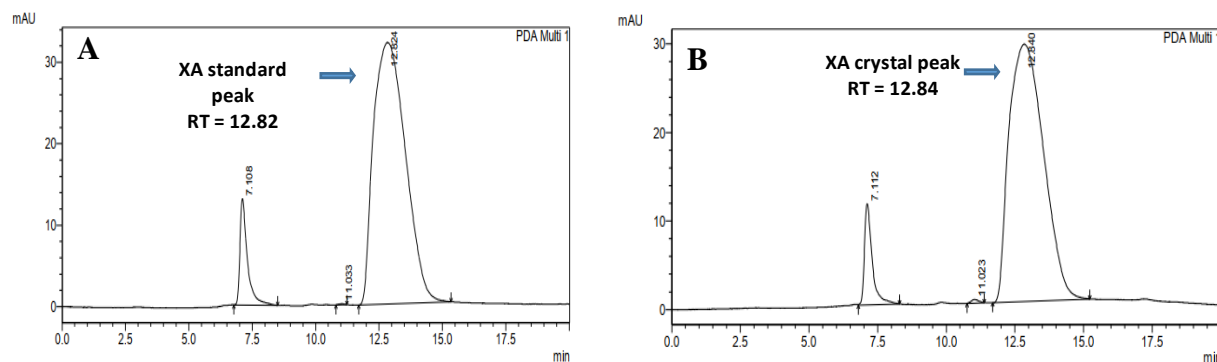


Fig.6.6. HPLC chromatogram of (A) xylic acid standard (B) purified xylic acid crystal

6.3.5. Xylonic acid and anti-microbial activity

Bacterial cultures on MHA plates were incubated with xylonic acid (1 – 10 mgmL⁻¹) loaded discs. A clear zone of inhibition started forming at a concentration of 4 mgmL⁻¹ after 24 h incubation at 37°C, indicating that this is the minimum effective concentration for inhibiting the growth of these pathogenic microorganisms (Fig.6.7). This means that xylonic acid was able to display antibacterial activity at a concentration of 4 mgmL⁻¹ or higher. However, it is important to note that this data is based on a disc study and further research is needed to confirm the effectiveness of xylonic acid in other forms and *in vivo*.

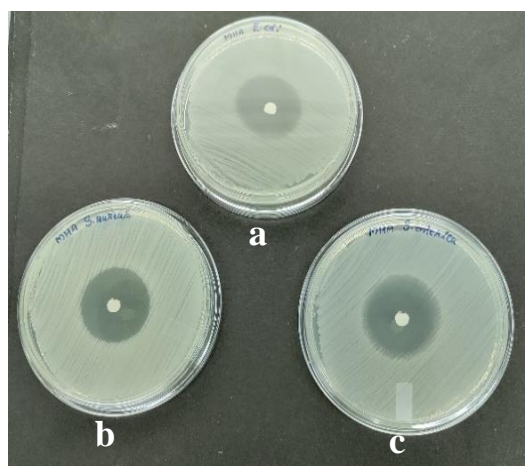


Fig.6.7. Antimicrobial effect of xylonic acid against (a) *Staphylococcus aureus* MTCC 96, (b) *Escherichia coli* MTCC 443 and (c) *Salmonella enterica* MTCC 3224

6.4. Discussion

The key factor in achieving a feasible bioprocess for xylonic acid is the development of effective production and purification methods. To separate and purify xylonic acid from the fermentation broth, multi-step process was standardized which comprised of activated charcoal treatment, pH adjustment, ion exchange resins, chromatographic methods, or liquid-liquid

extraction. Impurities in the fermented broth were found to precipitate at lower temperatures (20°C) and alkaline pH (8.0) in the presence of 5% (wv⁻¹) lead acetate. Concentrating the broth by 10-fold and using low temperature resulted in better impurity precipitation. The protein removal efficiency of this process was found to be 87.7%.

Charcoal treatment is an inexpensive and efficient method to remove colour from fermented broth. Its effectiveness was enhanced by extracting protein and other impurities from the concentrated fermented broth. To remove the dark brown colour of APL in the fermented broth, charcoal treatment (20 % wv⁻¹) was applied at 50°C and pH 6.0 for 60 min. The decolourization percentage of $92.4 \pm 1.6\%$ was calculated using a previously described procedure (Martínez et al., 2015).

Different downstream strategies were reported for xylonic acid recovery from fermentation broth which are as follows,

Ion exchange chromatography, which is a widely used technique for separating xylonic acid from other organic acids in the fermented broth. The anionic exchange resin (D311) is used for separation. The technique is based on the selective adsorption of xylonic acid onto the resin. The resin is then eluted with a buffer solution (1 molL⁻¹ NH₃) to recover the purified xylonic acid (Wang et al. 2016). The advantages of this technique include high purity and yield of the final product, but the disadvantages include the high cost of the resin and the potential for fouling.

Bipolar membrane electrodialysis (BMED), is another technology used to separate xylonic acid from other organic acids and impurities in the fermented broth. During the process, electric current causes the salt ion conjugated xylonic acid to migrate towards the bipolar membrane, where they get separated in the medium. Applying BMED approach 92% yield of

xylonic acid obtained from a fermentation broth containing 100 gL^{-1} of sodium xylonic acid. But the disadvantages include membrane damage and the potential for fouling of the membrane (Cao and Xu 2019).

Solvent extraction and crystallization is the technique involves the use of an organic solvent to extract xylonic acid from the fermented broth. The solvent is then cooled or evaporated to induce crystallization. The crystals are then separated and dried to recover the purified xylonic acid (Liu et al. 2012).

In this study, via ethanol precipitation and crystallization could recover xylonic acid with purity of 95.5 % from synthetic CGXII medium and that of with 89 % purity from sawdust APL based CGXII medium. The advantages of this technique over other downstream process includes high yield and purity of final product and simple operation.

In terms of its biological significance, xylonic acid has been found to have antimicrobial properties, making it a potential candidate for various applications in health care and food industries. It is assumed that the fluorescent nature as well as the acidic pH of xylonic acid is affecting the membrane potential of bacteria and thus inhibiting their growth. According to our experiments the minimum inhibitory concentration (MIC) obtained was high (4 mgmL^{-1}), and is not suitable for clinical applications. However, xylonic acid still finds application as an antibacterial agent in paints, adhesives and lignin rich nanocellulose (LRNC) films (Luo et al. 2020).

6.5. Summary

The process of recovery of xyloonic acid started with the removal of biomass by centrifugation, following the clarification of the broth by removing protein and other impurities by precipitation. Activated charcoal treatment removed the colour retained in the clarified fermented broth. Among the different strategies, solvent extraction with ethanol was found to be effective in the separation of xyloonic acid from fermentation broth. 40.81 gL⁻¹ (95.5 % purity) and 30.80 gL⁻¹ (89 % purity) of xyloonic acid crystals were recovered after downstream processing with 64.4 % and 63.5 % recovery from synthetic CGXII medium and sawdust APL-CGXII medium. LCMS-MS, NMR spectrum analysis, and HPLC confirmation of the purified crystals were done against analytical standards. High purity and carbonyl functional group makes it a promising chemical for the development of new pharmaceuticals. Being non-toxic and highly water soluble acid finds application as meat tenderizing agent in food industry. Also the purified xyloonic acid crystals exhibited fluorescence property and antibacterial activity against pathogenic microorganisms, making it a potential candidate for use as a natural preservative and additive.

Chapter 7

Bioconversion of xylose to xylonic acid by xylose dehydrogenase immobilized on ferromagnetic nanoparticles

7.1. Introduction

Xylose dehydrogenase (EC number: XDH: 1.1.1.175) belongs to the family of oxidoreductases, and catalyses the oxidation of xylose in the presence of NADP^+ . Although it may utilise both NADP^+ and NAD^+ , the enzyme has a high preference for NADP^+ . This is one of the key enzymes in the oxidative Weimberg pathway and Dahms metabolic pathways where xylose is catabolised into xylonic acid (Brüsseler et al. 2019). Different metabolic pathways involving the catalysis of xylose dehydrogenase along with other enzymes in microbial species were elucidated for xylonic acid production (Yim et al. 2017).

Immobilization of enzymes on an appropriate matrix has improved their kinetics, stability, and reusability, allowing them to be used in a variety of industrial processes (Liang et al. 2020). As immobilized enzymes are more stable than native enzymes at varied pH and temperatures, biocatalysts based on immobilized enzymes have gained a lot of interest in the last decade (Smuleac et al. 2011; Bilal et al. 2018; Drout et al. 2019). It is observed that the support structure and topology can have a significant impact on the characteristics of enzymes (Barbosa et al. 2013; Tully et al. 2016). Interestingly, the use of nanoparticles as immobilization scaffold has revolutionised their prospective in recent years. Nanoparticles have special characteristics like high bio-catalytic and enzyme loading efficiency, improved mass transfer resistance, large surface to volume ratio, efficient storage and high adsorption capacity (Ahmad and Sardar 2015; Zhang and Hay 2020; Khoo et al. 2020). Nowadays, researchers are using magnetic nanoparticles to fix the catalysts. Magnetic nanoparticles outrank other varieties, including heat stability, pH tolerance, and ease of nanoparticle separation with a simple magnet. Furthermore, they have numerous applications in the biomedical field and in the food industry (Husain 2016). In this study, an attempt was made to immobilize xylose dehydrogenase enzyme on ferro

magnetic nanoparticles for xylose to xylonic acid bioconversion. The immobilization mechanism, various parameters influencing immobilization and the catalytic activity of the biocatalyst in bioconversion are discussed.

7.2. Materials and Methods

Iron oxide (Fe_3O_4), procured from Merck (Cat 637106, Sigma, India), 3-Aminopropyltriethoxysilane (APTES) (99%), glutaraldehyde and the Luria Bertani culture medium were purchased from Himedia (Mumbai, India).

7.2.1. *Heterologous expression and purification of xylose dehydrogenase of *Caulobacter crescentus**

Xylose dehydrogenase (*xylB*) gene was amplified from xylose inducible *xyIXABCD* operon of *Caulobacter crescentus* by polymerase chain reaction with gene specific primers designed. The purified amplicon (747 bp *xylB*) was confirmed by DNA sequencing (chapter 3 (3.3.3.)) and sub-cloned into restriction site (*Eco RI/Bam HI*) of expression vector pET 28a. The recombinant plasmid pET 28a-*xylB*, was transformed into competent *E. coli* DH5 α (100 μL) and screened on LB plates containing 25 $\mu\text{g mL}^{-1}$ kanamycin (Stephens et al. 2007). The isolated plasmid pET 28a-*xylB* was used to transform the competent cells of *E. coli*, BL21 (DE3) cells (Novagen, USA) for expression studies. The bacterial strains, vectors and oligonucleotides used in the study are given in Table 7.1.

For the expression and purification of xylose dehydrogenase enzyme, single colony of recombinant *E. coli* BL21(pET28a-*xylB*) was inoculated and incubated overnight at 37°C. 1 mL of pre-inoculum ($\text{OD}_{600 \text{ nm}}$ 0.8) was added to 100 mL of LB broth. The culture was incubated at 37°C until an $\text{OD}_{600 \text{ nm}}$ of 0.6 – 0.8, IPTG (1mM) induction was done and subsequently

incubated at 37°C for 3 h. The cells were harvested by centrifugation, frozen, thawed, and resuspended in 0.5 M phosphate buffer. The cell resuspension was sonicated (Time: 6 min Pulse: 10 s on and 10 s off, Amplitude: 40 %) using ultrasonic homogenizer (Vibra cell, Sonics and materials Inc, USA) and centrifuged on an orbital shaker for 30 min at 13,000 g. The cell free supernatant was filtered (0.2 mm filter) and allowed to pass through His-Trap HP nickel affinity column (GE health care), and an imidazole gradient in buffer (50 mM Na₃PO₄ buffer pH 7.2, and 300 mM NaCl) was used to elute the recombinant protein bound to the column. The purified protein was collected and stored at -80°C.

Table 7.1. Bacterial strains, vectors and primers used in the study

Strains / vectors	Specifications	Reference
Bacterial strains		
<i>Escherichia coli</i> DH5α	Maximizes transformation efficiency, with three mutations, recA1, endA1 and lacZΔM15	(Hanahan 1983)
<i>Escherichia coli</i> BL21(DE3)	F- ompT gal dcm lon hsdSB(rB- mB-) λ(DE3)	Novagen, USA
Plasmid vectors		
pET 28a	Bacterial expression vector	Novagen, USA
Xylose operon	Xylose inducible <i>xylXABCD</i> operon	Gifted by Prof. Dr. Volker F Wendisch, Bielefeld University, Germany
Primer (sequences 5'–3')		
<i>xyl B</i> pET F'	GATGATGGATCCATGTCCTCAGCCA TCTATCC (BamHI)	This study
<i>xyl B</i> pET R'	TATTATGAATTCCTCAACGCCAGCCG GCGTCGATCCAG (EcoRI)	This study

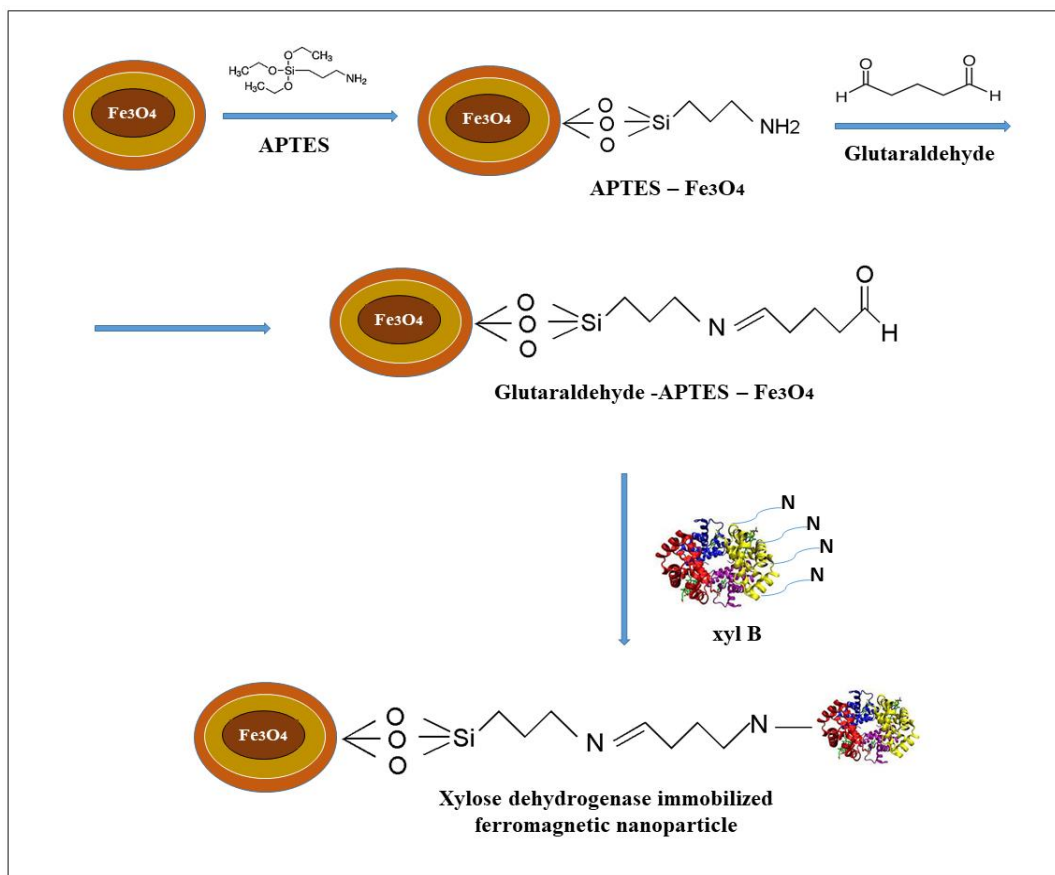
7.2.2. Determination of xylose dehydrogenase activity and bioconversion of xylose to xylonic acid

In the enzymatic bioconversion assay, the reaction volume 1.0 mL, contained 13.5 μM xylose dehydrogenase, 50 mM Na_3PO_4 buffer (pH 7.2), 275 mM xylose, and 1.25 mM NAD^+ . Under the above reaction conditions, 0.14 U (μMmin^{-1}) of enzyme catalysed the conversion of one μM of substrate (xylose) per minute into xylonic acid. The Bradford assay method was used to determine the protein content (Bradford 1987). After 72h of reaction at 30°C, the activity of xylose dehydrogenase was determined by quantification of xylonic acid formation by HPLC. Organic acid column, Phenomenex, with dimension (250 mm \times 4.6 mm \times 5 μm) was used for xylonic acid quantification. It was operated in with a flow rate of 0.6 mLmin⁻¹, where 0.01 N H_2SO_4 served as the mobile phase (Chapter 2, (2.4.2)).

7.2.3. Immobilization of xylose dehydrogenase on magnetic nanoparticles

To get a homogeneous suspension, magnetite nanoparticles (1g) were dispersed in a 1:1 combination of ethanol and water, and the obtained suspension was sonicated for 40 min with 15 s on and 15 s off pulse. This mixture was then treated with APTES (3.4 mL), resulting in a 1:4 molar ratio of magnetite to APTES. The reaction was carried out at 40°C for 2 h in a nitrogen environment with continuous stirring. The magnetite particles (100 mg) modified with APTES was mixed with 10 mL of 8% glutaraldehyde solution (vv⁻¹) and the mixture was incubated overnight at 30°C with continuous stirring. The functionalization and modification of magnetic nanoparticles were performed following the modified methodologies in literature (Can et al. 2009; Costa et al. 2016). Xylose dehydrogenase was allowed to react with modified nanoparticles for 3 h at 4°C. Enzyme that bound to the nanoparticles in the reaction medium was separated using a magnet. The enzyme loading was varied (10-50 μM) and the immobilization

efficiency and enzyme activity were calculated. The mechanism of biocatalyst immobilization is depicted in (Fig. 7.1).



APTES - (3-Aminopropyl)triethoxysilane, Fe₃O₄ – Iron oxide, *xylB* – xylose dehydrogenase

Fig. 7.1. Functionalization of ferromagnetic nanoparticles with APTES and glutaraldehyde for xylose dehydrogenase immobilization.

7.2.4. Optimization of immobilization conditions by statistical tool

The RSM tool was used to find the parameters that have a significant impact on the bioconversion of xylose into xylonic acid. An independent quadratic design *i.e.*, the Box Behnken experimental Design (BBD) (Sarabia and Ortiz 2009) with four independent variables that affect xylonic acid bioconversion was studied, such as the substrate, xylose, (100–400 mM), the

enzyme, xylose dehydrogenase, (10– 25 μM), co-factor, NAD^+ , (0.5–2.00 mM), and pH (5.5–10.5). The conversion yield (mM) of xylonic acid was used to measure the response. Using Minitab 17 software the statistics and ANOVA of the model were evaluated. The level of variance in the group *i.e* the parameter chosen was calculated using p-value, F value, effect value and regression co-efficient.

7.2.5. Enzyme kinetics of xylose dehydrogenase

For both free and immobilized xylose dehydrogenase (13.5 μM each), enzyme kinetic parameters like K_m , V_{max} , and catalytic efficiency were calculated with various concentrations (50 – 500 mM) of substrate. The Lineweaver Burk plot was used to study the kinetic parameters.

7.2.6. Validation of enzyme immobilization by FTIR and XRD

The Fourier Transform Infrared (IRTracer - 100, Shimadzu, Japan) spectroscopy was performed to characterize the ferromagnetic nanoparticles as such and to analyse the chemical modifications made with APTES and glutaraldehyde, thereby confirming the progressive functionalization of free magnetic nanoparticles for enzyme immobilization. FTIR data confirmed the presence of amide bonds in the xylose dehydrogenase enzyme and that of the enzyme immobilised on the surface of functionalized nanoparticles. Each sample's transmittance (percent) was measured in the 400 - 4000 cm^{-1} wavenumber range.

The crystal structure and phase analysis of ferromagnetic nanoparticles were determined using X-ray diffraction (XRD) patterns obtained from a PANalyticalX'pert Pro-diffractometer (Philips, Netherlands) with Ni-filtered Cu K radiation (= 1.54060) taken in the angular range of 10 -70° with a step size of 0.0170°, with the tube voltage and electric current held at 45 kV and 30 mA, respectively.

7.2.7. Reusability of immobilized xylose dehydrogenase

To assess the reusability of the immobilised biocatalyst, the magnetic nanoparticles carrying the xylose dehydrogenase (1 mg) were added to the reaction mixture and the xyloonic acid bioconversion was quantified after 72 h of reaction. To separate the supernatant from the solid fraction, a simple magnet was used to collect the nanoparticles on the surface of the reaction vial and then recovered. The nanoparticles were then washed twice with assay buffer (50 mM phosphate, pH 7.2) to remove any reaction mixture or products. The enzyme assay was carried out for 10 successive cycles to check the efficacy of the biocatalyst in recycling. The activity of the immobilized xylose dehydrogenase in the first cycle was taken as 100%.

7.3. Results

7.3.1. Expression and purification of xylose dehydrogenase

The coding region of xylose dehydrogenase enzyme i.e, *xylB* from xylose inducible *xylXABCD* operon of *C. crescentus* was cloned into the pET28a expression vector. The recombinant plasmid pET28a-*xylB* was confirmed by sequencing and restriction analysis. *E. coli* strain BL21 (DE3) carrying the recombinant vector was grown in liquid LB medium until an OD_{600 nm} of 0.6 – 0.8 and then IPTG (1 mM) induction was done after 3 h for protein expression. The homogeneity of the purified protein was tested on a 12% SDS-PAGE (Fig.7.2). The SDS-PAGE analysis revealed the size of the recombinant protein is about 32 kDa.

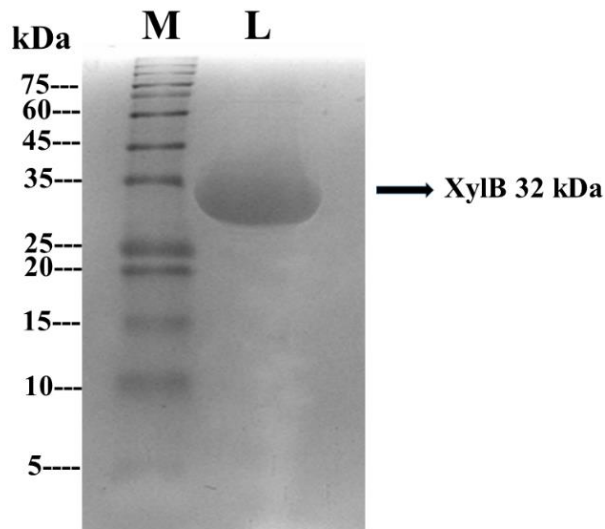


Fig. 7.2. Expression of recombinant xylose dehydrogenase
Lane M, pre-stained protein ladder; Lane 1, purified *xyl B*

7.3.2. Xylose dehydrogenase immobilization on magnetic nanoparticles

APTES, which imparts amine groups to the nanoparticles, was used to functionalize magnetic nanoparticles. These amine-functionalized nanoparticles exhibit a higher affinity for covalent interaction with the xylose dehydrogenase enzyme. The irreversible chemical bonding of the enzyme to nanoparticles is ensured by the -NH_2 and -COOH -coupling (Huang et al. 2010). To calculate immobilization efficiency, the actual enzyme bound onto the nanoparticle was estimated to the total enzyme used and the unbound fraction of enzyme eliminated *via* washing. After reaction, 76% of the total enzyme immobilized on nanoparticles (Table 7.2). The enzyme nature, its conformation, and the type of the nanoparticles have an impact on immobilization efficiency.

Table 7.2. Optimization of xylose dehydrogenase binding on magnetic nanoparticles

Total enzyme added (IU)	Enzyme bound on beads (IU)	Immobilization Efficiency (%)
10	7.2	72.0
20	14.7	73.4
30	22.8	76.0
40	30.1	75.3
50	37.3	74.6

7.3.3. Optimization of the parameters for xylose conversion to xylonic acid

Process parameter optimization of the *in vitro* assay medium for maximum xylonic acid production was done using Box behnken design (BBD). In the BBD, a 15-run experimental matrix was designed for optimising the four distinct parameters. The BBD and the response (xylonic acid) are given in Table 7.3.

Table 7.3. Box–Behnken design matrix with response xylonic acid bioconversion by immobilized xylose dehydrogenase

Run Order	Xylose (mM)	Xylose dehydrogenase (μM)	NAD ⁺ (mM)	pH	Xylonic acid (mM)
1	400	13.5	0.50	10.5	300 \pm 0.1
2	275	13.5	1.25	5.5	100 \pm 0.5
3	275	25	2.00	5.5	100 \pm 0.2
4	275	25	2.00	10.5	200 \pm 0.3
5	100	10	0.50	10.5	50 \pm 0.2
6	275	10	0.50	7.5	200 \pm 0.8
7	275	15	1.25	7.5	250 \pm 0.4
8	275	15	2.00	7.5	250 \pm 0.2
9	400	25	0.50	5.5	150 \pm 0.1
10	275	15	1.25	7.5	250 \pm 0.5

11	275	13.5	1.25	7.5	250 ± 0.3
12	275	13.5	2.00	7.5	250 ± 0.1
13	100	10	0.50	5.5	40 ± 0.2
14	275	15	1.25	10.5	200 ± 0.6
15	400	10	2.00	10.5	300 ± 0.4

The validation equation derived for the matrix is as followed:

$$\begin{aligned} \text{Xylonic acid (mM)} = & - 52.7 - 0.32 X_1 + 4.1 X_2 + 0.213 X_3 + 3.067 X_4 - 0.017 X_1^2 \\ & - 0.2219 X_2^2 - 0.0313 X_3^2 - 0.01853 X_4^2 - 0.064 X_1 X_2 + 0.0516 X_1 X_3 \\ & - 0.0128 X_1 X_4 + 0.436 X_2 X_3 + 0.0372 X_2 X_4 - 0.00212 X_3 X_4 \end{aligned}$$

(X₁ is xylose, X₂ is xylose dehydrogenase, X₃ is NAD⁺ and X₄ is pH)

A conversion yield of 250 ± 0.3 mM xylonic acid from 275 mM xylose was obtained from runs 7, 8, 10, 11, and 12. The least concentration of substrate, enzyme, co-factor, and optimum pH with maximum conversion was reflected in Run No.11, where the concentration of parameters were, xylose 275 mM, xylose dehydrogenase 13.5 μM, NAD⁺ 1.25 mM, and pH 7.5 (Table 7.3.). It indicates that the optimum concentration of these parameters has a remarkable positive impact on xylonic acid bioconversion. The contour plot displaying the relationship of two factors and the optimal concentration of the variables and its interaction for maximum bioconversion is shown in Fig. 7.3 A-F. The major interactions analysed were of the concentration between XDH and xylose (A), pH and xylose (B), NAD⁺ and xylose (C), pH and XDH (D), NAD⁺ and XDH (E) and, pH and NAD⁺ (F). The model was evaluated using ANOVA (Table 7.4). The p-value of lack of fit, p>0.05 implies that the proposed model fits the experimental data and the independent parameters have considerable effects on the response. The large F-value (5.54) indicates the statistical significance of the model. The higher R-square value

(95.55%) implies that the regression model fits the observed data well and also indicates that the model is a better fit.

Table 7.4. ANOVA for xylonic acid production using immobilized xylose dehydrogenase

Source	DF	Adj SS	Adj MS	F	P
Regression	8	97739	12217.4	5.54	0.176
Interaction	4	645	645.5	1.45	0.421
Square	4	22657	5664.3	5.84	0.143
Linear	4	56322	14080.5	8.22	0.105
Residual error	6	4554	759.0		
Lack of fit	5	4554	910.8		
Pure error	1	0	0.0		
Total	14	102293			

S=9.5449, R-Sq=95.55%, R-Sq (pred)=0.00% and R-Sq (adj)=89.61%

The contour plots display the relationship between independent variables (xylose, xylose dehydrogenase, NAD^+ , pH) and a dependent variable (xylonic acid). Fig. 7.3A. shows that high xylonic acid conversion *i.e.*, > 300 mM was attained with a combination of xylose dehydrogenase in the range of 10–24 μM and xylose greater than 250 mM (to 400 mM). In Fig. 7.3B. high xylonic acid conversion was obtained from combination of pH ranging between 7.5-9.5 and xylose greater than 300 mM. In the combination of NAD^+ and xylose in Fig. 7.3C., high xylonic acid conversion was reflected with NAD^+ concentration > 1.25 and xylose concentration > 300 mM.

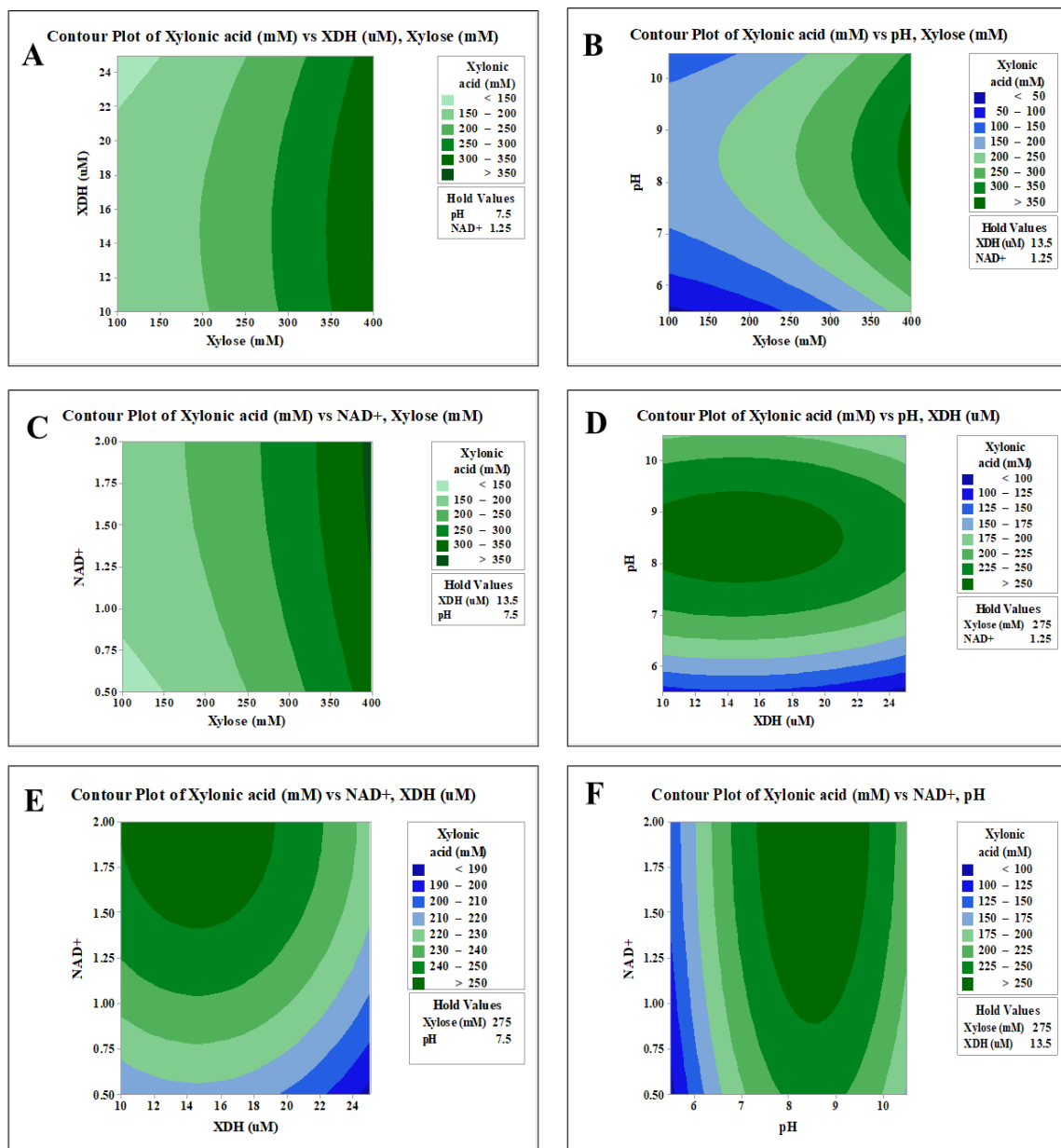


Fig.7.3. Contour plot showing the effect of various parameters on bioconversion of xylose into xylonic acid by immobilized xylose dehydrogenase. XDH and xylose concentrations (A), pH and xylose concentrations (B), NAD⁺ and xylose concentrations (C), pH and XDH concentrations (D), NAD⁺ and XDH concentrations (E), and pH and NAD⁺ concentrations (F).

In Fig. 7.3D. xylonic acid conversion of >250 mM was obtained from combination of pH range (7.5 - 9.5) and xylose dehydrogenase 10 - 20 μM . Similarly, in contour plots Fig. 7.3E. and

Fig .7.3F. also xyloic acid conversion greater than 250 mM was obtained from mixture of NAD^+ in the range of 1.25 – 2.00 mM, xylose dehydrogenase 10 -18 μM and pH in the range of 7.5 - 9.5.

From the hold values in each contour plot the optimum concentration of each parameter for maximum bioconversion obtained is as follows pH (7.5), NAD^+ (1.25 mM), xylose (275 mM) and xylose dehydrogenase (13.5 μM). Thus, with RSM tool the crucial parameters and its optimal concentration range were screened down for maximum output.

7.3.4. Enzyme kinetics of free and immobilized xylose dehydrogenase

The rate of the bioconversion reaction catalysed by xylose dehydrogenase was studied with different substrate concentrations, and the kinetic constants were validated using Lineweaver-Burk plots (Fig. 7.4), and the V_{\max} , K_m , and K_{cat} values are given in Table 7.5.

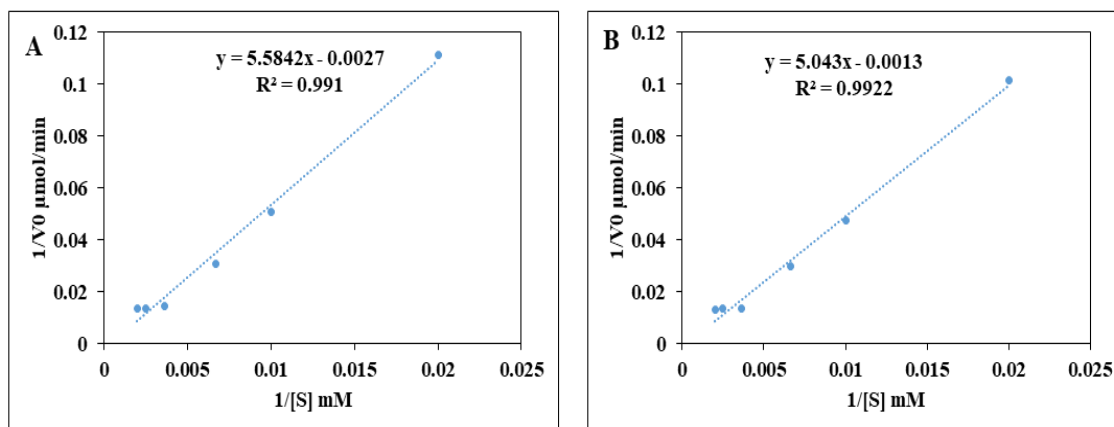


Fig.7.4. Lineweaver-Burk plots of free (A) and immobilized (B) xylose dehydrogenase.

Here, the maximum velocity of immobilized xylose dehydrogenase was found to increase two-fold more than that of free xylose dehydrogenase. The k_{cat} value of immobilized xylose

dehydrogenase was observed to be $12.31 \times 10^7 \text{ min}^{-1}$ while that of free xylose dehydrogenase was $5.93 \times 10^7 \text{ min}^{-1}$. The turnover rate of the enzyme increased on immobilization.

Table 7.5. Kinetic constants of free and immobilized xylose dehydrogenase

Kinetic constants	Free xylose dehydrogenase	Immobilized xylose dehydrogenase
V_{\max} (μmolmin^{-1})	370.37	769.20
Kcat (min^{-1})	5.93×10^7	12.31×10^7
Km (mM)	2068.22	3879.07

7.3.5. Structural characterization of ferromagnetic nanoparticles and immobilized xylose dehydrogenase

FTIR studies were performed on blank magnetic nanoparticles, with amino functionalization i.e, after treatment with aminosilane APTES and glutaraldehyde as controls, and on enzyme-attached nanoparticles. The peak of Fe_3O_4 (Fe-O bonding) was found at 545 cm^{-1} and the peak at 3398 cm^{-1} refers to stretching of OH bonds present on the surface of nanoparticles. The amide bond (i.e, C = O bonding) of enzyme observed at 1641 cm^{-1} , and amino function peaks were found at 2924 cm^{-1} (N-H bonding) (Fig. 7.5A). The final nanoparticle-enzyme bio-conjugate was irradiated with continuous spectrum of infrared energy and the vibration bands of single or functional groups of specific molecules present in iron particles, APTES, glutaraldehyde, and enzyme correlated to the stretchings obtained from functionalization and immobilization steps. All the specific peaks are clearly visible in the final bio-conjugate, indicating the successful immobilization of biocatalyst on magnetic nanoparticles (Fig. 7.5B). The FTIR data obtained are comparable to those previously published in the literature (Costa et al. 2016; Alam et al. 2018).

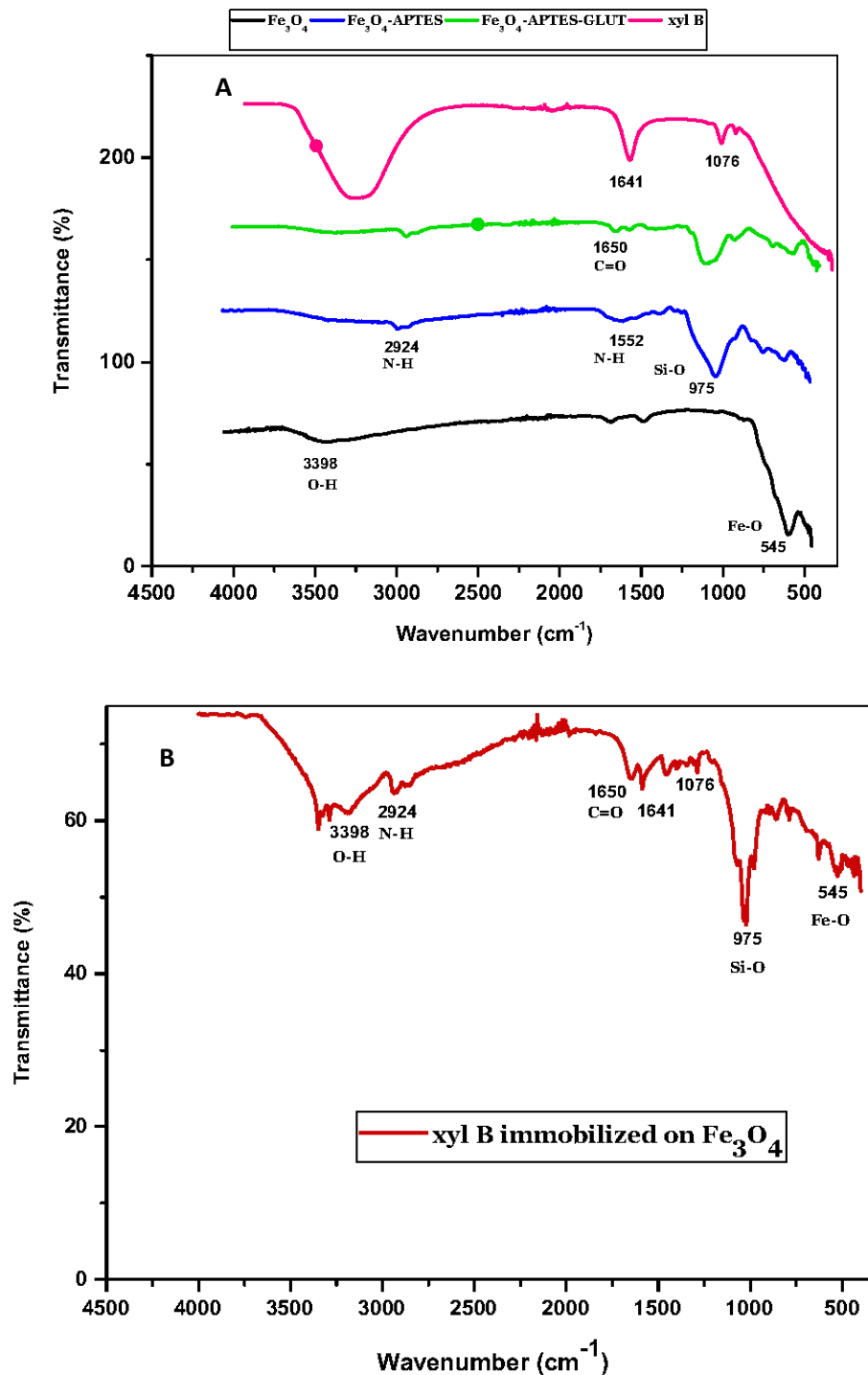


Fig.7.5. FTIR data of individual peaks of Fe_3O_4 iron particle, APTES – Glutaraldehyde modification and xylose dehydrogenase binding (A). Fe_3O_4 magnetic nanoparticle with immobilized xylose dehydrogenase (B).

Power X-ray diffraction was used to determine the crystalline structure and phase purity of ferromagnetic nanoparticle. The diffraction peaks observed were corresponding to the 2θ angle (220), (311), (400), (422), (511) and (440), which represents the cell parameter change, crystal structure of magnetite, confirming that the spatial arrangements of the atoms in the crystal phase are that of typical cubic iron oxide Fe_3O_4 (Fig. 7.6). The XRD pattern i.e., the position of diffraction peaks obtained is in close proximity with the Fe_3O_4 XRD data discussed in the literature by Wang et al. 2013.

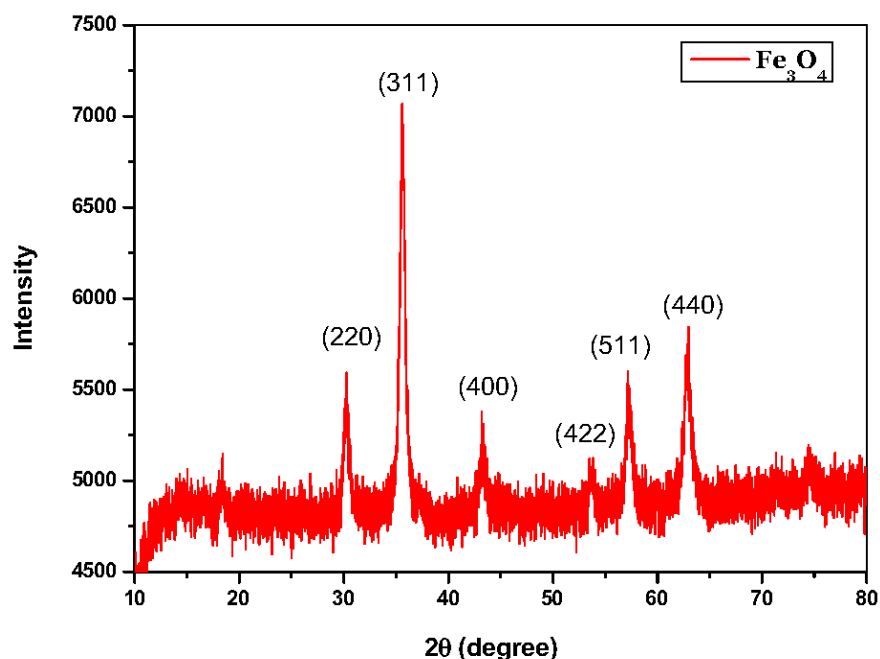


Fig.7.6. X-Ray Diffraction (XRD) pattern of magnetic nanoparticles (Fe_3O_4)

7.3.6. Bioconversion of xylose into xylonic acid by immobilized xylose dehydrogenase under optimized parameters

Bioconversion study was carried out under the optimized parameters, such as xylose (275 mM), xylose dehydrogenase (13.5 μM), NAD^+ (1.25 mM) and pH 7.5, derived from statistical

analysis for a period of 72 h. Under this condition a maximum of 250 ± 0.3 mM xylonic acid was formed from 275 mM xylose with a conversion efficiency of 91% (Fig. 7.7). Quantification of xylonic acid was done in HPLC. An HPLC chromatogram of xylonic acid bioconversion in the presence of immobilized biocatalyst is shown in Fig.7.8.

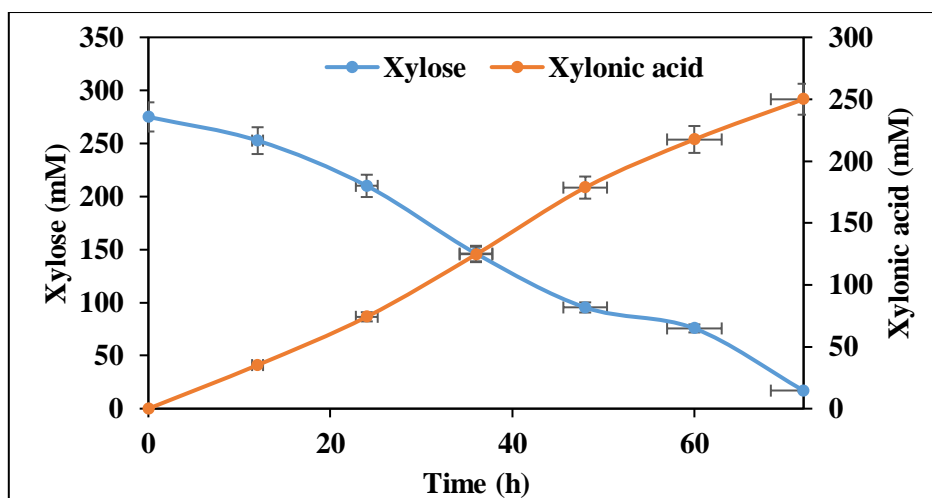


Fig.7.7. Bioconversion of xylose into xylonic acid by immobilized xylose dehydrogenase

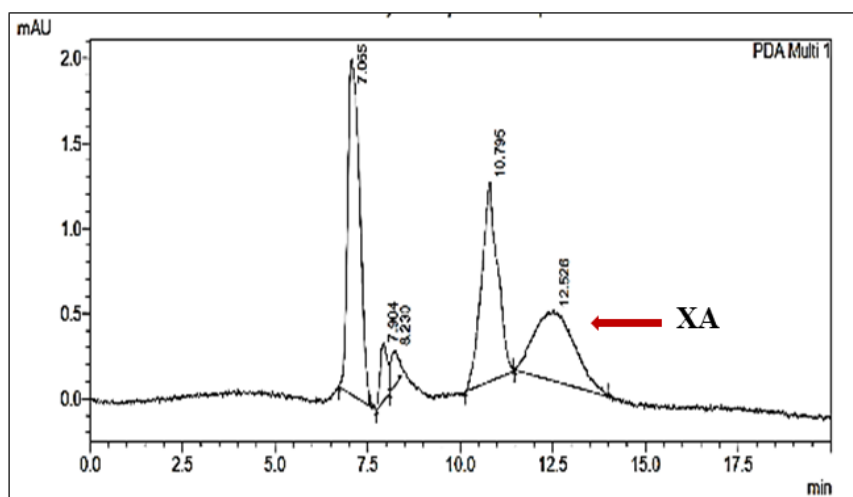


Fig.7.8. HPLC chromatogram of xylonic acid formation from xylose in the presence of immobilized xylose dehydrogenase

7.3.7. Reusability of immobilized biocatalyst

Reusability of biocatalyst is one of the significant advantages of enzymatic reactions based on magnetic nanoparticles. Repeated use of the immobilized biocatalyst was evaluated by incubating the same fraction of biocatalyst for multiple reaction cycles. It was observed that 93% of the activity was retained by the enzyme after 10 successive cycles (Fig. 7.9). Reusability of L-asparaginase is discussed in literature (Mu et al. 2014) and the enzyme retained 95.7% of its activity after recycle which is comparable to the results obtained in this study.

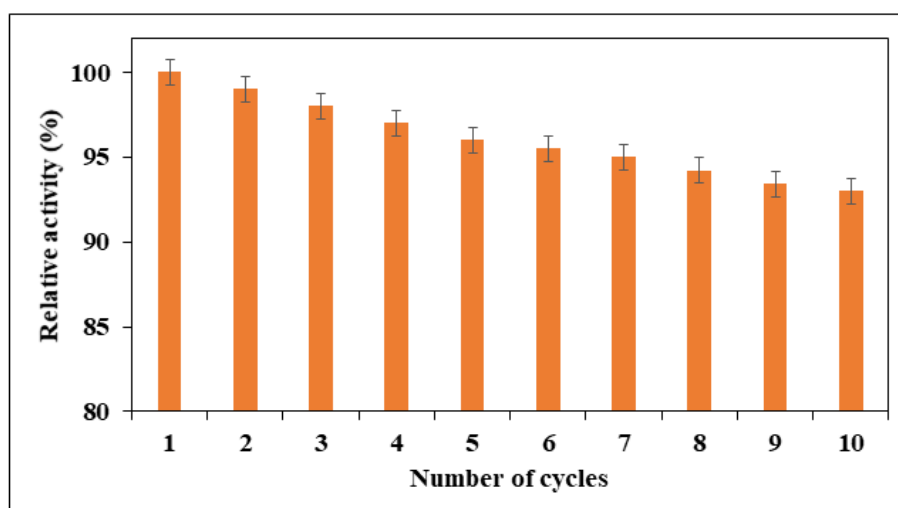


Fig.7.9. Operational stability of immobilized xylose dehydrogenase

7.4. Discussion

Xylose dehydrogenase has been immobilized onto diverse scaffolds for xylose conversion into xylonic acid. Bachosz et al., (2019) co-immobilized xylose dehydrogenase and alcohol dehydrogenase onto silica core-shell for xylose conversion to xylonic acid and co-factor regeneration (Bachosz et al. 2019). Similarly, glucose dehydrogenase and xylose dehydrogenase

were immobilized onto mesoporous amorphous silica for co-production of gluconic acid and xylonic acid (Zdarta et al. 2019). Zdarta et al (2018) demonstrated enzymatic production of xylonic acid and gluconic acid from biomass derived xylose and glucose via immobilization of xylose dehydrogenase and glucose dehydrogenase onto porous silica nanoparticles (Zdarta et al. 2018).

However, immobilization resulted in an increase in the K_m value, implying that the enzyme's affinity for its substrate has decreased. Perhaps, the disturbance in the stability of the enzyme and conformational and orientation changes occurred during immobilization, steric hindrance and the enzyme's diffusional limit to the substrate contributed to the decrease in enzyme affinity to the substrate (Cristovao et al. 2020). This is in line with the observation reported by Alam et al (2021), where they immobilized asparaginase on magnetic nanoparticles to alleviate acrylamide formation in potato chips (Alam et al. 2018).

Here, in this study, ferromagnetic (iron) nanoparticles were used for xylose dehydrogenase immobilization and the immobilized enzyme retained 93% catalytic efficiency after 10 consecutive cycles of reaction, leading to the productivity of 250 ± 0.3 mM xylonic acid from 275 mM xylose. In the case of silica up to 5 consecutive cycles are reported and thus it looks ferromagnetic conjugation is more stable. Magnetic nanoparticle immobilization aids easy separation and recovery, enhanced catalytic activity and selectivity of product. Thus, the enzyme-iron nanoparticle bioconjugate could be a promising long-drawn strategy for continuous bioconversion of xylose into xylonic acid. Additionally, the chemical stability, storage stability, robustness and reusability of iron nanoparticle for continual reaction aided improved productivity of xylonic acid.

7.5. Summary

Xylose dehydrogenase enzyme was purified and immobilized on ferromagnetic (iron) nanoparticles for the bioconversion of xylose into xylonic acid. FTIR and X-ray diffraction analysis were done for the structural characterization of nanoparticles and immobilized xylose dehydrogenase. The signature peak of Fe_3O_4 (Fe-O bonding) nanoparticles at 545cm^{-1} was obtained in the FTIR spectrum, the amide bond (i.e., C=O bonding) of the enzyme observed at 1641 cm^{-1} , and amino (N-H bonding) function peaks at 2924 cm^{-1} in spectrum along with Fe_3O_4 peak confirmed the successful immobilization of biocatalyst on ferromagnetic nanoparticle. Bioconversion study was carried out under optimized parameters, such as xylose (275 mM), xylose dehydrogenase (13.5 μM), NAD^+ (1.25 mM) and pH 7.5, derived from statistical analysis for a period of 72 h. Under this condition, a maximum of 250 ± 0.3 mM xylonic acid was formed from 275 mM xylose with a conversion efficiency of 91%. The immobilized enzyme retained 93% catalytic efficiency after 10 consecutive cycles of reaction.

Chapter 8

Summary and Conclusion

Pentose fraction of lignocellulosic biomass represents non-negligible portion (20-30 %) of sugars (especially D-xylose) at variable concentrations depends on the biomass. Acid hydrolysis of the biomass releases cellulose and hemicelluloses. The Acid pre-treated liquor (APL) generated by the process mainly contains pentose sugars, hexose sugars, and sugar degradation products. APL contains non negligible amount of pentose sugars which can be utilized for the production of value-added products. Due to the heterogeneous nature of the APL, its direct utilization by any chemical process is almost impossible. The bioprocess strategies of value addition using microorganisms were failed in most cases, due to the presence of growth inhibitors such as furfurals, 5-hydroxyl methyl furfurals and phenolics present in the APL.

Corynebacterium glutamicum is a versatile industrial microbe and the availability of genetic engineering tools makes it a rapid and rational manipulation host for diverse platform chemicals. *C. glutamicum* strain ATCC 31831 is selected as the host system for biomass value addition as it showed remarkable resistance towards inhibitors generated from various biomasses and besides it harbours an inbuilt AraE, a pentose transporter which facilitates the easy uptake of pentose sugars such as xylose and arabinose. Since wild type *C. glutamicum* lacks natural pathways for pentose sugar (xylose) metabolism which makes it an efficient system for the biotransformation of pentose sugars by avoiding non-specific sugar channelling towards regular metabolism. Thus, *C. glutamicum* ATCC 31831 was engineered for the utilization of xylose, the major pentose sugar fraction for value addition.

Xylonic acid is one of the important value-added products which can easily generate from xylose present in the APL through bioprocess. Synthesis of xylonic acid from xylose is a two-step enzymatic oxidation reaction supported by enzymes xylose dehydrogenase (XylB) and xylonolactonase (XylC), where xylose dehydrogenase in the presence of reducing equivalents

(NAD(P)⁺ catalyse the conversion of xylose into xylonolactone, an intermediate form. Xylonolactone is then hydrolysed either through a non-enzymatic process or through the action of xylonolactonase enzyme to form xylonic acid.

To develop an efficient conversion system for xylonic acid from xylose, the functional xylose dehydrogenase (*xylB*) and xylonolactonase (*xylC*) genes were isolated from *Caulobacter crescentus* xylose-inducible *xylXABCD* operon (CC0823–CC0819) and over expressed in *C. glutamicum* ATCC 31831 (chapter 3). The resulting transformants *C. glu-xylB* and *C. glu-xylBC* were able to grow in mineral medium containing xylose and converted it into xylonic acid. The transformant *C. glu-xylC* could neither uptake xylose nor produce xylonic acid. Among the transformants the maximum xylonic acid production was obtained using *C. glu-xylB* followed by *C. glu-xylBC* indicating non-enzymatic hydrolysis of xylonolactone into xylonic acid. The strain *C. glu-xylB* produced $56.32 \pm 0.3 \text{ gL}^{-1}$ xylonic acid from 60 gL^{-1} xylose with a conversion efficiency of 76.4 % in CGXII medium in the flask level with a yield of 1.04 gg^{-1} xylose and productivity $0.5 \text{ gL}^{-1}\text{h}^{-1}$ (chapter 4). The protein expression profile of *C. glu-xylB* upon IPTG (1mM) induction showed over expression of recombinant xylose dehydrogenase (32 kDa) enzyme in SDS-PAGE. A comparative analysis of xylonic acid production by recombinant *C. glutamicum* ATCC 13032 (wild type strain lacking AraE pentose transporter) and *C. glutamicum* ATCC 31831 (harbouring AraE pentose transporter) revealed the importance of the pentose transporter as an increase in 9.7 % of production was noticed with the strain *C. glutamicum* ATCC 31831 having *araE* transporter gene. This indicated the presence and functionality of *araE* pentose transporter gene in *C. glutamicum* ATCC 31831 (chapter 4).

After analysing various types of biomass for xylonic acid production and assessing their potential for value addition, sawdust was selected as the optimal raw material based on its

higher sugar concentration and lower levels of inhibitors. The transformant *C. glu-xytB* could also grow in and resist the inhibitors present in acid pre-treated sawdust liquor and produced xylonic acid with high efficiency. The process was optimized up to a 2.5L scale fermenter. $48.5 \pm 0.2 \text{ gL}^{-1}$ xylonic acid was obtained from 60 gL^{-1} xylose (using CGXII medium supplemented with xylose in sawdust APL) after 168 h fermentation with 66 % conversion efficiency and yield of 0.89 gg^{-1} xylose. $48.5 \pm 0.2 \text{ gL}^{-1}$ xylonic acid is a competitive result in comparison to CGXII synthetic medium ($56.32 \pm 0.3 \text{ gL}^{-1}$) under batch fermentation (chapter 5). Increased inoculum size (13 % (v v^{-1})), controlled DO level (2.5 vvm) and sugar ratio (1:3, Glucose: Xylose) are some of the critical factors positively influenced xylonic acid production in fermenter studies (chapter 5). The increased concentrations of total sugar ($> 80 \text{ gL}^{-1}$) tend to inhibit xylonic acid production by *C. glu-xytB*. APL concentrate containing more than 80 gL^{-1} of total sugars and higher concentrations of inhibitors ($1.5 \pm 0.02 \text{ gL}^{-1}$ furfurals, $1.0 \pm 0.01 \text{ gL}^{-1}$ HMF) also showed reduced (66.6 %) growth in comparison to synthetic CGXII medium. Subsequently, INDION PA 500 resin was employed to detoxify APL concentrate and thus removed 85 % of inhibitors present in the APL. The bacterial growth and production increased (51 %) after detoxification of the APL with INDION PA 500 resin. The overall process is shown in Fig 8.1.

The xylonic acid was purified and crystallized by multistep process (chapter 6). The fermented medium was filtered and concentrated using a rotary evaporator (65°C), after removing the bacterial biomass from it. The clarified broth was decolorized by charcoal treatment (20%, w v^{-1}) at high temperature (50°C) and low pH (6.0). Separation of xylonic acid from the decolorized broth was achieved by ethanol precipitation. The prismatic pure crystals of xylonic acid 40.81 gL^{-1} (95.5% purity) and 30.80 gL^{-1} (89% purity) were recovered after downstream processing from synthetic CGXII medium and sawdust APL-CGXII medium with

64.4% and 63.5% recovery respectively. Further confirmation of the xylonic acid crystals was made with FTIR and NMR analysis.

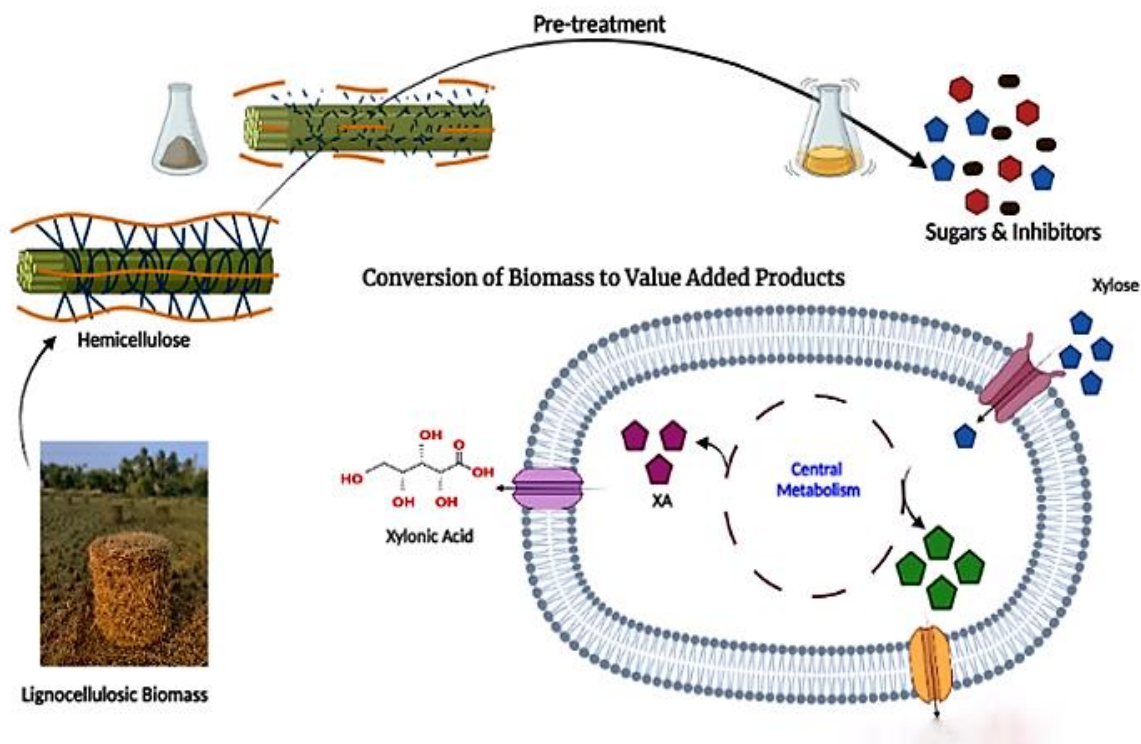


Fig 8.1. Schematic representation of bioprocess for xylonic acid production from lignocellulosic biomass (sawdust APL). Heterologous xylonic acid biosynthetic pathway established in recombinant *C. glutamicum* ATCC 31831 strain *C.glu-xy1B*. Acid pre-treatment of sawdust biomass releases xylose is up taken into recombinant *C. glutamicum* and metabolised into xylonic acid via action of xylose dehydrogenase and xylonolactonase enzymes.

An enzyme-based biotransformation approach was also attempted for the *invitro* conversion of xylose to xylonic acid (chapter 7). Xylose dehydrogenase enzyme has been immobilized on ferromagnetic nanoparticle and used as the biocatalyst and it displayed proficient conversion efficiency (91%). Xylose dehydrogenase enzyme activity was observed to be 0.14 U (μMmin^{-1}) of enzyme required for the conversion of one μM of xylose per minute into xylonic

acid. The biocatalyst exhibited excellent storage stability and recyclability of 93% catalytic efficiency after 10 consecutive cycles of reaction.

Our results on the antimicrobial activity of xylonic acid against *Staphylococcus aureus* MTCC 96, *Escherichia coli* MTCC 443 and *Salmonella enterica* MTCC 3224 showed its potential applications as an antibacterial agent in paints, adhesives and lignin rich nanocellulose (LRNC) films. However, we concluded that it is not suitable for biomedical applications due to its higher MIC (4 mgmL⁻¹) (chapter 6). Crystallization and recovery of xylonic acid were successful, as it can be easily processed into fine crystals *via* solvent precipitation.

Biorefineries can make the entire biofuel program economically viable by utilizing biomass APL for the production of value-added chemicals. However, for a biofuel production plant to be successful, it is necessary to target other products which can be made from overall process as well. A logical approach to this would be to convert xylose, which is a major fraction of APL, into value added chemicals. In this regard, *C. glutamicum* has been reported for producing many chemicals like amino acids, diamines, sugar alcohols, etc, and our study demonstrates that this host can be used for the production of sugar acid like xylonic acid as well. The global xylonic acid market is expected to reach USD 170 million by 2027, growing at a CAGR of 5.5% from 2020 to 2027. Asia Pacific is the largest market for xylonic acid, with China being the major producer and consumer of xylonic acid in the region.

A process framework was developed that will provide a blueprint not only for further evolution in xylonic acid bioprocessing but also in other bio-manufacturing processes. The higher stability of the engineered strain (*C. glutamicum*) and its ability to adapt to different biomass niches and carbon assimilation turned to achieve industrially applicable xylonic acid

productivity. Similarly, in pharmaceutical and fine chemical industries, the biotransformation process using immobilized enzyme system can act as a game changer.

Bibliography

- Abe S**, Takayama K-I, Kinoshita S (1967) Taxonomical Studies On Glutamic Acid-Producing Bacteria. *J Gen Appl Microbiol* 13:279–301. <https://doi.org/10.2323/jgam.13.279>
- Ahmad R**, Sardar M (2015) Enzyme Immobilization: An Overview on Nanoparticles as Immobilization Matrix. *Biochem Anal Biochem* 4. <https://doi.org/10.4172/2161-1009.1000178>
- Akinterinwa O**, Khankal R, Cirino PC. (2008) Metabolic engineering for bioproduction of sugar alcohols. *Curr Opin Biotechnol*. Oct;19(5):461-7. doi: 10.1016/j.copbio.2008.08.002. *Epub* 2008 Sep 16. PMID: 18760354.
- Alam S**, Ahmad R, Pranaw K, et al (2018) Asparaginase conjugated magnetic nanoparticles used for reducing acrylamide formation in food model system. *Bioresour Technol* 269:121–126. <https://doi.org/10.1016/j.biortech.2018.08.095>
- Alvira P**, Tomás-Pejó E, Ballesteros M, Negro MJ (2010) Pretreatment technologies for an efficient bioethanol production process based on enzymatic hydrolysis: A review. *Bioresour Technol* 101:4851–4861. <https://doi.org/10.1016/J.BIORTECH.2009.11.093>
- Arnone JT** (2020) Genomic Considerations for the Modification of *Saccharomyces cerevisiae* for Biofuel and Metabolite Biosynthesis (2020). *Microorg* 2020, Vol 8, Page 321 8:321. <https://doi.org/10.3390/MICROORGANISMS8030321>

- Bachosz K**, Synoradzki K, Staszak M, et al (2019) Bioconversion of xylose to xylonic acid via co-immobilized dehydrogenases for conjunct cofactor regeneration. *Bioorg Chem* 93: <https://doi.org/10.1016/J.BIOORG.2019.01.043>
- Bañares, A.B.**, Nisola GM, Valdehuesa KNG, et al (2021) Understanding D-xylonic acid accumulation: a cornerstone for better metabolic engineering approaches. *Appl Microbiol Biotechnol* 105:5309–5324. <https://doi.org/10.1007/S00253-021-11410-Y>
- Barbosa O**, Ortiz C, Berenguer-Murcia Á, et al (2013) Glutaraldehyde in bio-catalysts design: a useful crosslinker and a versatile tool in enzyme immobilization. *RSC Adv* 4:1583–1600. <https://doi.org/10.1039/C3RA45991H>
- Baritugo KAG**, Kim HT, David YC, et al (2018) Recent advances in metabolic engineering of *Corynebacterium glutamicum* as a potential platform microorganism for biorefinery. *Biofuels, Bioprod Biorefining* 12:899–925. <https://doi.org/10.1002/BBB.1895>
- Baruah J**, Nath BK, Sharma R, et al (2018) Recent trends in the pretreatment of lignocellulosic biomass for value-added products. *Front Energy Res* 6:141. <https://doi.org/10.3389/FENRG.2018.00141/BIBTEX>
- Becker J**, Rohles CM, Wittmann C (2018) Metabolically engineered *Corynebacterium glutamicum* for bio-based production of chemicals, fuels, materials, and healthcare products. *Metab Eng.* 50:122–141. <https://doi.org/10.1016/j.ymben.2018.07.008>
- Bilal M**, Asgher M, Cheng H, et al (2018) Multi-point enzyme immobilization, surface chemistry, and novel platforms: a paradigm shift in biocatalyst design. <https://doi.org/101080/0738855120181531822> 39:202–219.

- Bondar M**, da Fonseca MMR, Cesário MT (2021) Xylonic acid production from xylose by *Paraburkholderia sacchari*. *Biochem Eng J* 170:107982.
<https://doi.org/10.1016/j.bej.2021.107982>
- Box, G.E.P.** and Behnken, D.W. (1960) Some New Three Level Designs for the Study of Quantitative Variables. *Technometrics*, 2, 455-475.
<http://dx.doi.org/10.1080/00401706.1960.10489912>
- Bradford, M. M.**, (1976). A rapid and sensitive method for the quantitation of microgram quantities of protein utilizing the principle of protein-dye binding. *Analytical Biochemistry*. 72 (1-2), 248-254
- Brat D**, Boles E, Wiedemann B (2009) Functional Expression of a Bacterial Xylose Isomerase in *Saccharomyces cerevisiae*. *Appl Environ Microbiol* 75:2304.
<https://doi.org/10.1128/AEM.02522-08>
- Brüsseler C**, Späth A, Sokolowsky S, Marienhagen J (2019) Alone at last! – Heterologous expression of a single gene is sufficient for establishing the five-step Weimberg pathway in *Corynebacterium glutamicum*. *Metab Eng Commun* 9:e00090.
<https://doi.org/10.1016/j.mec.2019.e00090>
- Buchert J**, Viikari L (1988) The role of xylonolactone in xylonic acid production by *Pseudomonas fragi*. *Appl Microbiol Biotechnol* 27:333–336.
<https://doi.org/10.1007/BF00251763>
- Buchert Johanna**, Viikari Liisa (1988) Oxidative D-xylose metabolism of *Gluconobacter oxydans*. *Appl Microbiol Biotechnol* 29:375–379

Buschke N, Becker J, Schäfer R, et al (2013) Systems metabolic engineering of xylose-utilizing *Corynebacterium glutamicum* for production of 1,5-diaminopentane. *Biotechnol J* 8:557–570. <https://doi.org/10.1002/biot.201200367>

Byong-Wa C, Benita D, Macuch PJ, et al (2006) The Development of Cement and Concrete Additive. *Appl Biochem Biotechnol* 131:645–658. <https://doi.org/10.1385/abab:131:1:645>

Cabulong RB, Lee W-K, Bañares AB, et al (2018) Engineering *Escherichia coli* for glycolic acid production from D-xylose through the Dahms pathway and glyoxylate bypass. *Appl Microbiol Biotechnol* 102:2179–2189. <https://doi.org/10.1007/s00253-018-8744-8>

Can K, Ozmen M, Ersoz M (2009) Immobilization of albumin on aminosilane modified superparamagnetic magnetite nanoparticles and its characterization. *Colloids Surfaces B Biointerfaces* 71:154–159. <https://doi.org/10.1016/j.colsurfb.2009.01.021>

Cao R, Xu Y (2019) Efficient Preparation of Xylonic Acid from Xylonate Fermentation Broth by Bipolar Membrane Electrodialysis. *Appl Biochem Biotechnol* 187:396–406. <https://doi.org/10.1007/s12010-018-2827-y>

Cao Y, Xian M, Zou H, Zhang H (2013) Metabolic Engineering of *Escherichia coli* for the Production of Xylonate. *PLoS One* 8:e67305. <https://doi.org/10.1371/journal.pone.0067305>

Castilla-Archilla J, O’Flaherty V, Lens PNL (2019) Biorefineries: Industrial Innovation and Tendencies. *Biorefinery* 3–35. https://doi.org/10.1007/978-3-030-10961-5_1

Chandel AK, da Silva SS, Singh O V. (2013) Detoxification of Lignocellulose Hydrolysates: Biochemical and Metabolic Engineering Toward White Biotechnology. *Bioenergy Res* 6:388–401. <https://doi.org/10.1007/S12155-012-9241-Z/METRICS>

- Chen L**, Huang Y, Zou R, et al (2021) Regulating TiO₂/MXenes catalysts to promote photocatalytic performance of highly selective oxidation of D-xylose. *Green Chem* 23:1382–1388. <https://doi.org/10.1039/D0GC03628E>
- Cheng YS**, Zheng Y, Yu CW, et al (2010) Evaluation of High Solids Alkaline Pretreatment of Rice Straw. *Appl Biochem Biotechnol* 162:1768. <https://doi.org/10.1007/S12010-010-8958-4>
- Choi JW**, Jeon EJ, Jeong KJ (2019) Recent advances in engineering *Corynebacterium glutamicum* for utilization of hemicellulosic biomass. *Curr Opin Biotechnol* 57:17–24. <https://doi.org/10.1016/J.COPBIO.2018.11.004>
- Chun B-W**, Dair B, Macuch P, et al (2006) The development of cement and concrete additive: based on xylonic acid derived via bioconversion of xylose. *Appl Biochem Biotechnol*
- Conrady M**, Lemoine A, Limberg MH, et al (2019) Carboxylic acid consumption and production by *Corynebacterium glutamicum*. *Biotechnol Prog* 35:e2804. <https://doi.org/10.1002/BTPR.2804>
- Costa VM**, De Souza MCM, Fechine PBA, et al (2016) Nanobiocatalytic systems based on lipase-Fe₃O₄ and conventional systems for isoniazid synthesis: A comparative study. *Brazilian J Chem Eng* 33:661–673. <https://doi.org/10.1590/0104-6632.20160333s20150137>
- Cristovao RO**, Almeida MR, Barros MA, et al (2020) Development and characterization of a novel l -asparaginase/MWCNT nanobioconjugate. *RSC Adv* 10:31205–31213. <https://doi.org/10.1039/D0RA05534D>

- Dai L, Jiang W, Zhou X, Xu Y** (2020) Enhancement in xylonate production from hemicellulose pre-hydrolysate by powdered activated carbon treatment. *Bioresour Technol* 316:123944. <https://doi.org/10.1016/J.BIORTECH.2020.123944>
- de Sá LRV, Faber M de O, da Silva ASA, et al** (2020) Biohydrogen production using xylose or xylooligosaccharides derived from sugarcane bagasse obtained by hydrothermal and acid pretreatments. *Renew Energy* 146:2408–2415. <https://doi.org/10.1016/j.renene.2019.08.089>
- Dhar KS, Wendisch VF, Nampoothiri KM** (2016) Engineering of *Corynebacterium glutamicum* for xylitol production from lignocellulosic pentose sugars. *J Biotechnol* 230:63–71. <https://doi.org/10.1016/j.jbiotec.2016.05.011>
- Dhiman SS, Kalyani D, Jagtap SS, et al** (2012) Characterization of a novel xylanase from *Armillaria gemina* and its immobilization onto SiO₂ nanoparticles. *Appl Microbiol Biotechnol* 2012 973 97:1081–1091. <https://doi.org/10.1007/S00253-012-4381-9>
- Digman MF, Shinnars KJ, Casler MD, et al** (2010) Optimizing on-farm pretreatment of perennial grasses for fuel ethanol production. *Bioresour Technol* 101:5305–5314. <https://doi.org/10.1016/J.BIORTECH.2010.02.014>
- Domingues R, Bondar M, Palolo I, et al** (2021) Xylose Metabolism in Bacteria—Opportunities and Challenges towards Efficient Lignocellulosic Biomass-Based Biorefineries. *Appl Sci* 2021, Vol 11, Page 8112 11:8112. <https://doi.org/10.3390/APP11178112>

- Drout RJ**, Robison L, Farha OK (2019) Catalytic applications of enzymes encapsulated in metal–organic frameworks. *Coord Chem Rev* 381:151–160.
<https://doi.org/10.1016/J.CCR.2018.11.009>
- Fanger BO** (1987) Adaptation of the Bradford protein assay to membrane-bound proteins by solubilizing in glucopyranoside detergents. *Anal Biochem* 162:11–17.
[https://doi.org/10.1016/0003-2697\(87\)90004-2](https://doi.org/10.1016/0003-2697(87)90004-2)
- Fehér A**, Fehér C, Rozbach M, et al (2018) Treatments of Lignocellulosic Hydrolysates and Continuous-Flow Hydrogenation of Xylose to Xylitol. *Chem Eng Technol* 41:496–503.
<https://doi.org/10.1002/CEAT.201700103>
- Garba A**, Garba A (2020) Biomass Conversion Technologies for Bioenergy Generation: An Introduction. *Biotechnol Appl Biomass*. <https://doi.org/10.5772/INTECHOPEN.93669>
- Ghaffar A**, Yameen M, Aslam N, et al (2017) Acidic and enzymatic saccharification of waste agricultural biomass for biotechnological production of xylitol. *Chem Cent J* 11:1–6.
<https://doi.org/10.1186/s13065-017-0331-z>
- Goldemberg J** (2007) Ethanol for a sustainable energy future. *Science* (80-) 315:808–810.
https://doi.org/10.1126/SCIENCE.1137013/ASSET/DF795B22-5631-48DE-AE36-3535A165725A/ASSETS/GRAPHIC/315_808_F2.JPEG
- Gopinath V**, Meiswinkel TM, Wendisch VF, Nampoothiri KM (2011) Amino acid production from rice straw and wheat bran hydrolysates by recombinant pentose-utilizing *Corynebacterium glutamicum*. *Appl Microbiol Biotechnol* 92:985–996.
<https://doi.org/10.1007/s00253-011-3478-x>

Gopinath V, Murali A, Dhar KS (2012) *Corynebacterium glutamicum* as a potent biocatalyst for the bioconversion of pentose sugars to value-added products. 95–106.

<https://doi.org/10.1007/s00253-011-3686-4>

Han J, Hua X, Zhou X, et al (2021) A cost-practical cell-recycling process for xylonic acid bioproduction from acidic lignocellulosic hydrolysate with whole-cell catalysis of *Gluconobacter oxydans*. *Bioresour Technol* 333:125157.

<https://doi.org/10.1016/J.BIORTECH.2021.125157>

Hanahan D, Harbor CS (1983) Studies on transformation of *Escherichia coli* with plasmids. *J Mol Biol* 166:557–580. [https://doi.org/10.1016/S0022-2836\(83\)80284-8](https://doi.org/10.1016/S0022-2836(83)80284-8)

Herrera CRJ, Vieira VR, Benoliel T, Carneiro CVGC, De Marco JL, de Moraes LMP, de Almeida JRM, Torres FAG. Engineering *Zymomonas mobilis* for the Production of Xylonic Acid from Sugarcane Bagasse Hydrolysate. *Microorganisms*. 9:1–14. doi:

<https://doi.org/10.3390/microorganisms9071372>

Hoffert MI, Caldeira K, Benford G, et al (2002) Engineering: Advanced technology paths to global climate stability: Energy for a greenhouse planet. *Science* (80-) 298:981–987.

<https://doi.org/10.1126/SCIENCE.1072357/ASSET/677B06D9-78CC-4AA8-9DD2-3B4682D6F3DF/ASSETS/GRAPHIC/SE4320994003.JPEG>

Hou W, Zhang M, Bao J (2018) Cascade hydrolysis and fermentation of corn stover for production of high titer gluconic and xylonic acids. *Bioresour Technol* 264:395–399.

<https://doi.org/10.1016/j.biortech.2018.06.025>

- Huang YF**, Wang YF, Yan XP (2010) Amine-functionalized magnetic nanoparticles for rapid capture and removal of bacterial pathogens. *Environ Sci Technol* 44:7908–7913.
<https://doi.org/10.1021/ES102285N>
- Huang, C.**, Ragauskas, AJ., Wu, X., et al (2018) Co-production of bio-ethanol, xylonic acid and slow-release nitrogen fertilizer from low-cost straw pulping solid residue. *Bioresour Technol* 250:365–373. <https://doi.org/10.1016/J.BIORTECH.2017.11.060>
- Hudzicki J** (2009) Kirby-Bauer Disk Diffusion Susceptibility Test Protocol. *Am Soc Microbiol* 23
- Husain Q** (2016) Magnetic nanoparticles as a tool for the immobilization/stabilization of hydrolases and their applications: An overview. *Biointerface Res Appl Chem* 6:1585–1606.
<https://doi.org/10.2016/Published>
- Ibrahim MM**, El-Zawawy WK, Abdel-Fattah YR, et al (2011) Comparison of alkaline pulping with steam explosion for glucose production from rice straw. *Carbohydr Polym* 83:720–726. <https://doi.org/10.1016/J.CARBPOL.2010.08.046>
- Iqbal HMN**, Asgher M, Bhatti HN (2011) Optimization of physical and nutritional factors for synthesis of lignin degrading enzymes by a novel strain of *Trametes versicolor*. *BioResources* 6:1273–1287. <https://doi.org/10.15376/biores.6.2.1273-1287>
- Ishizaki H**, Ihara T, Yoshitake J, et al (1973) D-Xylonic Acid Production by *Enterobacter cloacae*. *J Agric Chem Soc Japan* 47:755–761.
<https://doi.org/10.1271/nogeikagaku1924.47.755>

- Isikgor FH**, Remzi Becer C (2015) Polymer Chemistry Lignocellulosic Biomass: A Sustainable Platform for Production of Bio-Based Chemicals and Polymers. *Polym Chem.*
<https://doi.org/10.1039/C5PY00263J>
- Jilani SB**, Dev C, Eqbal D, et al (2020) Deletion of *pgi* gene in *E. coli* increases tolerance to furfural and 5-hydroxymethyl furfural in media containing glucose-xylose mixture. *Microb Cell Fact* 19:1–13. <https://doi.org/10.1186/S12934-020-01414-0/TABLES/2>
- Jin D**, Ma J, Li Y, et al (2022) Development of the synthesis and applications of xylonic acid: A mini review. *Fuel* 314:122773. <https://doi.org/10.1016/J.FUEL.2021.122773>
- Kawaguchi H**, Sasaki M, Vertes AA, et al (2009) Identification and Functional Analysis of the Gene Cluster for L-Arabinose Utilization in *Corynebacterium glutamicum*. *Appl Environ Microbiol* 75:3419–3429. <https://doi.org/10.1128/AEM.02912-08>
- Keilhauer C**, Eggeling L, Sahm H. Isoleucine synthesis in *Corynebacterium glutamicum*: molecular analysis of the *ilvB-ilvN-ilvC* operon. *J Bacteriol.* 1993 Sep;175(17):5595-603. doi: 10.1128/jb.175.17.5595-5603.1993. PMID: 8366043; PMCID: PMC206616.
- Khoo KS**, Chia WY, Tang DYY, et al (2020) Nanomaterials Utilization in Biomass for Biofuel and Bioenergy Production. *Energies* 2020, Vol 13, Page 892 13:892.
<https://doi.org/10.3390/EN13040892>
- Kim SJ**, Sim HJ, Kim JW, et al (2017) Enhanced production of 2,3-butanediol from xylose by combinatorial engineering of xylose metabolic pathway and cofactor regeneration in pyruvate decarboxylase-deficient *Saccharomyces cerevisiae*. *Bioresour Technol* 245:1551–1557. <https://doi.org/10.1016/j.biortech.2017.06.034>

- Kitade Y**, Hiraga K, Inui M (2020) Aromatic Compound Catabolism in *Corynebacterium glutamicum*. 323–337. https://doi.org/10.1007/978-3-030-39267-3_11
- Kogure T**, Inui M (2018) Recent advances in metabolic engineering of *Corynebacterium glutamicum* for bioproduction of value-added aromatic chemicals and natural products. *Appl Microbiol Biotechnol* 102:8685–8705. <https://doi.org/10.1007/S00253-018-9289-6/TABLES/3>
- Köhler KA**, Blank, L.M., Frick, O., Schmid, A. (2015) D-Xylose assimilation via the Weimberg pathway by solvent-tolerant *Pseudomonas taiwanensis* VLB120. *Environ Microbiol* 17:156–170. <https://doi.org/10.1111/1462-2920.12537>
- Kudahettige-Nilsson RL**, Helmerius J, Nilsson RT, et al (2015) Biobutanol production by *Clostridium acetobutylicum* using xylose recovered from birch Kraft black liquor. *Bioresour Technol* 176:71–79. <https://doi.org/10.1016/j.biortech.2014.11.012>
- Kumar AK**, Sharma S (2017) Recent updates on different methods of pretreatment of lignocellulosic feedstocks: a review. *Bioresour Bioprocess* 2017 41 4:1–19. <https://doi.org/10.1186/S40643-017-0137-9>
- Kumar R**, Wyman CE (2009) Effects of cellulase and xylanase enzymes on the deconstruction of solids from pretreatment of poplar by leading technologies. *Biotechnol Prog* 25:302–314. <https://doi.org/10.1002/BTPR.102>

- Kumar V**, Binod P, Sindhu R, et al (2018) Bioconversion of pentose sugars to value added chemicals and fuels: Recent trends, challenges and possibilities. *Bioresour Technol* 269:443–451. <https://doi.org/10.1016/J.BIORTECH.2018.08.042>
- Kwak S**, Jin YS (2017) Production of fuels and chemicals from xylose by engineered *Saccharomyces cerevisiae*: a review and perspective. *Microb Cell Factories* 2017 161 16:1–15. <https://doi.org/10.1186/S12934-017-0694-9>
- Lachke A** (2002) Biofuel from D-xylose — The second most abundant sugar. *Reson* 2002 75 7:50–58. <https://doi.org/10.1007/BF02836736>
- Lekshmi Sundar MS**, Nampoothiri KM (2022) Xylose Dehydrogenase Immobilized on Ferromagnetic Nanoparticles for Bioconversion of Xylose to Xylonic Acid. *Bioconjug Chem*. https://doi.org/10.1021/ACS.BIOCONJCHEM.2C00159/SUPPL_FILE/BC2C00159_SI_001.PDF
- Li M**, Zhong LX, Chen W, et al (2021) Regulating the electron–hole separation to promote selective oxidation of biomass using ZnS@Bi₂S₃ nanosheet catalyst. *Appl Catal B Environ* 292: <https://doi.org/10.1016/J.APCATB.2021.120180>
- Liang S**, Wu XL, Xiong J, et al (2020) Metal-organic frameworks as novel matrices for efficient enzyme immobilization: An update review. *Coord Chem Rev* 406:213149. <https://doi.org/10.1016/J.CCR.2019.213149>
- Lin K**, Han S, Zheng S (2022) Application of *Corynebacterium glutamicum* engineering display system in three generations of biorefinery. *Microb Cell Factories* 2022 211 21:1–12. <https://doi.org/10.1186/S12934-022-01741-4>

- Lin T-H**, Huang C-F, Guo G-L, et al (2012) Pilot-scale ethanol production from rice straw hydrolysates using xylose-fermenting *Pichia stipitis*. *Bioresour Technol* 116:314–319.
<https://doi.org/10.1016/j.biortech.2012.03.089>
- Liu H**, Valdehuesa KNG, Nisola GM, et al (2012) High yield production of d-xyloonic acid from d-xylose using engineered *Escherichia coli*. *Bioresour Technol* 115:244–248.
<https://doi.org/10.1016/j.biortech.2011.08.065>
- Liu S**, Okuyama Y, Tamura M, et al (2015) Selective transformation of hemicellulose (xylan) into n-pentane, pentanols or xylitol over a rhenium-modified iridium catalyst combined with acids. *Green Chem* 18:165–175. <https://doi.org/10.1039/C5GC02183A>
- Luo J**, Huang K, Zhou X, Xu Y (2020) Preparation of highly flexible and sustainable lignin-rich nanocellulose film containing xyloonic acid (XA), and its application as an antibacterial agent. *Int J Biol Macromol* 163:1565–1571.
<https://doi.org/10.1016/J.IJBIOMAC.2020.07.281>
- Ma J**, Liu Z, Song J, et al (2018) Au@h-Al₂O₃ analogic yolk-shell nanocatalyst for highly selective synthesis of biomass-derived D-xyloonic acid via regulation of structure effects. *Green Chem* 20:5188–5195. <https://doi.org/10.1039/C8GC02618A>
- Ma J**, Zhong L, Peng X, Sun R (2016) D-Xyloonic acid: a solvent and an effective biocatalyst for a three-component reaction. *Green Chem* 18:1738–1750.
<https://doi.org/10.1039/C5GC01727K>

- Martínez EA**, Canettieri E V., Bispo JAC, et al (2015) Strategies for xylitol purification and Crystallization: A review. *Sep Sci Technol* 50:2087–2098.
<https://doi.org/10.1080/01496395.2015.1009115>
- Mathews SL**, Pawlak J, Grunden AM (2015) Bacterial biodegradation and bioconversion of industrial lignocellulosic streams. *Appl Microbiol Biotechnol* 99:2939–2954.
<https://doi.org/10.1007/s00253-015-6471-y>
- McClintock**, M.K., Wang, J., Zhang, K. (2017) Application of Nonphosphorylative Metabolism as an Alternative for Utilization of Lignocellulosic Biomass. *Front Microbiol* 8:
<https://doi.org/10.3389/FMICB.2017.02310>
- McIntosh S**, Vancov T (2010) Enhanced enzyme saccharification of Sorghum bicolor straw using dilute alkali pretreatment. *Bioresour Technol* 101:6718–6727.
<https://doi.org/10.1016/J.BIORTECH.2010.03.116>
- Mehtio T**, Toivari M, Wiebe MG, et al (2016) Production and applications of carbohydrate-derived sugar acids as generic biobased chemicals. *Crit Rev Biotechnol* 36:904–916.
<https://doi.org/10.3109/07388551.2015.1060189>
- Meiswinkel TM**, Gopinath V, Lindner SN, et al (2013) Accelerated pentose utilization by *Corynebacterium glutamicum* for accelerated production of lysine, glutamate, ornithine and putrescine. *Microb Biotechnol* 6:131–140. <https://doi.org/10.1111/1751-7915.12001>
- Miao Y**, Zhou X, Xu Y, Yu S (2015) Draft genome sequence of *Gluconobacter oxydans* NL71, a strain that efficiently biocatalyzes xylose to xylonic acid at a high concentration. *Genome Announc* 3:2–3. <https://doi.org/10.1128/genomeA.00615-15>

- Mohd Azhar SH**, Abdulla R, Jambo SA, et al (2017) Yeasts in sustainable bioethanol production: A review. *Biochem Biophys Reports* 10:52–61.
<https://doi.org/10.1016/J.BBREP.2017.03.003>
- Moysés DN**, Reis VCB, Almeida JRM de, et al (2016) Xylose Fermentation by *Saccharomyces cerevisiae*: Challenges and Prospects. *Int J Mol Sci* 2016, Vol 17, Page 207 17:207.
<https://doi.org/10.3390/IJMS17030207>
- Mu X**, Qiao J, Qi L, et al (2014) Poly(2-vinyl-4,4-dimethylazlactone)-functionalized magnetic nanoparticles as carriers for enzyme immobilization and its application. *ACS Appl Mater Interfaces* 6:21346–21354. <https://doi.org/10.1021/AM5063025>
- Niu Wei**, Molefe N Mapitso, Frost J W (2003) Microbial Synthesis of the Energetic Material Precursor 1,2,4-Butanetriol. *J Am Chem Soc* 125:12998–12999
- Nygård Y**, Toivari MH, Penttilä M, et al (2011) Bioconversion of d-xylose to d-xylonate with *Kluyveromyces lactis*. *Metab Eng* 13:383–391.
<https://doi.org/10.1016/j.ymben.2011.04.001>
- Oliveira-Filho, ER.**, Gomez, JGC., Taciro, MK., Silva L (2021) *Burkholderia sacchari* (synonym *Paraburkholderia sacchari*): An industrial and versatile bacterial chassis for sustainable biosynthesis of polyhydroxyalkanoates and other bioproducts. *Bioresour Technol* 337: <https://doi.org/10.1016/J.BIORTECH.2021.125472>
- Osman AI**, Mehta N, Elgarahy AM, et al (2021) Conversion of biomass to biofuels and life cycle assessment: a review. *Environ Chem Lett* 2021 196 19:4075–4118.
<https://doi.org/10.1007/S10311-021-01273-0>

- Pérez-García F**, Peters-Wendisch P, Wendisch VF (2016) Engineering *Corynebacterium glutamicum* for fast production of L-lysine and L-pipecolic acid. *Appl Microbiol Biotechnol* 100:8075–8090. <https://doi.org/10.1007/s00253-016-7682-6>
- Peters-Wendisch PG**, Schiel B, Wendisch VF, Katsoulidis E, Möckel B, Sahm H, Eikmanns BJ (2001) Pyruvate carboxylase is a major bottleneck for glutamate and lysine production by *Corynebacterium glutamicum*. *J Mol Biol Biotechnol* 3(2):295–300
- Phwan CK**, Chew KW, Sebayang AH, et al (2019) Effects of acids pre-treatment on the microbial fermentation process for bioethanol production from microalgae. *Biotechnol Biofuels* 2019 12:1–8. <https://doi.org/10.1186/S13068-019-1533-5>
- Qiao Y**, Li C, Lu X, et al (2021) Transporter engineering promotes the co-utilization of glucose and xylose by *Candida glycerinogenes* for d-xylonate production. *Biochem Eng J* 175:108150. <https://doi.org/10.1016/J.BEJ.2021.108150>
- Rafaïdeen T**, Baranton S, Coutanceau C (2019) Highly efficient and selective electrooxidation of glucose and xylose in alkaline medium at carbon supported alloyed PdAu nanocatalysts. *Appl Catal B Environ* 243:641–656. <https://doi.org/10.1016/J.APCATB.2018.11.006>
- Ramos TGS**, Justen F, Carneiro CVGC, et al (2021) Xylonic acid production by recombinant *Komagataella phaffii* strains engineered with newly identified xylose dehydrogenases. *Bioresour Technol Reports* 16:100825. <https://doi.org/10.1016/J.BITEB.2021.100825>
- Ruiz HA**, Rodríguez-Jasso RM, Fernandes BD, et al (2013) Hydrothermal processing, as an alternative for upgrading agriculture residues and marine biomass according to the

biorefinery concept: A review. *Renew Sustain Energy Rev* 21:35–51.

<https://doi.org/10.1016/j.rser.2012.11.069>

S Kinoshita, S Udaka, M Shimono (2004) Studies on the amino acid fermentation. Part 1.

Production of L-glutamic acid by various microorganisms. *J Gen Appl Microbiol* 50

(6):331–343

Sambrook BJ, Maccallum P, Russell D (2006) *Molecular Cloning: A Laboratory Manual* to

order or request additional information: *Molecular Cloning: A Laboratory Manual Third*

Edition. I:1–3

Sapcı B, Akpınar O, Bolukbasi U, Yılmaz L (2016) Evaluation of cotton stalk hydrolysate for

xylitol production. *Prep Biochem Biotechnol* 46:474–482.

<https://doi.org/10.1080/10826068.2015.1084511>

Sarabia LA, Ortiz MC (2009) Response Surface Methodology. *Compr Chemom* 1:345–390.

<https://doi.org/10.1016/B978-044452701-1.00083-1>

Sassner P, Mårtensson CG, Galbe M, Zacchi G (2008) Steam pretreatment of H₂SO₄-

impregnated *Salix* for the production of bioethanol. *Bioresour Technol* 99:137–145.

<https://doi.org/10.1016/J.BIORTECH.2006.11.039>

Shuai L, Yang Q, Zhu JY, et al (2010) Comparative study of SPORL and dilute-acid

pretreatments of spruce for cellulosic ethanol production. *Bioresour Technol* 101:3106–

3114. <https://doi.org/10.1016/J.BIORTECH.2009.12.044>

Sluiter A, Hames B, Ruiz R, Scarlata C, Sluiter J, Templeton D, and Crocker D. (2012).

Determination of Structural Carbohydrates and Lignin in Biomass. *Laboratory Analytical*

Procedure (LAP). Issue Date: April 2008 Revision Date: August 2012. (Version 08-03-2012). NREL http://www.nrel.gov/biomass/analytical_procedures.html

Smuleac V, Varma R, Baruwati B, et al (2011) Nanostructured Membranes for Enzyme Catalysis and Green Synthesis of Nanoparticles. *ChemSusChem* 4:1773–1777.

<https://doi.org/10.1002/cssc.201100211>

Stephens C, Christen B, Fuchs T, et al (2007) Genetic Analysis of a Novel Pathway for D-Xylose Metabolism in *Caulobacter crescentus*. *J Bacteriol* 189:2181–2185.

<https://doi.org/10.1128/JB.01438-06>

Sun R, Lawther JM, Banks WB (1995) Influence of alkaline pre-treatments on the cell wall components of wheat straw. *Industrial Crop Prod* 2:127–145

Sun Y, Cheng JJ (2005) Dilute acid pretreatment of rye straw and bermudagrass for ethanol production. *Bioresour Technol* 96:1599–1606.

<https://doi.org/10.1016/J.BIORTECH.2004.12.022>

Sundar Lekshmi M S, Susmitha A, Soumya M P, et al (2019) Bioconversion of D-xylose to D-xylonic acid by *Pseudoduganella danionis*. *Indian J Exp Biol* 57:821–824

Sundar MSL, Susmitha A, Rajan D, Hannibal S, Sasikumar K, Wendisch VF, Nampoothiri KM (2020) Heterologous expression of genes for bioconversion of xylose to xylonic acid in *Corynebacterium glutamicum* and optimization of the bioprocess. *AMB Express*. 2020 Apr 15;10(1):68. doi: 10.1186/s13568-020-01003-9. PMID: 32296988; PMCID: PMC7158973.

Takata E, Tsuruoka T, Tsutsumi K, et al (2014) Production of xylitol and tetrahydrofurfuryl alcohol from xylan in napier grass by a hydrothermal process with phosphorus oxoacids

followed by aqueous phase hydrogenation. *Bioresour Technol* 167:74–80.

<https://doi.org/10.1016/j.biortech.2014.05.112>

Takkellapati S, Li T, Gonzalez MA (2018) An Overview of Biorefinery Derived Platform Chemicals from a Cellulose and Hemicellulose Biorefinery. *Clean Technol Env Policy* 20:1615–1630. <https://doi.org/10.1007/s10098-018-1568-5>

Tathod A, Kane T, Sanil ES, Dhepe PL (2014) Solid base supported metal catalysts for the oxidation and hydrogenation of sugars. *J Mol Catal A Chem* 388–389:90–99. <https://doi.org/10.1016/J.MOLCATA.2013.09.014>

Toivari M, Nygård Y, Kumpula EP, et al (2012) Metabolic engineering of *Saccharomyces cerevisiae* for bioconversion of d-xylose to d-xylonate. *Metab Eng* 14:427–436. <https://doi.org/10.1016/j.ymben.2012.03.002>

Toivari M, Vehkomäki ML, Nygård Y, et al (2013) Low pH d-xylonate production with *Pichia kudriavzevii*. *Bioresour Technol* 133:555–562. <https://doi.org/10.1016/J.BIORTECH.2013.01.157>

Toivari MH, Nygård Y, Penttilä M, et al (2012) Microbial D-xylonate production. *Appl Microbiol Biotechnol* 2012 961 96:1–8. <https://doi.org/10.1007/S00253-012-4288-5>

Toivari MH, Ruohonen L, Richard P, et al (2010) *Saccharomyces cerevisiae* engineered to produce D-xylonate. *Appl Microbiol Biotechnol* 88:751–760. <https://doi.org/10.1007/s00253-010-2787-9>

Torres-Mayanga PC, Lachos-Perez D, Mudhoo A, et al (2019) Production of biofuel precursors and value-added chemicals from hydrolysates resulting from hydrothermal processing of

biomass: A review. *Biomass and Bioenergy* 130:105397.

<https://doi.org/10.1016/J.BIOMBIOE.2019.105397>

Tully J, Yendluri R, Lvov Y (2016) Halloysite Clay Nanotubes for Enzyme Immobilization.

Biomacromolecules 17:615–621. <https://doi.org/10.1021/ACS.BIOMAC.5B01542>

van der Rest ME, Lange C, Molenaar D (1999) A heat shock following electroporation induces

highly efficient transformation of *Corynebacterium glutamicum* with xenogeneic plasmid

DNA. *Appl Microbiol Biotechnol* 52:541–545. <https://doi.org/10.1007/s002530051557>

Wang C, Wei D, Zhang Z, et al (2016) Production of xylonic acid by *Klebsiella pneumoniae*.

Appl Microbiol Biotechnol 100:10055–10063. <https://doi.org/10.1007/s00253-016-7825-9>

Wang S, Su P, Huang J, et al (2013) Magnetic nanoparticles coated with immobilized alkaline

phosphatase for enzymolysis and enzyme inhibition assays. *J Mater Chem B* 1:1749–1754.

<https://doi.org/10.1039/c3tb00562c>

Wang Y, Hu J, Sun M, et al (2022) Efficient Purification of 2'-Fucosyllactose by

Membrane Filtration and Activated Carbon Adsorption. *Ferment* 2022, Vol 8, Page 655

8:655. <https://doi.org/10.3390/FERMENTATION8110655>

Wendisch VF, Nampoothiri KM, Lee JH (2022) Metabolic Engineering for Valorization of

Agri- and Aqua-Culture Sidestreams for Production of Nitrogenous Compounds by

Corynebacterium glutamicum. *Front Microbiol* 13.

<https://doi.org/10.3389/FMICB.2022.835131>

- Wilbanks TJ**, Fernandez SJ (2014) Climate change and infrastructure, urban systems, and vulnerabilities: Technical Report for the U.S. Department of Energy in Support of the National Climate Assessment Island Press Washington
- William, S.**, Feil, H., 2012. Bacterial genomic DNA isolation using CTAB. Sigma. 50-6876
- Wu J**, Hu J, Zhao S, et al (2018) Single-cell Protein and Xylitol Production by a Novel Yeast Strain *Candida intermedia* FL023 from Lignocellulosic Hydrolysates and Xylose. *Appl Biochem Biotechnol* 185:163–178. <https://doi.org/10.1007/s12010-017-2644-8>
- Xu J**, Thomsen MH, Thomsen AB (2009) Pretreatment on corn stover with low concentration of formic acid. *J Microbiol Biotechnol* 19:845–850
- Yim SS**, Choi JW, Lee SH, et al (2017) Engineering of *Corynebacterium glutamicum* for Consolidated Conversion of Hemicellulosic Biomass into Xylonic Acid. *Biotechnol J* 12:1700040. <https://doi.org/10.1002/BIOT.201700040>
- Zahoor A**, Otten A, Wendisch VF (2014) Metabolic engineering of *Corynebacterium glutamicum* for glycolate production. *J Biotechnol* 192:366–375. <https://doi.org/10.1016/j.jbiotec.2013.12.020>
- Zamora F**, Bueno M, Molina I, et al (2000) *Stereoregular copolyamides* derived from D-xylose and L-arabinose. *Macromolecules* 33:2030–2038. <https://doi.org/10.1021/MA9916436/ASSET/IMAGES/LARGE/MA9916436F00004.JPEG>
- Zdarta J**, Bachosz K, Deg O, et al (2019) Co-Immobilization of Glucose Dehydrogenase and Xylose Dehydrogenase as a New Approach for Simultaneous Production of Gluconic and xylonic acid. *Materials (Basel)* 12:1–16

- Zdarta J**, Pinelo M, Jesionowski T, Meyer AS (2018) Upgrading of biomass monosaccharides by immobilized glucose dehydrogenase and xylose dehydrogenase. *ChemCatChem*
- Zhang H**, Han X, Wei C, Bao J (2017) Oxidative production of xylonic acid using xylose in distillation stillage of cellulosic ethanol fermentation broth by *Gluconobacter oxydans*. *Bioresour Technol*. <https://doi.org/10.1016/j.biortech.2016.11.039>
- Zhang H**, Han X, Wei C, Bao J (2017) Oxidative production of xylonic acid using xylose in distillation stillage of cellulosic ethanol fermentation broth by *Gluconobacter oxydans*. *Bioresour Technol*. <https://doi.org/10.1016/j.biortech.2016.11.039>
- Zhang H**, Hay AG (2020) Magnetic biochar derived from biosolids via hydrothermal carbonization: Enzyme immobilization, immobilized-enzyme kinetics, environmental toxicity. *J Hazard Mater* 384: <https://doi.org/10.1016/J.JHAZMAT.2019.121272>
- Zhang H**, Liu G, Zhang J, Bao J (2016) Fermentative production of high titer gluconic and xylonic acids from corn stover feedstock by *Gluconobacter oxydans* and techno-economic analysis. *Bioresour Technol* 219:123–131.
<https://doi.org/10.1016/J.BIORTECH.2016.07.068>
- Zhang W**, Yang Y, Liu X, et al (2019) Development of a secretory expression system with high compatibility between expression elements and an optimized host for endoxylanase production in *Corynebacterium glutamicum*. *Microb Cell Fact* 18:.
<https://doi.org/10.1186/s12934-019-1116-y>

- Zhang Z**, Yang Y, Wang Y, et al (2020) Ethylene glycol and glycolic acid production from xylonic acid by *Enterobacter cloacae*. *Microb Cell Fact* 19:1–16.
<https://doi.org/10.1186/s12934-020-01347-8>
- Zhao Z**, Xian M, Liu M, Zhao G (2020) Biochemical routes for uptake and conversion of xylose by microorganisms. *Biotechnol Biofuels* 13:1–12. <https://doi.org/10.1186/S13068-020-1662-X/figures/2>
- Zhou X**, Huang L, Xu Y, Yu S (2017) A two-step bioprocessing strategy in pentonic acids production from lignocellulosic pre-hydrolysate. *Bioprocess Biosyst Eng* 40:1581–1587.
<https://doi.org/10.1007/s00449-017-1814-y>
- Zhou X**, Lü S, Xu Y, et al (2015) Improving the performance of cell biocatalysis and the productivity of xylonic acid using a compressed oxygen supply. *Biochem Eng J* 93:196–199. <https://doi.org/10.1016/J.BEJ.2014.10.014>
- Zhou X**, Xu Y (2019) Eco-friendly consolidated process for co-production of xylooligosaccharides and fermentable sugars using self-providing xylonic acid as key pretreatment catalyst. *Biotechnol Biofuels* 12: <https://doi.org/10.1186/s13068-019-1614-5>
- Zhou X**, Xu Y, Yu S (2016) Simultaneous Bioconversion of Xylose and Glycerol to Xylonic Acid and 1,3-Dihydroxyacetone from the Mixture of Pre-Hydrolysates and Ethanol-Fermented Waste Liquid by *Gluconobacter oxydans*. *Appl Biochem Biotechnol* 178:1–8.
<https://doi.org/10.1007/s12010-015-1853-2>

- Zhou X**, Zhou X, Tang X, Xu Y (2018) Process for calcium xylonate production as a concrete admixture derived from in-situ fermentation of wheat straw pre-hydrolysate. *Bioresour Technol* 261:288–293. <https://doi.org/10.1016/j.biortech.2018.04.040>
- Zhou X**, Zhou X, Zhang H, et al (2018) Improving the performance of cell biocatalysis and the productivity of acetoin from 2,3-butanediol using a compressed oxygen supply. *Process Biochem* 64:46–50. <https://doi.org/10.1016/j.procbio.2017.09.027>
- Zhu J**, Rong Y, Yang J, et al (2015) Integrated Production of Xylonic Acid and Bioethanol from Acid-Catalyzed Steam-Exploded Corn Stover. *Appl Biochem Biotechnol* 2015 1765 176:1370–1381. <https://doi.org/10.1007/S12010-015-1651-X>
- Zhu M**, Sun L, Lu X, et al (2019) Establishment of a transient CRISPR-Cas9 genome editing system in *Candida glycerinogenes* for co-production of ethanol and xylonic acid. *J Biosci Bioeng* 128:283–289. <https://doi.org/10.1016/j.jbiosc.2019.03.009>
- Zoghalmi A**, Paës G (2019) Lignocellulosic Biomass: Understanding Recalcitrance and Predicting Hydrolysis. *Front Chem* 7: <https://doi.org/10.3389/fchem.2019.00874>

ANNEXURE I

LIST OF INSTRUMENTS USED

Instruments	Model and country
Autoclave	Labline, India
Balance	Mettler Toledo, Mumbai, India
Centrifuge	Kubota 7780, Japan; Eppendorf, Germany; MICRO CL17, Thermo Fisher Scientific, India
Cold room	Rinac Pvt. Ltd, India
Deep freezer (-80°C)	Elanpro, India; Haier, China
DNA sequencer	3500 Genetic Analyzer, Applied Biosystems, Hitachi, Japan
Electrophoresis unit	Bio-Rad, USA
Electroporator	Eppendorf, Germany
Fermenter	InforsHT Sixfors, Switzerland
Gel documentation	ChemiDoc, Biorad, USA
Heating water bath	B20G, Lab companion, South Korea
Hot air Oven	Kemi Instruments, India
HPLC	Shimadzu, Japan
Incubator	Infors Ht, Switzerland
Incubating water bath	Julabo, Germany
Ion exchange column	Amersham Biosciences, UK
Laminar air flow chamber	Labline, India
Lyophilizer	Operon, Korea
Microplate reader	Infinite M200 Pro, Tecan, Switzerland,
Nanodrop spectrophotometer	ND1000, Thermo Fisher Scientific, India
NMR Analysis	Bruker Advance III 500 MHz

pH meter	Eutech, Thermo Fisher Scientific, India
PCR machine	MyCycler, Bio-Rad, USA
Phase contrast microscope	Leica DMLS, Leica Microsystems, Germany
NMR Spectrometer	Bruker Avance II-500, Bruker Co., USA
Scanning electron microscope	Zeiss EVO 18 cryo-SEM, Germany
Sonicator	Vibra cell, Sonics and Materials Inc., USA
Transmission electron microscope	JEM2010, JEOL, Japan
Thermostat	Eppendorf, USA
UV-Vis Spectrophotometer	UV-160A, Shimadzu, Japan
Fourier Transform-Infrared Spectrometer	Nexus-870 FT-IR, Thermo Nicolet Corporation, Madison, WI, USA
Stirred tank bioreactor	Minifors, Infors HT, Switzerland

ANNEXURE II

MEDIA COMPOSITION

I. LB Medium

Constituents	Concentration (gL ⁻¹)
Tryptone	10.00
NaCl	10.00
Yeast Extract	5.00
Agar (for solid medium)	15.00

Adjusted the pH to 7.0 by 1 N HCl/ NaOH, and sterilized by autoclaving

III. Brain Heart Infusion (BHI) medium

Constituents	Concentration (gL ⁻¹)
Beef heart infusion	2.50
Calf brain infusion	6.25
Glucose	1.75
Peptone	5.00
NaCl	2.50

Adjusted the pH to 7.0 by 1 N HCl/ NaOH, and sterilized by autoclaving

III. CGXII Basal medium

Constituents	Concentration (gL⁻¹)
(NH ₄) ₂ SO ₄	20.00
Urea	5.00
K ₂ HPO ₄	1.00
KH ₂ PO ₄	1.00
MgSO ₄ . 7H ₂ O	0.25
MOPS	5.00
*Stock solution 1 (1% CaCl ₂)	1.0 mL
*Stock solution 2 (0.02% Biotin)	0.1 mL
*Stock solution 3 (FeSO ₄ .7H ₂ O (1%), MnSO ₄ . H ₂ O (1%), ZnSO ₄ .7H ₂ O (0.1%), CuSO ₄ .5H ₂ O (0.03%) & NiCl ₂ .6H ₂ O (0.002%)	1.0 mL
*Stock solution 4 (3% Protocatechuate)	1.0 mL
# Sugar solution (Glucose/ Xylose/Arabinose)	Upto 40
<i>Made up the volume to 1000 mL (pH 6.5) and filter sterilized through 0.2 µm filters</i>	

IV. SOC Medium

Constituents	Concentration (gL⁻¹)
Glucose	20 mM
Bacto-tryptone	20.00
Yeast Extract	5.00
MgCl ₂	10 mM
KCl	0.19
NaCl	0.5

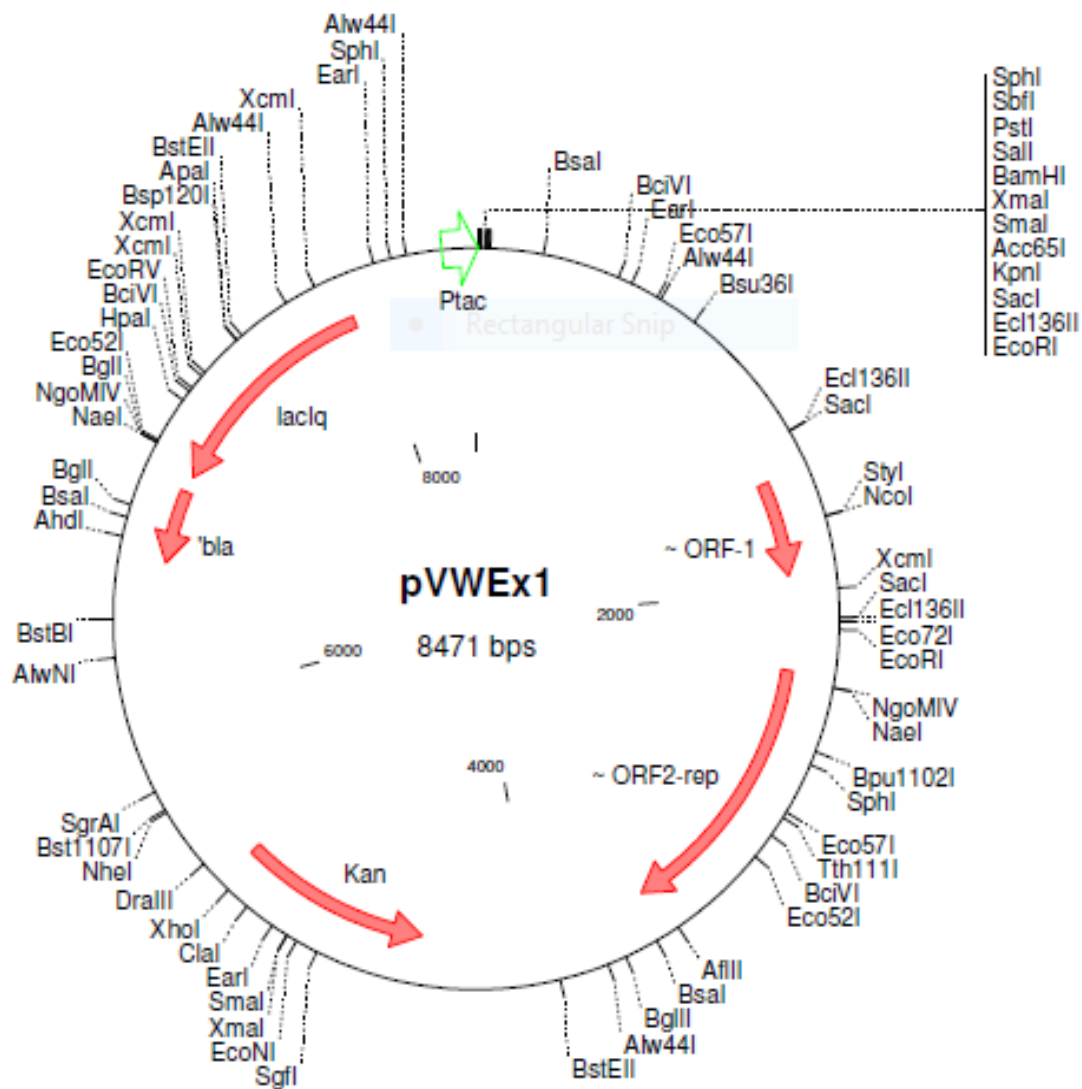
IV. Epo Medium

Constituents	Concentration (gL⁻¹)
Tryptone	10.0
Yeast Extract	5.0
Isonicotinic acid	4.0
Tween 80	1 ml
Glycine	25.0
NaCl	10.0

ANNEXURE III

VECTOR MAP AND SEQUENCE

1. pVWEx1 (8471 bp)



```

AAGCTTGCATGCCTGCAGGTGCGACTCTAGAGGATCCCCGGGTACCGAGCTCGAATTCCTGGCCGTCG
TTTTACAGCCAAGCTTGGCTGTTTTGGCGGATGAGAGAAGATTTTCAGCCTGATACAGATTAAATCAG
AACGCAGAAGCGGTCTGATAAAAACAAATTTGCCTGGCGGCAGTAGCGCGGTGGTCCCACCTGACCCCA
TGCCGAACTCAGAAGTGAACGCGGTAGCGCCGATGGTAGTGTGGGGTCTCCCCATGCGAGAGTAGG
GAACTGCCAGGCATCAAATAAAACGAAAGGCTCAGTCGAAAGACTGGGCCTTTTCGTTTTATCTGTTGT
TTGTCGGTGAACGCTCTCCTGAGTAGGACAAATCCGCCGGGAGCGGATTTGAACGTTGCGAAGCAACG

```

GCCCGGAGGGTGGCGGGCAGGACGCCCGCCATAAACTGCCAGGCATCAAATTAAGCAGAAGGCCATC
 CTGACGGATGGCCTTTTTGCGTTTCTACAAACTCTTTTGTATTTTTCTAAATACATTCAAATATGTAT
 CCGTCTATGAGACAATAACCCTGATAAATGCTTCAATAATATTGAAAAAGGAAGAGTATGAGTATTCA
 ACATTTCCGTGTCGCCCTTATTCCCTTTTTGCGGCATTTTGCCTTCTGTTTTTGTCTACCCAGAAACG
 CTGGTGAAGTAAAAGATGCTGAAGATCAGTTGGGTGCACGAGTGGGTACATCGAACTGGATCTCAA
 CAGCGGTAAGATCCTTGAGAGTTTTCGCCCCGAAGAACGTTTTCCAATGATGAGCACTTTTGATCCCC
 TGCGGCGTGCCTGATCGCCCTCGCGACGTTGTGCGGGTGGCTTGTCCCTGAGGGCGCTGCGACAGATA
 GCTAAAAATCTGCGTCAGGATCGCCGTAGAGCGCGCGTGCCTGATTGGAGGCTTCCCTTTGGTTG
 ACGGTCTTCAATCGCTCTACGGCGATCCTGACGCTTTTTTGTGCGTACCGTCGATCGTTTTATTTCTGT
 CGATCCCCGAAAAAGTTTTTGCCTTTTGTAAAAAACTTCTCGGTGCCCCGCAAATTTTCGATTCCAGAT
 TTTTTAAAAACCAAGCCAGAAATACGACACACCGTTTTGCAGATAATCTGTCTTTTCGAAAAATCAAGT
 GCGATACAAAATTTTAGCACCCCTGAGCTGCGCAAAGTCCCGCTTCGTGAAAAATTTTCGTGCCGCGTG
 ATTTTCCGCCAAAACTTTAACGAACGTTTCGTTATAATGGTGTGATGACCTTCACGACGAAGTACCAA
 AATTGGCCCGAATCATCAGCTATGGATCTCTCTGATGTCGCGCTGGAGTCCGACGCGCTCGATGCTGCC
 GTCGATTTAAAAACGGTGATCGGATTTTTCCGAGCTCTCGATACGACGACGCGCCAGCATCACGAGA
 CTGGGCGAGTGGCGGAGCGACCTAGAAACTCTCGTGGCGGATCTTGAGGAGCTGGCTGACGAGTGC
 GTGCTCGGCAGCGCCAGGAGGACGCACAGTAGTGGAGGATCGAATCAGTTGCGCCTACTGCGGTGGC
 CTGATTCCTCCCCGCGCTGACCCGCGAGGACGGCGCGCAAATATTGCTCAGATGCGTGTCTGTGCCG
 AGCCAGCCGCGAGCGCGCAAACAACGCCACGCCGAGGAGCTGGAGGCGGCTAGGTTCGCAAATGGCG
 CTGGAAGTGCCTCCCCGAGCGAAATTTGGCCATGGTTCGTCACAGAGCTGGAAGCGGCAGCGAGAA
 TTATCCGCGATCGTGGCGCGGTGCCCGCAGGCATGACAAACATCGTAAATGCCGCGTTTTCGTGTGGCC
 GTGGCCGCCAGGACGTGTGACGCGCCGCCACCACCTGCACCGAATCGGCAGCAGCGTCCGCGCTCGA
 AAAAGCGCACAGGCGGCAAGAAGCGATAAGCTGCACGAATACCTGAAAAATGTTGAACGCCCCGTGA
 GCGGTAACCTCACAGGGCGTCCGCTAACCCCCAGTCCAAACCTGGGAGAAAGCGCTCAAAAATGACTC
 TAGCGGATTCACGAGACATTGACACACCGGCCTGGAAATTTTCCGCTGATCTGTTGACACCCATCCC
 GAGCTCGCGCTGCGATCACGTGGCTGGACGAGCGAAGACCCGCCGAATTCCTCGCTCACCTGGGCGAG
 AGAAAATTTCCAGGGCAGCAAGACCCGCGACTTCGCCAGCGCTTGATCAAAGACCCGGACACGGGA
 GAAACACAGCCGAAGTTATACCGAGTTGGTTCAAATCGCTTGCCCGGTGCCAGTATGTTGCTCTGAC
 GCACGCGCAGCACGACGCCGTGCTTGTCTGGACATTGATGTGCCGAGCCACCAGGCCGCGGGAAA
 ATCGAGCACGTAAACCCCGAGGTCTACGCGATTTTGGAGCGCTGGGCACGCCTGGAAAAAGCGCCAG
 CTTGGATCGGCGTGAATCCACTGAGCGGGAAATGCCAGTCTATCTGGCTCATTGATCCGGTGTATGCC
 GCAGCAGGCATGAGCAGCCGAATATGCGCCTGCTGGCTGCAACGACCGAGGAAATGACCCGCGTTTT
 CGGCGCTGACCAGGCTTTTTACATAGGCTGAGCCGGTGGCCACTGCACGTCTCCGACGATCCCACCG
 CGTACCGCTGGCATGCCCAGCACAAATCGCGTGGATCGCTAGCTGATCTTATGGAGGTTGCTCGCATG
 ATCTCAGGCACAGAAAAACCTAAAAACGCTATGAGCAGGAGTTTTCTAGCGGACGGGCACGTATCG
 AAGCGGCAAGAAAAGCCACTGCGGAAGCAAAGCACTTGCCACGCTTGAAGCAAGCCTGCCGAGCGC
 CGCTGAAGCGTCTGGAGAGCTGATCGACGGCGTCCGTGTCTCTGGACTGCTCCAGGGCGTGCCGCC
 GTGATGAGACGGCTTTTCGCCACGCTTTGACTGTGGGATACCAGTTAAAAGCGGCTGGTGTGAGCGCCTA
 AAAGACACCAAGATCATCGACGCCTACGAGCGTGCCTACACCGTCGCTCAGGCGGTGCGGAGCAGCG
 GCCGTGAGCCTGATCTGCCGCCGATGCGTGACCGCCAGACGATGGCGCGACGTTGTGCGCGGCTACGTC
 GCTAAAGGCCAGCCAGTTCGTCCTGCTCGTACAGCAGAGACGACGAGCAGCCGAGGCGGAAAGCTC
 TGGCCACTATGGGAAGACGTGGCGGTA AAAAGGCCGCGAGAACGCTGGAAAGACCCAAACAGTGAGTA
 CGCCCAGCACAGCGAGAAAAACTAGCTAAGTCCAGTCAACGACAAGCTAGGAAAGCTAAAGGAAAT
 CGCTTGACCATTGCAGGTTGGTTTATGACTGTTGAGGGAGAGACTGGCTCGTGGCCGACAATCAATGA
 AGCTATGTCTGAATTTAGCGTGTACGTCAGACCGTGAATAGAGCACTTAAGTCTGCGGGCATTGAAC
 TTCCACGAGGACGCCGTAAGCTTTCCAGTAAATGTGCCATCTCGTAGGCAGAAAACGGTTCCCCCG
 TAGGGGTCTCTCTTTGGCTCCTTTCTAGGTGCGGCTGATTGCTCTTGAAGCTCTTAGGGGGGCTCA
 CACCATAGGCAGATAACGGTTCCCCACCGGCTCACCTCGTAAGCGCACAAAGGACTGCTCCCAAAGATC
 TTCAAAGCCACTGCCGCGACTCCGCTTCGCGAAGCCTTGCCCCGCGGAAATTTCTCCACCGAGTTCGT
 GCACACCCCTATGCCAAGCTTCTTTACCCTAAATTCGAGAGATTGGATTCTTACCGTGGAATTTCTTC
 GCAAAAATCGTCCCCTGATCGCCCTTGCAGCTTGCTCGCGGCGGTGCCGCTGGTTGCGCTTGGCTTGA
 CCGACTTGATCCTCCGGCGTTCAGCCTGTGCCACAGCCGACAGGATGGTGACCACCATTTGCCCATAT
 CACCGTCCGTAATGATCCCGTTCGTAATAAACCGAACCCTACACCTGAGCATCAAATCTTTTATCA
 GTTGGATCATGTCCGGCGTTCGCGGCCAAGACGGTTCGAGCTTCTTACCAGAATGACATCACCTTCC
 TCCACCTTATCTCAGCAAATCCAGCCCTTCCCGATCTGTTGAACTGCCGGATGCCTTGTCCGGTAAAG
 ATGCGGTTAGCTTTTACCCTGCATCTTTGAGCGCTGAGGTCTGCCTCGTGAAGAAGGTGTTGCTGACT

CATACCAGGCCTGAATCGCCCCATCATCCAGCCAGAAAGTGAGGGAGCCACGGTTGATGAGAGCTTTG
 TTGTAGGTGGACCAGTTGGTGATTTTGAACCTTTTGTCTTGCCACGGAACGGTCTGCGTTGTCGGGAAGA
 TGCGTGATCTGATCCTTCAACTCAGCAAAAGTTTCGATTTATTCAACAAAGCCGCCGTCCCGTCAAGTCA
 GCGTAATGCTCTGCCAGTGTACAACCAATTAACCAATTCTGATTAGAAAACTCATCGAGCATCAAA
 TGAAACTGCAATTTATTCATATCAGGATTATCAATACCATATTTTTGAAAAAGCCGTTTCTGTAATGAA
 GGAGAAAACTCACCGAGGCAGTTCCATAGGATGGCAAGATCCTGGTATCGGTCTGCGATTCCGACTCG
 TCCAACATCAATAACAACCTATTAATTTCCCTCGTCAAAAATAAGGTTATCAAGTGAGAAATCACCAT
 GAGTGACGACTGAATCCGGTGAGAATGGCAAAAGCTTATGCATTTCTTTCCAGACTTGTTCAACAGGC
 CAGCCATTACGCTCGTCATCAAAATCACTCGCATCAACCAAACCGTTATTCATTTCGTGATTGCGCCTGA
 GCGAGACGAAATACGCGATCGCTGTTAAAAGGACAATTACAAACAGGAATCGAATGCAACCGGCGCA
 GGAACACTGCCAGCGCATCAACAATATTTTACCTGAATCAGGATATCTTCTAATACCTGGAATGCTG
 TTTTCCCGGGGATCGCAGTGGTGAGTAACCATGCATCATCAGGAGTACGGATAAAATGCTTGATGGTC
 GGAAGAGGCATAAATTCGTCAGCCAGTTTAGTCTGACCATCTCATCTGTAACATCATTGGCAACGCT
 ACCTTTGCCATGTTTCAGAAACAACCTCTGGCGCATCGGGCTTCCCATACAATCGATAGATTGTCGCACC
 TGATTGCCGACATTATCGCGAGCCCATTTATACCCATATAAATCAGCATCCATGTTGGAATTTAATCG
 CGCCTCGAGCAAGACGTTTCCCGTTGAATATGGCTCATAAACACCCCTTGTATTACTGTTTATGTAAGC
 AGACAGTTTTATTGTTTCATGATGATATATTTTTATCTTGTGCAATGTAACATCAGAGATTTTGAGACAC
 AACGTGGCTTTGTTGAATAAATCGAACTTTTGCTGAGTTGAAGGATCAGATCACGCATCTTCCCGACA
 ACGCAGACCGTTCCGTGGCAAAGCAAAGTTCAAAAATCACCAACTGGTCCACCTACAACAAAGCTCTC
 ATCAACCGTGGCTCCCTCACTTTCTGGCTGGATGATGGGGCGATTACGGCCTGGTATGAGTCAGCAAC
 ACCTTCTTACGAGGCAGACCTCAGCGCTAGCGGAGTGTATACTGGCTTACTATGTTGGCACTGATGA
 GGGTGTCAAGTGAAGTCTTCATGTGGCAGGAGAAAAAGGCTGCACCGGTGCGTCAGCAGAATATGT
 GATACAGGATATATTCCGCTTCCCTCGTCACTGACTCGCTACGCTCGGTGCTTCGACTGCGGCGAGCGG
 AAATGGCTTACGAACGGGGCGGAGATTTCTGGAAGATGCCAGGAAGATACTTAACAGGGGAAGTGAG
 AGGGCCGCGCAAAGCCGTTTTTCCATAGGCTCCGCCCCCTGACAAGCATCACGAAATCTGACGCTC
 AAATCAGTGGTGGCGAAACCCGACAGGACTATAAAGATAACCAGGCGTTTCCCTGGCGGCTCCCTCG
 TGCGCTCTCCTGTTCCCTGCCTTTCCGTTTACCGGTGTCATTCCGCTGTTATGGCCGCGTTTGTCTCATT
 CACGCCTGACACTCAGTTCGGGTAGGCAGTTCGCTCCAAGCTGGACTGTATGCACGAACCCCCGTT
 CAGTCCGACCGCTGCGCCTTATCCGGTAACATCGTCTTGAGTCCAACCCGAAAGACATGCAAAAGC
 ACCACTGGCAGCAGCCACTGGTAATTGATTTAGAGGAGTTAGTCTTGAAGTCATGCGCCGGTTAAGGC
 TAAACTGAAAGGACAAGTTTTGGTGACTGCGCTCCTCCAAGCCAGTTACCTCGGTTCAAAGAGTTGGT
 AGCTCAGAGAACCTTCGAAAAACCGCCCTGCAAGGCGGTTTTTTTCGTTTTTCAGAGCAAGAGATTACGC
 GCAGACCAAAAACGATCTCAAGAAGATCATCTTATTAAGGGGTCTGACGCTCAGTGGAACGAAAACTC
 ACGTTAAGGGATTTTGGTCATGAGATTATCAAAAAGGATCTTCACCTAGATCCTTTTAAATTAAAAATG
 AAGTTTTAAATCAATCTAAAGTATATATGAGTAACTTGGTCTGACAGTTACCAATGCTTAATCAGTGA
 GGCACCTATCTCAGCGATCTGTCTATTTTCGTTTCATCCATAGTTGCCTGACTCCCCGTCGTGTAGATAAC
 TACGATACGGGAGGGCTTACCATCTGGCCCCAGTGTGCAATGATACCGCGAGACCCACGCTCACCGG
 CTCCAGATTTATCAGCAATAAACCAGCCAGCCGGAAGGGCCGAGCGCAGAAGTGGTCTGCAACTTTA
 TCCGCTCCATCCAGTCTATTAATTGTTGCCGGGAAGCTAGAGTAAGTGTTCGCGAGTTAATAGTTTG
 CGCAACGTTGTTGCCATTGCCGATGATAAGCTGTCAAACATGGCCTGTCGCTTGGCGTATTCGGAATCT
 TGCACGCCCTCGCTCAAGCCTTCGTCACTGGTCCCGCCACCAAACGTTTTCGGCGAGAAGCAGGCCATT
 ATCGCCGGCATGGCGGCCGACGCGCGGGAGAGCGGTTTTGCGTATTGGGCGCCAGGGTGGTTTTTCT
 TTTACCAAGTGAGACGGGCAACAGCTGATTGCCCTTACCGCCTGGCCCTGAGAGAGTTGCAGCAAGC
 GGTCCACGCTGGTTTTGCCCCAGCAGGCGAAAAATCCTGTTTGATGGTGGTTAACGGCGGGATATAACAT
 GAGCTGTCTTCGGTATCGTCGTATCCACTACCGAGATATCCGCACCAACGCGCAGCCCGGACTCGGT
 AATGGCGCGCATTGCGCCCAGCGCCATCTGATCGTTGGCAACCAGCATCGCAGTGGGAACGATGCCCT
 CATTACGATTTGCATGGTTTTGTTGAAAACCGGACATGGCACTCCAGTTCGCTTCCCGTTCCGCTATCG
 GCTGAATTTGATTGCGAGTGAGATATTTATGCCAGCCAGCCAGACGCAGACGCGCCGAGACAGAATT
 AATGGGCCCCTAACAGCGGATTTGCTGGTGACCCAATGCGACCAGATGCTCCACGCCAGTCGCGT
 ACCGTCTTCATGGGAGAAAATAATACTGTTGATGGGTGTCTGGTCAGAGACATCAAGAAAATAACGCCG
 GAACATTAGTGCAGGCAGCTTCCACAGCAATGGCATCCTGGTCATCCAGCGGATAGTTAATGATCAGC
 CCACTGACGCGTTGCGCGAGAAGATTGTGCACCGCCGCTTTACAGGCTTCGACGCCGCTTCGTTCTACC
 ATCGACACCACCAGCTGGCACCCAGTTGATCGGCGCGAGATTTAATCGCCGCGACAATTTGCGACCG
 CGGTGACAGGGCCAGACTGGAGGTGGCAACGCCAATCAGCAACGACTGTTTGGCCGCCAGTTGTTGTG
 CCACGCGGTTGGGAATGTAATTCAGCTCCGCCATCGCCGCTTCCACTTTTTCCCGCGTTTTTCGCAGAAA
 CGTGGCTGGCTGGTTACCACGCGGAAACGGTCTGATAAGAGACACCGGCATACTCTGCGACATCG

TGATGATGATGATGGCTGCTGCCCATGGTATATCTCCTTCTTAAAGTTAAACAAAATTATTTCTAGAGG
 GGAATTGTTATCCGCTACAATCCCCTATAGTGAGTCGTATTAATTCGCGGGATCGAGATCTCGATC
 CTCTACGCCGGACGCATCGTGGCCGGCATCACCGGCGCCACAGGTGCGGTTGCTGGCGCTATATCGC
 CGACATCACCGATGGGGAAGATCGGGCTCGCCACTTCGGGCTCATGAGCGCTTGTTCGGCGTGGGTA
 TGGTGGCAGGCCCGTGGCCGGGGACTGTTGGGCGCCATCTCCTTGCATGCACCATTCCTTGGCGCG
 GCGGTGCTCAACGGCCTAACCTACTACTGGGCTGCTTCCTAATGCAGGAGTCGCATAAGGGAGAGCG
 TCGAGATCCCGGACACCATCGAATGGCGCAAAACCTTTCGCGGTATGGCATGATAGCGCCCGGAAGA
 GAGTCAATTCAGGGTGGTGAATGTGAAACCAGTAACGTTATACGATGTCGCAGAGTATGCCGGTGTCT
 CTTATCAGACCGTTCCTCCGCGTGGTGAACCAGGCCAGCCACGTTTCTGCGAAAACCGGGGAAAAAGTG
 GAAGCGGCGATGGCGGAGCTGAATTACATTCCCAACCGCGTGGCACAACAACCTGGCGGGCAAACAGT
 CGTTGCTGATTGGCGTTGCCACCTCCAGTCTGGCCCTGCACGCGCCGTCGCAAATTGTCGCGGCGATTA
 AATCTCGCGCCGATCAACTGGGTGCCAGCGTGGTGGTGTGATGGTAGAACGAAGCGGCGTCAAGC
 CTGTAAAGCGGCGGTGCACAATCTTCTCGCGCAACGCGTCAGTGGGCTGATCATTAACCTATCCGCTGG
 ATGACCAGGATGCCATTGCTGTGGAAGCTGCCTGACTAATGTTCCGGCGTTATTTCTTGATGTCTCTG
 ACCAGACACCCATCAACAGTATTATTTCTCCCATGAAGACGGTACGCGACTGGGCGTGGAGCATCTG
 GTCGCATTGGGTACACAGCAAATCGCGCTGTTAGCGGGCCCATTAAGTTCTGTCTCGGCGCGTCTGCGT
 CTGGCTGGCTGGCATAAATATCTCACTCGCAATCAAATTCAGCCGATAGCGGAACGGGAAGGCGACTG
 GAGTGCCATGTCCGGTTTTCAACAAACCATGCAAATGCTGAATGAGGGCATCGTTCCCACTGCGATGC
 TGGTTGCCAACGATCAGATGGCGCTGGGCGCAATGCGCGCCATTACCGAGTCCGGGCTGCGCGTTGGT
 GCGGATATCTCGGTAGTGGGATACGACGATACCGAAGACAGCTCATGTTATATCCCGCCGTTAACCAC
 CATCAAACAGGATTTTCGCTGCTGGGGCAAACAGCGTGGACCGCTTGCTGCAACTCTCTCAGGGCC
 AGGCGGTGAAGGGCAATCAGCTGTTGCCGCTCTCACTGGTGAAAAGAAAAACCACCCTGGCGCCCAA
 TACGCAAACCGCCTCTCCCCGCGGTTGGCCGATTCATTAATGCAGCTGGCACGACAGGTTTCCCGACT
 GGAAAGCGGGCAGTGAGCGCAACGCAATTAATGTAAGTTAGCTCACTCATTAGGCACCGGGATCTCG
 ACCGATGCCCTTGAGAGCCTTCAACCCAGTCAGCTCCTTCCGGTGGGCGCGGGGCATGACTATCGTCG
 CCGCACTTATGACTGTCTTCTTTATCATGCAACTCGTAGGACAGGTGCCGGCAGCGCTCTGGGTCAATT
 TCGGCGAGGACCGCTTTCGCTGGAGCGCGACGATGATCGGCCTGTCGCTTGCGGTATTCGGAATCTTG
 CACGCCCTCGCTCAAGCCTTCGTCACTGGTCCCGCCACCAAACGTTTCCGGCGAGAAGCAGGCCATTAT
 CGCCGGCATGGCGGCCCCACGGGTGCGCATGATCGTGCTCCTGTGCTGAGGACCCGGCTAGGCTGGC
 GGGGTTGCCTTACTGGTTAGCAGAATGAATCACCGATACGCGAGCGAACGTGAAGCGACTGCTGCTGC
 AAAACGTCTGCGACCTGAGCAACAACATGAATGGTCTTCGGTTTTCCGTGTTTCGTAAGTCTGGAAAC
 GCGGAAGTCAGCGCCCTGCACCATTATGTTCCGGATCTGCATCGCAGGATGCTGCTGGCTACCCTGTG
 GAACACCTACATCTGTATTAACGAAGCGCTGGCATTGACCCTGAGTGATTTTTCTCTGGTCCCGCCGA
 TCCATACCGCCAGTTGTTTACCCTCACACGTTCCAGTAACCGGGCATGTTTCATCATCAGTAACCCGTA
 TCGTGAGCATCCTCTCTCGTTTCATCGGTATCATTACCCCATGAACAGAAATCCCCCTTACACGGAGG
 CATCAGTGACCAAACAGGAAAAAACCGCCCTAACATGGCCCGCTTTATCAGAAGCCAGACATTAACG
 CTTCTGGAGAACTCAACGAGCTGGACGCGGATGAACAGGCAGACATCTGTGAATCGTTACAGACCA
 CGCTGATGAGCTTACCGCAGCTGCCTCGCGCGTTTCGGTGATGACGGTGAAAACCTCTGACACATGC
 AGCTCCCGGAGACGGTCACAGCTTGTCTGTAAGCGGATGCCGGGAGCAGACAAGCCCGTCAGGGCGC
 GTCAGCGGGTGTGGCGGGTGTGGGGCGCAGCCATGACCCAGTCACGTAGCGATAGCGGAGTGTAT
 ACTGGCTTAACTATGCGGCATCAGAGCAGATTGTAAGTACTGAGAGTGCACCATATATGCGGTGTGAAATAC
 CGCACAGATGCGTAAGGAGAAAATACCGCATCAGGCGCTTTCGGCTTCCTCGCTCACTGACTCGCTG
 CGCTCGGTGCTTCGGCTGCGGCGAGCGGTATCAGCTCACTCAAAGCGGTAATACGGTTATCCACAGA
 ATCAGGGGATAACGCAGGAAAGAACATGTGAGCAAAGGCCAGCAAAGGCCAGGAACCGTAAAAA
 GGCCGCGTTGCTGGCGTTTTTCCATAGGCTCCGCCCCCTGACGAGCATCACAAAAATCGACGCTCAA
 GTCAGAGGTGGCGAAACCCGACAGGACTATAAAGATACCAGGCGTTTTCCCTGGAAGCTCCCTCGTG
 CGCTCTCCTGTTCCGACCCTGCCGCTTACCGGATACCTGTCCGCTTTCTCCCTTCGGGAAGCGTGGCG
 CTTTCTCATAGCTCACGCTGTAGGTATCTCAGTTCGGTGTAGGTGCTTCGCTCCAAGCTGGGCTGTGTG
 CACGAACCCCGGTTACGCCGACCGCTGCGCCTTATCCGGTAACTATCGTCTTGAGTCCAACCCGGTA

AGACACGACTTATCGCCACTGGCAGCAGCCACTGGTAACAGGATTAGCAGAGCGAGGTATGTAGGCG
GTGCTACAGAGTTCTTGAAGTGGTGGCCTAACTACGGCTACACTAGAAGGACAGTATTTGGTATCTGC
GCTCTGCTGAAGCCAGTTACCTTCGGAAAAAGAGTTGGTAGCTCTTGATCCGGCAAACAAACCACCG
TGGTAGCGGTGGTTTTTTTTGTTTGCAAGCAGCAGATTACGCGCAGAAAAAAGGATCTCAAGAAGATC
CTTTGATCTTTTCTACGGGGTCTGACGCTCAGTGGAACGAAACTCACGTTAAGGGATTTTGGTCATGA
ACAATAAAACTGTCTGCTTACATAAACAGTAATACAAGGGGTGTTATGAGCCATATTCAACGGGAAAC
GTCTTGCTCTAGGCCGCGATTAAATTCCAACATGGATGCTGATTTATATGGGTATAAATGGGCTCGCGA
TAATGTCTGGCAATCAGGTGCGACAATCTATCGATTGTATGGGAAGCCCGATGCGCCAGAGTTGTTTC
TGAAACATGGCAAAGGTAGCGTTGCCAATGATGTTACAGATGAGATGGTCAGACTAACTGGCTGAC
GGAATTTATGCCTCTTCCGACCATCAAGCATTTTATCCGTACTCCTGATGATGCATGGTTACTCACCAC
TGCGATCCCCGGGAAAACAGCATTCCAGGTATTAGAAGAATATCCTGATTCAGGTGAAAATATTGTTG
ATGCGCTGGCAGTGTTCTGCGCCGGTTGCATTTCGATTCTGTTTGTAAATTGTCCTTTTAACAGCGATC
GCGTATTTTCGTCTCGCTCAGGCGCAATCACGAATGAATAACGGTTTTGGTTGATGCGAGTGATTTTGATG
ACGAGCGTAATGGCTGGCCTGTTGAACAAGTCTGGAAGAAATGCATAAACTTTTGCCATTCTCACCG
GATTCAGTCGTCACTCATGGTGATTTCTCACTTGATAACCTTATTTTTGACGAGGGGAAATTAATAGGT
TGTATTGATGTTGGACGAGTCGGAATCGCAGACCGATAACCAGGATCTTGCCATCCTATGGAACCTGCCT
CGGTGAGTTTTCTCCTTCATTACAGAAACGGCTTTTTCAAAAATATGGTATTGATAATCCTGATATGAA
TAAATTGCAGTTTCATTTGATGCTCGATGAGTTTTTCTAAGAATTAATTCATGAGCGGATACATATTTG
AATGTATTTAGAAAAATAAACAATAGGGGTTCCGCGCACATTTCCCCGAAAAGTGCCACCTGAAATT
GTAAACGTTAATATTTTGTAAATTCGCGTTAAATTTTTGTAAATCAGCTCATTTTTTAACCAATAGG
CCGAAATCGGCAAATCCCTTATAAATCAAAAAGAATAGACCGAGATAGGGTTGAGTGTTGTTCCAGTT
TGGAACAAGAGTCCACTATTAAGAACGTGGACTCCAACGTCAAAGGGCGAAAAACCGTCTATCAGG
GCGATGGCCACTACGTGAACCATCACCCCTAATCAAGTTTTTTGGGGTCGAGGTGCCGTAAAGCACTA
AATCGGAACCCTAAAGGGAGCCCCGATTTAGAGCTTGACGGGAAAGCCGGCGAACGTGGCGAGAA
AGGAAGGGAAGAAAGCGAAAGGAGCGGGCGCTAGGGCGCTGGCAAGTGTAGCGGTCACGCTGCGCG
TAACCACCACACCCGCGCGCTTAATGCGCCGCTACAGGGCGCGTCCCATTCCGCA

ANNEXURE IV
AcSIR Course Work

Sl No.	Level & Course No.	Title	Status
Level 100			
1.	BIO-101	Biostatistics	Completed
2.	BIO-102	Bioinformatics	Completed
3.	BIO-103	Basic Chemistry	Completed
4.	BIO-104	Research Methodology, communication/ ethics/ safety	Completed
Level 200			
1.	BIO-NIIST-201	Biotechnology and Instrumentation	Completed
2.	BIO-NIIST-206	Protein Sciences and Proteomics	Completed
3.	BIO-NIIST-239	Basic Molecular Biology	Completed
Level 300			
1.	BIO-NIIST-301	Seminar Course	Completed
2.	BIO-NIIST-337	Bioprocess Technology	Completed
3.	BIO-NIIST-369	Enzymology and Enzyme Technology	Completed
Level 400			
1.		Review	Completed
2.		Project Proposal	Completed
Level 800			
1.		CSIR 800 Project	Completed

ABSTRACT OF THE THESIS

Name of the Student: **Lekshmi Sundar M S**Registration No.: **10BB17J39013**Faculty of Study: **Biological Sciences**Year of Submission: **2023**AcSIR academic centre/CSIR Lab: **CSIR-NIIST, Trivandrum Kerala**Name of the Supervisor: **Dr. K. Madhavan Nampoothiri**Title of the thesis: **Integrated bioprocess for conversion of xylose to xylonic acid by recombinant *Corynebacterium glutamicum***

Reliance on depleted fossil fuels accompanied by global warming and climate change has driven the world to explore and develop new strategies for global sustainable development. Hence, new value-added products have been developed from renewable resources like lignocellulosic biomass. One of the platform chemicals synthesized from biomass is xylonic acid which is a sugar acid derived from pentose sugar xylose. Our study was to develop a bioprocess for the synthesis of xylonic acid from sawdust APL using a well-established industrial microbe *Corynebacterium glutamicum*. The xylose utilizing genes (*xylB*) and (*xylC*) of *Caulobacter crescentus* were expressed in *C. glutamicum* ATCC 31831. $56.32 \pm 0.3 \text{ gL}^{-1}$ xylonic acid was obtained from 60 gL^{-1} xylose (using synthetic sugar in CGXII medium) with a yield of 1.04 gg^{-1} xylose and 76.4% conversion after 120 h fermentation and it was $48.5 \pm 0.2 \text{ gL}^{-1}$ xylonic acid from 60 gL^{-1} xylose (using CGXII medium supplemented with xylose in sawdust APL) with a yield of 0.93 gg^{-1} xylose and 66 % conversion after 168 h fermentation. Effective downstream process developed for recovery, purification and crystallization of xylonic acid. Xylose dehydrogenase enzyme has been immobilized on ferromagnetic nanoparticle and used as the biocatalyst and it displayed efficient conversion efficiency (91%). The biocatalyst exhibited excellent storage stability and recyclability of 93% catalytic efficiency after 10 consecutive cycles of reaction.

Thus, an integrated bioprocess strategy comprising a fermentative production of xylonic acid using a recombinant *C. glutamicum* strain and an *invitro* enzymatic conversion of xylose to xylonic acid was put forward in this thesis. The developed framework will provide a blueprint not only for further evolution in xylonic acid bioprocessing but also in other bio-manufacturing processes.

List of Publications

a) Details of the publications emanating from the thesis work

1. **Sundar, M. S.**, Susmitha, A., Rajan, D., Hannibal, S., Sasikumar, K., Wendisch, V. F., & Nampoothiri, K. M. (2020). Heterologous expression of genes for bioconversion of xylose to xylonic acid in *Corynebacterium glutamicum* and optimization of the bioprocess. *AMB Express*, 10 (1), 1-11. <https://doi.org/10.1186/s13568-020-01003-9>
2. **Lekshmi Sundar M S**, K Madhavan Nampoothiri (2022). Xylose Dehydrogenase Immobilized on Ferromagnetic Nanoparticles for Bioconversion of Xylose to Xylonic Acid. *Bioconjugate Chemistry*, 33 (5), 948-955. DOI: 10.1021/acs.bioconjchem.2c00159
3. **Lekshmi Sundar M S**, Madhavan Nampoothiri K (2022). Sustainable production of xylonic acid from acid pre-treated sawdust liquor and subsequent downstream process (Manuscript under preparation).

b) Review article

1. **Lekshmi Sundar, M.S.**, & Madhavan Nampoothiri, K. (2022). An overview of the metabolically engineered strains and innovative processes used for the value addition of biomass derived xylose to xylitol and xylonic acid. *Bioresource Technology*, 345, 126548, 1-13. <https://doi.org/10.1016/j.biortech.2021.126548>

c) Details of the publications from other work

1. Susmitha A, Arya JS, **Sundar L**, Maiti KK, Nampoothiri KM. (2023). Sortase E-mediated site-specific immobilization of green fluorescent protein and xylose dehydrogenase on gold nanoparticles. *J Biotechnol.* Apr 10; 367:11-19. doi: 10.1016/j.jbiotec.2023.03.007. Epub 2023 Mar 25. PMID: 36972749.

2. **Sundar Lekshmi M S**, Susmitha A, Soumya M P, Keerthi Sasikumar, K Madhavan Nampoothiri (2019) Bioconversion of D-xylose to D-xylonic acid by *Pseudoduganella danionis*. Indian J Exp Biol 57 (11): 821–824.

d) Book chapter

1. Keerthi Sasikumar, **Lekshmi Sundar M S**, K Madhavan Nampoothiri (2022). Microbial Production of Sugar alcohols. Handbook of Bio-refinery Research and Technology. (Under review)

e) List of conference presentations

1. **Lekshmi Sundar M S**, Susmitha A, Soumya MP and K. Madhavan Nampoothiri, Bioconversion of pentose sugar to sugar acids by *Pseudoduganella danionis* (2018). Poster presented at the International Conference on Biotechnological research and innovation for sustainable development (BioSD-2018), November 22-25, CSIR -IICT, Hyderabad, India.
2. **Lekshmi Sundar M S** and K Madhavan Nampoothiri (2019), D- Xylonic acid production by genetically engineered *Corynebacterium glutamicum*. Poster presented at the International conference on New Horizons in Biotechnology (NHBT 2019), November 20-24, CSIR NIIST, Trivandrum, India.
3. **Lekshmi Sundar M S** and K. Madhavan Nampoothiri (2021), Biotransformation of xylose into xylonic acid using ferro-magnetic nanoparticles immobilized with xylose dehydrogenase. Poster presented at the International Conference on Biotechnology for Resource Efficiency, Energy, Environment, Chemicals and Health (BRE3CH-2021), December 1-4, CSIR - IIP, Dehradun, India.

Correction to “Xylose Dehydrogenase Immobilized on Ferromagnetic Nanoparticles for Bioconversion of Xylose to Xylonic Acid”

Lekshmi Sundar M. S. and K. Madhavan Nampoothiri*

Bioconjugate Chem. 2022, 33 (5), 948–955. DOI: 10.1021/acs.bioconjchem.2c00159



Cite This: *Bioconjugate Chem.* 2022, 33, 2428–2428



Read Online

ACCESS |

Metrics & More

Article Recommendations

“CSIR-HRDG Campus, Uttar Pradesh” must be removed in the affiliation for both the corresponding author and first author. This change is reflected in the affiliations of this Correction.

AUTHOR INFORMATION

Corresponding Author

K. Madhavan Nampoothiri – *Microbial Processes and Technology Division, CSIR–National Institute for Interdisciplinary Science and Technology (NIIST), Thiruvananthapuram 695019 Kerala, India; Academy of Scientific and Innovative Research (AcSIR), Ghaziabad 201002, India; orcid.org/0000-0003-4151-0974; Email: madhavan@niist.res.in*

Author

Lekshmi Sundar M. S. – *Microbial Processes and Technology Division, CSIR–National Institute for Interdisciplinary Science and Technology (NIIST), Thiruvananthapuram 695019 Kerala, India; Academy of Scientific and Innovative Research (AcSIR), Ghaziabad 201002, India*

Complete contact information is available at:

<https://pubs.acs.org/10.1021/acs.bioconjchem.2c00505>

Published: November 16, 2022



Xylose Dehydrogenase Immobilized on Ferromagnetic Nanoparticles for Bioconversion of Xylose to Xylonic Acid

Lekshmi Sundar M. S. and K. Madhavan Nampoothiri*



Cite This: <https://doi.org/10.1021/acs.bioconjchem.2c00159>



Read Online

ACCESS |



Metrics & More

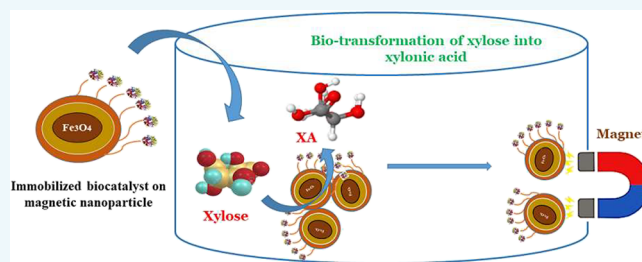


Article Recommendations



Supporting Information

ABSTRACT: D-Xylonic acid (XA), derived from pentose sugar xylose, is a multifunctional high-value chemical with a wide range of applications in the fields of medicines, food, agriculture and is a valuable chemical reagent for the synthesis of other useful commodity chemicals. In the bacterial system, xylose dehydrogenase (XDH) catalyzes the oxidation of D-xylose into D-xylonolactone, consuming NAD⁺ or NADP⁺ as a cofactor. The D-xylonolactone then undergoes auto-oxidation into D-xylonic acid. Herein, the XDH enzyme overexpressed in *Escherichia coli* is purified and immobilized on ferromagnetic nanoparticles, effectively converting xylose into xylonic acid. Parameters deciding the bioconversion were statistically optimized and obtained a maximum of 91% conversion rate. Kinetic parameters of immobilized xylose dehydrogenase showed a 2-fold increase in the maximum velocity of the reaction and catalytic efficiency compared to free enzyme. The operational stability test for the enzyme–nanoparticle conjugate retained 93% relative activity after 10 successive experiments, exhibiting the good recyclability of the biocatalyst for XA production.



INTRODUCTION

Xylonic acid (XA), which is derived mostly from xylose, is a new multipurpose platform chemical with extensive application in industrial sectors.¹ According to the US Department of Energy, xylonic acid is one of the top 30 chemicals with the most potential.² Xylonic acid application has enormous socio-economic benefits, and it has also helped safeguard the environment, thereby increasing the demand for its biosynthesis.³ It is required for the production of 1,2,4-butanetriol or energetic materials.^{4,5} In fiber fabrication, the characteristic properties like heat absorption, moisture absorption, and strong flexibility of xylonic acid were adopted for the production of fiber fabric with a cooling effect.⁶ For the Biginelli reaction, xylonic acid is used as both a catalyst and green solvent.⁷ The use of xylonic acid and its derivatives in building is now cost-effective, and it is predicted to eventually substitute gluconic acid in the construction sector as a cement water reducer.⁸

Xylose dehydrogenase belongs to the family of oxidoreductases and catalyzes the oxidation of D-xylose in the presence of NADP⁺. Although it may utilize both NADP⁺ and NAD⁺, the enzyme has a high preference for NADP⁺. This is one of the key enzymes in the oxidative Weimberg pathway and Dahms metabolic pathways where xylose is catabolized into xylonic acid.⁹ Different metabolic pathways involving the catalysis of xylose dehydrogenase along with other enzymes in microbial species were elucidated for xylonic acid production.¹⁰ Sundar et al. reported the metabolic engineering of *Corynebacterium glutamicum* 31831 for xylonic acid production

by overexpressing the xylose dehydrogenase gene of *Caulobacter crescentus*. In the CGXII synthetic medium, the modified strain produced 56.32 g/L xylonic acid from xylose and 42.94 g/L xylonic acid from rice straw hydrolysate-derived xylose.¹¹

Immobilization of enzymes on an appropriate matrix has improved their kinetics, stability, and reusability, allowing them to be used in a variety of industrial processes.¹² As immobilized enzymes are more stable than native enzymes at varied pH levels and temperatures, biocatalysts based on immobilized enzymes have gained a lot of interest in the past decade.^{13–15} It is observed that the support structure and topology can have a significant impact on the characteristics of enzymes.^{16,17} Interestingly, the use of nanoparticles as an immobilization scaffold has revolutionized their prospect in recent years. Nanoparticles have special characteristics like high biocatalytic and enzyme loading efficiency, improved mass transfer resistance, large surface-to-volume ratio, efficient storage, and high adsorption capacity.^{18–20} Nowadays, researchers are using magnetic nanoparticles to fix the catalysts. Magnetic nanoparticles outrank other varieties, including heat stability, pH

Received: March 31, 2022

Revised: April 16, 2022

tolerance, and ease of nanoparticle separation with a simple magnet. Furthermore, they have numerous applications in the biomedical field and in the food industry.²¹ In this study, an attempt was made to immobilize xylose dehydrogenase on ferromagnetic nanoparticles for xylose-to-xylic acid bioconversion. The immobilization mechanism, various parameters influencing immobilization, and the catalytic activity of the biocatalyst in bioconversion are discussed.

RESULTS

Xylose Dehydrogenase Expression and Analysis. For protein expression, the coding region of xylose dehydrogenase enzyme, i.e., *xylB*, from *C. crescentus* is cloned into the pET28a expression vector. The recombinant plasmid pET28a-*xylB* was confirmed by sequencing and restriction analysis. The *Escherichia coli* strain (BL21 DE3) carrying the recombinant vector was grown in liquid LB medium until an OD of 0.6–0.7 was reached, and then IPTG (0.5 mM) induction was done for 3 h for protein expression. The homogeneity of the purified protein was tested on 12% SDS-PAGE (Figure 1). The SDS-PAGE analysis revealed the size of the recombinant protein corresponding to the bands with a molecular weight of 32 kDa.

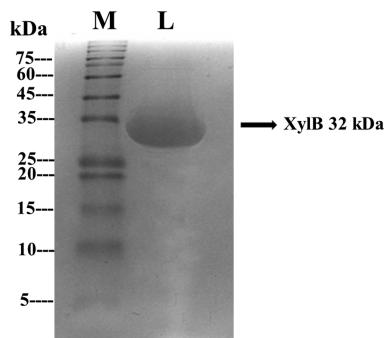


Figure 1. Expression of recombinant xylose dehydrogenase of *C. crescentus* ATCC 19089. Lane M, prestained protein ladder; Lane L, purified *xylB*.

Xylose Dehydrogenase Immobilization on Magnetic Nanoparticles. APTES, which imparts amine groups to the nanoparticles, was used to functionalize magnetic nanoparticles. These amine-functionalized nanoparticles exhibit a higher affinity for covalent interaction with the xylose dehydrogenase enzyme. The irreversible chemical bonding of the enzyme to nanoparticles is ensured by $-\text{NH}_2$ and $-\text{COOH}$ coupling.²⁸ To calculate the immobilization efficiency, the actual enzyme bound onto the nanoparticle was estimated to the total enzyme used and the unbound fraction of enzyme eliminated via washing. After reaction, 76% of the total enzyme remained immobilized on nanoparticles (Table 1). The enzyme nature, its conformation, and the type of nanoparticle have an impact on immobilization efficiency.

Validation of Statistical Tool: BBD and Optimization of Bioconversion Parameters. Operational reaction parameter optimization of the *in vitro* assay medium was carried out for maximum xylose bioconversion into xylic acid. In the BBD, a 15-run experimental matrix was designed for optimizing the four distinct parameters. The validation equation derived for the matrix is as follows:

Table 1. Optimization of Xylose Dehydrogenase Binding on Magnetic Nanoparticles

total enzyme added (IU)	enzyme bound on beads (IU)	immobilization efficiency (%)
10	7.2	72
20	14.7	73.4
30	22.8	76
40	30.1	75.3
50	37.3	74.6

xylic acid (mM)

$$\begin{aligned}
 &= -52.7 - 0.32X_1 + 4.1X_2 + 0.213X_3 + 3.067X_4 \\
 &\quad - 0.017X_1^2 - 0.2219X_2^2 - 0.0313X_3^2 - 0.01853X_4^2 \\
 &\quad - 0.064X_1X_2 + 0.0516X_1X_3 - 0.0128X_1X_4 \\
 &\quad + 0.436X_2X_3 + 0.0372X_2X_4 - 0.00212X_3X_4
 \end{aligned}$$

X_1 is xylose, X_2 is xylose dehydrogenase, X_3 is NAD^+ , and X_4 is pH.

A higher conversion yield of 250 mM xylic acid from 275 mM xylose was obtained from runs 7, 8, 10, 11, and 12. The least concentration of substrate, enzyme, cofactor, and optimum pH with maximum conversion was reflected in run no. 11, where the concentrations of parameters were as follows: xylose, 275 mM; xylose dehydrogenase, 13.5 μM ; NAD^+ , 1.25 mM; pH 7.5. It indicates that the optimum concentration of these parameters has a remarkable positive impact on xylic acid bioconversion. The contour plot displaying the relationship of two factors and the optimal concentration of the variables and its interaction for maximum bioconversion is shown in Figure 2A–F. The major interactions analyzed were of the concentration between XDH and xylose (A), pH and xylose (B), NAD^+ and xylose (C), pH and XDH (D), NAD^+ and XDH (E), and pH and NAD^+ (F). The model was evaluated using ANOVA (Table 2). The p -value of lack of fit, $p > 0.05$, implies that the proposed model fits the experimental data and the independent parameters have considerable effects on the response. The large F -value (5.54) indicates the statistical significance of the model. The higher R^2 value (95.55%) implies that the regression model fits the observed data well and also indicates that the model is a better fit.

The contour plots display the relationship between independent variables (xylose, xylose dehydrogenase, NAD^+ , and pH) and a dependent variable (xylic acid). Figure 2A shows that high xylic acid conversion, i.e., >300 mM, was attained with a combination of xylose dehydrogenase in the range of 10–24 μM and xylose with greater than 250 mM (to 400 mM) concentration. In Figure 2B, high xylic acid conversion was obtained from a combination of pH ranging between 7.5 and 9.5 and xylose with greater than 300 mM concentration. In the combination of NAD^+ and xylose in Figure 2C, high xylic acid conversion was reflected with a NAD^+ concentration of >1.25 and a xylose concentration of >300 mM. In Figure 2D, xylic acid conversion of >250 mM was obtained from a combination of pH range (7.5–9.5) and xylose dehydrogenase (10–20 μM). Similarly, in contour plots in Figure 2E,F, also, xylic acid conversion greater than 250 mM was obtained from the mixture of NAD^+ in the range of 1.25–2.00 mM, xylose dehydrogenase (10–18 μM), and pH in the range of 7.5–9.5. From the hold values in each contour

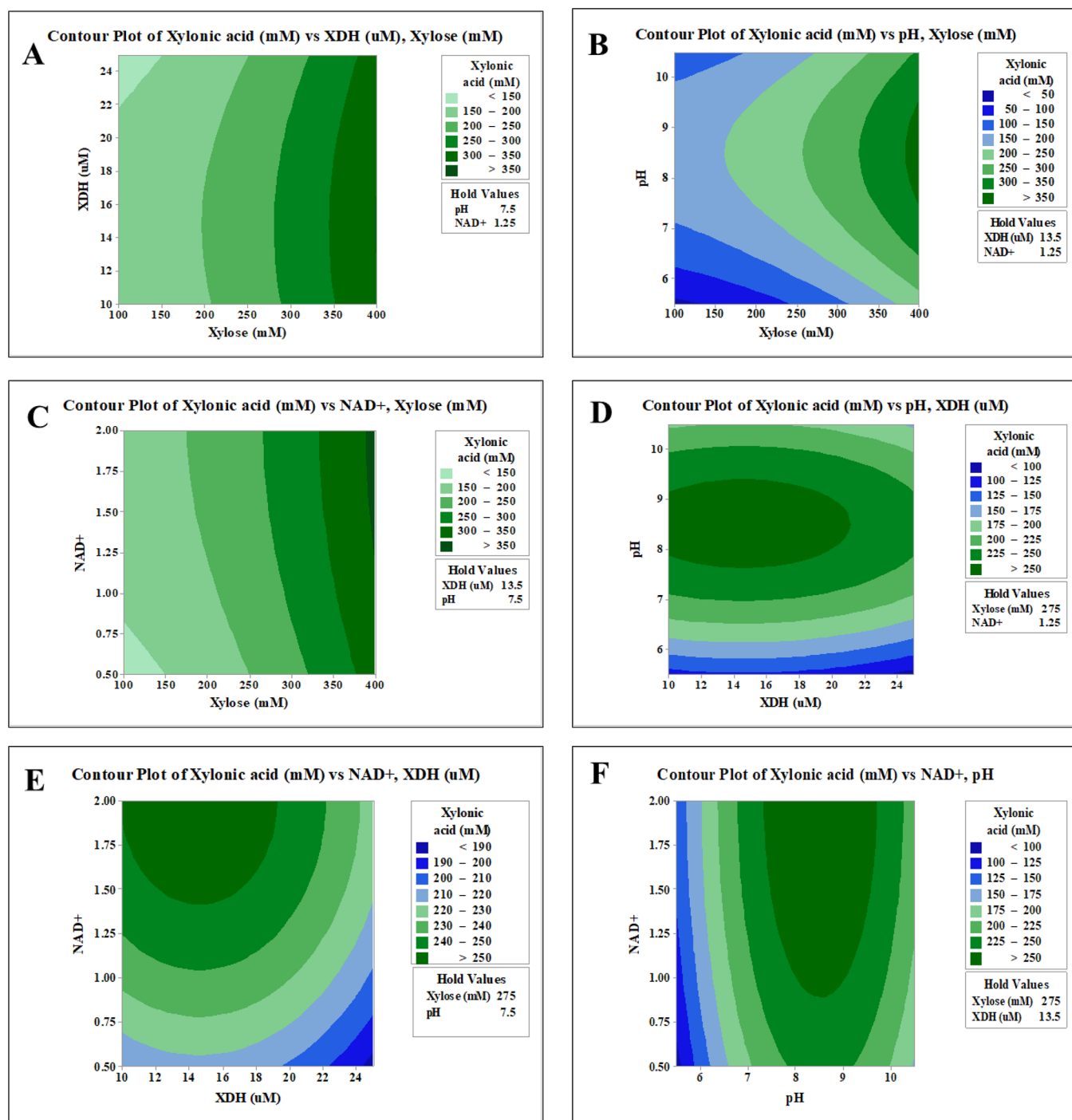


Figure 2. Contour plots showing the effect of various parameters on bioconversion of xylose into xylonic acid by immobilized xylose dehydrogenase. XDH and xylose concentrations (A), pH and xylose concentrations (B), NAD⁺ and xylose concentrations (C), pH and XDH concentrations (D), NAD⁺ and XDH concentrations (E), and pH and NAD⁺ concentrations (F).

plot, the optimum concentration of each parameter for maximum bioconversion obtained is as follows: pH 7.5; NAD⁺, 1.25 mM; xylose, 275 mM; xylose dehydrogenase, 13.5 μ M. Thus, with the RSM tool, the crucial parameters and the optimal concentration range were screened down for maximum output.

Enzyme Kinetic Study of Free and Immobilized Xylose Dehydrogenase. The rate of the bioconversion reaction catalyzed by xylose dehydrogenase was studied with different substrate concentrations, the kinetic constants were

validated using Lineweaver–Burk plots (Figure S1), and the V_{max} , K_m , and K_{cat} values are given in Table 3. Here, the maximum velocity of immobilized xylose dehydrogenase was found to increase 2-fold more than that of free xylose dehydrogenase. However, immobilization resulted in an increase in the K_m value, implying that the enzyme's affinity for its substrate has decreased. Perhaps, the disturbance in the stability of the enzyme and conformational and orientation changes occurred during immobilization, and steric hindrance and the enzyme's diffusional limit to the substrate contributed

Table 2. ANOVA for Xylonic Acid Production by Immobilized Xylose Dehydrogenase^a

source	DF	adj. SS	adj. MS	F	P
regression	8	97,739	12217.4	5.54	0.176
interaction	4	645	645.5	1.45	0.421
square	4	22,657	5664.3	5.84	0.143
linear	4	56,322	14080.5	8.22	0.105
residual error	6	4554	759.0		
lack of fit	5	4554	910.8		
pure error	1	0	0.0		
total	14	102,293			

^aS = 9.5449, R² = 95.55%, R² (pred.) = 0.00%, and R² (adj.) = 89.61%.

Table 3. Kinetic Constants of Free and Immobilized Xylose Dehydrogenase

kinetic constants	free xylose dehydrogenase	immobilized xylose dehydrogenase
V _{max} (μmol/min)	370.37	769.20
K _{cat} (min ⁻¹)	5.93 × 10 ⁷	12.31 × 10 ⁷
K _m (mM)	2068.22	3879.07

to the decrease in enzyme affinity to the substrate.²⁹ This is in line with the observation reported by Alam et al., where they immobilized asparaginase on magnetic nanoparticles to alleviate acrylamide formation in potato chips.³⁰ Here, the K_{cat} value of immobilized xylose dehydrogenase is 12.31 × 10⁷ min⁻¹, while that of free xylose dehydrogenase is 5.93 × 10⁷ min⁻¹. The turnover rate of the enzyme increased on immobilization.

Structural Characterization of Ferromagnetic Nanoparticles and Immobilized Xylose Dehydrogenase.

FTIR studies were performed on blank magnetic nanoparticles, with amino functionalization, i.e., after treatment with aminosilane APTES and glutaraldehyde as controls, and on enzyme-attached nanoparticles. The peak of Fe₃O₄ (Fe–O bonding) was found at 545 cm⁻¹, and the peak at 3398 cm⁻¹ refers to the stretching of OH bonds present on the surface of nanoparticles. The amide bond (i.e., C=O bonding) of the enzyme was observed at 1641 cm⁻¹, and amino function peaks were found at 2924 cm⁻¹ (N–H bonding) (Figure 3A). The final nanoparticle–enzyme bioconjugate was irradiated with continuous spectrum of infrared energy, and the vibration bands of single or functional groups of specific molecules present in iron particles, APTES, glutaraldehyde, and enzyme correlated with the stretchings obtained from functionalization and immobilization steps. All the specific peaks are clearly visible in the final bioconjugate, indicating the successful immobilization of the biocatalyst on magnetic nanoparticles (Figure 3B). The FTIR data obtained are comparable to those previously published in the literature.^{26,30}

Power X-ray diffraction was used to determine the crystalline structure and phase purity of the ferromagnetic nanoparticle. The diffraction peaks observed corresponded to the 2θ angles of (220), (311), (400), (422), (511), and (440), which represent the cell parameter change of the crystal structure of magnetite, confirming that the spatial arrangements of the atoms in the crystal phase are those of typical cubic iron oxide Fe₃O₄ (Figure S2). The XRD pattern, i.e., the position of diffraction peaks obtained, is in close proximity to the data discussed in the literature.³¹

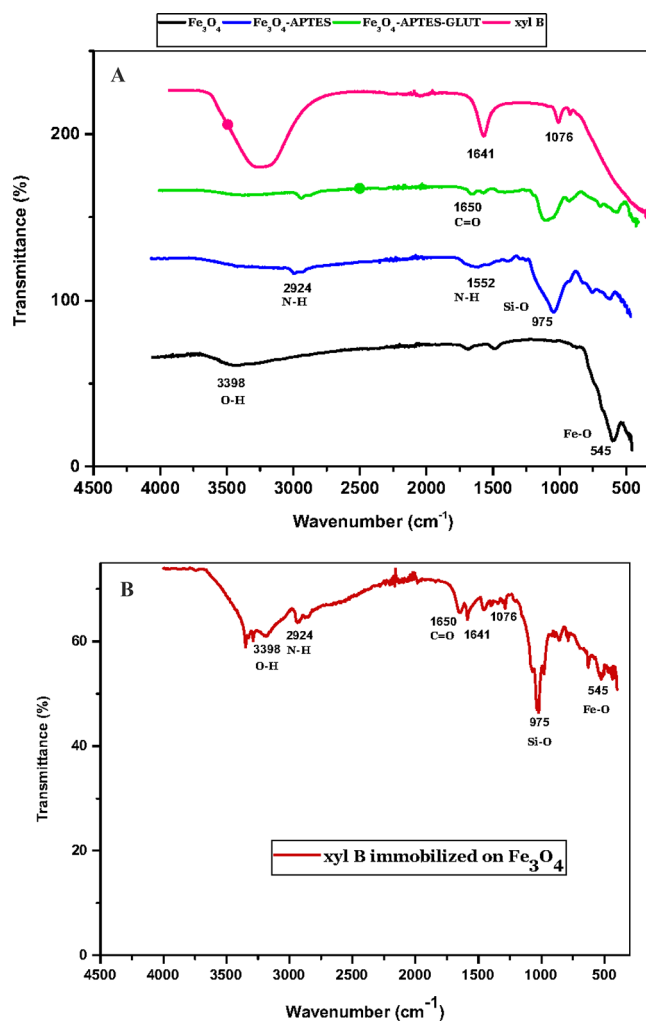


Figure 3. FTIR data of individual peaks of Fe₃O₄ iron particle, APTES–glutaraldehyde modification, and xylose dehydrogenase (xyl B) binding (A). Fe₃O₄ magnetic nanoparticle with immobilized xylose dehydrogenase (B).

Bioconversion of Xylose into Xylonic Acid by Immobilized Xylose Dehydrogenase under Optimized Parameters. Bioconversion study was carried out under the optimized parameters, such as xylose (275 mM), xylose dehydrogenase (13.5 μM), NAD⁺ (1.25 mM) and pH 7.5, derived from statistical analysis for a period of 72 h. Under this condition, a maximum of 250 mM xylonic acid was formed from 275 mM xylose with a conversion efficiency of 91% (see Figure 4). Quantification of xylonic acid was done by HPLC. An HPLC chromatogram of xylonic acid bioconversion in the presence of the immobilized biocatalyst is shown in Figure S3.

Reusability of Xylose Dehydrogenase Immobilized on Magnetic Nanoparticles. Reusability of the biocatalyst is one of the superlative advantages of enzymatic reactions based on magnetic nanoparticles. Repeated use of the immobilized biocatalyst was evaluated by incubating the same fraction of the biocatalyst for multiple reaction cycles. It was observed that 93% of the activity is retained by the enzyme after 10 successive cycles (see Figure 5). Reusability of L-asparaginase is discussed in the literature,³² and the enzyme retained 95.7% of its activity after recycle, which is comparable to the results obtained in this study.

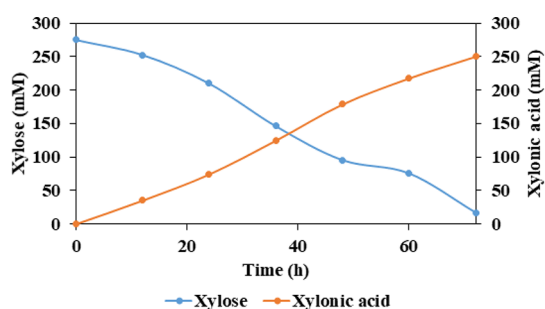


Figure 4. Bioconversion of xylose into xylonic acid by immobilized xylose dehydrogenase.

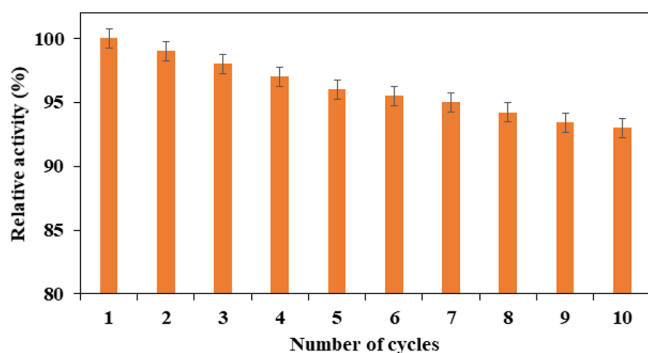


Figure 5. Operational stability of immobilized xylose dehydrogenase.

DISCUSSION

Xylose dehydrogenase has been immobilized onto diverse scaffolds for xylose conversion into xylonic acid. Bachosz et al. co-immobilized xylose dehydrogenase and alcohol dehydrogenase onto silica core–shell for xylose conversion to xylonic acid and cofactor regeneration.³³ Similarly, glucose dehydrogenase and xylose dehydrogenase were immobilized onto mesoporous amorphous silica for coproduction of gluconic acid and xylonic acid.³⁴ Zdarta et al. demonstrated enzymatic production of xylonic acid and gluconic acid from biomass-derived xylose and glucose via immobilization of xylose dehydrogenase and glucose dehydrogenase onto porous silica nanoparticles.³⁵ Here, in this study, ferromagnetic (iron)

nanoparticles were used for xylose dehydrogenase immobilization and the immobilized enzyme retained 93% catalytic efficiency after 10 consecutive cycles of reaction, leading to the productivity of 250 mM xylonic acid. In the case of silica, up to five consecutive cycles are reported and, thus, it looks like ferromagnetic conjugation is more stable. Thus, the enzyme–iron nanoparticle bioconjugate could be a promising long-drawn strategy for continuous bioconversion of xylose into xylonic acid. Additionally, the chemical stability, storage stability, robustness, and reusability of iron nanoparticles for continual reaction aided the improved productivity of xylonic acid.

CONCLUSIONS

Enzyme immobilization onto or within a support matrix physically or chemically enhances the enzyme's activity, stability, and reusability in aqueous and non-aqueous media. A stable heterogeneous immobilized enzyme system can overcome the drawbacks of conventional biological whole-cell reactions and heterogeneous chemical catalysts. Because of their compact size, extremely large surface area, high immobilization efficiency, and excellent reusability, magnetic nanoparticles are ideal for the immobilization of enzymes for different applications. The production of xylonic acid can benefit from immobilized enzymatic cofactor-dependent monosaccharide conversion. Resistance toward environmental changes and higher stability of the immobilized enzymes than free enzymes are added advantages. The interesting fact is that the heterogeneity of immobilized enzyme systems enables repeated enzymatic reactions with facile product recovery and quick reaction termination. They offer a commercial advantage over tedious downstream processing, leading to the possibility of pure product isolation. Compared to the chemical route, via chemical oxidation using platinum and gold catalysts, the immobilized enzyme system is considered an environmentally friendly and economical approach for xylonic acid biosynthesis. The immobilization of the key catalytic enzymes could be a promising and cost-effective platform for the production of various commodity chemicals such as xylonic acid.

Table 4. Bacterial Strains, Vectors, and Oligonucleotides Used in the Study²³

Strains / vectors	Specifications	Reference
Bacterial strains		
<i>Caulobacter crescentus</i>	ATCC19089, wild type	<i>Caulobacter vibrioides</i> Henrici and Johnson (ATCC 19089)
<i>Escherichia coli</i> DH5 α	Maximizes transformation efficiency, with three mutations, recA1, endA1 and lac Δ M15 ²³	
Plasmid vectors		
pET 28a	Bacterial expression vector	Harvard Medical School
Primers(sequences 5'–3')		
Xyl B pET F'	GATGATGGATCCATGTCTCAGCCATCTATCC BamHI	This study
Xyl B pET R'	TATTATGAATTC AACGCCAGCCGGCGTCGAT CCAG EcoRI	This study

MATERIALS AND METHODS

Chemicals. Iron oxide (Fe_3O_4) was procured from Merck (cat. 637,106, Sigma), Germany. 3-Aminopropyltriethoxysilane (APTES) (99%), glutaraldehyde, and the Luria Bertani culture medium were purchased from Himedia (Mumbai, India).

Molecular Methodology and Plasmid Construction. Xylose dehydrogenase (*xylB*) gene was amplified from the xylose operon of *C. crescentus* by polymerase chain reaction with specific primers designed. The purified amplicons (747 bp *xylB*) were confirmed by DNA sequencing and subcloned into the restriction site (*Eco* RI/*Bam* HI) of the expression vector pET 28a. The recombinant plasmid pET 28a-*xylB* was transformed into competent *E. coli* DH5 α and screened on LB plates containing 25 $\mu\text{g mL}^{-1}$ kanamycin.²² The bacterial strains, vectors, and oligonucleotides used in the study are given in Table 4.

Expression and Purification of Xylose Dehydrogenase. A single colony of recombinant *E. coli* (BL21-pET28a-*xylB*) was inoculated and incubated overnight at 37 °C. One milliliter of pre-inoculum ($\text{OD}_{600\text{ nm}} = 0.8$) was added to 100 mL of LB broth. The culture was incubated at 37 °C until an OD of 0.4–0.6 was reached, IPTG (1 mM) induction was done, and the culture was again incubated at 37 °C for 3 h. The cells were harvested by centrifugation, frozen, thawed, and resuspended in 0.5 M phosphate buffer. The cell resuspension was sonicated (time: 6 min; pulse: 10 s on and 10 s off; amplitude: 40%) and centrifuged on an orbital shaker for 30 min at 13,000g. The cell-free supernatant was filtered (0.2 mm filter) and allowed to pass through a His-Trap HP column, and an imidazole gradient in buffer (50 mM Na_3PO_4 buffer (pH 7.2) and 300 mM NaCl) was used to elute the recombinant protein bound to the column. The purified protein was collected and stored at -80 °C.

Determination of Xylose Dehydrogenase Activity and Quantification of Xylonic Acid. In the enzymatic bioconversion assay, the reaction volume of 1.0 mL contained 13.5 μM xylose dehydrogenase, 50 mM Na_3PO_4 buffer (pH 7.2), 275 mM xylose, and 1.25 mM NAD^+ . Under the above reaction conditions, 0.14 U ($\mu\text{M}/\text{min}$) of enzyme catalyzed the conversion of 1 μM substrate (xylose) per minute into xylonic acid. The Bradford assay method was used to determine the protein content.²⁴ After 72 h of reaction at 30 °C, the activity of xylose dehydrogenase was determined by quantification of xylonic acid formation by HPLC. An organic acid column, Phenomenex, with a dimension of 250 mm \times 4.6 mm \times 5 μm was used for xylonic acid quantification. It was operated with a flow rate of 0.6 mL/min, where 0.01 N H_2SO_4 served as the mobile phase.

Surface Activation of Nanoparticles and Immobilization of Xylose Dehydrogenase (*xylB*). To get a homogeneous suspension, magnetite nanoparticles (1 g) were dispersed in a 1:1 combination of ethanol and water, and the obtained suspension was sonicated for 40 min with 15 s on and 15 s off pulse. This mixture was then treated with APTES (3.4 mL), resulting in a 1:4 molar ratio of magnetite to APTES. The reaction was carried out at 40 °C for 2 h in a nitrogen environment with continuous stirring. The magnetite particles (100 mg) modified with APTES were mixed with 10 mL of 8% glutaraldehyde solution, and the mixture was incubated overnight at 30 °C with continuous stirring. The functionalization and modification of magnetic nanoparticles were performed following the modified methodologies in the

literature.^{25,26} Xylose dehydrogenase was allowed to react with modified nanoparticles for 3 h at 4 °C. The enzyme that was bound to the nanoparticles in the reaction medium was separated using a magnet. The enzyme loading was varied (10–50 μM), and the immobilization efficiency and enzyme activity were calculated. The mechanism of biocatalyst immobilization is depicted in Figure 6.

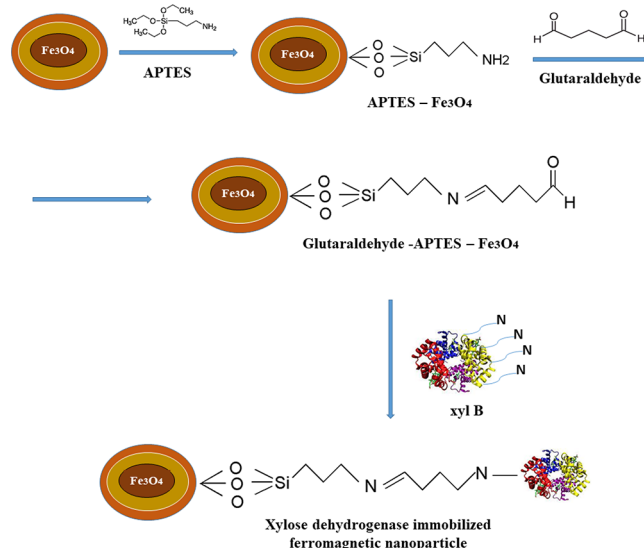


Figure 6. Functionalization of ferromagnetic nanoparticles with APTES and glutaraldehyde for xylose dehydrogenase immobilization.

Operational Parameter Optimization by the Statistical Tool Response Surface Methodology (RSM). The RSM tool was used to find the parameters that have a significant impact on the bioconversion of xylose into xylonic acid. An independent quadratic design, i.e., the Box–Behnken experimental design (BBD)²⁷ with four independent variables that affect xylonic acid bioconversion, such as substrate, xylose (100–400 mM), enzyme, xylose dehydrogenase (10–25 μM), cofactor, NAD^+ (0.5–2.00 mM), and pH (5.5–10.5), was studied. The conversion yield (mM) of xylonic acid was used to measure the response. Using the Minitab 17 software, the statistics and ANOVA of the model were evaluated. The level of variance in the group, i.e., the parameter chosen, was calculated using the *p*-value, *F*-value, effect value, and regression coefficient. The BBD and response (xylonic acid) are given in Table 5.

Enzyme Kinetics of Xylose Dehydrogenase. For both free and immobilized xylose dehydrogenase (13.5 μM each), enzyme kinetic parameters like K_m , V_{max} , and catalytic efficiency were calculated with various concentrations (50–500 mM) of the substrate. The Lineweaver–Burk plot was used to study the kinetic parameters.

FTIR and XRD for Confirmation of Enzyme Immobilization. Fourier transform infrared (IRTracer-100, Shimadzu, Japan) spectroscopy was performed to characterize the ferromagnetic nanoparticles as such and to analyze the chemical modifications made with APTES and glutaraldehyde, thereby confirming the progressive functionalization of free magnetic nanoparticles for enzyme immobilization. FTIR data confirmed the presence of amide bonds in the xylose dehydrogenase enzyme and that of the enzyme immobilized on the surface of functionalized nanoparticles. Each sample's

Table 5. Box–Behnken Design Matrix with Response (Xyloic Acid Bioconversion) by Immobilized Xylose Dehydrogenase

run order	xylose (mM)	xylose dehydrogenase (μM)	NAD ⁺ (mM)	pH	xyloic acid (mM)
1	400	13.5	0.50	10.5	300
2	275	13.5	1.25	5.5	100
3	275	25	2.00	5.5	100
4	275	25	2.00	10.5	200
5	100	10	0.50	10.5	50
6	275	10	0.50	7.5	200
7	275	15	1.25	7.5	250
8	275	15	2.00	7.5	250
9	400	25	0.50	5.5	150
10	275	15	1.25	7.5	250
11	275	13.5	1.25	7.5	250
12	275	13.5	2.00	7.5	250
13	100	10	0.50	5.5	40
14	275	15	1.25	10.5	200
15	400	10	2.00	10.5	300

transmittance (percent) was measured in the 400–4000 cm^{-1} wavenumber range.

The crystal structure and phase analysis of ferromagnetic nanoparticles were determined using X-ray diffraction (XRD) patterns obtained from a Philips PANalytical X'pert Pro diffractometer with Ni-filtered Cu K radiation (= 1.54060) taken in the angular range of 10–70° with a step size of 0.0170°, with the tube voltage and electric current held at 45 kV and 30 mA, respectively.

Reusability of Immobilized Xylose Dehydrogenase for Xyloic Acid Bioconversion. To assess the reusability of the immobilized biocatalyst, the magnetic nanoparticles carrying xylose dehydrogenase were added to the reaction mixture and the xyloic acid bioconversion was quantified after 72 h of reaction. To separate the supernatant from the solid fraction, a simple magnet was used to collect and then recover the nanoparticles on the surface of the reaction vial. The nanoparticles were then washed twice with assay buffer (50 mM phosphate, pH 7.2) to remove any reaction mixture or products. The enzyme bioconversion assay was carried out for 10 successive cycles to check the efficacy of the biocatalyst in recycling. The activity of immobilized xylose dehydrogenase in the first cycle was taken as 100%.

■ ASSOCIATED CONTENT

SI Supporting Information

The Supporting Information is available free of charge at <https://pubs.acs.org/doi/10.1021/acs.bioconjchem.2c00159>.

Figure S1: Lineweaver–Burk plots of free and immobilized xylose dehydrogenase; Figure S2: X-ray diffraction (XRD) pattern of magnetic nanoparticles (Fe_3O_4); Figure S3: HPLC chromatogram of xyloic acid (PDF)

■ AUTHOR INFORMATION

Corresponding Author

K. Madhavan Nampoothiri – *Microbial Processes and Technology Division, CSIR–National Institute for Interdisciplinary Science and Technology (NIIST), Thiruvananthapuram 695019 Kerala, India; Academy of*

Scientific and Innovative Research (AcSIR), CSIR–HRDG Campus, Ghaziabad, Uttar Pradesh 201002, India;
orcid.org/0000-0003-4151-0974; Email: madhavan@niist.res.in

Author

Lekshmi Sundar M. S. – *Microbial Processes and Technology Division, CSIR–National Institute for Interdisciplinary Science and Technology (NIIST), Thiruvananthapuram 695019 Kerala, India; Academy of Scientific and Innovative Research (AcSIR), Ghaziabad, 201002, India.*

Complete contact information is available at:

<https://pubs.acs.org/10.1021/acs.bioconjchem.2c00159>

Author Contributions

The first author L.S.M.S. performed the experimental part and prepared the draft of the manuscript, and the communicating author conceived the work and created the project. He did the critical reading and final editing of the manuscript.

Notes

The authors declare no competing financial interest.

■ ACKNOWLEDGMENTS

L.S.M.S. acknowledges Devi Rajan for her suggestions and help during the work and for the JRF and SRF Fellowships by CSIR, New Delhi. K.M.N. acknowledges the DBT BMBF (Indo German) grant. The authors thank Prof. Volker F. Wendisch, University of Bielefeld, Germany, for providing the *C. crescentus* operon for amplifying *xyl B* gene during the period in his lab.

■ REFERENCES

- Zhou, X.; Zhou, X.; Tang, X.; Xu, Y. Process for calcium xylonate production as a concrete admixture derived from in-situ fermentation of wheat straw pre-hydrolysate. *Bioresour. Technol.* **2018**, *261*, 288–293.
- Werpy, T. A.; Holladay, J. E.; White, J. F. *Top Value Added Chemicals From Biomass: I. Results of Screening for Potential Candidates from Sugars and Synthesis Gas*. U.S. Department of Energy Office of Scientific and Technical Information 2004, *1*, 76.
- Jin, D.; Ma, J.; Li, Y.; Jiao, G.; Liu, K.; Sun, S.; Zhou, J.; Sun, R. Development of the synthesis and applications of xyloic acid: A mini-review. *Fuel* **2022**, 122773.
- Wei, N.; Mapitso, M. N.; Frost, J. W. Microbial Synthesis of the Energetic Material Precursor 1,2,4-Butanetriol. *J. Am. Chem. Soc.* **2003**, *125*, 12998–12999.
- Yukawa, T.; Bamba, T.; Guirimand, G.; Matsuda, M.; Hasunuma, T.; Kondo, A. Optimization of 1,2,4-butanetriol production from xylose in *Saccharomyces cerevisiae* by metabolic engineering of NADH/NADPH balance. *Biotechnol. Bioeng.* **2021**, *118*, 175–185.
- Qingping, L.; Chunwei, L.; Shengzhong, Z.; Shengcheng, Z.; Jianmin, D.; Hongqin, W. S. 2011 Xyloic acid viscose fiber and Egyptian cotton interwoven big jacquard fabric. CN202144537U.
- Ma, J.; Zhong, L.; Peng, X.; Sun, R. D-Xyloic acid: A solvent and an effective biocatalyst for a three-component reaction. *Green Chem.* **2016**, *18*, 1738–1750.
- Byong-Wa, C.; Benita, D.; Macuch, P. J.; Debbie, W.; Charlotte, P.; Ara, J. The Development of Cement and Concrete Additive. *Appl. Biochem. Biotechnol.* **2006**, *131*, 645–658.
- Brü ssel, C.; Späth, A.; Sokolowsky, S.; Marienhagen, J. Alone at last! – Heterologous expression of a single gene is sufficient for establishing the five-step Weimberg pathway in *Corynebacterium glutamicum*. *Metab. Eng. Commun.* **2019**, *9*, No. e00090.

- (10) Yim, S. S.; Choi, J. W.; Lee, S. H.; Jeon, E. J.; Chung, W.-J.; Jeong, K. J. Engineering of *Corynebacterium glutamicum* for Consolidated Conversion of Hemicellulosic Biomass into Xylonic Acid. *Biotechnol. J.* **2017**, *12*, 1700040.
- (11) Sundar, M. S. L.; Susmitha, A.; Rajan, D.; Hannibal, S.; Sasikumar, K.; Wendisch, V. F.; Nampoothiri, K. M. Heterologous expression of genes for bioconversion of xylose to xylonic acid in *Corynebacterium glutamicum* and optimization of the bioprocess. *AMB Express* **2020**, *10*, 68.
- (12) Liang, S.; Wu, X. L.; Xiong, J.; Zong, M. H.; Lou, W. Y. Metal-organic frameworks as novel matrices for efficient enzyme immobilization: An update review. *Coord. Chem. Rev.* **2020**, *406*, 213149.
- (13) Bilal, M.; Asgher, M.; Cheng, H.; Yan, Y.; Iqbal, H. M. N. Multi-point enzyme immobilization, surface chemistry, and novel platforms: a paradigm shift in biocatalyst design. *Crit. Rev. Biotechnol.* **2018**, *39*, 202–219.
- (14) Drout, R. J.; Robison, L.; Farha, O. K. Catalytic applications of enzymes encapsulated in metal–organic frameworks. *Coord. Chem. Rev.* **2019**, *381*, 151–160.
- (15) Smuleac, V.; Varma, R.; Baruwati, B.; Sikdar, S.; Bhattacharyya, D. Nanostructured Membranes for Enzyme Catalysis and Green Synthesis of Nanoparticles. *ChemSusChem* **2011**, *4*, 1773–1777.
- (16) Tully, J.; Yendluri, R.; Lvov, Y. Halloysite Clay Nanotubes for Enzyme Immobilization. *Biomacromolecules* **2016**, *17*, 615–621.
- (17) Barbosa, O.; Ortiz, C.; Berenguer-Murcia, A.; Torres, R.; Rodrigues, R. C.; Fernandez-Lafuente, R. Glutaraldehyde in biocatalysts design: a useful crosslinker and a versatile tool in enzyme immobilization. *RSC Adv.* **2014**, *4*, 1583–1600.
- (18) Ahmad, R.; Sardar, M. Enzyme Immobilization: An Overview on Nanoparticles as Immobilization Matrix. *Biochem. Anal. Biochem.* **2015**, *1*.
- (19) Khoo, K. S.; Chia, W. Y.; Tang, D. Y. Y.; Show, P. L.; Chew, K. W.; Chen, W.-H. Nanomaterials Utilization in Biomass for Biofuel and Bioenergy Production. *Energies* **2020**, *13*, 892.
- (20) Zhang, H.; Hay, A. G. Magnetic biochar derived from biosolids via hydrothermal carbonization: Enzyme immobilization, immobilized-enzyme kinetics, environmental toxicity. *J. Hazard. Mater.* **2020**, *384*, 121272.
- (21) Husain, Q. Magnetic nanoparticles as a tool for the immobilization/stabilization of hydrolases and their applications: An overview. *Biointerface Res. Appl. Chem.* **2016**, *6*, 1585–1606.
- (22) Stephens, C.; Christen, B.; Fuchs, T.; Sundaram, V.; Watanabe, K.; Jenal, U.; Camino Real, E.; Clara, S. Genetic Analysis of a Novel Pathway for D-Xylose Metabolism in *Caulobacter crescentus*. *J. Bacteriol.* **2007**, *189*, 2181–2185.
- (23) Hanahan, D.; Harbor, C. S. Studies on transformation of *Escherichia coli* with plasmids. *J. Mol. Biol.* **1983**, *166*, 557–580.
- (24) Fanger, B. O. Adaptation of the Bradford protein assay to membrane-bound proteins by solubilizing in glucopyranoside detergents. *Anal. Biochem.* **1987**, *162*, 11–17.
- (25) Can, K.; Ozmen, M.; Ersoz, M. Immobilization of albumin on aminosilane modified superparamagnetic magnetite nanoparticles and its characterization. *Colloids Surf., B* **2009**, *71*, 154–159.
- (26) Costa, V. M.; De Souza, M. C. M.; Fechine, P. B. A.; Macedo, A. C.; Gonçalves, L. R. B. Nanobiocatalytic systems based on lipase-Fe₃O₄ and conventional systems for isoniazid synthesis: A comparative study. *Braz. J. Chem. Eng.* **2016**, *33*, 661–673.
- (27) Sarabia, L. A.; Ortiz, M. C. Response Surface Methodology. *Compr. Chemom.* **2009**, *1*, 345–390.
- (28) Huang, Y. F.; Wang, Y. F.; Yan, X. P. Amine-functionalized magnetic nanoparticles for rapid capture and removal of bacterial pathogens. *Environ. Sci. Technol.* **2010**, *44*, 7908–7913.
- (29) Cristovao, R. O.; Almeida, M. R.; Barros, M. A.; Nunes, J. C. F.; Boaventura, R. A. R.; Loureiro, J. M.; Faria, J. L.; Neves, M. C.; Freire, M. G.; Ebinuma-Santos, V. C.; Tavares, A. P. M.; Silva, C. G. Development and characterization of a novel l-asparaginase/MWCNT nanobiocatalytic. *RSC Adv.* **2020**, *10*, 31205–31213.
- (30) Alam, S.; Ahmad, R.; Pranaw, K.; Mishra, P.; Khare, S. K. Asparaginase conjugated magnetic nanoparticles used for reducing acrylamide formation in food model system. *Bioresour. Technol.* **2018**, *269*, 121–126.
- (31) Wang, S.; Su, P.; Huang, J.; Wu, J.; Yang, Y. Magnetic nanoparticles coated with immobilized alkaline phosphatase for enzymolysis and enzyme inhibition assays. *J. Mater. Chem. B* **2013**, *1*, 1749–1754.
- (32) Mu, X.; Qiao, J.; Qi, L.; Dong, P.; Ma, H. Poly(2-vinyl-4,4-dimethylazlactone)-functionalized magnetic nanoparticles as carriers for enzyme immobilization and its application. *ACS Appl. Mater. Interfaces* **2014**, *6*, 21346–21354.
- (33) Bachosz, K.; Synoradzki, K.; Staszak, M.; Pinelo, M.; Meyer, A. S. Bioorganic Chemistry Bioconversion of xylose to xylonic acid via co-immobilized dehydrogenases for conjunct cofactor regeneration. *Bioorg. Chem.* **2019**, *93*, 102747.
- (34) Zdarta, J.; Bachosz, K.; Deg, O.; Zdarta, A.; Kaczorek, E. Co-Immobilization of Glucose Dehydrogenase and Xylose Dehydrogenase as a New Approach for Simultaneous Production of Gluconic and xylonic acid. *Materials* **2019**, *12*, 3167.
- (35) Zdarta, J.; Pinelo, M.; Jesionowski, T.; Meyer, A. S. Upgrading of biomass monosaccharides by immobilized glucose dehydrogenase and xylose dehydrogenase. *ChemCatChem* **2018**, *5*, 164.



Review

An overview of the metabolically engineered strains and innovative processes used for the value addition of biomass derived xylose to xylitol and xylonic acid

M.S Lekshmi Sundar^{a,b}, K. Madhavan Nampoothiri^{a,*}

^a Microbial Processes and Technology Division, CSIR – National Institute for Interdisciplinary Science and Technology (NIIST), Thiruvananthapuram 695019, Kerala, India

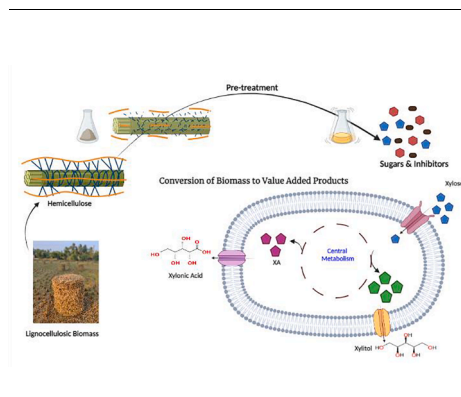
^b Academy of Scientific and Innovative Research (AcSIR), Ghaziabad, 201002, India



HIGHLIGHTS

- There is a need for progressive and innovative strategies for the biomass value addition.
- Xylose has to be utilized rationally for the commercial viability of biorefineries.
- Xylitol and xylonate are highly demanded commodity chemicals in food and pharma industries.
- There are natural and metabolically engineered strains utilizing xylose.

GRAPHICAL ABSTRACT



ARTICLE INFO

Keywords:

Agro-residual biomass
 Pentose
 Xylose
 Xylitol
 Xylonic acid

ABSTRACT

Xylose, the most abundant pentose sugar of the hemicellulosic fraction of lignocellulosic biomass, has to be utilized rationally for the commercial viability of biorefineries. An effective pre-treatment strategy for the release of xylose from the biomass and an appropriate microbe of the status of an Industrial strain for the utilization of this pentose sugar are key challenges which need special attention for the economic success of the biomass value addition to chemicals. Xylitol and xylonic acid, the alcohol and acid derivatives of xylose are highly demanded commodity chemicals globally with plenty of applications in the food and pharma industries. This review emphasis on the natural and metabolically engineered strains utilizing xylose and the progressive and innovative fermentation strategies for the production and subsequent recovery of the above said chemicals from pre-treated biomass medium.

1. Introduction

Biomass holds an inexhaustible, far, wide and low-cost wellspring of

sugars that can be used as renewable carbon source for the manufacture of synthetic compounds. Different horticultural build-ups contain around 20–30% hemicellulose (Iqbal et al., 2011). The second most

* Corresponding author.

E-mail address: madhavan@niist.res.in (K. Madhavan Nampoothiri).

<https://doi.org/10.1016/j.biortech.2021.126548>

Received 27 October 2021; Received in revised form 6 December 2021; Accepted 7 December 2021

Available online 11 December 2021

0960-8524/© 2021 Elsevier Ltd. All rights reserved.

prevalent sugar in these hydrolysates is D-xylose (30–40 %), an important bio-resource for diverse chemicals and added value products (Dhiman et al., 2012; Lachke, 2002; Moysés et al., 2016). Thus, plant biomass has the potential to be utilised as renewable source for a variety of fuels and chemicals. The conversion of xylose to ethanol has been the focus of much of these investigations (Mohd Azhar et al., 2017). However, several recent studies have demonstrated that bacteria can convert this pentose sugar to other valuable chemicals. (Kwak et al., 2017) Both indigenous or engineered microorganisms were reported in literature capable of producing variety of chemicals from biomass derived sugars (Isikgor and Remzi Becer, 2015).

Xylose derived sugar alcohol and sugar acid i.e., xylitol and xylonic acid have gained much attention in the last decade and are still a thriving area of research (Kumar et al., 2018). Researchers contribute dedicated piece of works related to different pre-treatment strategies, strain improvement, advanced fermentation strategies to enhance the titre of these chemicals (Ghaffar et al., 2017; Sapci et al., 2016; Takata et al., 2014). The gradual switching from C6 sugars to least utilized C5 sugars of biomass is an important twist in the rapid growth of the alternate carbon source utilization in white biotechnology.

2. Biomass as a raw material for value-added chemicals

As an alternative resource, biomass, a renewable, carbon-neutral, abundant, and locally accessible raw material become a natural choice. Lignocellulose being a complex carbohydrate polymer composed of cellulose, hemicellulose and an aromatic polymer lignin as well as the rich source of C6 sugars and C5 sugars (Ruiz et al., 2013). Better exploitation of these sugars can support a diverse application in different industrial sectors like pharmaceuticals, food, cosmetics and agriculture. Sugars are primarily used as the source of energy and the xylose is used for the production of bioethanol, biobutanol, biopolymer, bio-hydrogen, 1, 3-butanediol, 2, 3-propanediol, organic acids, furfural, xylitol, single-cell protein, amino acids and furans (furfural and 5-hydroxymethylfurfural: precursors for polyester, nylon, fuel, plastic, resin, fine chemicals) (de Sá et al., 2020; Kim et al., 2017; Kudahettige-Nilsson et al., 2015; Wu et al., 2018).

Saccharification is the prime and most important step in the processing of agricultural biomass. Chemical and enzymatic hydrolysis is the most prevalent saccharification techniques for the release and hydrolysis of polysaccharides in lignocellulosics. Chemical hydrolysis is of two types acid and alkali pre-treatment, where dilute acid treatment with hydrochloric acid, acetic acid and sulfuric acid is done for the maximal release of pentose sugars (Phwan et al., 2019). Combining microwave with a physical or chemical pre-treatment method increased decreasing fermentable sugar yields prior to the hydrolysis process by removing lignin or modifying the refractory biomass components. Another advantage of microwave pre-treatment is that the levels of inhibitor generated during the pre-treatment process chemicals were found to be insufficient to impede the fermentation process (Ethaib et al., 2014). Cellulose and lignin are likewise affected by steam explosion conditions. Cellulose molecules were disassembled and degraded to furfural at high pressures (5-hydroxymethylfurfural). Lignin undergoes condensation and cleavage processes that result in the formation of acid insoluble lignin molecules. Donohoe et al., 2008 proposes that lignin is melting, flowing, and condensing as beads on the surface of the cellulose microfibrils and thus increasing porosity. Because of the removal of moisture and volatiles, as well as the thermal destruction of hemicelluloses, steam explosion treatment increases the calorific value of biomass. The carbon content of the biomass rises, while oxygen and hydrogen are eliminated. Because of the presence of hydroxyl (OH) groups in hemicellulose and cellulose, biomass has a high hygroscopicity. As the quantity of accessible hydroxyl groups reduced indicating the severity and effectiveness of the steam explosion process. Hemicellulose removal alters the mechanical characteristics of the biomass (Stelte, 2013).

Considering the cost analysis and operational conditions, dilute acid pre-treatment appears to be a more advantageous method for xylose recovery from biomass. Shen and Wyman (2011) introduced a kinetic model explaining enhanced xylose yield from dilute sulfuric acid where total xylose yield increased significantly to 93.1% for pre-treatment with sulfuric acid (0.5 %) at 160 °C for 40 min compared to hydrothermal pre-treatment with maximum total xylose yield was only 71.5% after 30 min at 180 °C.

The update of D-xylose, the most bountiful pentose, to value-added biochemicals is monetarily imperative to cutting edge biorefineries and here we review the reports on the production of two most wanted commodity chemicals derived from biomass xylose.

3. Xylose assimilation network

The metabolic routes of xylose have not received significant attention than those of other fermentable sugars, particularly glucose. Very few natural strains from archaea domain and yeast *sps.* were reported for xylose utilisation (Zhao et al., 2020). To maximise pentose utilisation, genetic engineering approach based on molecular rewiring has been applied to develop recombinant microbial strains with improved potential to uptake and assimilate xylose (Kawaguchi et al., 2006; Wang et al., 2004). Xylose is primarily metabolised via three metabolic pathways: (i) the isomerase pathway; (ii) the oxidoreductase pathway; and (iii) the oxidative pathway, also known as the non-phosphorylative pathway (Cabulong et al., 2018)

4. Sugar alcohols

Sugar alcohols are molecules formed when the sugar aldo or keto group is reduced to the corresponding hydroxyl group, as the name suggests as such they are alcohols. Because sugars are polyhydroxy chemicals, the related sugar alcohols have only one extra group of alcohols, hence the group is also known as polyols, polyalcohols, or polyhydric alcohols. Sugar alcohols are chemically, physiologically, and physically similar to sugars, to the point where some are sweet to the taste and one (xylitol) is being evaluated as a food sweetener. They are essentially similar to the plant sugar (typically ketose) in biogenesis and metabolism, and they replace sugar in many activities in many species, particularly fungus. As a result, it's been rational to think of them as distinct sugar types in terms of their metabolic functions. (Awuci and Echeta, 2019).

They are derived from their corresponding aldose sugars. Triteritols, pentitols and hexitols are more representative of sugar alcohols. There are three possible straight-chained triteritols; naturally occurring erythritol (mesoerythritol) and D-threitol, plus L-threitol. Ribitol (adonitol), xylitol, D-arabitol (D-arabinitol, D-lyxitol) and L-arabitol (L-arabinitol, L-lyxitol) are four pentitols, all of which are contained in nature. There are ten straight-chain hexitols, of which at least five occur in plants, and are possible: Sorbitol (D-glucitol), iditol (L-iditol, sorbierite), mannitol (D-mannitol), allitol (D- or L-allitol, allodulcitol) and galactitol (melampyrite, D- or L-galactitol, Dulcitol, mesogalactitol). Sorbitol, mannitol, galactitol and xylitol have been generated directly from lignocellulosic biomass such as Japanese cedar, eucalyptus, bagasse, empty fruit bunches, and rice straw (Aswal et al., 2002) Fig. 1 shows the general classification flow chart and Fig. 2, the chemical structure of major sugar alcohols.

4.1. Xylitol

According to the analysis conducted by the US Department of Energy on the development of bio-based fuels and fine chemicals, xylitol hits as one among the 12 platform chemicals with industrial importance. Xylitol, sugar alcohol, is naturally seen distributed in strawberries, plums and raspberries (Werpy et al., 2004). Xylitol being a penta hydroxy polyol found extensive application in food industry. The anti-

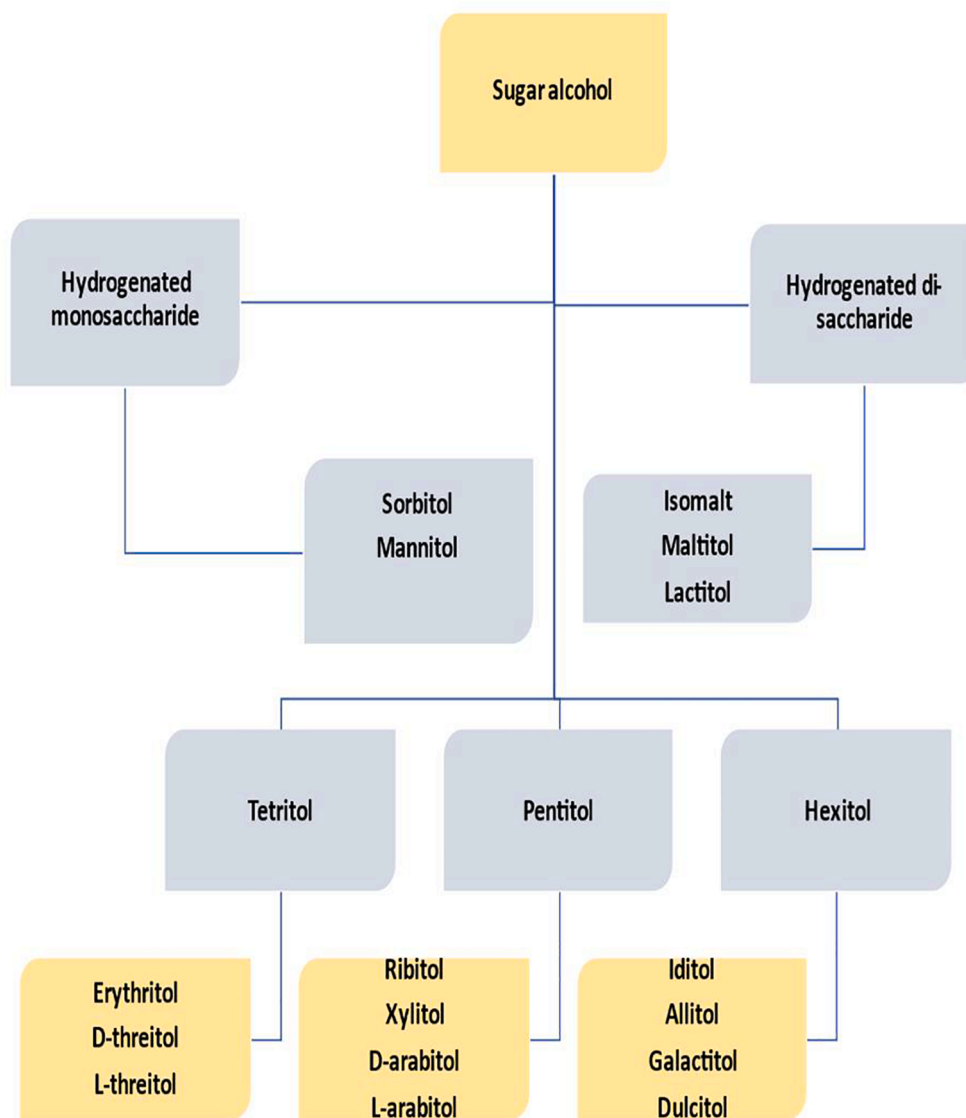


Fig. 1. Classification of sugar alcohols.

diabetic, anti-oxidant, anti-carcinogenic and other biochemical properties of xylitol extended their application in various sectors of nutraceuticals. In industries different biomass derived xylose is chemically reduced to xylitol, but the high energy requirement for industrial processes along with the environmental concern raised by greenhouse gas emission and other toxic by-products (Ni 2 +) demand a much green strategy for xylitol production (Su et al., 2015).

4.1.1. Market value and demand

Due to the increasing demand and per capita income the xylitol market will control the global economy by 2025 (grandviewresearch.com/global-xylitol-market). The rise in the incidence of lifestyle disorders like obesity, heart disease and diabetes has fueled demand for low-calorie sweeteners. Xylitol's health benefits, such as its anti-cavity characteristics and low glycemic index, have spurred its use in a variety of applications. The Asia Pacific region's growing demand for confectionery, sugar-free chewing gum and oral care product plays the pivotal role in driving the worldwide xylitol market. In terms of application the multiple health benefits connected with xylitol like its protection against tooth and enamel decay, cavities and demineralization, and increasing interest for it in chewing gum is predicted to increase in the forthcoming years. Due to increased consumer health awareness, the

chewing gum application segment is expected to expand at the fastest CAGR of 6.2 percent from 2016 to 2025 (grandviewresearch.com/global-xylitol-market). One of the major xylitol producer is Shanghai just import and export Co., Ltd China. This company alone produces approximately 55,000 tonnes of xylitol per year. The introduction of novel xylitol extraction technology is enabling large xylitol producers to cut their production costs and environmental footprint.

4.1.2. Xylitol production from biomass by natural and engineered strains

Several natural microbial producers were reported for the production of xylitol from pure xylose, but very few stated the potential of utilizing biomass derived xylose for xylitol synthesis. *Corynebacterium* sps was the first among the natural bacteria ever reported for xylitol production from xylose way back in 1970. Yeast species such as *Pichia*, *Saccharomyces*, *Candida* and *Rhodotorula* are natural producers of xylitol from pure xylose (Borokhova and Mikhailova, 1996; Granström et al., 2005; Xu et al., 2011). However, as an effort to find alternative carbon sources, the implication of metabolic engineering strategies created an opportunity for the microbes to alter their genetic make-up. As a result, new recombinant strains were introduced for xylitol production.

4.1.2.1. Natural strains producing xylitol from biomass. Among the

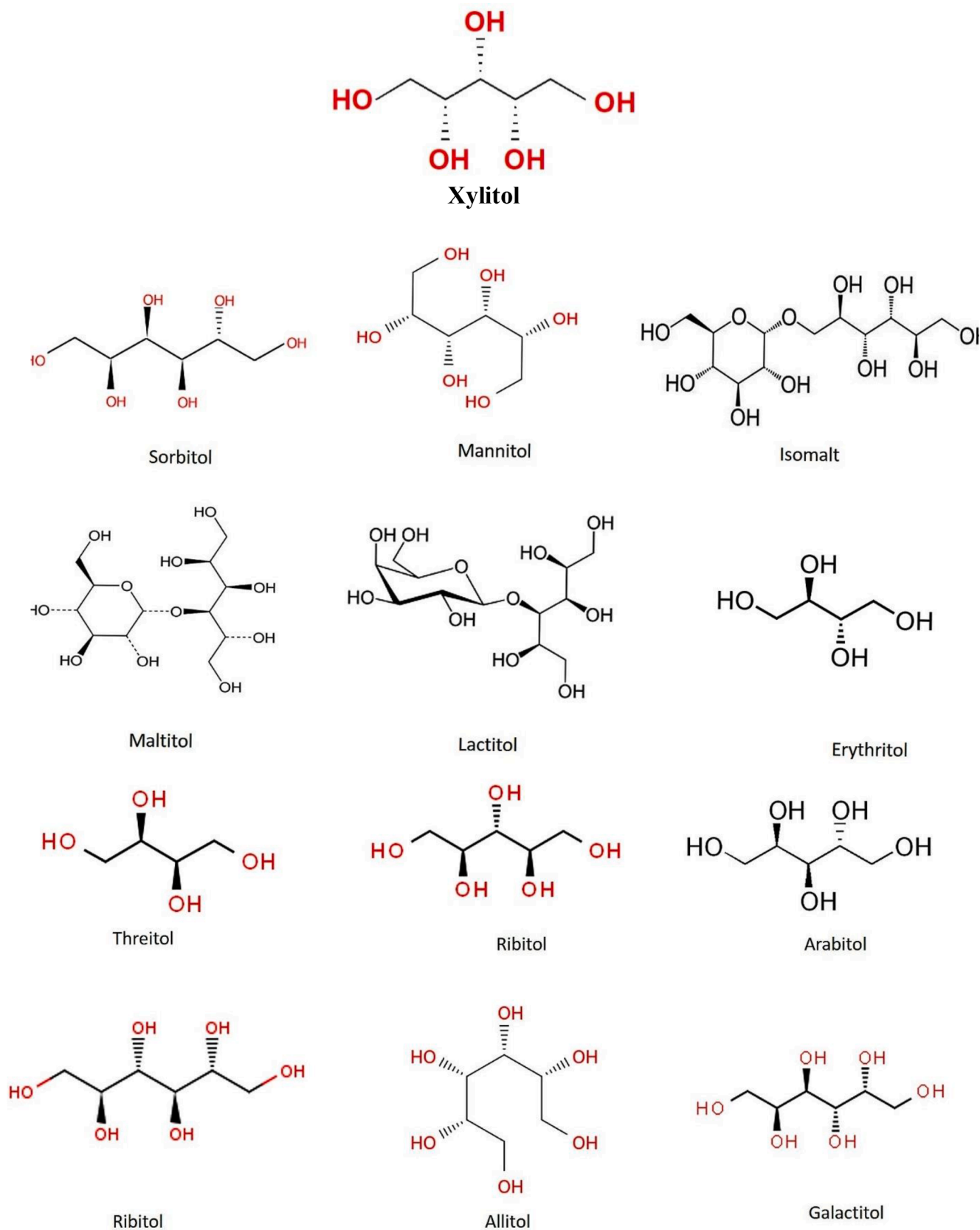


Fig. 2. Sugar alcohols and their chemical structure.

microbial community, *Candida* species are the major xylitol producers (Granström et al., 2007; Li et al., 2015; Mateo et al., 2015). *Candida tropicalis* effectively exploited to convert hemicellulosic hydrolysate from corn cob to xylitol (Li et al., 2015). Detoxified acid hydrolysate of birch wood was used for xylitol production using *Candida magnolia* (xylitol yield 0.74 g xylitol/g xylose, volumetric productivity 1.0 g/L/h) (Miura et al., 2015). Xylitol production from various hemicelluloses hydrolysates without detoxification using adapted strains of *Candida tropicalis* and *Candida magnoliae* have achieved, and the maximum production was 71 % (w/w) (Huang et al., 2011; Misra et al., 2013; Tada et al., 2012). Rapeseed straw hemicellulosic hydrolysate used as the carbon source by two yeast strains *Candida guilliermondii* and *Debaryomyces hansenii* for xylitol production. *Candida guilliermondii* showed increased tolerance to inhibitors than *D. hansenii* (López-Linares et al., 2018). *Candida intermedia* a novel yeast strain reported for single-cell protein and xylitol production from corn cob hydrolysate. The strain was tolerant to inhibitors like acetic acid, syringaldehyde and furfural in the hydrolysate and produced 45.7 g/L xylitol from xylose with the productivity of 0.38 g/L/h and the yield of

0.57 g/g xylose (Wu et al., 2018). *Candida tropicalis* M43 expanded its substrate spectrum to chestnut hull hydrolysate where optimization of detoxification parameters and concentration level achieved higher xylitol concentration of 6.30 g/L with productivity and yield of 0.11 g/L/h and 19.13 % respectively (Eryasar-Orer, 2021). *Candida mogi* demonstrated high xylitol production potential of 20.19 g and yield of 0.89 g/g xylose ingested after 120 h fermentation from prairie cordgrass hydrolysate (Rudrangi and West, 2020). *Candida tropicalis* exhibited high tolerance to acid hydrolysate of sugarcane bagasse at lower pH (4.6) and produced 109.5 g/L xylitol with a yield of 0.86 g/g of xylose, and with a productivity of 2.81 g/L/h, from biomass (Morais et al., 2019). Sisal fiber is one of the low-cost and readily available lignocellulosic materials with higher hemicellulosic than other biomass. *C. tropicalis* fermented sisal fiber hydrolysate, for the combined production of xylitol (0.32 g/g) and ethanol (0.27 g/g) without any detoxification steps (Damião Xavier et al., 2018).

After *Candida* sps, *Scheffersomyces amazonensis* from the yeast family reported for the efficient xylitol production from biomass i.e., xylitol yield of (1.04 g/g) from rice hull hydrolysate (Cadete et al., 2016). *Barnettozyma populi*, a newly isolated yeast strain selectively produced xylitol from mixed sugars i.e, both xylose and arabinose in corn stover hemicellulosic hydrolysate. *Cyberlindner asaturnus*, tropical mangrove yeast could grow and assimilate xylose, yielding, a massive proportion of xylitol (38.63 g/L). After 144 h of growth on corn cob hydrolysate (CCH) containing 65 g/L xylose, a maximum yield of 0.54 g/g was attained by *C. asaturnus* (Kamat et al., 2013). Rissi et al., (2018) introduced macro basidiomycete for sugar alcohol production from plant biomass. *Trametes membranacea* simultaneously produced ethanol and xylitol from enzymatic hydrolysate of sugar cane bagasse. *Pichia fermentans* also produced high levels of xylitol from sugarcane bagasse (SCB) and olive pit (OP) hydrolysates. A co-fermentation technique to assess *Pichia fermentans*' capacity for xylitol production yielded 86.6 g/L and 71.9 g/L from SCB and OP hydrolysates respectively (Narisetty et al., 2021).

Rarely, some enzymatic conversion of xylose to xylitol was also reported. Enzymatic production of bio-xylitol from saw dust hydrolysate i. e., using xylose reductase (XR) from *Candida tropicalis* isolated for the bio-xylitol production with a yield of 71 % (w/w) (Rafiqul et al., 2015)

4.1.2.2. Xylitol producing pathway from xylose. Xylose isomerase (XI) pathway: Xylose is assimilated by converting xylose to xylulose and then phosphorylating it to xylulose-5-phosphate, which is then metabolised in the pentose phosphate pathway (Cunha et al., 2019; Pal et al., 2013). This is commonly employed by prokaryotes, notably by *E. coli* and *Bacillus sp.*, (Lawlis et al., 1984; Lokman et al., 1991; Rygus et al., 1991; Stephens et al., 2007). In detail, the enzyme xylose isomerase initially metabolise xylose to xylulose in the isomerase pathway. Xylose kinase

then phosphorylates xylulose to xylulose-5-phosphate.

The oxidoreductase pathway also known as the xylose reductase (XR) and xylose dehydrogenase (XDH) pathway (XR-XDH pathway) where XR catalyse direct reduction of xylose to xylitol, preferentially using NADPH as cofactor; xylitol then subsequently oxidised to xylulose via xylitol dehydrogenase, solely using NAD + as cofactor and enters pentose phosphate pathway as xylulose-5-phosphate via phosphorylation by xylose kinase (Fig. 3.). Both xylose dehydrogenase and xylose reductase are co-factor (NAD + and NADP +) dependent enzymes. The regeneration and availability of co-factor is indispensable in microbial xylitol production. The oxido-reductase pathway is found mostly in eukaryotic bacteria (Kwak and Jin, 2017).

4.1.2.3. Engineered strains reported for xylitol production. Recombinant *E. coli* was introduced for the xylitol production from lignocellulosic hydrolysate. Xylose reductase gene from *Neurospora crassa* was cloned into *E. coli* for the assimilation of pentose sugar, along with which the PEP phosphotransferase system (ptsG) was disrupted to eliminate CCR mechanism enabling uptake of both xylose and glucose. Two genes xylA and xylB encoding xylose isomerase and xylose kinase were also removed inhibiting xylose catabolism in *E. coli*. The recombinant strain effectively produced xylitol from hemicellulosic sugar (Su et al., 2015). Xylose reductase, for xylose utilisation, and glucose dehydrogenase, for gluconic acid production, were expressed in *E. coli* and used as a whole-cell catalyst for the conversion of cornstalk hydrolysate derived xylose into xylitol coupled with gluconate production (Chang et al., 2018). Based on this, a combinatorial strategy, deleting ptsG gene along with crp mutation was applied for efficient xylitol synthesis from corncob hydrolysates (Yuan et al., 2020).

Corynebacterium glutamicum, one of the potent industrial hosts exploited for producing diverse biochemicals. Dhar et al., (2016) reported xylitol production from lignocellulosic pentose sugars using genetically engineered *C. glutamicum*. Heterologous expression of xylose reductase (xr) gene along with the co-expression of three different polycistronic genes from different microbial sources resulted in the direct conversion of sorghum stover derived pentoses into xylitol. The recombinant strain synthesised 27 ± 0.3 g/L xylitol from sorghum stover liquor (SAPL) which was comparable to the production from synthetic source (31 ± 0.5 g/L).

Lack of xylose assimilating metabolic network in *Saccharomyces cerevisiae* and its sensitivity towards biomass inhibitors are crucial barriers to the economical production of lignocellulosic biofuels. This problem was resolved through a genetic approach i.e., cell surface engineering of *S. cerevisiae*. Cell surface display of xylose reductase (XR) along with xylan degrading enzymes directly converted the rice straw hydrolysate derived xylose to xylitol. Further nanofiltration technology for inhibitor removal facilitated better xylitol yield in bioprocessing (Guirimand et al., 2016). Later, cell surface expression of critical genes showed double the increment in xylitol productivity i.e 0.54 g/g xylose from cellobiose/xylose co-utilization (Guirimand et al., 2019). *S. cerevisiae* was genetically engineered to overexpress a xylose transporter gene SUT1 and an aldose reductase gene GRE3 for xylitol production from corn cob hydrolysate (Kogje and Ghosalkar, 2017). *Saccharomyces cerevisiae* strains tolerant to WXML (Waste Xylose Mother Liquor) were given the ability to express xylose reductase, pentose transporter, and pentose phosphate pathway enzymes and this strain showed a significant capacity to produce xylitol from xylose in WXML (He et al., 2021). In addition, *Pichia fermentans*, a novel yeast strain for sugar alcohol synthesis from agro-residual hydrolysate was recently identified. Chemical mutagenesis of xylose-assimilating *P. fermentans* with ethyl methane sulphonate (EMS) produced a mutant strain with the highest xylose bioconversion efficiency (Prabhu et al., 2020).

Zhang et al (2021) engineered *Candida tropicalis*, an uracil deficient mutant strain, for xylitol fermentation from XML (Xylose Mother Liquor). Gene deletion to block xylitol assimilation and heterologous

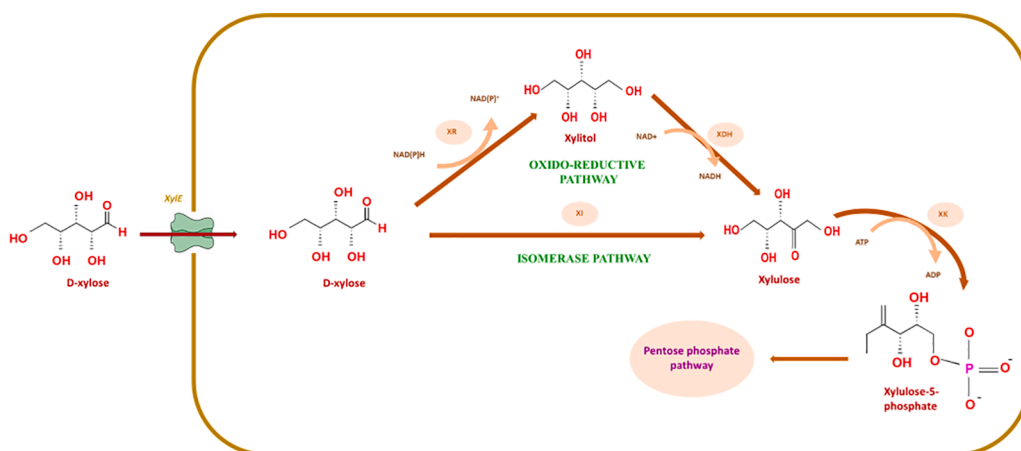


Fig. 3. Xylitol biosynthetic pathway. Xylose enters the cell via xylose transporter (xyleE). Oxido-reductive pathway; Xylose is catalytically converted to xylitol by xylose reductase (XR) followed by reduction of xylitol to xylulose by the enzyme xylitol dehydrogenase (XDH). Xylulokinase (XX) phosphorylates xylulose to xylulose-5-phosphate and enters the PP Pathway. Isomerase pathway; Xylose is directly converted to xylulose by xylose isomerase (XI) and enters PP Pathway as xylulose-5-phosphate.

expression of dehydrogenase genes (for NADPH regeneration system) from *Yarrowia lipolytica* created a recombinant strain and it produced 97.10 g/L xylitol from 300 g/L XML within 120 h fermentation.

4.1.3. Innovative production strategies for xylitol

A novel process of integrated inhibitor degradation, explaining xylitol and ethanol fermentation by *Candida tropicalis* W103 from acid pre-treated and non-detoxified corncob hydrolysate was put forward by the researchers. *C. tropicalis* W103 degraded furfural, acetate and hydroxymethylfurfural totally after 60 h fermentation. 17.1 g/L xylitol and 25.3 g/L ethanol was produced corresponding to 82 % of theoretical yield (Cheng et al., 2014). Complementing *Candida tropicalis*, *Bacillus subtilis* was modified for one-pot biotransformation of waste xylose mother liquor (WXML) to xylitol, this study demonstrates that one-pot process a feasible choice for the value addition of WXML to produce platform chemicals increasing its economic value (Wang et al., 2016a, Wang et al., 2016b).

Tathod and Dhepe, (2015) developed a one-pot method for directly converting hemicellulosic and agricultural wastes into sugar alcohol. Pt-Sn bimetallic catalyst (PtSn/c-Al₂O₃) is used for the conversion of substrates like C6 sugars, C5 sugars, hemicelluloses and agricultural wastes into sugar alcohols. An efficient bimetallic catalyst mediated conversion of biomass into sugar alcohol in a wide range of reaction conditions attained with higher yield (49–72%) and recyclability. The immobilisation and application of recombinant *E. coli* co-expressing XR and GDH for xylitol synthesis proved successful. The maximal activity recovery after immobilisation was 80.3 percent. The immobilised cells were stable in terms of pH, temperature, and functioning. Batch tests revealed that the immobilised cells could retain 70.5 percent of their initial activity after being recycled 10 times, and yielded 11.5 g/L xylitol from waste xylose mother liquor (Jin et al., 2019).

Two-step transformation into xylitol i.e., phosphorous oxoacid mediated hydrothermal processing followed by Pd/C catalytic hydrogenation of napier grass was attempted by Takata and team. Xylose obtained by phosphorous acid (3.0 wt%) hydrothermal treatment from the napier grass was subsequently converted into xylitol by Pd/c (5.0 wt %) hydrogenation with 51.6 % yield of xylan (Takata et al., 2014). Phosphorus oxoacids, can replace sulphuric acid for biomass pretreatment as it is eco-friendly and less corrosive. It is also effective in high pentose release while decreasing inhibitor concentration, and the residual phosphate salts are used as micro-nutrients and fertilizers (Lenihan et al., 2010; Orozco et al., 2011).

Apart from free cells, immobilized cells were also reported for xylitol production. Calcium alginate immobilised *Candida* cells produced xylitol from poplar wood hydrolysate with a novel detoxification technique. Process combination for inhibitor degradation, where hemicellulose hydrolysate detoxified employing a unique method of vacuum

evaporation followed by removal of inhibitors by solvent separation, producing toxin free hydrolysate while preserving high quantities of C5 and C6 sugars (Dalli et al., 2017). Another technique i.e., soaking in aqueous ammonia (SAA) was the pre-treatment strategy used to minimise the inhibitors and the detoxified corncob hydrolysate was subjected to fermentation by immobilized *Candida* cells for xylitol production and the results showed higher productivity using detoxified corn cob hydrolysate as substrate (Deng et al., 2014).

Ultra-sonication assisted production of xylitol using *C. tropicalis* from biomass, *C. tropicalis* immobilized on PU foam applied with 37 kHz sonication during fermentation under optimum condition resulted in intensified fermentation kinetics with xylitol yield of 0.66 g/g xylose in 15 h. Optimization of operational parameter, i.e., steam pre-treatment of 24 hr pre-soaked (in H₂SO₄) rice straw at 121 °C for 30 min and neutralization with barium hydroxide, produced notably reduced HMF and furfurals. *C. tropicalis* fermented rice straw hydrolysate with 0.6 g/g yield (Singh et al., 2021).

A kind of Inhibitor add-on technique was also reported like the presence of inhibitor derived from lignocellulosic biomass enhances the xylose metabolism in *Candida magnoliae*. The fermentation medium supplemented with furfural and glucose enhanced xylitol production from xylose in *C. magnoliae*. After fermentation, a significant production rate (0.169 g/g h) and productivity (1.04 g/L/h) were maintained whereas in the absence of inhibitors and sugars, the overall production rate decreased below 35 % (Wannawilai et al., 2017).

Combined fermentation i.e., fermentation by *Kluyveromyces* and *Saccharomyces cerevisiae* for xylitol production from wheat bran-corn cob hydrolysates. Acid hydrolysis followed by enzymatic hydrolysis and combined microbial fermentation resulted in high yields and productivity of xylitol from both wheat bran and corn cob biomass (Ghaffar et al., 2017). *Candida guilliermondii* and *Kluyveromyces marxianus* harbouring xylose reductase and xylitol dehydrogenase metabolized xylose present in apple pomace for alcohol production. *Candida guilliermondii* produced xylitol (9.35 g/L) whereas *Kluyveromyces marxianus* produced both xylitol (9.10 g/L) and ethanol (10.47 g/L) adding value to apple pomace raw materials as well as apple production chain (Leonel et al., 2020). *Kluyveromyces marxianus* could ferment biomass derived sugars for ethanol and xylitol production. A suitable expression cassette harbouring xylose reductase was constructed and incorporated in *K. marxianus*. The modified strain produced 58.62 ± 0.15 g of xylitol along with ethanol, to be used as a single biocatalyst for multiproduct biorefinery application (Dasgupta et al., 2019).

A detoxification procedure for inhibitor elimination from corn cob hydrolysate has been devised for optimum xylitol synthesis and recovery. Corn cob acid hydrolysate was successfully removed from 60 percent salts and 90 percent phenolic compounds using an optimised technique. *Candida tropicalis* fermentation performance was greatly

improved, with the detoxification process and through downstream processing of carbonation, ion exchange, and activated charcoal, xylitol purity of above 90% was obtained (Kumar et al., 2019).

An interesting two-stage fermentation strategy was employed, where both ethanol and xylitol were co-produced from corn cob hydrolysate using *K. marxianus* (Du et al., 2020). *S. cerevisiae* PE-2 strain with an innate potential of accumulating xylitol was overexpressed with GRE-3 and xylose reductase gene from *Pichia stipites* for xylitol production. The recombinant strain fermented xylose to xylitol in a whole slurry of corn cob hydrolysate (Baptista et al., 2018). Table 1 summarises the yield and volumetric productivity of xylitol reported for different microbial strains (natural and engineered) from biomass.

4.1.4. Recovery and purification of xylitol from fermented broth

Purity is an important criterion for pharmaceutical and nutraceutical substances. Colorants, cell debris, residual sugars and other organic compounds are among the impurities in fermentation broth that must be removed in order to produce a high-quality end-product. Activated charcoal treatment is highly efficient for broth clarification and removal of colorants. To remove ionic/charged contaminants, ion-exchange resins (cation and anion-exchange resins) are also used. Cation-exchange resins are employed for the removal of salts and other positively charged organic chemicals, while anion exchange resins are for eliminating anionic coloured compounds. The use of activated charcoal in combination with ion exchange resins is an efficient and cost-effective technique to remove the majority of contaminants (Silva et al., 2020; Martínez et al., 2015). Nanofiltration (NF) membranes are used to separate molecules based on particle size differences. Faneer et al., (2017) developed a polyethersulfone NF membrane for the recovery of xylitol from other contaminants with higher purity. More than 90% of xylitol and a tiny fraction of sugars were preserved after nanofiltration with a polyethersulfone NF membrane from the fermentation broth.

5. Sugar acid

Sugar acids are mainly synthesised via oxidation of corresponding mono or oligosaccharides. Both chemical and biological methods are used for sugar acid production. Aldonic, aldaric, and uronic acids are the

three major class of sugar acids. The biorefinery concept of producing biofuels and commodity chemicals from natural resource is gaining high interest due to its replacement with those produced from petroleum basis along with which sugar acids are also generating a lot of attention due to their potential as high value chemicals, and specifically as precursors of bio-plastics. Sugar acids are used as latent acid in food industry, and other application as pH regulator, sequestering agent and in pharmaceuticals. Xylose derived, sugar acid, xylonic acid generate interest as of the use of this molecule in the manufacture of synthetic polymers, including polyamides, polyesters and hydrogels. Further advancement of this xylonic acid would result in higher production volumes and thus help sustain the next generation biorefineries (Mehtio et al., 2016).

5.1. Xylonic acid

D-xylonic acid, an oxidised five carbon derivative of xylose, is an excellent chemical platform with multifarious applications in the food, medicinal and agricultural fields. It is regarded as one of the top 30 highest-value chemicals by the U.S. National Renewable Energy Laboratory (NREL) and finds a number of applications in different fields as precursor for synthesis of 1,2,4-butanetriol, chelator and polyamides (Toivari et al., 2012a). The two potential routes for the synthesis of xylonic acid are chemical and biological oxidation. In chemical process XA oxidation is through a chemical catalyst (Pt/Au). In biological process biocatalysts dehydrogenase and lactonase oxidise xylose into XA. Biological oxidation is more sustainable, eco-friendly and cost-effective for industrial need compared to chemical process due to the lack of selectivity of the process (Mathews et al., 2015).

5.2. Xylonic acid production from biomass by natural and engineered strains

5.2.1. Native producers of xylonate

The biological conversion of pentoses to pentanoic acid is mainly attained by aerobic bacterial fermentation. At the end of the nineteenth century, microbial production of xylonate was recognised from pure xylose and several species like *Gluconobacter*, *P. sacchari*, *Pseudomonas*,

Table 1
Microbial species reported for the production of xylitol from biomass.

Species	Yield (g/g)	Biomass	Volumetric productivity (g/L/h)	Reference
<i>Candida tropicalis</i> JA2	0.86	Sugarcane bagasse	2.81	Morais Junior et al., 2019
<i>Candida guilliermondii</i> FTI 20,037	0.6	Sugarcane straw	0.34	Hernández-Pérez et al., 2016
<i>Pichia fermentans</i>	0.54	Sugarcane bagasse	–	Prabhu et al., 2020
<i>Candida boidinii</i> XMO2G	0.52	Cocoa pod husk hemi-cellulose hydrolysate	–	Santana et al., 2018
<i>Candida Tropicalis</i> Kuen 1022	–	Cotton Stalk	0.06	Sapci et al., 2016
<i>Saccharomyces cerevisiae</i> PE –2 strain	0.93	Corn cob	0.54	Baptista et al., 2018
<i>Candida Tropicalis</i> MTCC 6192	0.6	Rice Straw	–	Singh et al., 2021
<i>E. coli</i>	–	Corn cob	1.40	Su et al., 2015
<i>Candida tropicalis</i> X828 & <i>Bacillus Subtilis</i> Bs 12	0.75	Waste Xylose Mother Liquor	–	Wang et al., 2016a, Wang et al., 2016b
<i>Candida magnoliae</i> TISTR 5663	–	Furfural	1.04	Wannawilai et al., 2017
<i>Scheffersomyces amazonensis</i>	1.04	Rice hull hydrolysate (RHH)	–	Cadete et al., 2016
<i>Candida tropicalis</i>	0.32	Corn cob	–	Cheng et al., 2014
<i>Kluyveromyces marxianus</i>	0.82	Corn cob	–	Du et al., 2020
<i>Saccharomyces cerevisiae</i> & <i>Kluyveromyces</i>	87.716	Wheat straw & Corn cob	0.018	Ghaffar et al., 2017
<i>Candida tropicalis</i> JH 030	0.71	Rice straw hydrolysate	–	Huang et al., 2011
<i>Cyberlindnera saturnus</i>	0.54	Corn cob	–	Kamat et al., 2013
<i>Saccharomyces cerevisiae</i>	–	Corn cob	0.212	Kogje and Ghosalkar, 2017
<i>Debaromyces hansenii</i>	0.45	Rapeseed straw	–	López-Linares et al., 2018
<i>Candida guilliermondii</i>	0.55	Rapeseed straw	–	López-Linares et al., 2018
<i>Candida tropicalis</i> NBRC 0618	1.20	Olive pruning	–	Mateo et al., 2015
<i>Candida magnoliae</i>	0.74	Birch wood hydrolysate	1.0	Miura et al., 2015
<i>Candida intermedia</i> FL023	0.57	Corn cob	0.38	Wu et al., 2018
<i>Candida tropicalis</i> CCT 1516	0.32	Sisal fiber hemicellulose hydrolysate	–	Damião Xavier et al., 2018
<i>E. coli</i> W3110	–	Corn cob	3.04	Yuan et al., 2020

Pseudoduganella, *Erwinia* and other microorganisms were reported to produce xylonic acid (Bondar et al., 2021; Sundar Lekshmi et al., 2019; Toivari et al., 2012a). *Burkholderia sacchari* is a well-known industrial producer strain with a high capacity for incorporation into a bio refinery that uses biomass residues. The wild-type *B. sacchari* produced both xylitol and xylonic acid comparable with other high production hosts. The genetic level rewiring of its metabolic route, along with improvements in molecular modification methods and a better knowledge of metabolic fluxes through upcoming studies, will integrate its potential as a micro-production platform (Oliveira-Filho et al., 2021). Native xylonic acid producers, yield and titre reported are compiled in Table 2. For the production of xylonate with theoretical yield, metabolic engineering approaches based on genetic modulation were introduced in the 2000 s.

5.2.2. Xylonic acid biosynthetic pathway

The oxidative pathway is divided into two routes: The Weimberg pathway and the Dahms pathways (Fig. 4). Native bacteria such as *G. oxydans*, *B. xenovorans*, *P. sacchari*, *C. crescentus*, and *P. taiwanensis* utilise this pathway to assimilate xylose into D-xylonolactone via enzyme xylose dehydrogenase (XDH) (Köhler et al., 2015; McClintock et al., 2017; Stephens et al., 2007). D-xylonolactone is then converted to D-xylonic acid by xylonolactonase (XL), which is further converted to the common intermediate, 2-keto-3-deoxy-xylonate, between the two pathways. 2-keto-3-deoxy-xylonate is converted to α -ketoglutarate via

Table 2
Native strains reported for xylonic acid production.

Species	Yield (g/g)	Titer (g/L)	Volumetric productivity (g/L/h)	Process	Reference
<i>Gluconobacter oxydans</i> ATCC 621	1.1	109	2.5	Batch	Toivari et al., 2012a
<i>Gluconobacter oxydans</i> ATCC 621	1.1	51	1.8	Batch	VTT
<i>Gluconobacter oxydans</i> ATCC 621	1.0	41	1.0	Batch	VTT
<i>Gluconobacter oxydans</i> DSM 2003	–	66.42	–	Batch	Zhang et al., 2017
<i>Gluconobacter oxydans</i> DSM 2003	0.9	38.86	–	Batch	Zhang et al., 2016
<i>Gluconobacter oxydans</i> NL71	–	143.6	4.48	Batch	Dai et al., 2020
<i>Gluconobacter oxydans</i> NL71	0.98	586.3	4.69	Batch	Zhou et al., 2015
<i>Gluconobacter oxydans</i>	–	329	6.7	Batch	Zhou and Xu, 2019
<i>Gluconobacter oxydans</i>	–	102.3	–	Batch	Zhou et al., 2016
<i>Gluconobacter oxydans</i> NL71	0.9	54.97	–	Batch	Zhu et al., 2015
<i>Enterobacter cloacae</i>	~ 1	190	~ 1	Batch	Ishizaki et al., 1973
<i>Pseudomonas fragi</i> ATCC 4973	1.1	162	1.4	Batch	Buchert and Viikari 1988
<i>Pichia kudriavzevii</i>	1.0	171	1.4	Fed-Batch	Toivari et al., 2013
<i>Klebsiella pneumoniae</i>	1.11	103	1.30	Fed-Batch	Wang et al., 2016a, Wang et al., 2016b
<i>Paraburkholderia sacchari</i>	1.11	390	6.41	Fed-Batch	Bondar et al., 2021
<i>Pseudoduganella danionis</i>	0.65	6.5	–	Batch	Sundar Lekshmi et al., 2019

the Weimberg pathway, alternatively 2-keto-3-deoxy-xylonate is hydrolysed to pyruvate and glucoaldehyde via the Dahms pathway (Brüsseler et al., 2019).

The non-phosphorylative metabolic route has significant advantages over the oxidoreductase and isomerase pathways as it directly transforms D-xylose to pyruvate and -ketoglutarate without entering PPP, reducing enzymatic conversions and ATP consumption. The incorporation of oxidative pathway enzymes aided the evolution of new recombinant strains producing a variety of useful chemicals (Bañares et al., 2021; Domingues et al., 2021).

5.2.3. Engineered strains producing xylonate

E. coli is an interesting model for producing biotechnologically valuable chemicals, because its metabolic routes and physiology are well understood, and there are several genetic and bioinformatic tools accessible. However, its prime genetic pathway for xylose metabolism is the XI pathway, *E. coli* does not natively produce xylonate from xylose. Nevertheless, metabolic engineering can be used to get around this limitation. In fact, the genetically modified strain accumulated xylonic acid after co-expression of two genes encoding xylose dehydrogenase (xdh) and xylonolactonase (xylC) from a heterologous Gram negative bacteria *Caulobacter crescentus*, as well as deletion of the genes encoding xylose isomerase and xylose kinase to block xylose utilisation via its native xylose isomerase pathway (Cao et al., 2013; Liu et al., 2012a). After *E. coli*, very recently *Corynebacterium glutamicum* has been reported for its potential in xylonic acid production from agro-residue. *Corynebacterium glutamicum* is a potent industrial host reported for the production of diverse products like organic acids, alcohols, vitamins, recombinant proteins, nucleic acid, sugar alcohol, etc. In 2017 Yim et al explored *Corynebacterium glutamicum* for its potential in bioconversion of hemicellulosic biomass into speciality chemicals i.e xylan into xylonic acid. Heterologous expression of xylose specific transporter gene, xylE, of *Escherichia coli* along with xylose dehydrogenase and xylonolactonase genes, involved in xylonic acid metabolism, from *Caulobacter crescentus* were cloned for xylonic acid production. The metabolically engineered *C. glutamicum* successfully produced xylonic acid from biomass (Yim et al., 2017). Based on this, Sundar et al (2020) carried out metabolic engineering in *C. glutamicum* ATCC 31831, where incorporation of xylose dehydrogenase and xylonolactonase into the central metabolic pathway produced a recombinant strain successfully converting xylose, derived from rice straw hydrolysate, into xylonic acid. The relatively high conversion efficiency of this organism is owing to the presence of an inbuilt AraE pentose transporter, which facilitates the intake of C5 sugars promoting pentose metabolism (Sundar et al., 2020). D-xylose dehydrogenase gene from *Caulobacter crescentus* was also expressed in yeast *Pichia kudriavzevii* VTT C-79090 T for xylonic acid production and the modified strain showed 100% conversion (Toivari et al., 2013). Herrera et al., (2021) engineered *Zymomonas mobilis* for conversion of sugarcane bagasse derived xylose to xylonic acid. The recombinant strain expressing xylose dehydrogenase gene (of *Paraburkholderia xenovorans*) allowed effective production of xylonic acid in shake flasks. The yeasts *Saccharomyces cerevisiae* and *Kluyveromyces lactis* were also modified in such a way showing the potential of prokaryotic systems for xylonic acid production (Nygård et al., 2011; Toivari et al., 2012a). The studies on this sugar acid took a deviation to the practical application of xylonic acid as a concrete add-mixture in 2018. Zhou et al., (2018) exploited *G. oxydans* for xylonic acid production from wheat straw hydrolysate as an economical source for industrial application. High titer of upto 210 g xylonic acid was produced by *G. oxydans* within one day catalysis (Han et al., 2021). Calcium xylonate from lignocellulosic pre-hydrolysate (CXL) demonstrated to be a promising commercial precursor for concrete add-mixture with improved characteristics as a potential water reducer with high retardation capacity and compressive strength reinforcement and as a cost-competitive approach it has boosted the comprehensive utilization of lignocellulosic for xylonic acid production.

Klebsiella pneumoniae a mutant strain (Δgad) reported for producing

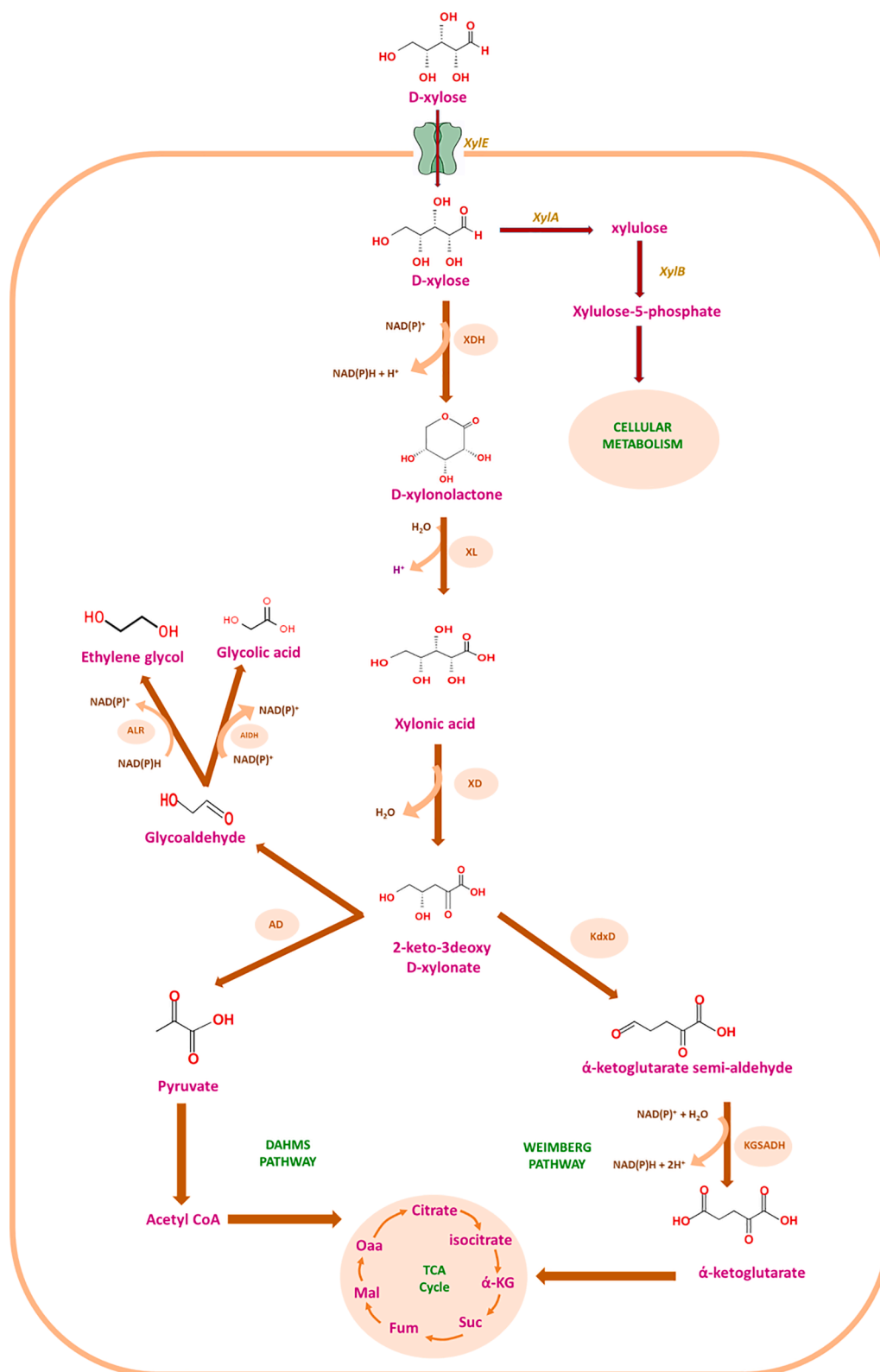


Fig. 4. Xylose oxidative pathway for xylonic acid biosynthesis. Xylose is converted to xylonolactone by xylose dehydrogenase (XDH) and then to xylonic acid by xylonolactonase (XL). Xylonic acid again converted to 2-keto 3-deoxy D-xylonate by xylonate dehydratase (XD). 2-keto 3-deoxy D-xylonate is the common intermediate in both the Dahm’s pathway and Weimberg pathway. In Dahm’s pathway 2-keto 3-deoxy D-xylonate splits into pyruvate and glycoaldehyde via enzyme aldolase (AD) pyruvate enters into TCA cycle as acetyl CoA, glycoaldehyde again converted to ethylene glycol via aldehyde dehydrogenase (ALR) and/or converted to glycolic acid via aldehyde dehydrogenase (AIDH), whereas in Weimberg pathway 2-keto 3-deoxy D-xylonate is oxidised to α-keto-glutarate semi-aldehyde by Keto-deoxy-Xylonate dehydratase (KdxD) and then enters TCA cycle as α-keto-glutarate by the enzymatic action of α-keto glutarate semi-aldehyde dehydrogenase (KGSADH).

both gluconic acid and xylonic acid from bamboo hydrolysate, where 14 g/L xylonate and 33 g/L gluconate were produced (Wang et al., 2016a, Wang et al., 2016b). *G. oxydans* the natural xylonate producer that has undergone extensive studied for this metabolite's synthesis reported with maximum yield of 586 g/L (Zhou et al., 2015). Miao et al., 2015, sequenced the complete genome of *G. oxydans* NL 71 to understand the overall metabolism of xylose as well as the genome sequence elucidation paved the basis for both evolutionary studies and in the enhancement of the organism's biotechnological applications. This whole genome data is influential in understanding the metabolic mechanism occurring in the bacterial cells for the biotransformation of xylose into xylonic acid and the cellular resistance towards highly concentrated xylonic acid, xylose and inhibitors in the crude lignocellulosic hydrolysate. Table.3 compiles the metabolically engineered strains reported for xylonic acid production.

CRISPR-Cas9 technology is a dynamic genome editing tool, the vast scope of this technology will change the near future of biotechnology. A transitory CRISPR-Cas9 gene editing in *Candida glycerinogenes* enabled the co-production of xylonic acid and ethanol from lignocellulosic hydrolysate. For decades, *Candida glycerinogenes*, a potent industrial yeast with strong inhibitor resistance, has been used to produce glycerol. The absence of reduction division, whole genome, and the dearth of molecular tools, however, limited its genetic manipulation. The CRISPR-Cas9 system altered the genetic make-up of *C. glycerinogenes*. Single and multiple gene knock-outs were produced by targeting counter selectable marker genes (TRP1, URA3), and the auxotroph created employed as a background for targeting other genes (HOG1) with an 80 percent mutation efficiency. Furthermore, by knocking in the xylose dehydrogenase gene, a recombinant *C. glycerinogenes* strain was created, co-producing both ethanol (28 g/L) and xylonic acid (9 g/L) from xylose rich biomass hydrolysate. This strategy could countersign to unlock the application of CRISPR-cas9 genome editing in more organisms paving pathways producing diverse biochemicals (Zhu et al., 2019).

Table 3
Metabolically engineered strains reported for xylonic acid production.

Species	Process	Yield (g/g)	Titer (g/L ⁻¹)	Volumetric productivity (g/L/h)	Reference
<i>Saccharomyces cerevisiae Xyd1</i>	Batch	0.4	4	0.03	Toivari et al., 2010
<i>Saccharomyces cerevisiae xylB</i>	Batch	0.8	17	0.23	Toivari et al., 2012b
<i>Kluyveromyces lactis Xyd1</i>	Batch	0.6	19	0.16	Nygård et al., 2011
<i>Kluyveromyces lactis Xyd1 ΔXYL1</i>	Batch	0.4	8	0.13	Nygård et al., 2011
<i>Aspergillus niger ATCC 1015</i>	Batch	0.8	10	0.12	VTT
<i>E. coli W3110 EWX4</i>	Batch	0.98	39.2	1.09	Liu et al., 2012a
<i>E. coli BL21 ΔxylAB/pA-xdhxylC</i>	Batch	0.91	27.3	1.8	Cao et al., 2013
<i>Corynebacterium glutamicum (ATCC 13032)</i>	Batch	1.04	20.71	1.02	Yim et al., 2017
<i>Corynebacterium glutamicum (ATCC 31831)</i>	Batch	1	56.32	0.93	Sundar et al., 2020
<i>Zymomonas mobilis</i>	Batch	1.04	26.17	1.85	Herrera et al., 2021

5.3. Improvised bioprocesses and xylonic acid recovery

Hou et al., (2018) illustrated the cascade hydrolysis and fermentation (CHF) strategy for the co-production of both gluconic acid and xylonic acid from highly viscous corn stover hydrolysate slurry. The high fermentation product yields of gluconic and xylonic acid (118.9 g/L and 59.3 g/L respectively) were reported exploiting *Gluconobacter oxydans* DSM 2003. This study signifies the economy and efficacy of CHF over traditional distinct hydrolysis and fermentation (SHF) as a practical fermentation strategy to be broadly extended to other value-added chemicals. Powdered activated carbon treatment improves xylonate synthesis from hemicellulose pre-hydrolysate. The use of powdered activated carbon lowered the viscosity of concentrated pre-hydrolysate and other non-sugar molecules, allowing lignocellulosic xylonic acid synthesis to be scaled up in an air-aerated and agitated bioreactor (Dai et al., 2020). Using straw pulping solid residue, a unique bio-refinery sequence was created, providing a variety of co-products such as xylonic acid, nitrogen fertiliser and ethanol. This method employs neutral sulfite pretreatment, which resulted in 64.3 % delignification and also preserving cellulose and xylan (90 and 67.3%) under optimal conditions. Semi-simultaneous saccharification and fermentation (S-SSF) and bio-catalysis methods were investigated after pretreatment. With various solid loading, nearly 100 % xylonic acid got yielded from bio-catalysis of xylose remained in fermentation broth (Huang et al., 2018).

For industrial applications, purity is a key criterion. Activated charcoal treatment and solvent extraction are the major downstream processes employed for xylonic acid recovery. Charcoal clarified broth is concentrated by rotary evaporator (usually at 70 °C) and xylonic acid precipitate is recovered by ethanol precipitation (3:1 ratio). Another recovery process is the use of ion-exchange resin and crystallization, where anion exchange resin (D311) is employed for xylonic acid purification. The resin extracted eluate is concentrated into pure xylonic acid crystals (Liu et al., 2012b; Wang et al., 2016a, Wang et al., 2016b; Zhang et al., 2020).

6. Conclusion

Xylose is the supreme and most attractive sugar obtained from hemicellulosic fraction of lignocellulosic biomass. Biological processes that use pentose-rich biomass as the sole carbon source will help to minimise raw material prices while also ensuring process sustainability. The major bio-resource for xylitol and xylonic acid production through either chemical or biotechnological paths is pentose-rich hemicellulosic hydrolysates. The bottleneck in the complete utilization of xylose in many microorganisms is the lack of a well-established xylose utilization pathway. Metabolic engineering via rewiring one or two paths enhanced xylose assimilation in microbial cells. Novel bioprocessing and innovative production strategies reflected higher titers of xylonic acid and xylitol from biomass derived xylose. Xylonic acid as an added value chemical will replace gluconic acid in a variety of applications considering the versatility and novelty of this five carbon sugar acid. Other artificial sweeteners will be put back by xylitol in a short time considering its health benefits. Value addition of biomass derived xylitol and xylonic acid will enrich white biotechnology and biorefinery. The production of more superlative commodity chemicals from xylose-stream of hemicellulose will be a reality in the near future.

Ethical approval

No ethical issues in this review article

CRedit authorship contribution statement

M.S. Lekshmi Sundar: Conceptualization, Data curation. **K. Madhavan Nampoothiri:** Outline, Validation.

Declaration of Competing Interest

The authors declare that they have no known competing financial interests or personal relationships that could have appeared to influence the work reported in this paper.

Acknowledgements

Lekshmi Sundar acknowledges the Junior and Senior Research Fellowships by CSIR, New Delhi.

References

- Aswal, D.K., Singh, A., Sen, S., Kaur, M., Viswandham, C.S., Goswami, G.L., Gupta, S.K., 2002. Effect of grain boundaries on paraconductivity of YBa₂Cu₃Ox. *J. Phys. Chem. Solids* 63 (10), 1797–1803.
- Awuci, C.G., Echeta, K.C., 2019. Current developments in sugar alcohols: chemistry, nutrition, and health concerns of sorbitol, xylitol, glycerol, arabitol, inositol, maltitol, and lactitol. *Int. J. Adv. Acad. Res.* 5, 2488–9849.
- Bañares, A.B., Nisola, G.M., Valdehuesa, K.N.G., Lee, W.-K., Chung, W.-J., 2021. Understanding D-xylonic acid accumulation: a cornerstone for better metabolic engineering approaches. *Appl. Microbiol. Biotechnol.* 105 (13), 5309–5324.
- Baptista, S.L., Cunha, J.T., Romani, A., Domingues, L., 2018. Xylitol production from lignocellulosic whole slurry corn cob by engineered industrial *Saccharomyces cerevisiae* PE-2. *Bioresour. Technol.* 267, 481–491. <https://doi.org/10.1016/j.biortech.2018.07.068>.
- Bondar, M., da Fonseca, M.M.R., Cesário, M.T., 2021. Xylonic acid production from xylose by *Paraburkholderia sacchari*. *Biochem. Eng. J.* 170, 107982. <https://doi.org/10.1016/j.bej.2021.107982>.
- Borokhova, O.E., Mikhailova, N.P., 1996. Microbial conversion of D-xylose. *Mikrobiologiya* 65, 581–588.
- Brüsseler, C., Späth, A., Sokolowsky, S., Marienhagen, J., 2019. Alone at last! – Heterologous expression of a single gene is sufficient for establishing the five-step Weimberg pathway in *Corynebacterium glutamicum*. *Metab. Eng. Commun.* 9, e00090. <https://doi.org/10.1016/j.mec.2019.e00090>.
- Buchert, Johanna, Viikari, Liisa, 1988. The role of xylonolactone in xylonic acid production by *Pseudomonas fragi*. *Appl. Microbiol. Biotechnol.* 27 (4), 333–336. <https://doi.org/10.1007/BF00251763>.
- Cabulong, R.B., Lee, W.-K., Bañares, A.B., Ramos, K.R.M., Nisola, G.M., Valdehuesa, K.N.G., Chung, W.-J., 2018. Engineering *Escherichia coli* for glycolic acid production from D-xylose through the Dahms pathway and glyoxylate bypass. *Appl. Microbiol. Biotechnol.* 102 (5), 2179–2189. <https://doi.org/10.1007/s00253-018-8744-8>.
- Cadete, R.M., Melo-Cheab, M.A., Viana, A.L., Oliveira, E.S., Fonseca, C., Rosa, C.A., 2016. The yeast *Scheffersomyces amazonensis* is an efficient xylitol producer. *World J. Microbiol. Biotechnol.* 32 (12) <https://doi.org/10.1007/s11274-016-2166-5>.
- Cao, Y., Xian, M.o., Zou, H., Zhang, H., Cirino, P.C., 2013. Metabolic Engineering of *Escherichia coli* for the Production of Xylonate. *PLoS ONE* 8 (7), e67305. <https://doi.org/10.1371/journal.pone.0067305>. <https://doi.org/10.1371/journal.pone.0067305.g00110.1371/journal.pone.0067305.g00210.1371/journal.pone.0067305.g00310.1371/journal.pone.0067305.g00410.1371/journal.pone.0067305.g00510.1371/journal.pone.0067305.t00110.1371/journal.pone.0067305.s00110.1371/journal.pone.0067305.s002>.
- Chang, Z., Liu, D., Yang, Z., Wu, J., Zhuang, W., Niu, H., Ying, H., 2018. Efficient Xylitol Production from Cornstalk Hydrolysate Using Engineered *Escherichia coli* Whole Cells. *J. Agric. Food Chem.* 66 (50), 13209–13216. <https://doi.org/10.1021/acs.jafc.8b04666>.
- Cheng, K.K., Wu, J., Lin, Z.N., Zhang, J.A., 2014. Aerobic and sequential anaerobic fermentation to produce xylitol and ethanol using non-detoxified acid pretreated corn cob. *Biotechnol. Biofuels* 7, 1–9. <https://doi.org/10.1186/s13068-014-0166-y>.
- Cunha, J.T., Soares, P.O., Romani, A., Thevelein, J.M., Domingues, L., 2019. Xylose fermentation efficiency of industrial *Saccharomyces cerevisiae* yeast with separate or combined xylose reductase/xylitol dehydrogenase and xylose isomerase pathways. *Biotechnol. Biofuels* 12 (1). <https://doi.org/10.1186/s13068-019-1360-8>.
- Silva, E.G., Borges, A.S., Maione, N.R., Castiglioni, G.L., Suarez, C.A.G., Montano, I.D.C., 2020. Fermentation of hemicellulosic liquor from Brewer's spent grain using *Scheffersomyces stipitis* and *Pachysolen tannophilus* for production of 2G ethanol and xylitol. *Biofuels. Bioprod. Biorefining* 14 (2), 127–137. <https://doi.org/10.1002/bbb.2072>.
- Dai, L., Jiang, W., Zhou, X., Xu, Y., 2020. Enhancement in xylonate production from hemicellulose pre-hydrolysate by powdered activated carbon treatment. *Bioresour. Technol.* 316, 123944. <https://doi.org/10.1016/j.biortech.2020.123944>.
- Dalli, S.S., da Silva, S.S., Upreti, B.K., Rakshit, S.K., 2017. Enhanced Production of Xylitol from Poplar Wood Hydrolysates Through a Sustainable Process Using Immobilized New Strain *Candida tropicalis* UFMG BX 12-a. *Appl. Biochem. Biotechnol.* 182 (3), 1053–1064.
- Damião Xavier, F., Santos Bezerra, G., Florentino Melo Santos, S., Sousa Conrado Oliveira, L., Luiz Honorato Silva, F., Joice Oliveira Silva, A., Maria Conceição, M., 2018. Evaluation of the Simultaneous Production of Xylitol and Ethanol from Sisal Fiber. *Biomolecules* 8 (1), 2. <https://doi.org/10.3390/biom8010002>.
- Dasgupta, D., Junghare, V., Nautiyal, A.K., Jana, A., Hazra, S., Ghosh, D., 2019. Xylitol Production from Lignocellulosic Pentosans: A Rational Strain Engineering Approach toward a Multiproduct Biorefinery. *J. Agric. Food Chem.* 67 (4), 1173–1186. <https://doi.org/10.1021/acs.jafc.8b05509>.
- de Sá, L.R.V., Faber, M.d.O., da Silva, A.S., Cammarota, M.C., Ferreira-Leitão, V.S., 2020. Biohydrogen production using xylose or xyloligosaccharides derived from sugarcane bagasse obtained by hydrothermal and acid pretreatments. *Renew. Energy* 146, 2408–2415. <https://doi.org/10.1016/j.renene.2019.08.089>.
- Deng, L.-H., Tang, Y., Liu, Y., 2014. Detoxification of corn cob acid hydrolysate with SAA pretreatment and xylitol production by immobilized *Candida tropicalis*. *Sci. World J.* 2014, 1–11. <https://doi.org/10.1155/2014/214632>.
- Dhar, K.S., Wendisch, V.F., Nampoothiri, K.M., 2016. Engineering of *Corynebacterium glutamicum* for xylitol production from lignocellulosic pentose sugars. *J. Biotechnol.* 230, 63–71. <https://doi.org/10.1016/j.jbiotec.2016.05.011>.
- Dhiman, S.S., Kalyani, D., Jagtap, S.S., Haw, J.-R., Kang, Y.C., Lee, J.-K., 2013. Characterization of a novel xylanase from *Armillaria gemina* and its immobilization onto SiO₂ nanoparticles. *Appl. Microbiol. Biotechnol.* 97 (3), 1081–1091.
- Domingues, R., Bondar, M., Palolo, I., Queirós, O., Almeida, C.D. de, Cesário, M.T., 2021. Xylose Metabolism in Bacteria—Opportunities and Challenges towards Efficient Lignocellulosic Biomass-Based Biorefineries. *Appl. Sci.* 2021, Vol. 11, Page 8112 11, 8112. <https://doi.org/10.3390/APP11178112>.
- Donohoe, B.S., Decker, S.R., Tucker, M.P., Himmel, M.E., Vinzant, T.B., 2008. Visualizing lignin coalescence and migration through maize cell walls following thermochemical pretreatment. *Biotechnol. Bioeng.* 101 (5), 913–925.
- Du, C., Li, Y., Zong, H., Yuan, T., Yuan, W., Jiang, Y.u., 2020. Production of bioethanol and xylitol from non-detoxified corn cob via a two-stage fermentation strategy. *Bioresour. Technol.* 310, 123427. <https://doi.org/10.1016/j.biortech.2020.123427>.
- Ethaib, S., Omar, R., Kamal, S.M.M., Biak, D.R.A., 2014. Microwave-assisted pretreatment of lignocellulosic biomass: A review. *J. Eng. Sci. Technol. Spec. Issue SOMCHE* 97–109.
- Faneer, K.A., Rohani, R., Mohammad, A.W., Ba-Abbad, M.M., 2017. Evaluation of the operating parameters for the separation of xylitol from a mixed sugar solution by using a polyethersulfone nanofiltration membrane. *Korean J. Chem. Eng.* 34 (11), 2944–2957. <https://doi.org/10.1007/s11814-017-0186-y>.
- Ghaffar, A., Yameen, M., Aslam, N., Jalal, F., Noreen, R., Munir, B., Mahmood, Z., Saleem, S., Rafiq, N., Falak, S., Tahir, I.M., Noman, M., Farooq, M.U., Qasim, S., Latif, F., 2017. Acidic and enzymatic saccharification of waste agricultural biomass for biotechnological production of xylitol. *Chem. Cent. J.* 11, 1–6. <https://doi.org/10.1186/s13065-017-0331-z>.
- Granström, T.B., Izumori, K., Leisola, M., 2007. A rare sugar xylitol. *Appl. Microbiol. Biotechnol.* 74 (2), 277–281. <https://doi.org/10.1007/s00253-006-0761-3>.
- Granström, T.B., Takata, G., Morimoto, K., Leisola, M., Izumori, K., 2005. L-Xylose and L-xylose production from xylitol using *Alcaligenes 701B* strain and immobilized L-rhamnose isomerase enzyme. *Enzyme Microb. Technol.* 36 (7), 976–981. <https://doi.org/10.1016/j.enzmictec.2005.01.027>.
- Guirimand, G., Sasaki, K., Inokuma, K., Bamba, T., Hasunuma, T., Kondo, A., 2016. Cell surface engineering of *Saccharomyces cerevisiae* combined with membrane separation technology for xylitol production from rice straw hydrolysate. *Appl. Microbiol. Biotechnol.* 100 (8), 3477–3487. <https://doi.org/10.1007/s00253-015-7179-8>.
- Guirimand, G.G.Y., Bamba, T., Matsuda, M., Inokuma, K., Morita, K., Kitada, Y., Kobayashi, Y., Yukawa, T., Sasaki, K., Ogino, C., Hasunuma, T., Kondo, A., 2019. Combined Cell Surface Display of β-D-Glucosidase (BGL), Maltose Transporter (MAL11), and Overexpression of Cytosolic Xylose Reductase (XR) in *Saccharomyces cerevisiae* Enhance Cellobiose/Xylose Coutilization for Xylitol Bioproduction from Lignocellulosic B. *Biotechnol. J.* 14, 1–10. <https://doi.org/10.1002/biot.201800704>.
- Han, J., Hua, X., Zhou, X., Xu, B., Wang, H., Huang, G., Xu, Y., 2021. A cost-practical cell-recycling process for xylonic acid bioproduction from acidic lignocellulosic hydrolysate with whole-cell catalysis of *Glucanobacter oxydans*. *Bioresour. Technol.* 333, 125157. <https://doi.org/10.1016/j.biortech.2021.125157>.
- He, Y., Li, H., Chen, L., Zheng, L., Ye, C., Hou, J., Bao, X., Liu, W., Shen, Y.u., 2021. Production of xylitol by *Saccharomyces cerevisiae* using waste xylose mother liquor and corn cob residues. *Microb. Biotechnol.* 14 (5), 2059–2071. <https://doi.org/10.1111/1751-7915.13881>.
- Santana, N.B., Dias, J.C.T., Rezende, R.P., Franco, M., Oliveira, L.K.S., Souza, L.O., Arora, P.K., 2018. Production of xylitol and bio-detoxification of cocoa pod husk hemicellulose hydrolysate by *Candida boidinii* XM02G. *PLoS ONE* 13 (4), e0195206. <https://doi.org/10.1371/journal.pone.0195206>. <https://doi.org/10.1371/journal.pone.0195206.g00110.1371/journal.pone.0195206.g00210.1371/journal.pone.0195206.g00310.1371/journal.pone.0195206.g00410.1371/journal.pone.0195206.t00110.1371/journal.pone.0195206.t00210.1371/journal.pone.0195206.t00310.1371/journal.pone.0195206.t00410.1371/journal.pone.0195206.t00510.1371/journal.pone.0195206.s00110.1371/journal.pone.0195206.s002>.
- Hernández-Pérez, A.F., de Arruda, P.V., Felipe M. das G. de A., 2016. Sugarcane straw as a feedstock for xylitol production by *Candida guilliermondii* FTI 20037. *Braz. J. Microbiol.* 47 (2), 489–496. <https://doi.org/10.1016/j.bjm.2016.01.019>.
- Herrera, C.R.J., Vieira, V.R., Benoliel, T., Carneiro, C.V.G.C., De Marco, J.L., de Moraes, L.M.P., de Almeida, J.R.M., Torres, F.A.G., 2021. Engineering *Zymomonas mobilis* for the production of xylonic acid from sugarcane bagasse hydrolysate. *Microorganisms* 9, 1–14. <https://doi.org/10.3390/microorganisms9071372>.
- Hou, W., Zhang, M., Bao, J., 2018. Cascade hydrolysis and fermentation of corn stover for production of high titer gluconic and xylonic acids. *Bioresour. Technol.* 264, 395–399. <https://doi.org/10.1016/j.biortech.2018.06.025>.
- Huang, C., Ragauskas, A.J., Wu, X., Huang, Y., Zhou, X., He, J., Huang, C., Lai, C., Li, X., Yong, Q., 2018. Co-production of bio-ethanol, xylonic acid and slow-release nitrogen fertilizer from low-cost straw pulping solid residue. *Bioresour. Technol.* 250, 365–373. <https://doi.org/10.1016/J.BIORTECH.2017.11.060>.

- Huang, C.-F., Jiang, Y.-F., Guo, G.-L., Hwang, W.-S., 2011. Development of a yeast strain for xylitol production without hydrolysate detoxification as part of the integration of co-product generation within the lignocellulosic ethanol process. *Bioresour. Technol.* 102 (3), 3322–3329. <https://doi.org/10.1016/j.biortech.2010.10.111>.
- Iqbal, H.M.N., Asgher, M., Bhatti, H.N., 2011. Optimization of physical and nutritional factors for synthesis of lignin degrading enzymes by a novel strain of *Trametes versicolor*. *BioResources* 6, 1273–1287. <https://doi.org/10.15376/biores.6.2.1273-1287>.
- Ishizaki, H., Ihara, T., Yoshitake, J., Shimamura, M., Imai, T., 1973. D-Xyloic Acid Production by *Enterobacter cloacae*. *J. Agric. Chem. Soc. Japan* 47 (12), 755–761. <https://doi.org/10.1271/nogeikagaku1924.47.755>.
- Isikgor, F.H., Remzi Becer, C., 2015. Polymer Chemistry Lignocellulosic Biomass: A Sustainable Platform for Production of Bio-Based Chemicals and Polymers. *Polym. Chem.* <https://doi.org/10.1039/C5PY00263J>.
- Jin, L.-Q., Yang, B.o., Xu, W., Chen, X.-X., Jia, D.-X., Liu, Z.-Q., Zheng, Y.-G., 2019. Immobilization of recombinant *Escherichia coli* whole cells harboring xylose reductase and glucose dehydrogenase for xylitol production from xylose mother liquor. *Bioresour. Technol.* 285, 121344. <https://doi.org/10.1016/j.biortech.2019.121344>.
- Kamat, S., Gaikwad, S., Ravi Kumar, A., Gade, W.N., 2013. Xylitol production by *Cyberlindnera (Williopsis) saturnus*, a tropical mangrove yeast from xylose and corn cob hydrolysate. *J. Appl. Microbiol.* 115 (6), 1357–1367. <https://doi.org/10.1111/jam.12327>.
- Kawaguchi, H., Vertès, A.A., Okino, S., Inui, M., Yukawa, H., 2006. Engineering of a xylose metabolic pathway in *Corynebacterium glutamicum*. *Appl. Environ. Microbiol.* 72 (5), 3418–3428. <https://doi.org/10.1128/AEM.72.5.3418-3428.2006>.
- Kim, S.J., Sim, H.J., Kim, J.W., Lee, Y.G., Park, Y.C., Seo, J.H., 2017. Enhanced production of 2,3-butanediol from xylose by combinatorial engineering of xylose metabolic pathway and cofactor regeneration in pyruvate decarboxylase-deficient *Saccharomyces cerevisiae*. *Bioresour. Technol.* 245, 1551–1557. <https://doi.org/10.1016/j.biortech.2017.06.034>.
- Kogej, A.B., Ghosalkar, A., 2017. Xylitol production by genetically modified industrial strain of *Saccharomyces cerevisiae* using glycerol as co-substrate. *J. Ind. Microbiol. Biotechnol.* 44, 961–971. <https://doi.org/10.1007/s10295-017-1914-3>.
- Köhler, K.A., Blank, L.M., Frick, O., Schmid, A., 2015. D-Xylose assimilation via the Weimberg pathway by solvent-tolerant *Pseudomonas taiwanensis* VLB120. *Environ. Microbiol.* 17, 156–170. <https://doi.org/10.1111/1462-2920.12537>.
- Kubra Eryasar-Orer, I., S.K.-Y. 2, 2021. Optimization of activated charcoal detoxification and concentration of chestnut shell hydrolysate for xylitol production. *Biotechnol Lett* 43, 1195–1209. <https://doi.org/10.1007/s10529-021-03087-0>.
- Kudahettige-Nilsson, R.L., Helmerius, J., Nilsson, R.T., Sjöblom, M., Hodge, D.B., Rova, U., 2015. Biobutanol production by *Clostridium acetobutylicum* using xylose recovered from birch Kraft black liquor. *Bioresour. Technol.* 176, 71–79. <https://doi.org/10.1016/j.biortech.2014.11.012>.
- Kumar, V., Sandhu, P.P., Ahluwalia, V., Mishra, B.B., Yadav, S.K., 2019. Improved upstream processing for detoxification and recovery of xylitol produced from corncob. *Bioresour. Technol.* 291, 121931. <https://doi.org/10.1016/j.biortech.2019.121931>.
- Kumar, V., Binod, P., Sindhu, R., Gnansounou, E., Ahluwalia, V., 2018. Bioconversion of pentose sugars to value added chemicals and fuels: Recent trends, challenges and possibilities. *Bioresour. Technol.* 269, 443–451. <https://doi.org/10.1016/j.biortech.2018.08.042>.
- Kwak, S., Jin, Y.-S., 2017. Production of fuels and chemicals from xylose by engineered *Saccharomyces cerevisiae*: a review and perspective. *Microb. Cell Fact.* 16 (1) <https://doi.org/10.1186/s12934-017-0694-9>.
- Kwak, S., Kim, S.R., Xu, H., Zhang, G.-C., Lane, S., Kim, H., Jin, Y.-S., 2017. Enhanced isoprenoid production from xylose by engineered *Saccharomyces cerevisiae*. *Biotechnol. Bioeng.* 114 (11), 2581–2591.
- Lachke, A., 2002. Biofuel from D-xylose — The second most abundant sugar. *Reson* 7 (5), 50–58.
- Lawlis, V.B., Dennis, M.S., Chen, E.Y., Smith, D.H., Henner, D.J., 1984. Cloning and sequencing of the xylose isomerase and xylose kinase genes of *Escherichia coli*. *Appl. Environ. Microbiol.* 47 (1), 15–21.
- Lenihan, P., Orozco, A., O'Neill, E., Ahmad, M.N.M., Rooney, D.W., Walker, G.M., 2010. Dilute acid hydrolysis of lignocellulosic biomass. *Chem. Eng. J.* 156 (2), 395–403. <https://doi.org/10.1016/j.cej.2009.10.061>.
- Leonel, L.V., Sene, L., da Cunha, Mário.Antônio.A., Dalanol, Kátia.C.França., de Almeida Felipe, M.das.Graças., 2020. Valorization of apple pomace using bio-based technology for the production of xylitol and 2G ethanol. *Bioprocess Biosyst Eng* 43 (12), 2153–2163.
- Li, Z., Guo, X., Feng, X., Li, C., 2015. An environment friendly and efficient process for xylitol bioconversion from enzymatic corncob hydrolysate by adapted *Candida tropicalis*. *Chem. Eng. J.* 263, 249–256. <https://doi.org/10.1016/j.cej.2014.11.013>.
- Liu, H., Valdehuesa, K.N.G., Nisola, G.M., Ramos, K.R.M., Chung, W.-J., 2012a. High yield production of d-xyloic acid from d-xylose using engineered *Escherichia coli*. *Bioresour. Technol.* 115, 244–248. <https://doi.org/10.1016/j.biortech.2011.08.065>.
- Liu, H., Valdehuesa, K.N.G., Nisola, G.M., Ramos, K.R.M., Chung, W., 2012b. Bioresource Technology High yield production of D-xyloic acid from D-xylose using engineered *Escherichia coli*. *Bioresour. Technol.* 115, 244–248. <https://doi.org/10.1016/j.biortech.2011.08.065>.
- Lokman, B.C., van Santen, P., Verdoes, J.C., Krüse, J., Leer, R.J., Posno, M., Pouwels, P. H., 1991. Organization and characterization of three genes involved in d-xylose catabolism in *Lactobacillus pentosus*. *MGG Mol. Gen. Genet.* 230 (1-2), 161–169. <https://doi.org/10.1007/BF00290664>.
- López-Linares, J.C., Romero, I., Cara, C., Castro, E., Mussatto, S.I., 2018. Xylitol production by *Debaryomyces hansenii* and *Candida guilliermondii* from rapeseed straw hemicellulosic hydrolysate. *Bioresour. Technol.* 247, 736–743. <https://doi.org/10.1016/j.biortech.2017.09.139>.
- Martínez, E.A., Canetti, E. V., Bispo, J.A.C., Giuliotti, M., De Almeida e Silva, J.B., Converti, A., 2015. Strategies for xylitol purification and Crystallization: A review. *Sep. Sci. Technol.* 50, 2087–2098. <https://doi.org/10.1080/01496395.2015.1009115>.
- Mateo, S., Puentes, J.G., Moya, A.J., Sánchez, S., 2015. Ethanol and xylitol production by fermentation of acid hydrolysate from olive pruning with *Candida tropicalis* NBRC 0618. *Bioresour. Technol.* 190, 1–6. <https://doi.org/10.1016/j.biortech.2015.04.045>.
- Mathews, S.L., Pawlak, J., Grunden, A.M., 2015. Bacterial biodegradation and bioconversion of industrial lignocellulosic streams. *Appl. Microbiol. Biotechnol.* 99 (7), 2939–2954. <https://doi.org/10.1007/s00253-015-6471-y>.
- McClintock, M.K., Wang, J., Zhang, K., 2017. Application of Nonphosphorylative Metabolism as an Alternative for Utilization of Lignocellulosic Biomass. *Front. Microbiol.* 8 <https://doi.org/10.3389/fmicb.2017.02310>.
- Mehtio, T., Toivari, M., Wiebe, M.G., Harlin, A., Penttilä, M., Koivula, A., 2016. Production and applications of carbohydrate-derived sugar acids as generic biobased chemicals. *Crit. Rev. Biotechnol.* 36 (5), 904–916. <https://doi.org/10.3109/07388551.2015.1060189>.
- Miao, Y., Zhou, X., Xu, Y., Yu, S., 2015. Draft genome sequence of *Gluconobacter oxydans* NL71, a strain that efficiently biocatalyzes xylose to xylonic acid at a high concentration. *Genome Announc.* 3, 2–3. <https://doi.org/10.1128/genomeA.00615-15>.
- Misra, S., Raghuvanshi, S., Saxena, R.K., 2013. Evaluation of corncob hemicellulosic hydrolysate for xylitol production by adapted strain of *Candida tropicalis*. *Carbohydr. Polym.* 92 (2), 1596–1601. <https://doi.org/10.1016/j.carbpol.2012.11.033>.
- Miura, M., Shimotori, Y., Nakatani, H., Harada, A., Aoyama, M., 2015. Bioconversion of Birch Wood Hemicellulose Hydrolyzate to Xylitol. *Appl. Biochem. Biotechnol.* 176 (3), 947–955. <https://doi.org/10.1007/s12010-015-1604-4>.
- Mohd Azhar, S.H., Abdulla, R., Jambo, S.A., Marbawi, H., Gansau, J.A., Mohd Faik, A.A., Rodrigues, K.F., 2017. Yeasts in sustainable bioethanol production: A review. *Biochem. Biophys. Reports* 10, 52–61. <https://doi.org/10.1016/j.bbrep.2017.03.003>.
- Morais Junior, W.G., Pacheco, T.F., Trichez, D., Almeida, J.R.M., Gonçalves, S.B., 2019. Xylitol production on sugarcane biomass hydrolysate by newly identified *Candida tropicalis* JA 2 strain. *Yeast* 36, 349–361. <https://doi.org/10.1002/yea.3394>.
- Moysés, D.N., Reis, V.C.B., Almeida, J.R.M. de, Moraes, L.M.P. de, Torres, F.A.G., 2016. Xylose Fermentation by *Saccharomyces cerevisiae*: Challenges and Prospects. *Int. J. Mol. Sci.* 2016, Vol. 17, Page 207 17, 207. <https://doi.org/10.3390/IJMS17030207>.
- Narisetty, V., Castro, E., Durgapal, S., Coulon, F., Jacob, S., Kumar, D., Kumar Awasthi, M., Kishore Pant, K., Parameswaran, B., Kumar, V., 2021. High level xylitol production by *Pichia fermentans* using non-detoxified xylose-rich sugarcane bagasse and olive pits hydrolysates. *Bioresour. Technol.* 342, 126005. <https://doi.org/10.1016/j.biortech.2021.126005>.
- Nygård, Y., Toivari, M.H., Penttilä, M., Ruohonen, L., Wiebe, M.G., 2011. Bioconversion of d-xylose to d-xylofuranose with *Kluyveromyces fragilis*. *Metab. Eng.* 13 (4), 383–391. <https://doi.org/10.1016/j.ymben.2011.04.001>.
- Oliveira-Filho, E.R., Gomez, José.Gregório.C., Tacio, M.K., Silva, L.F., 2021. Burkholderia sacchari (synonym Paraburkholderia sacchari): An industrial and versatile bacterial chassis for sustainable biosynthesis of polyhydroxyalkanoates and other bioproducts. *Bioresour. Technol.* 337, 125472. <https://doi.org/10.1016/j.biortech.2021.125472>.
- Orozco, A.M., Al-Muhtaseb, A.H., Albadarin, A.B., Rooney, D., Walker, G.M., Ahmad, M.N.M., 2011. Dilute phosphoric acid-catalysed hydrolysis of municipal bio-waste wood shavings using autoclave Parr reactor system. *Bioresour. Technol.* 102 (19), 9076–9082. <https://doi.org/10.1016/j.biortech.2011.07.006>.
- Pal, S., Choudhary, V., Kumar, A., Biswas, D., Mondal, A.K., Sahoo, D.K., 2013. Studies on xylitol production by metabolic pathway engineered *Debaryomyces hansenii*. *Bioresour. Technol.* 147, 449–455. <https://doi.org/10.1016/j.biortech.2013.08.065>.
- Phwan, C.K., Chew, K.W., Sebayang, A.H., Ong, H.C., Ling, T.C., Malek, M.A., Ho, Y.-C., Show, P.L., 2019. Effects of acids pre-treatment on the microbial fermentation process for bioethanol production from microalgae. *Biotechnol Biofuels* 12 (1). <https://doi.org/10.1186/s13068-019-1533-5>.
- Prabhu, A.A., Bosakomranut, E., Amraoui, Y., Agrawal, D., Coulon, F., Vivekanand, V., Thakur, V.K., Kumar, V., 2020. Enhanced xylitol production using non-detoxified xylose rich pre-hydrolysate from sugarcane bagasse by newly isolated *Pichia fermentans*. *Biotechnol. Biofuels* 13, 1–15. <https://doi.org/10.1186/s13068-020-01845-2>.
- Rafiqul, I.S.M., Sakinah, A.M.M., Zularisam, A.W., 2015. Enzymatic Production of Bioxylitol from Sawdust Hydrolysate: Screening of Process Parameters. *Appl. Biochem. Biotechnol.* 176 (4), 1071–1083. <https://doi.org/10.1007/s12010-015-1630-2>.
- Rissi, S., Fontana, R.C., Reck, M.A., da Silveira, R.M.B., Dillon, A.José.P., Camassola, M., 2018. Production of ethanol and xylitol by *Trametes membranacea*. *Bioprocess Biosyst. Eng.* 41 (7), 1017–1028. <https://doi.org/10.1007/s00449-018-1931-2>.
- Rudrang, S.S.R., West, T.P., 2020. Effect of pH on xylitol production by *Candida* species from a prairie cordgrass hydrolysate. *Zeitschrift für Naturforsch. - Sect. C J. Biosci.* 75, 489–493. <https://doi.org/10.1515/znc-2020-0140>.
- Ruiz, H.A., Rodríguez-Jasso, R.M., Fernandes, B.D., Vicente, A.A., Teixeira, J.A., 2013. Hydrothermal processing, as an alternative for upgrading agriculture residues and marine biomass according to the biorefinery concept: A review. *Renew. Sustain. Energy Rev.* 21, 35–51. <https://doi.org/10.1016/j.rser.2012.11.069>.

- Rygus, T., Scheler, A., Allmansberger, R., Hillen, W., 1991. Molecular cloning, structure, promoters and regulatory elements for transcription of the *Bacillus megaterium* encoded regulon for xylose utilization. *Arch. Microbiol.* 155 (6), 535–542. <https://doi.org/10.1007/BF00245346>.
- Sapci, B., Akpınar, O., Bolukbasi, U., Yilmaz, L., 2016. Evaluation of cotton stalk hydrolysate for xylitol production. *Prep. Biochem. Biotechnol.* 46 (5), 474–482. <https://doi.org/10.1080/10826068.2015.1084511>.
- Shen, J., Wyman, C.E., 2011. A novel mechanism and kinetic model to explain enhanced xylose yields from dilute sulfuric acid compared to hydrothermal pretreatment of corn stover. *Bioresour. Technol.* 102 (19), 9111–9120. <https://doi.org/10.1016/j.biortech.2011.04.001>.
- Singh, S., Kaur, D., Yadav, S.K., Krishania, M., 2021. Process scale-up of an efficient acid-catalyzed steam pretreatment of rice straw for xylitol production by *C. tropicalis* MTCC 6192. *Bioresour. Technol.* 320, 124422. <https://doi.org/10.1016/j.biortech.2020.124422>.
- Stelte, W., 2013. Steam explosion for biomass pre-treatment. *Danish Technol. Inst.* 1–15.
- Stephens, C., Christen, B., Fuchs, T., Sundaram, V., Watanabe, K., Jenal, U., 2007. Genetic analysis of a novel pathway for D-xylose metabolism in *Caulobacter crescentus*. *J. Bacteriol.* 189, 2181–2185. <https://doi.org/10.1128/JB.01438-06>.
- Su, B., Wu, M., Zhang, Z., Lin, J., Yang, L., 2015. Efficient production of xylitol from hemicellulosic hydrolysate using engineered *Escherichia coli*. *Metab. Eng.* 31, 112–122. <https://doi.org/10.1016/j.ymben.2015.07.003>.
- Sundar Lekshmi, M.S., Susmitha, A., Soumya, M.P., Keerthi, S., Nampoothiri Madhavan, K., 2019. Bioconversion of D-xylose to D-xylonic acid by *Pseudoduganella danionis*. *Indian J. Exp. Biol.* 57, 821–824.
- Sundar, M.S.L., Susmitha, A., Rajan, D., Hannibal, S., Sasikumar, K., Wendisch, V.F., Nampoothiri, K.M., 2020. Heterologous expression of genes for bioconversion of xylose to xylonic acid in *Corynebacterium glutamicum* and optimization of the bioprocess. *AMB Express* 10, 68. <https://doi.org/10.1186/s13568-020-01003-9>.
- Tada, K., Kanno, T., Horiuchi, J.-ichi., 2012. Enhanced production of bioxylitol from corn cobs by *Candida magnoliae*. *Ind. Eng. Chem. Res.* 51 (30), 10008–10014. <https://doi.org/10.1021/ie202800h>.
- Takata, E., Tsuruoka, T., Tsutsumi, K., Tsutsumi, Y., Tabata, K., 2014. Production of xylitol and tetrahydrofurfuryl alcohol from xylan in napier grass by a hydrothermal process with phosphorus oxoacids followed by aqueous phase hydrogenation. *Bioresour. Technol.* 167, 74–80. <https://doi.org/10.1016/j.biortech.2014.05.112>.
- Tathod, A.P., Dhepe, P.L., 2015. Efficient method for the conversion of agricultural waste into sugar alcohols over supported bimetallic catalysts. *Bioresour. Technol.* 178, 36–44. <https://doi.org/10.1016/j.biortech.2014.10.036>.
- Toivari, M.H., Ruohonen, L., Richard, P., Penttilä, M., Wiebe, M.G., 2010. *Saccharomyces cerevisiae* engineered to produce D-xylonate. *Appl. Microbiol. Biotechnol.* 88 (3), 751–760. <https://doi.org/10.1007/s00253-010-2787-9>.
- Toivari, M., Vehkomäki, M.L., Nygård, Y., Penttilä, M., Ruohonen, L., Wiebe, M.G., 2013. Low pH D-xylonate production with *Pichia kudriavzevii*. *Bioresour. Technol.* 133, 555–562. <https://doi.org/10.1016/j.biortech.2013.01.157>.
- Toivari, M., Nygård, Y., Kumpula, E.-P., Vehkomäki, M.-L., Bencina, M., Valkonen, M., Maaheimo, H., Andberg, M., Koivula, A., Ruohonen, L., Penttilä, M., Wiebe, M.G., 2012a. Metabolic engineering of *Saccharomyces cerevisiae* for bioconversion of d-xylose to d-xylonate. *Metab. Eng.* 14 (4), 427–436. <https://doi.org/10.1016/j.ymben.2012.03.002>.
- Toivari, M.H., Nygård, Y., Penttilä, M., Ruohonen, L., Wiebe, M.G., 2012b. Microbial d-xylonate production. *Appl. Microbiol. Biotechnol.* 961 (96), 1–8. <https://doi.org/10.1007/S00253-012-4288-5>.
- Wang, C., Wei, D., Zhang, Z., Wang, D., Shi, J., Kim, C.H., Jiang, B., Han, Z., Hao, J., 2016a. Production of xylonic acid by *Klebsiella pneumoniae*. *Appl. Microbiol. Biotechnol.* 100 (23), 10055–10063. <https://doi.org/10.1007/s00253-016-7825-9>.
- Wang, H., Li, L., Zhang, L., An, J., Cheng, H., Deng, Z., 2016b. Xylitol production from waste xylene mother liquor containing miscellaneous sugars and inhibitors: One-pot biotransformation by *Candida tropicalis* and recombinant *Bacillus subtilis*. *Microb. Cell Fact.* 15, 1–12. <https://doi.org/10.1186/s12934-016-0480-0>.
- Wang, Y., Shi, W.-L., Liu, X.-Y., Shen, Y., Bao, X.-M., Bai, F.-W., Qu, Y.-B., 2004. Establishment of a xylose metabolic pathway in an industrial strain of *Saccharomyces cerevisiae*. *Biotechnol. Lett.* 26 (11), 885–890. <https://doi.org/10.1023/B:bile.0000025897.21106.92>.
- Wannawilai, S., Lee, W.C., Chisti, Y., Sirisansaneeyakul, S., 2017. Furfural and glucose can enhance conversion of xylose to xylitol by *Candida magnoliae* TISTR 5663. *J. Biotechnol.* 241, 147–157. <https://doi.org/10.1016/j.jbiotec.2016.11.022>.
- Werpy, T.A., Holladay, J.E., White, J.F., 2004. Top Value Added Chemicals From Biomass: I. Results of Screening for Potential Candidates from Sugars and Synthesis Gas. U.S. Dep. energy 1, 76. <https://doi.org/10.2172/926125>.
- Wu, J., Hu, J., Zhao, S., He, M., Hu, G., Ge, X., Peng, N., 2018. Single-cell Protein and Xylitol Production by a Novel Yeast Strain *Candida intermedia* FLO23 from Lignocellulosic Hydrolysates and Xylose. *Appl. Biochem. Biotechnol.* 185 (1), 163–178. <https://doi.org/10.1007/s12010-017-2644-8>.
- Xu, P., Bura, R., Doty, S.L., 2011. Genetic analysis of D-xylose metabolism by endophytic yeast strains of *Rhodotorula graminis* and *Rhodotorula mucilaginosa*. *Genet. Mol. Biol.* 34 (3), 471–478. <https://doi.org/10.1590/S1415-47572011000300018>.
- Yim, S.S., Choi, J.W., Lee, S.H., Jeon, E.J., Chung, W.-J., Jeong, K.J., 2017. Engineering of *Corynebacterium glutamicum* for Consolidated Conversion of Hemicellulosic Biomass into Xylonic Acid. *Biotechnol. J.* 12 (11), 1700040. <https://doi.org/10.1002/biot.v12.1110.1002/biot.201700040>.
- Yuan, X., Tu, S., Lin, J., Yang, L., Shen, H., Wu, M., 2020. Combination of the CRP mutation and ptsG deletion in *Escherichia coli* to efficiently synthesize xylitol from corncob hydrolysates. *Appl. Microbiol. Biotechnol.* 104 (5), 2039–2050. <https://doi.org/10.1007/s00253-019-10324-0>.
- Zhang, H., Han, X., Wei, C., Bao, J., 2017. Oxidative production of xylonic acid using xylose in distillation stillage of cellulosic ethanol fermentation broth by *Gluconobacter oxydans*. *Bioresour. Technol.* 224, 573–580. <https://doi.org/10.1016/j.biortech.2016.11.039>.
- Zhang, H., Liu, G., Zhang, J., Bao, J., 2016. Fermentative production of high titer gluconic and xylonic acids from corn stover feedstock by *Gluconobacter oxydans* and techno-economic analysis. *Bioresour. Technol.* 219, 123–131. <https://doi.org/10.1016/j.biortech.2016.07.068>.
- Zhang, L., Chen, Z., Wang, J., Shen, W., Li, Q., Chen, X., 2021. Stepwise metabolic engineering of *Candida tropicalis* for efficient xylitol production from xylose mother liquor. *Microb. Cell Fact.* 20 (1). <https://doi.org/10.1186/s12934-021-01596-1>.
- Zhang, Z., Yang, Y., Wang, Y., Gu, J., Lu, X., Liao, X., Shi, J., Kim, C.H., Lye, G., Baganz, F., Hao, J., 2020. Ethylene glycol and glycolic acid production from xylonic acid by *Enterobacter cloacae*. *Microb. Cell Fact.* 19, 1–16. <https://doi.org/10.1186/s12934-020-01347-8>.
- Zhao, Z., Xian, M., Liu, M., Zhao, G., 2020. Biochemical routes for uptake and conversion of xylose by microorganisms. *Biotechnol. Biofuels* 13, 1–12. <https://doi.org/10.1186/s13068-020-1662-x>.
- Zhou, X., Shanshan, L., Yong, X., Yixian, M., Shiyuan, Y., 2015. Improving the performance of cell biocatalysis and the productivity of xylonic acid using a compressed oxygen supply. *Biochem. Eng. J.* 93, 196–199. <https://doi.org/10.1016/j.bej.2014.10.014>.
- Zhou, X., Xu, Y., 2019. Eco-friendly consolidated process for co-production of xylooligosaccharides and fermentable sugars using self-providing xylonic acid as key pretreatment catalyst. *Biotechnol. Biofuels* 12 (1). <https://doi.org/10.1186/s13068-019-1614-5>.
- Zhou, X., Xu, Y., Yu, S., 2016. Simultaneous Bioconversion of Xylose and Glycerol to Xylonic Acid and 1,3-Dihydroxyacetone from the Mixture of Pre-Hydrolysates and Ethanol-Fermented Waste Liquid by *Gluconobacter oxydans*. *Appl. Biochem. Biotechnol.* 178 (1), 1–8. <https://doi.org/10.1007/s12010-015-1853-2>.
- Zhou, X., Zhou, X., Tang, X., Xu, Y., 2018. Process for calcium xylonate production as a concrete admixture derived from in-situ fermentation of wheat straw pre-hydrolysate. *Bioresour. Technol.* 261, 288–293. <https://doi.org/10.1016/j.biortech.2018.04.040>.
- Zhu, J., Rong, Y., Yang, J., Zhou, X., Xu, Y., Zhang, L., Chen, J., Yong, Q., Yu, S., 2015. Integrated production of xylonic acid and bioethanol from acid-catalyzed steam-exploded corn stover. *Appl. Biochem. Biotechnol.* 176 (5), 1370–1381. <https://doi.org/10.1007/s12010-015-1651-x>.
- Zhu, M., Sun, L., Lu, X., Zong, H., Zhuge, B., 2019. Establishment of a transient CRISPR-Cas9 genome editing system in *Candida glycerinogenes* for co-production of ethanol and xylonic acid. *J. Biosci. Bioeng.* 128 (3), 283–289. <https://doi.org/10.1016/j.jbiosc.2019.03.009>.